

A New Schiff Base Mercury(II) Complex: Synthesis, Spectroscopy, HOMO, LUMO and MEP Analysis

Raziyeh Mohammadi^a, Morteza Montazerzohori^{a,*}, Leila Taghizadeh^a, Ardavan Masoudiasl^a and Shiva Joohari^b

^aDepartment of Chemistry, Faculty of Sciences, Yasouj University, Yasouj, Iran

^bDepartment of Basic Sciences, Yasooj Branch, Islamic Azad University, Yasooj, Iran

Corresponding author Email: mmzohory@yahoo.com

1. Introduction

In recent years, the coordination chemistry of mercury has received considerable attention because mercury compounds exhibit high toxicity to living organisms [1]. The increased concentration of mercury in the biosphere and the presence of mercury in industrial wastes have attracted interest to the mercury coordination chemistry [2,3]. The d^{10} configuration of Hg(II) is associated with a flexible coordination environment, thus, the geometries of these complexes can vary from linear to octahedral or even distorted hexagonal bipyramidal [4]. Also, Schiff base ligands are among the most chelating systems in coordination chemistry and form complexes with both transition and p-block metals [5,6].

2. Experimental

The Schiff base ligand (L) was synthesized by reaction between 2-methylpentane-1,5-diamine (1mmol) and cinnamaldehyde (2 mmol) in ethanol. Yield: 71%. UV–Vis in CH_2Cl_2 [λ_{max} ; nm]: 286. FT-IR (KBr, cm^{-1}): 2830(w), 1635(vs). For synthesis of $HgLI_2$ complex, a solution of ligand was added to ethanolic solution of mercury iodide salt. Product obtained as cream precipitate. Yield: 86%. UV–Vis in CH_2Cl_2 [λ_{max} ; nm]: 285. FT-IR (KBr, cm^{-1}): 2854(w), 1629(vs). DFT calculations have been carried out at the B3LYP/LanL2DZ level of theory.

3. Result and discussion

In the FT-IR spectrum of ligand, the presence of a sharp band at 1635 cm^{-1} has been attributed to the stretching vibrations of the azomethine groups. In complex, this band shifted 6 cm^{-1} to lower wave numbers indicating the involvement of iminic nitrogens in coordination [7]. Furthermore, the appearance of a doublet peak at 8.05 ppm in the 1H NMR spectrum of ligand confirms its formation. The shifting of this peak to downer fields in the spectrum of complex (8.19 ppm) indicates that nitrogens are coordinated to metal center.

The optimized structure of $HgLI_2$ complex has been shown in Fig. 1. Some important calculated geometrical parameters are listed in Table 1. The geometry of the metal center in this complex can be described as distorted tetrahedral geometry based on τ_4 angular index defined by Houser ($\tau_4 = 0.83$) [8]. The HOMO and LUMO surfaces of complex are depicted in Fig. 2. HOMO is mainly localized on iodide anions while LUMO is delocalized on one side of Schiff base ligand. On the MEP surface (Fig. 3), the regions having the maximum negative potential is over the iodide anions and the regions having the maximum positive potential are mainly over the hydrogen atoms.

4. Conclusion

A new mercury complex has been prepared by reaction mercury iodide salt and a bidentate Schiff base ligand (L) and characterized by different physical and spectroscopic techniques. The optimization of geometry of complex showed a distorted tetrahedral environment. Furthermore, HOMO, LUMO and MEP map of complex were investigated.

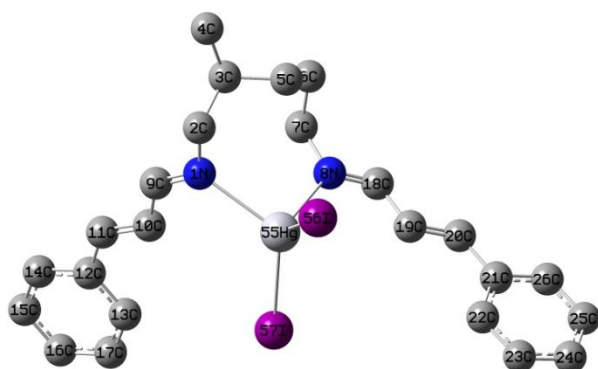


Fig. 1. The optimized structure of HgLI₂ complex.

Table 1 Bond lengths (Å) and bond angles (°) calculated at B3LYP/LANL2DZ level.

Bond length (Å)	
Hg55—N1	2.520
Hg55—N8	2.506
Hg55—I56	2.872
Hg55—I57	2.886
Bond angle (°)	
N1—Hg55—N8	91.67
N1—Hg55—I56	103.53
N1—Hg55—I57	116.04
N8—Hg55—I56	110.46
N8—Hg55—I57	102.51
I56—Hg55—I57	126.95

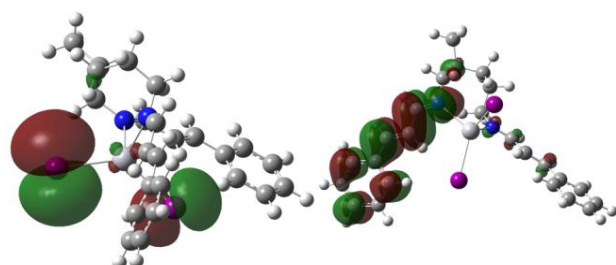


Fig. 2. HOMO (left) and LUMO (right) surfaces of HgLI₂ complex.

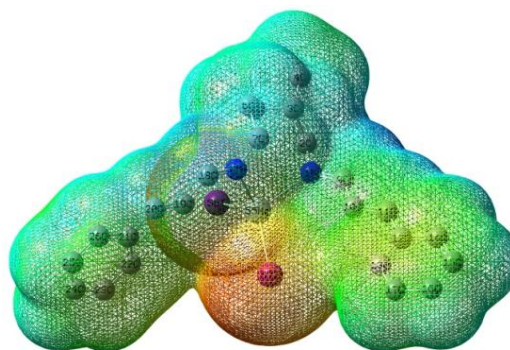


Fig. 3. The MEP surface of HgLI₂ complex.

5. References

- [1] I. Onyido, A. R. Norris, E. Buncel, *Chem. Rev.*, **2004**, 104, 5911-5929.
- [2] X. Wang, L. Andrews, *Inorg. Chem.*, **2005**, 44, 108-113.
- [3] J. G. Melnick, G. Parkin, *Science*, **2007**, 17, 225-227.
- [4] A. Morsali, M. Y. Masoomi, *Coord. Chem. Rev.*, **2009**, 253, 1882-1905.
- [5] D. A. Atwood, M.J. Harvey, *Chem. Rev.*, **2001**, 101, 37-52.
- [6] C. -M. Che, J. -S. Huang, *Coord. Chem. Rev.*, **2003**, 242, 97-113.
- [7] J. Chakraborty, S. Thakurta, B. Samanta, A. Ray, G. Pilet, S. R. Batten, P. Jensen, S. Mitra, *Polyhedron*, **26** (2007) 5139. **2007**, 26, 5139-5149.
- [8] L. Yang, D. R. Powell, R. P. Houser, *Dalton Trans.*, **2007**, 955-964.

Carbon-Oxygen Bond-Forming Reductive Elimination from Diacetate Platinum(IV) Complexes

Marzieh Dadkhah Aseman^a, S. Masoud Nabavizadeh^{a*}

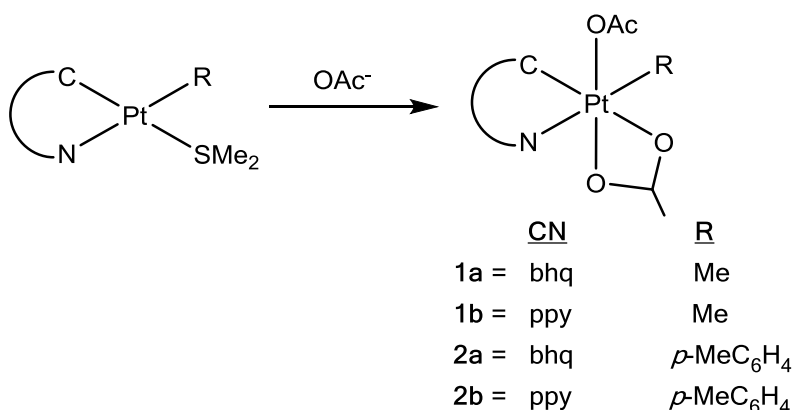
^a Department of Chemistry, College of Sciences, Shiraz University, Shiraz, Iran
nabavi@chem.susc.ac.ir

Introduction:

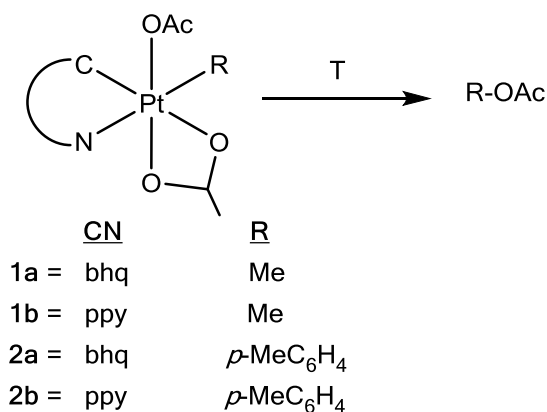
Reductive elimination is a fundamental organometallic reaction and a critical product-release step in a number of industrially important catalytic processes.[1] In particular, reductive elimination reactions which form C-O bonds from Pt(IV) have been proposed as product forming steps in the functionalization of alkanes by Pt(II) catalysts (Shilov's oxidations and the system recently reported by Catalytica).[2-3] Only a limited number of examples of reductive eliminations which form carbon-heteroatom (C-O, C-N, C-S) bonds from model complexes are known. These reactions primarily occur at low valent d^8 metal centers (Pd(II), Ni(II)) and involve aryl and acyl carbon groups.[4] Examples of carbon-heteroatom reductive couplings which occur from high valent d^6 metal centers such as Pd(IV), Pt(IV), Rh(III), or Ir(III), as well as those which involve alkyl carbon groups, are extremely rare. This contribution reports the first direct observation and study of high yield alkyl C-O reductive elimination from a d^6 octahedral Pt(IV) metal center.[4]

Methods / Experimentals:

The reaction of organoplatinum(II) precursor $[PtR(SMe_2)(CN)]$ complexes with 1 equivalent of acetate source at room temperature gave stable octahedral platinum (IV) diacetate $[Pt(CN)R(OAc)_2]$, **1-2**, complexes (Scheme 1). These complexes were characterized by 1H and ^{13}C -NMR, Mass spectroscopy and also IR spectroscopy.



According to Scheme 2, thermolysis of Pt(IV) complexes lead to direct C-O bond formation.



Scheme 2

Results and Discussion:

As is depicted in Scheme 1, the reaction of organoplatinum(II) precursor [PtR(SMe₂)(CN)] complexes with acetate source, in acetone, gave in good yield, the complex [Pt(CN)R(OAc)₂]. These Pt(IV) complexes are an air-stable white solid that are stable in solutions for several hours at room temperature. This complexes was fully characterized by multinuclear (¹H, ¹³C) NMR and Mass and IR spectroscopy. For instance, in the ¹H- NMR spectrum of complex **2a**, the H atom of two acetate group were appeared as a singlet signal at δ = 1.7 ppm, the H atoms of *Para* tolyl ligand were appeared at 2.3 ppm as a singlet signal. Thermal decomposition of platinum complex **1**, **2**, occurs smoothly at 80 °C in toluene. Based on ¹H-NMR spectroscopy after almost one day all the signals related to complex **1**, **2** were disappeared and the signal of R-OAc was appeared.

Conclusion:

We present our studies toward the synthesis and comparative reactivity of a series of Pt(IV) diacetate complexes According to NMR spectroscopy, our results indicate that Pt(IV) complexes contain two acetate groups that shows C-O reductive elimination during thermolysis.

References:

- [1] A. R. Dick, J. W. Kampf, M. S. Sanford, *J. Am. Chem. Soc.* **2005**, *127*, 12790-1279.
- [2] Y. Fu, Z. Li, S. Liang, Q. X. Guo, L. Liu, *Organometallics*. **2008**, *27*, 3736–3742.
- [3] J. R. Khusnutdinova, A. N. Vedernikov, *J. Am. Chem. Soc.* **2008**, *130*, 2174-2175.
- [4] A. K. Cook, M. S. Sanford, *J. Am. Chem. Soc.* **2015**, *137*, 3109-3118.

CuSO₄ catalyzed One-pot approach for the synthesis of 2-aryl benzothiazoles via an oxidative condensation of benzothiazoles and toluene derivatives using K₂S₂O₈

Marzieh roosta^a, Dariush Khalili^{a,*}, Ali Khalafi-nezhad^a

^a Department of Chemistry, College of Sciences, Shiraz University, Shiraz 71454, Iran

Email address: Khalili@shirazu.ac.ir

Introduction:

During the past decades, tandem processes involve multiple chemical transformations in a single-pot has undergone great development [1]. Especially, utilizing a single catalyst that could promotes multiple transformation in a selective manner attracted greater attention. This innovative strategy result in a reduced number of operations, giving significant time-cost benefits as well as preventing side product formation and loss of starting material [2]. 2-Benzothiazoles are important aromatic nitrogen heterocycles due to their ubiquitous presence and wide applications in many chemical, pharmaceutical and biological areas [3]. Therefore, their synthesis is a frequently encountered mission for both organic and medicinal chemists. Recently, various alternative routes have been developed for these heterocycles [4]. In this work, we wish to report that 2-arylbenzothiazoles can be synthesized via K₂S₂O₈-mediated oxidative condensation of benzothiazoles with toluene derivatives using CuSO₄ as catalyst. This one-pot transformation involves the oxidative opening of the thiazole ring, oxidation of toluene to aldehyde and oxidative condensation of the resultant 2-amino thiophenol with the aldehyde.

Methods / Experimentals:

To a solution of benzothiazole (1 mmol) and alkyl benzene (2 mmol) in DMSO/H₂O (2:0.5 mL), K₂S₂O₈ (1 mmol) and CuSO₄ (30 mgr) were added. The reaction mixture was heated in oil bath (60 °C) for 5 h. after completion of the reaction indicated by TLC, the reaction mixture was diluted with water and extracted with ethyl acetate. The combined organic extracts were dried with anhydrous Na₂SO₄ and concentrated under vacuum to afford crude product which was purified by column chromatography (silica gel, hexane/ethyl acetate to give 2-aryl substituted benzothiazole.

Results and Discussion:

Encouraged by this unprecedented oxidative condensation optimizations were carried out with various Cu(I) and Cu(II) salts (entries 1–11, Table 1) among the various copper salts, CuSO₄·5H₂O was found to be superior (entry 2, Table 1). Next, the oxidant effect in this reaction was investigated, and several oxidants were tested (entries 12-16 and 2, Table 1), in which K₂S₂O₈ afforded the highest yield.

Having established the optimized conditions for the formation of the 2-aryl substituted benzothiazole, the substrate scope of the protocol was then surveyed. The effects of substituents on the alkylbenzenes were investigated under the optimized reaction conditions (Table 2).

Table 1. Screening of reaction conditions.

Run	Copper salt	Oxidants	Yield (%)
1	Cu(OAc) ₂	K ₂ S ₂ O ₈	0
2	CuSO ₄ ·5H ₂ O	K ₂ S ₂ O ₈	86
3	CuSO ₄ .anhydrous	K ₂ S ₂ O ₈	9
4	Cu(CO ₃) ₂	K ₂ S ₂ O ₈	61
5	Cu(NO ₃) ₂ ·3H ₂ O	K ₂ S ₂ O ₈	56
6	CuCl ₂ ·2H ₂ O	K ₂ S ₂ O ₈	0
7	CuI	K ₂ S ₂ O ₈	0
8	CuCl	K ₂ S ₂ O ₈	0
9	CuO	K ₂ S ₂ O ₈	63
10	Cu(SO ₄)(NH ₄)	K ₂ S ₂ O ₈	trace
11	Cu(OH)(CO ₃)	K ₂ S ₂ O ₈	32
12	CuSO ₄ ·5H ₂ O	Air	0
13	CuSO ₄ ·5H ₂ O	TBHP	0
14	CuSO ₄ ·5H ₂ O	Oxone	44
15	CuSO ₄ ·5H ₂ O	H ₂ O ₂	0
16	CuSO ₄ ·5H ₂ O	DDQ	0

Table 2. Substrate Scope for Benzothiazole.

 2a , 1 h, 91%	 3a , 1 h, 92%
 1a , 5 h, 86%	 4a , 5 h, 83%
 5a , 5 h, 60%	 6a , 8 h, 0%

Conclusion: In Conclusion, a novel method for the synthesis of 2-aryl benzothiazoles from benzothiazoles and toluene derivatives was developed. By treating benzothiazoles and alkyl benzenes with K₂S₂O₈ in DMSO and H₂O, the benzothiazoles were found to undergo oxidative ring opening to produce 2-amino thiophenols, which subsequently underwent oxidative cyclization with the alkyl benzene to give a variety of 2-aryl benzothiazoles in yields ranging from 60 to 92%. The reaction also worked well when benzothiazole was replaced with 2-amino thiophenol.

References

- [1] J.C. Wasilke; S.J. Obrey; R.T. Baker; G.C. Bazan. *Chem. Rev.*, **2005**, *105*, 1001-1020.
- [2] P. Liu; Y.M. Pan; Y.L. Xu; H.S. Wang. *Org. Biomol. Chem.*, **2012**, *10*, 4696-4698.
- [3] A. R. Katritzky; C. A. Ramsden; E. F. V. Scriven; R. J. K. Taylor. *Comprehensive Heterocyclic Chemistry III*, Pergamon, Oxford, New York, USA, **2008**, vol. 4.
- [4] S. Ranjit; X. Liu. *Chem.-Eur. J.*, **2011**, *17*, 1105-1108.

Manganese(III) tetradenate Schiff base: A clue to the crystal structure, electrochemical properties and catalytic activities for the oxidation of sulfides and olefins

Elham Khodaei, Saeed Rayati *

Department of Chemistry, K.N. Toosi University of Technology, P.O. Box 16315-1618, Tehran 15418, Iran

Abstract

A Schiff base ligand derived from 5-bromo-2-hydroxybenzaldehyde and 2, 2'-dimethylpropylenediamine (H_2L) and its corresponding manganese(III) complex has been synthesized and characterized. X-ray crystal structure of complex has been determined. A practical catalytic method for efficient and highly selective oxidation of wide range of sulfides and olefins with urea hydrogen peroxide (UHP) or hydrogen peroxide as green oxidants in ethanol was investigated.

Introduction

Transition metal complexes with Schiff base ligands have been widely studied in the past few years because of their application in electrochemistry, biological and catalytic fields [1-4]. Schiff base ligands and their metal complexes are efficient catalysts under homogeneous and heterogeneous conditions. For this purpose, the synthesis of a Schiff base ligand derived from 5-bromo-2-hydroxybenzaldehyde and 2, 2'-dimethylpropylenediamine (H_2L) and its corresponding Manganese(III) complex as a homogeneous catalyst has been synthesized and characterized by X-ray crystal structure which used as a catalyst for the oxidation of sulfides and alkenes with Urea hydrogen peroxide (UHP) and H_2O_2 . Moreover, the electrochemical properties of the Schiff base complexes were investigated in CH_3CN by cyclic voltammetry.

Experimental

H_2L was prepared according to the described producer [5, 6]. The manganese complex was prepared as follows: the Schiff base ligand, H_2L (1 mmol) was dissolved in 20 ml of ethanol. An ethanolic solution of manganese(II) acetate (1mmol) was added and the reaction mixture was refluxed. The solution was concentrated to yield single crystal (Fig 1).

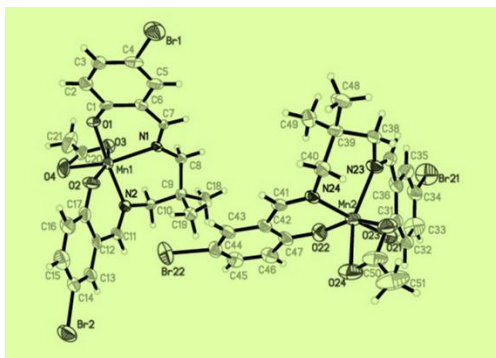


Fig. 1. Crystal structure of manganese complex

Result and discussion

The Schiff base ligand and its Mn(III) have been characterized by FTIR and electronic spectroscopy, elemental analysis and X-ray crystallography. Then catalytic activity of the Mn(III) complex in oxidation of sulfides and alkenes has been investigated. In order to achieve the appropriate condition for the oxidation of sulfides or olefins, different reaction conditions such as amount of imidazole as co-catalyst, amount of acetic anhydride as activator of oxidant, reaction time and the concentration of oxidant on the reaction conversion has been investigated. In addition, the electrochemical properties of the manganese complex have been studied. In order to demonstrate the efficiency of catalyst, oxidation of different sulfides and alkenes under optimized conditions has also been carried out.

Conclusion

In this study, the tetradenate Schiff base (N_2O_2) ligand and its corresponding manganese(III) complex have been synthesized and characterized by X-ray crystal structure. The potential catalytic activity of catalyst on the oxidation of different sulfides and alkenes and the electrochemical behavior of Schiff base complex under optimized conditions was investigated.

References

- [1] Wengnack N L, Hoard H M, Rusnak F (1999) J Am Chem Soc 9748
- [2] Usha A K, Chandra S (1992) Synth React Inorg Met Org Chem 2:1565
- [3] Martins M, Boas M, Castro B d, Freire A R (2005) Elechtrochim Acta 51:304-314
- [4] Moutet J C, Ourari A (1997) Electrochim Acta 42: 2525-2531
- [5] F. Heshmatpour, S. Rayati, M. Afghan Hajiabbas, P. Abdolalian, B. Neumuller, Polyhedron, 31 (2012) 443.
- [6] N. Doddapaneni, in: Proceedings of the 30th Power Sources Symposium, Electrochemical Society, Atlantic City, NJ, USA, 1982, p. 169

Molecular dynamics simulation studies of retinol aggregation in aqueous solution

Mousavi S. Habib-allah^{*a}, Fellah Elham^a

h.mousavi@pnu.ac.ir

introduction:

Retinol, is one of the animal form of vitamin A. Vitamin A is a fat-soluble vitamin and is made of compounds called retinoids, which forms vitamin A, and are available in nature in several ways. Retinoids, which include vitamin A (retinol) and its chemical derivatives, regulate and control diverse physiological functions. Because these compounds are lipophilic, binding proteins act as carriers for their inter- and intracellular transportation and release in the target cells. Several types of retinoid-binding proteins are known to exist. Due to its hydrophobicity, retinol makes molecular aggregation in aqueous solution. Thus, thermodynamic properties of molecular aggregation of retinol in water can clarify obscure aspects of the intracellular transportation of hydrophobic molecules [1,2].

The main objective of this study was to obtain thermodynamic properties and the impact of intermolecular forces in the accumulation of molecules in the water and to determine aggregation number and enthalpy, entropy and Gibbs free energy.

Method:

One of the best methods available to study the structure and behavior of materials, computer simulations. Gromacs software package for molecular dynamics simulations of many-body systems based on Newton's equations of motion has been expanded [3]. The software is widely used in the review exists within the simulation of biological systems.

In this study we have done simulations on the various numbers of retinol molecules in the cubic box. Retinol structure was optimized using software Gaussian 2003 and was stored in a pdb file format. Then, the prdrg site [4] was used to make molecular topology files with GROMOS43a1 force field. We made cubic boxes and filled with water, SPC model. Energy minimization is done at a later stage. The equilibrium stages were performed in two NVT and NPT ensembles. The final stage was MD production. Thermodynamic parameters were extracted from calculation results.

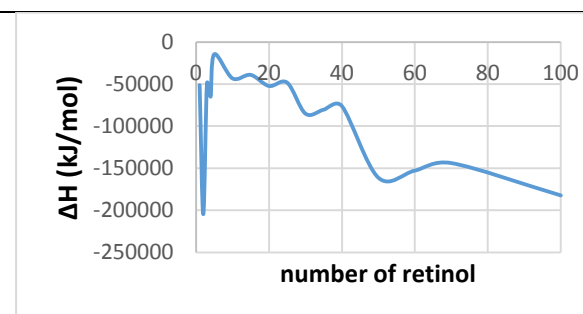


Figure 1

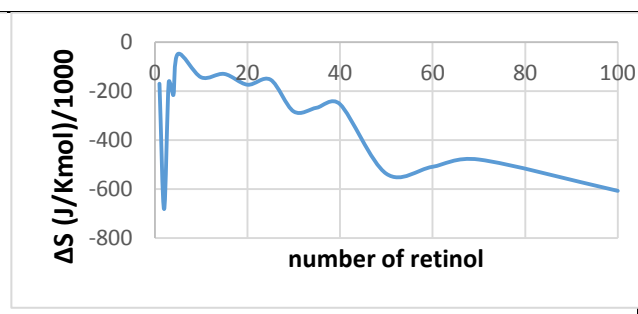


Figure 2

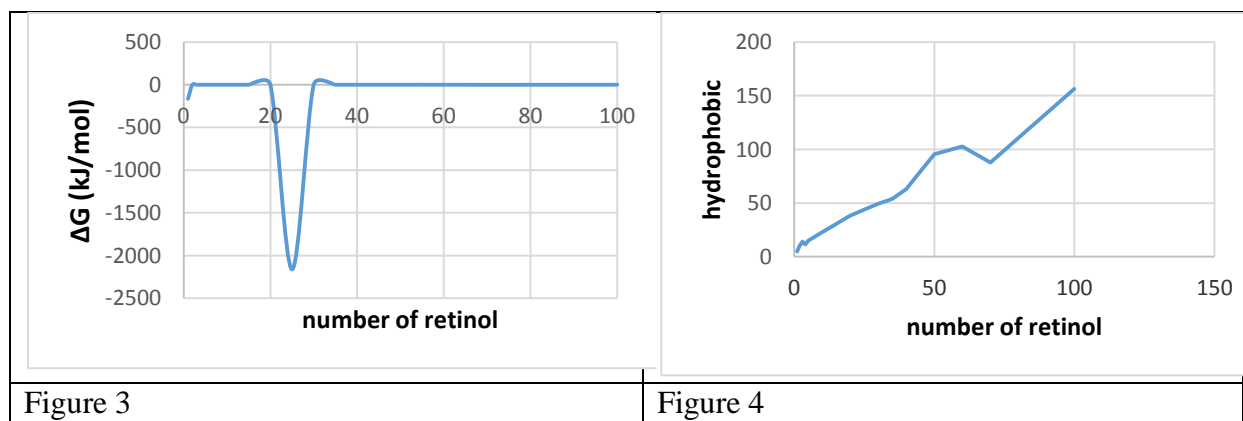
Results and discussion

Figure 1 shows the solvation enthalpy changes of retinol molecules versus the number of retinol molecules; which is negative in all numbers. Retinol has a hydroxyl group as polar head and a 20 carbon hydrophobic tail. Its solubility is very low in water solution [1]. Retinol solvation in water may be included contributions of hydration of the molecules and formation of molecular aggregation due to hydrophobic interactions. Hydration is only contribution in enthalpy changes for a single molecule solvation, whereas the contribution of formation of aggregation is added with increasing of the number of molecules. Considerable decreasing of enthalpy in the high number of molecules indicates that the hydrophobic contribution is dominant.

The changes of entropy versus number is shown in figure 2 which is negative at all numbers as enthalpy. The negative entropy means that the order is increased. It is may due to the formation of molecular aggregation as micell or other kinds of aggregations. However, entropy decreasing is unfavorable in the solvation process of retinol in water spontaneously.

The changes of Gibbs free energy versus the numbers is shown in figure 3. It is too slight at all numbers except at the number of 25 which it is showing a considerable decrease. The highly negative Gibbs free energy of the number 25 may due to start of the formation of new aggregated molecules. Enthalpy and entropy are in competition in the Gibbs free energy calculation. Despite the negative entropy, the negative enthalpy compensates its contribution and keep Gibbs free energy near to zero. However, both enthalpy and entropy are showing the formation of aggregated molecules.

Figure 4 shows the accessible hydrophobic surface area versus the number. It is increasing with the growth of the number which indicate that the aggregated particle have become bigger or more aggregations have been formed.



References:

- [1] Szuts E. Z., Harosi F. I. *Arshives Biochem. Biophys.* **1991**, 287, 297-304.
- [2] Bales B. L., Benrraous M., Zana R. *J. phys. Chem. B* **2002**, 106, 9033-9035.
- [3] <http://www.gromacs.org/>
- [4] <http://davapc1.bioch.dundee.ac.uk/cgi-bin/prodrg>

Investigation of the molecular interaction of platinum complex with Human Serum Albumin

M. M. Alavianmehr ^a, R. Yousefi ^b, Mohsen Golbon Haghighi ^c, A. Ashrafi ^{a*}

^a Department of Chemistry, Shiraz University of Technology, Shiraz 71555-313, Iran

^b Protein Chemistry Laboratory (PCL), Department of Biology, Shiraz University, Shiraz 71454, Iran

^c Department of Chemistry, Shahid Beheshti University, Evin, Tehran 19839-69411, Iran

(Email: ashrafiab@gmail.com)

Introduction: Plasma proteins play an important role in the transportation and deposition of substances such as fatty acids, hormones and medicinal drugs in the circulatory system. Therefore, it is important to reveal the interaction between drugs and proteins in the bloodstream, as it may affect the bioavailability, distribution and elimination of pharmaceutical or nutraceutical active compounds. Albumin is the main plasma protein, and its main function is to regulate colloidal osmotic pressure and transport substances in the bloodstream [1]. The interaction of human serum albumin with a wide range of chemically synthesized drugs used in medicine may influence their bioavailability and effectiveness [2].

Methods: The fluorescence spectra were recorded with a Cary-Eclipse spectrofluorimeter (Model Varian, Australia), equipped with an automatic temperature controller. In this study, quenching of Trp fluorescence was used to assess the interaction of Pt complex with HSA. To perform fluorescence titration experiment, a fixed concentration of HSA (3 μ M) was treated with different amounts of each Pt complex in the range 0–18 μ M (λ_{ex} = 295 nm, λ_{em} = 300–500 nm). Molecular dynamic simulation of HSA was performed by GROMACS 4.5.5 package. The molecular docking simulation of the Pt complexes into HSA was calculated by Molegro Virtual Docker (MVD) software. The chemical structure of Pt complex was optimized by Gaussian 09, using the B3LYP level of theory. The LANL2DZ basis set was chosen to describe Pt complex. Also, the 6–31G (d) basis set was applied for expressing the other atoms.

Results and Discussion: The present paper is devoted to studying the interaction of platinum complex with HSA by the means of fluorescence spectroscopy which are superior to conventional methods for drug protein interaction studies. Moreover, the thermodynamic parameters of binding of the Pt complex to HSA were analyzed by Stern-Volmer and van't Hoff equations. Such parameters help in studying the pharmacological response and designing dosage of drugs. Finally, a combination of molecular dynamics (MD) simulation and docking approaches were also applied to locate the Pt complex binding site on HSA. As can be observed in Figure 1, the addition of Pt complex (figure 2) has quenched HSA fluorescence in max intensity from 335 to 345 nm, implying the significant changes in the microenvironment of the fluorophore and the HSA conformation, by the polar solvent and the drug interaction. A Stern-Volmer equation, can help define the quenching mechanism according to following equation[3]:
$$\frac{F_0}{F} = 1 + k_q \tau_0 [Q] = 1 + K_{sv} [Q] \quad (1)$$

In this equation, F_0 and F represent the steady-state fluorescence intensities in the absence and presence of

quencher, respectively, $[Q]$ is the concentration of quencher which is Pt complex in this study, k_q is the quenching rate constant of biomolecule, and τ_0 is the average lifetime of the biomolecule without the quencher with a value of 10^{-8} s for HSA. As Table 1 shows, the K_{SV} values decrease with temperature. This behavior can be attributed to static quenching. Florescence quenching data for the interaction of Pt complex and HSA was also analyzed to obtain various binding parameters. The binding constant (K_A) and number of binding sites (n) were calculated according to the following [4]: $\log\left(\frac{F_0 - F}{F}\right) = n \log[Q] + \log K_A$ (2)

The number of binding sites (n) for the Pt complex are approximately unity. It means that one molecule of Pt complex binds to one molecule of HSA at 15, 30, and 37 °C. From the results given in Table 1, it can be deduced that by increasing the temperature, the values of binding constants decrease. The dependence of the thermodynamic parameters on temperature was examined to characterize the interaction between Pt complex and HSA. The main forces that exist between the Pt complex and ligands are hydrogen bonding, van der Waals force, electrostatic, and hydrophobic interactions. The thermodynamic parameters of enthalpy change (ΔH) and entropy change (ΔS) were determined using van't Hoff equation [5]: $\ln K = -\frac{\Delta H}{RT} + \frac{\Delta S}{R}$ (3)

The values of ΔH and ΔS were found to be -278 kJ/mol.lit and .798 kJ/mol.K, respectively. Also, the values of Gibbs free energy changes (ΔG) were retrieved from the following equation [6]: $\Delta G = -RT \ln K$ (4)

where R is the global gas constant. All the thermodynamic parameters are summarized in Table 1.

Conclusion: In this study, the interactions of platinum complex with HSA investigated by the means of fluorescence spectroscopy. The Pt complex quenches the fluorescence intensity of HSA through a dynamic mechanism. The results indicated that the main driving forces in Pt complex HSA interaction are van der Waals and hydrophobic interactions.

References

- [1] Li Y; He W.Y; Liu H; Yao X; Hu Z; *J. Mol. Struct.* **2007**, 831,144-150.
- [2] Varshney A; Sen P; Ahmad E; Rehan M; Subbarao N; Khan RH; *Chirality*, **2010**, 22, 77-87.
- [3] Wang Y.Q; Zhang H.-M; Zhang G.C; Tao W.-H., Tang , S.-H., *J. Mol. Struct*, **2007**, 830, 40–45.
- [4] Froehlich E; Mandeville J; Jennings. C; Sedaghat-Herati R; Tajmir-Riahi H; *J. Phys. Chem. B*, **2009**, 113, 6986–6993.
- [5] Hu Y.-J; Liu Y; Shen X.-S; Fang X.-Y; Qu S.-S, *J. Mol. Struct*, **2005**, 738, 143–147.
- [6] Ross P.D., Subramanian S, *Biochemistry*, 1981, 20, 3096–3102.

Table 1. Thermodynamics and Binding Parameters of the Pt Complex to HSA

T(K)	$K_B \times 10^4 (M^{-1})$	lnK	n	ΔH (kJ/mol)	ΔS (kJ/mol)	ΔG (kJ/mol)
288	3.27	20.2	1.703			-48.4
303	2.35	13.9	1.155	-0.278	0.798	-33.5
310	1.72	12.1	1.022			-28.9

Figure 1. Florescence intensity of binding of the Pt complex to human serum albumin.

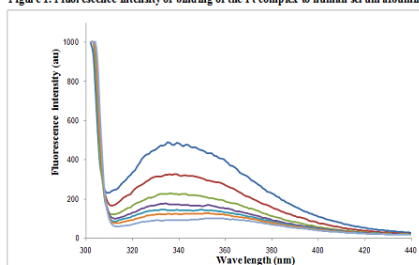
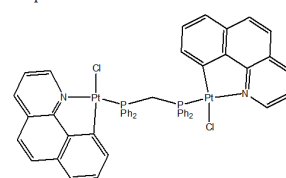


Fig. 2. Pt complex



Using of excitation-emission matrix fluorescence spectra combined with three-way chemometrics analysis to investigate the interaction of hemoglobin with pyrene and anthracene

S.Heidari^a, B.Hemmatinejad^{a,b,*}, S.Yousefinejad^a

^a Department of Chemistry, Shiraz University, Shiraz, Iran

^b Medicinal and Natural Products Chemistry Research Center, Shiraz University of Medical Sciences, Shiraz, Iran

E-mail: hemmatb@shirazu.ac.ir

Introduction: Hemoglobin (Hb), the major protein component of erythrocytes, is responsible for oxygen carrying from the lungs to respiring tissues. It is the major hemoprotein of redblood cells [1]. Heme is present in all cells, acting as a cofactor in essential metabolic pathways such as respiration and photosynthesis. Moreover, both heme and its degradation products have been ascribed important signaling roles [2]. Most of polycyclic aromatic hydrocarbons (PAHs) are considered to be environmental pollutants that can have a detrimental effect on the flora and fauna [3]. So, the effect of PAHs as biological contaminants on hemoglobin will be important.

Experimental: heme degradation study of Hb in presence of anthracene and pyrene were done by fluorescence spectroscopy. Fluorescence emission spectra were scanned from 380 nm to 500 nm by varying the Ex wavelength from 270 nm to 290 nm for Hb intrinsic fluorescence and from 305 nm to 335 nm for heme degradation product. Two cubes for titration of Hb with anthracene and pyrene were arranged in I×J×K three-way array. These three-way data sets were targeted by PARAFAC analysis.

Result and discussion: The results of analysis for determination of number of PARAFAC components indicate that three PARAFAC components are enough to well describe the modeled data, D.

Fluorescence study during titration of Hb with anthracene: Figure 1 shows Ex, Em and concentration profiles extracted from PARAFAC analysis of fluorescence data, gained from this titration. Concentration profile (Figure 1, C) indicates that the first factor (Hb spectrum) increases gradually which shows that Hb concentration fairly remains constant during titration and the second factor (anthracene spectrum) increases steadily by increasing anthracene concentration. The third factor has experienced an increase between the concentration of 0.0 and 2.0×10^{-6} M anthracene; however, in higher concentrations it has remained quite stable. This indicated that heme degradation product formed at anthracene concentrations of 2.0×10^{-6} M and higher.

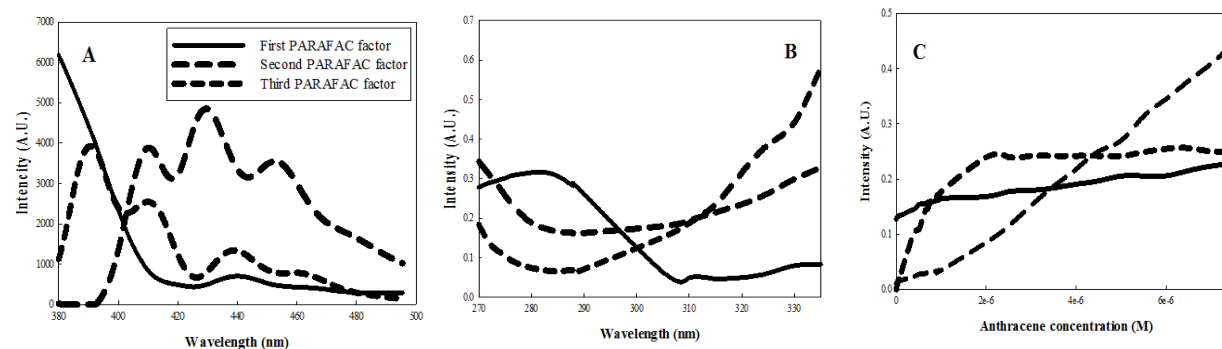


Figure 1 Em(A), Ex(B) and concentration (C) profiles gained from analysis of fluorescence data of titration of Hb with anthracene followed by PARAFAC analysis.

Fluorescence study during titration of Hb with pyrene: The resolved PARAFAC scores in three directions from analysis of fluorescence data of titration of Hb with pyrene are shown in Figure 2. In the case of contaminants with low concentration, intrinsic fluorescence peak of Hb didn't change, but formation of degradation products can be proved by their fluorescence intensity in the range of 380-600 nm.

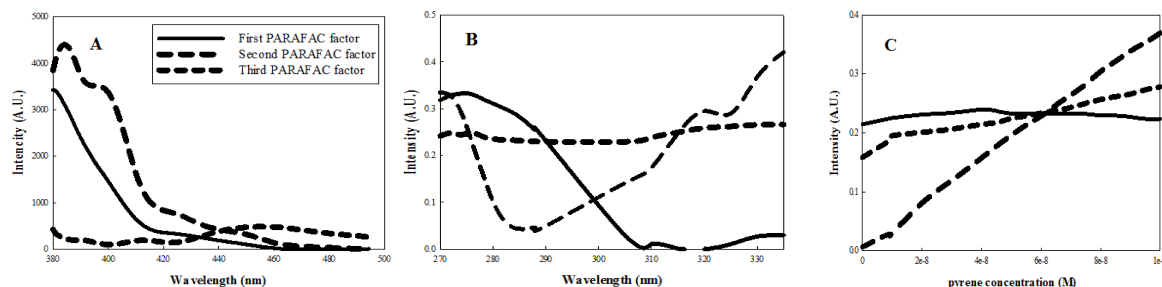


Figure 2 Ex(B), Em(A) and concentration(C) profiles gained from analysis of fluorescence data of titration of Hb with pyrene by PARAFAC analysis

Conclusion: Based on our experimental results, it was confirmed that the interactions between hemoglobin and poly aromatic hydrocarbons (anthracene and pyrene) leads to heme degradation. Because of high overlap in fluorescence spectra of poly aromatic hydrocarbons and hemoglobin, multivariate techniques can be useful. Using parallel factor analysis combined with fluorescence spectroscopy, helped in resolving component related to heme degradation product successfully.

References

- [1]. K. a Dill and H. S. Chan, *Nat. Struct. Biol.*, vol. 4, no. 1, pp. 10–19, 1997.
- [2]. L. J. Deterding, D. C. Ramirez, J. R. Dubin, R. P. Mason, and K. B. Tomer, *J. Biol. Chem.* vol. 279, no. 12, pp. 11600–11607, 2004.
- [3]. K. Liu, W. Han, W.-P. Pan, and J. T. Riley, *J. Hazard. Mater.*, vol. 84, no. 2–3, pp. 175–188, Jun. 2001.

Investigation of the effects of the chemical composition of Lubricants on the value of their viscosity index using multivariate calibration methods

Samaneh Ehsani^a, Ahmad Mani-Varnosfaderani^{*a}, Yadollah Yamini, Hatam Amanzadeh^a

a Department of Chemistry, Tarbiat Modares University, Tehran, Iran

* Corresponding author, email: a.mani@modares.ac.ir

Introduction

Lubricants are appreciable technical products defined by their chemical structures and their physical properties [1]. They have several properties to fulfill including high boiling point, thermal stability, high resistance to oxidation and high viscosity index. Among these properties viscosity index is a critical parameter. Consequently, we have attempted to use analytical techniques such as FT-IR spectroscopy and gas chromatography to relate such an important property to some special wavelengths or peaks in chromatograms, respectively. In order to achieve this goal, several multivariate calibration techniques have been applied for relating the viscosity index of lubricant to their chemical compositions.

Methods / Experimental

In this study a few samples of lubricating motor oils were purchased from Behran Oil Company and they have been extracted by HS-SPME at 140 C° and analyzed by GC [2]. Furthermore, IR spectra of 7 samples of lubricants were collected. Each sample was replicated three times. MATLAB software was used for implementation of the multivariate calibration codes. The calculations were implemented on a desktop computer with 'Windows 7 Pro' as the operating system, Intel(R) Core(TM) core i5 CPU and 8GB of RAM memory. The Matlab functions for GA-MLR algorithm have been written in house by authors.

Results and Discussion

The obtained FT-IR spectra and chromatograms have been used in this work to make the independent variables for the modeling procedure. The values of the viscosity index of the motor oils have been used to make the dependent variable. As a preliminary screening procedure, multiple linear regression (MLR) has been used for relating independent variables (i.e instrumental signals) to viscosity index. The results of the MLR technique are summarized in Table 1 in terms of root mean square error (RMSE) and coefficient of determination (R^2). As can be seen in this Table, the results obtained by MLR are not satisfactory. This can be due to the multicollinearity problem or lack of informative independent variables. In order to check this hypothesis, different variable selection strategies including stepwise selection and genetic algorithm (GA) have been used to select the best set of the fitting independent variables. As can be seen

in this Table, the GA-MLR technique reasonably selects the best set of the fitting independent variables. The developed GA-MLR model has been validated using leave-one-out (LOO) strategy. The R^2 and RMSE values for LOO procedure are given in Table 1. Reasonable values of R^2_{LOO} and RMSE_{LOO} for GA-MLR model reveals its prediction power and robustness. The obtained results in this work suggest that, the lack of fit of the MLR models can be enhanced using a thorough variable selection technique. While stepwise-MLR does not yield a good fit, surprisingly, GA could accurately extracts the best set of fitting independent variables. Moreover, the results in this work suggest that, it is thoroughly possible to predict and model the values of the viscosity index of motor oils using FT-IR spectroscopy. Following the development of a robust model, it is possible to accurately determine which compound is responsible for increasing the value of viscosity index in motor oils using HS-SPME-GC strategy followed by mass spectrometry.

MLR		Stepwise-MLR*		GA-MLR	
R^2_{train}	$\text{RMSE}_{\text{train}}$	R^2_{train}	$\text{RMSE}_{\text{train}}$	R^2_{train}	$\text{RMSE}_{\text{train}}$
0.0303	411.4209	-----	----	0.93	6.52
R^2_{LOO}	RMSE_{LOO}	R^2_{LOO}	RMSE_{LOO}	R^2_{LOO}	RMSE_{LOO}
0.0061	2.388	-----	-----	0.80	11.03

* The stepwise algorithm does not select even a variable for modeling the viscosity index.

Conclusion

In this work MLR model was developed and tested based on FT-IR spectroscopy of various samples of Lubricating motor oils and GA-MLR conducted over the FT-IR spectra showed satisfactory results. Therefore this fast, low-cost, and non-destructive FT-IR GA-MLR method opens a new possibility for determining spectral wavelengths which are responsible for corresponding viscosity index of a given lubricant [3].

References

- [1] Georg Kreisberger; Markus Himmelsbach ; Wolfgang Buchberger. Journal of Chromatography A, 2015, 1383, 169-174.
- [2] Dianne M. Levermore ; Mira Josowicz ; William S. Rees. Anal.Chem. 2001, 73, 1361-1365.
- [3] Leticia Maria de Souza; Hery Mitsutake; Lucas Caixeta Gontijo. Fuel, 2014, 130, 257-262.

Triplet States Properties of Short-Lived Red Phosphorescent Cationic Ir(III) Complexes Investigated from 1.5 K to 300 K

Mahboubeh Jamshidi^a, Rafal Czerwieniec^{b*}, Marion Graf^c, Hartmut Yersin^{b*}

^a Department of Chemistry, College of Sciences, Shiraz University, Shiraz 71467-13565, Iran

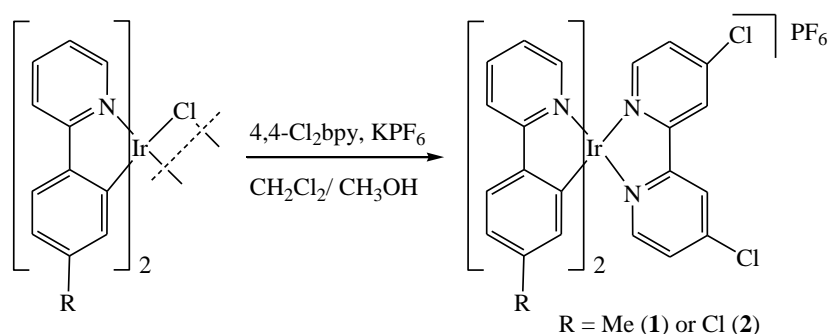
^b Institute of Physical Chemistry, University of Regensburg, Regensburg 93053, Germany

^c Department of Chemistry, Ludwig Maximilian University of Munich, Munich 81377, Germany

hartmut.yersin@ur.de rafal.czerwieniec@ur.de

Introduction: Ir(III) complexes as triplet emitters have been extensively investigated in electroluminescence devices (OLED and LEEC) due to their photo and thermal stabilities, color tuning abilities, and short emission decay times [1-3]. Investigation down to cryogenic temperatures makes it possible to study the triplet T_1 state in detail. It usually splits into three substates. Their individual properties determine the decay behavior crucially. In particular, the amount of splitting, the zero-field splitting (ZFS), is correlated to the metal participation in the T_1 state and thus, to the effectiveness of SOC that determines the substates' radiative decay times [4].

Methods: We describe detailed photophysical properties of two bis-cyclometalated compounds (Scheme 1) in PMMA films by measuring the temperature dependence of the emission spectra and decay time in the range from 1.5 to 298 K.



Scheme 1. Preparation of the Ir(III) complexes **1** and **2**.

Results and Discussion: The emission spectra are broad and the emission decay is approximately mono-exponential in the whole temperature range (Figure 1a). Accordingly, fast thermal equilibration occurs between the three triplet substates. Thus, the population is governed by a Boltzmann distribution. In Figure 1b, the emission decay time of complex **2** is plotted versus temperature. One observes a plateau between 1.5 and ≈ 6 K. This refers to the decay time

of the lowest T_1 substate I amounting to $\tau(I) = 142 \mu\text{s}$. With increasing temperature, the decay time decreases and reaches $\tau = 3.7 \mu\text{s}$ at $T = 77 \text{ K}$. The decay data from 1.5 K to 77 K can be fitted by a three-level Boltzmann-type equation [4]. The results are summarized in Figure 1c for both compounds.

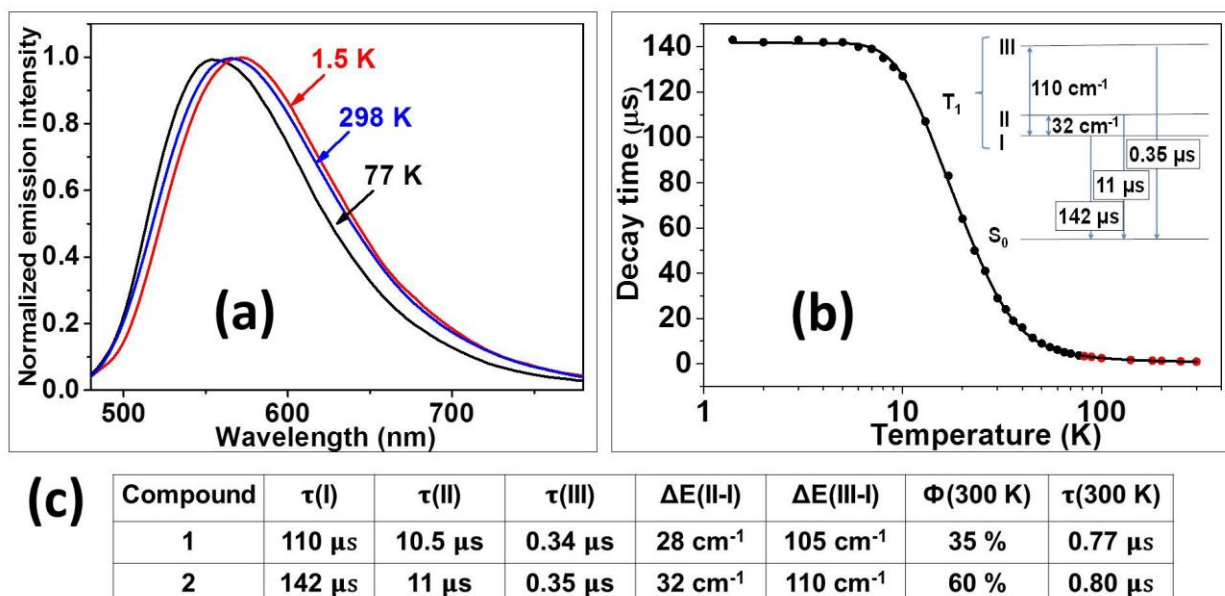


Figure 1. (a) Normalized emission spectra of **2** at different temperatures in PMMA. (b) Emission decay time of **2** versus temperature measured after pulsed excitation at $\lambda_{\text{exc}} = 378 \text{ nm}$ and detected at $\lambda_{\text{det}} = 569 \text{ nm}$. Inset: Energy level diagram for the three triplet substates, I, II, and III. (c) Properties of the triplet T_1 substates for **1** and **2**.

Conclusion: According to the large energy splitting of the emitting triplet state into substates, we classify this state as being dominantly of $^3\text{MLCT}$ character. The large ZFS is induced by very efficient SOC of the Iridium metal center. This crucially influences the emission decay time – apart from non-radiative processes.

References

- [1] H. Yersin. Ed., Highly efficient OLEDs with phosphorescent materials, *Wiley-VCH*, **2008**.
- [2] R. D. Costa; E. Ortí; D. Tordera; A. Pertegás; H. J. Bolink; S. Graber; C. E. Housecroft; L. Sachno; M. Neuburger; E. C. Constable. *Adv. Energy Mater* **1**, **2011**, 2, 282-290.
- [3] C. D. Ertl; L. Gil-Escrig; J. Cerdá; A. Pertegás; H. J. Bolink; J. M. Junquera-Hernández; A. Prescimone; M. Neuburger; E. C. Constable; E. Ortí. *Dalt. Trans.*, **2016**, 45, 11668-11681.
- [4] H. Yersin; A. F. Rausch; R. Czerwieniec; T. Hofbeck; T. Fischer. *Coord. Chem. Rev.*, **2011**, 255(21), 2622-2652..

Sensitivity enhancement of carbon monoxide gas sensor using palladium-doped tin oxide

Mahshad Sotoudehnavan^{a,b}, Mahdi Behzad^{a*}, Hamideh Samari Jahromi^b

^a Department of Chemistry, Semnan university, Semnan, Iran

^b Institute for Environmental Research and Biotechnology, RIPI, Tehran, Iran

Email: mbehzad@semnan.ac.ir

Introduction: Metal oxide nanostructures are of extensive interest for expansion of gas sensors [1,2]. Recently through the high level research it has been observed that sensing properties at working temperature, selectivity, and thermal stability can be greatly enhanced by controllable preparation with proper doping of metals [3-9]. Pd doping is constantly measured and evaluated by effectual method to improve the sensitivity and decrease the operating temperature. $\text{Pd}(1-x)\text{SnO}_2$ with various mol% nanoparticles were successfully synthesized by hydrothermal method and the 0.20% Pd-doped sample shows the maximum response to CO [10]. Carbon monoxide (CO) is a colorless, odorless, and tasteless but highly toxic gas. Exposure to a low concentration of approximately 35 ppm can cause headache and dizziness, whereas exposure to a higher concentration can result in convulsion, respiratory arrest, and even death. The current trend for CO sensor development is to increase sensitivity and reduce response time, as well as lowering the detection limit [11].

In this present work, synthesize and characterized Pd-SnO₂ nanoparticles by hydrothermal method to enhance CO gas-sensing performance at different temperatures and various concentrations with ultrafast response-recovery time, high responsivity, good stability, and reproducibility.

Methods/Experimentals: 0.2% Pd-doped SnO₂ nanoparticles have been synthesized by hydrothermal method. The amount of SnCl₄.5H₂O dissolving in 50 ml DI water (1).

The amount of PdCl₂ dissolving in 15 ml DI water with addition of amount of HCl drop wise (2).

Then, (2) has dissolved drop wise to (1) under constant stirring at 70 °C for 90 min.

After that sufficient amount of aqueous ammonia has added to the above solution as reducing agent till the formation of perfect gel.

The gel is transferred to teflon lined stainless steel autoclave and heating treatment of synthesized nanoparticles were conducted at 100 °C for 24 h.

The gel is filtered and washed with DI water, dried at 80 °C for 6 h.

Finally, annealing at 400 °C for 5 h.

Results and Discussion: The detailed characterization of Pd-doped SnO₂ was carried out using XRD, SEM with EDX and gas sensing analyzer. X-ray diffraction (XRD) spectrum of Pd-doped SnO₂ as shown in Fig. 1

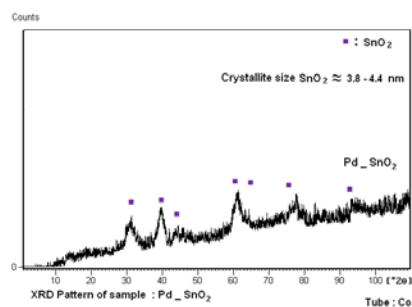


Fig 1. XRD spectrum of 0.2% Pd-doped SnO₂

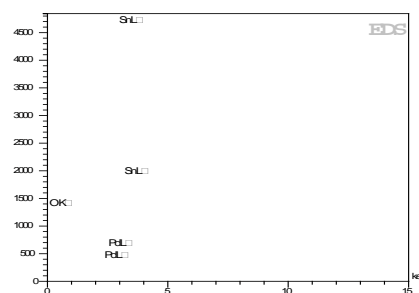


Fig 2. EDS image of 0.2% Pd-doped SnO₂

The surface morphology and elemental composition were observed by Scanning Electron Microscope (SEM) and EDS. The compositions of Pd-doped SnO₂ were examined by EDS as shown in Fig. 2. The SEM images of Pd-doped SnO₂ are shown in given Fig 3.

The observation obtained from SEM analysis also supports the XRD results and confirms the transition, crystalline state to the amorphous state for higher Pd concentrations and the EDS shows spectrum of 0.20% Pd doped SnO₂ nanoparticles.

The results showed that the prepared materials had very small, homogeneously distributed, spherical, and extremely crystalline nanoparticles and the particle sizes were in the range of 3.8-4.4 nm.

The sensitivity of palladium-doped tin oxide nanoparticles, at different temperatures(150-350 °C) and various concentrations of carbon monoxide gas (5,35,75,100 ppm) were investigated.

0.2% palladium-doped tin oxide exhibited the highest sensitivity and the best response to carbon monoxide at concentration of 35 ppm at 200 °C shown in Fig 4.

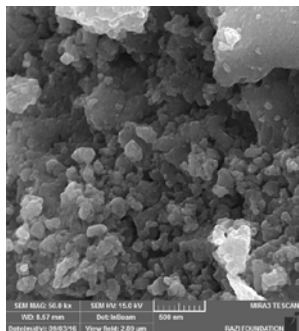


Fig 3. SEM Images of 0.2% Pd-doped SnO₂

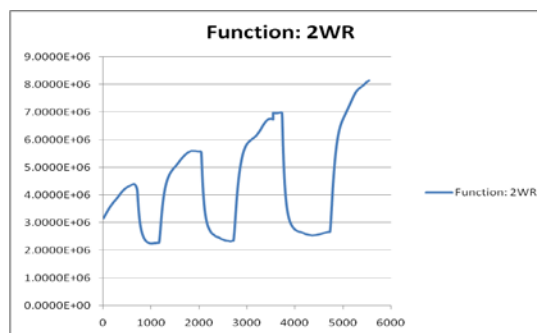


Fig 4.CO gas sensing

Conclusion:

The Pd-doped SnO₂ nanoparticles synthesized by hydrothermal method are found to have tetragonal rutile structure with crystallite sizes in range of 3.8-4.4 nm.

The SEM images of nanoparticles confirms the existence of very small, homogeneously distributed.

The 0.20% Pd-doped SnO₂ shows the maximum response to CO at concentration of 35 ppm at 200 °C.

The important point was the high lifetime of this sensor which was stable for about eight months.

References:

- [1] X. Chen; P. Li, H. Tong; T. Kako. Technol. Adv. Mater. 12 (2011) 044604.
- [2] B.H. Kim; S.Y. Oh; H.Y. Yu. Technol. Adv. Mater. 11 (2010) 065003.
- [3] S.H. Hahn; N. Barsan; U. Weimar. Sens. Actuators B 78 (2001) 64-68.
- [4] R. Janmanee; P. Pirakitikulr; N. Wetchakun. C. Phanichphant, Adv. Mater. Res. 55_57 (2008) 777-780.
- [5] M. Kwoka; L. Ottaviano; M. Passacantando. Sci. 254 (2008) 8089-8092.
- [6] P. Hanys; P. Janecek; V. Matolin. Sci. 600(2006) 4233-4238.
- [7] Shu-rong Wang; Ying-qiang Zhao; Jing Huang. Sci. 253 (2007) 3057-3061.
- [8] Yi-si Feng; Ri-sheng Yao; Li-de Zhang. Chem. Phys. 89 (2005) 311-314.
- [9] N.S. Ramgir; I.S. Mulla; K.P. Vijaymohan. Sens. Actuators B 107 (2005) 708-715.
- [10] Davender Singh; Virender Singh Kundu; A.S. Maan. Journal of Molecular Structure, 1100 (2015) 562-569
- [11] Do Dang Trung; Nguyen Duc Hoa; Pham Van Tong. Journal of Hazardous Materials 265 (2014) 124– 132

Column chromatography separation method or reaction medium

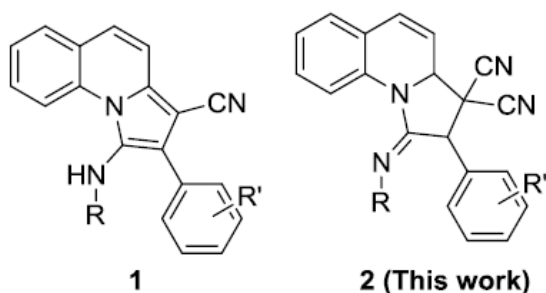
Seyed Ali Jehbez^a and Hamidreza Safaei^{b,*}

^a*Young Researchers and Elite Club, Shiraz Branch, Islamic Azad University, Shiraz, Iran*

^b*Department of Chemistry, Shiraz Branch, Islamic Azad University, Shiraz, Iran*

E-mail address: hrsafaei@yahoo.com

Introduction: The adduct formation was obtained from the reaction between quinoline and acetylenedicarboxylate by Huisgen in [1]. This pioneering work of Huisgen, impressive advances have been made in the synthesis of five and six membered heterocycles. In recent years, Nair and his coworkers envisaged that 1,4 zwitterionic intermediates generated in situ from quinoline or isoquinoline, and DMAD could be trapped by dipolarophiles [2] to produce six member rings. Recently, the reaction between aldehydes, malonitrile, isocyanide and quinoline in the presence of TiO_2 was reported and led to form Heterocycles **1**[3]. The HCN molecule was eliminated during column chromatography. As part of an ongoing development of efficient protocols for the preparation of biologically active heterocycles [4], here in, a new and efficient one-pot multi-component approach for the synthesis of novel Highly Substituted cyano heterocycles **2** is described. We believe that with passing the column chromatography the elimination of HCN was not occurred.

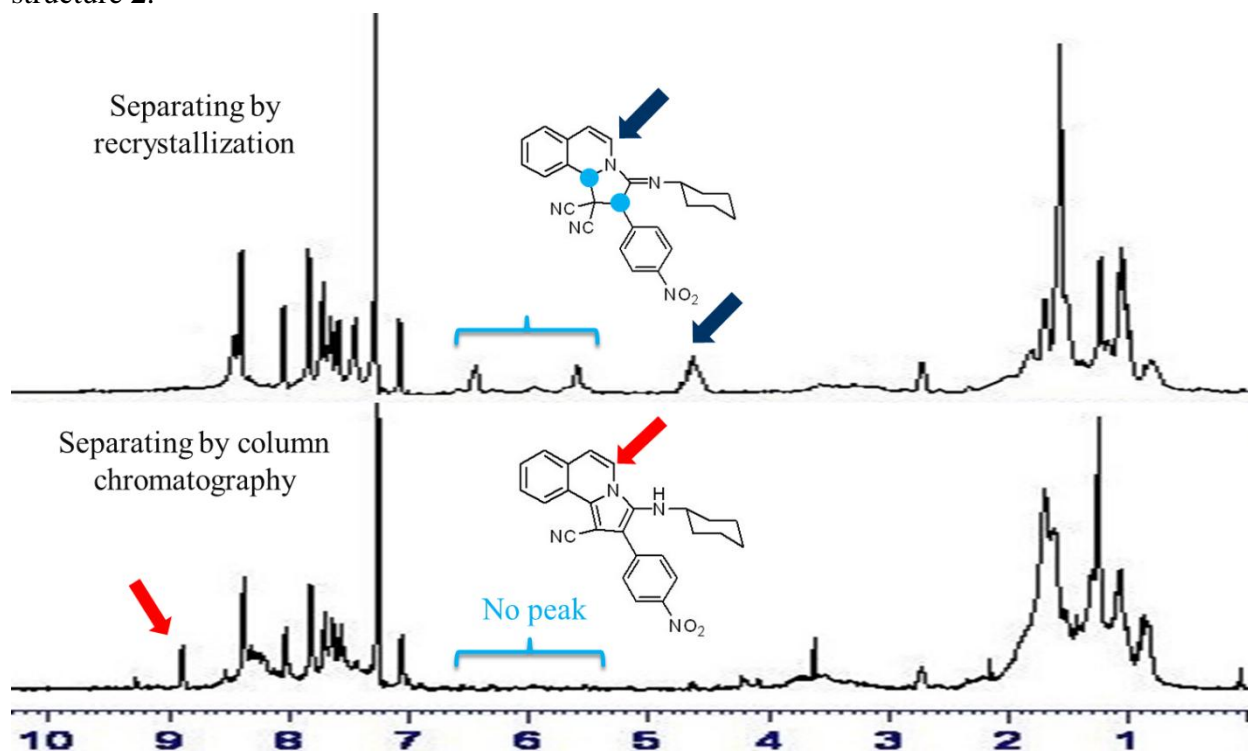


The structures of the products **2** were deduced from their elemental analyses and IR, ^1H and ^{13}C NMR spectra. The mass spectra of these compounds displayed molecular ion peaks at the appropriate m/z values.

Experimental: To a magnetically stirred solution of 2-benzylidenemalononitrile derivatives (1 mmol), isoquinoline (1 mmol) and isocyanides (1 mmol) in benzene (2 ml) as solvent under catalyst free conditions and 80°C . The reaction mixture was stirred for 3h. After completion of the reaction the solvent was evaporated under reduced pressure and to the residue was added a mixture of EtOH/ H_2O ether (5 ml, 1:1) which was added to precipitate a solid product.

Results and Discussion: Surprisingly, when column chromatography was used the compound **2** was not obtained. Instead, a color product was isolated with a ^1H NMR resonance at δ (H) 8.9 corresponding to a C-H moiety related to C_3 of quinolone. It is shown that this hydrogen is exposed to anisotropic effect of contains nitrogen quinolone ring due to aromatization. This

aromatization was occurred by HCN elimination in column chromatography. To establish the crucial role of column chromatography as mediator for the synthesis of **1**, the reaction was examined without column chromatography under optimized conditions and crystallization was used for purification. It was found that only compound **2** obtained as product. The ^1H NMR spectrum of the product exhibited three distinct signals at δ (H) 4.3 – 6.5 fully supporting the structure **2**.



Conclusion: Introducing highly efficient, catalyst free and green methods for synthesis of novel highly substituted cyano heterocyclic compounds. To the best of our knowledge for the first time we reported new approaches to column chromatography techniques that showed that Column chromatography plays an indispensable role in the elimination of HCN and formation of **1**. This will open the door for scientists either in chemistry, pharmaceutical fields to care about this matter in their synthetic protocols and find new applications for it.

References

- [1] R. Huisgen, M. Morikawa, K. Herbig, E. Brunn, *Chem. Ber.* 1967, 100, 1094.
- [2] V. Nair, S. Devipriya, E. Suresh, *Tetrahedron* 2008, 64, 3567.
- [3] M. T. Maghsoodlou, N. Hazeri, K. Khandan-Barani, S. M. Habibi-Khorasani, A. Abedi, *J. Heterocyclic Chem.*, 2014, 51, 152.
- [4] J. A. Gladysz, H. R. Safaei, S. Nouri, *Helv. Chim. Acta*; 2014, 97, 1539.

Synthesis and characterization of N',N^3 -dibenzylmalonamide and its complexes with Cu (II) salts

Seyyede Mina Hosseini, Mohammad Reza Iravani-Mohammad Abadi *, Abbas Rahmati

Department of Chemistry, University of Isfahan, Isfahan 81746-73441, Iran

Email address: m.r.iravani@sci.ui.ac.ir

Introduction: N,N' -Malonamide derivatives are privileged structures for their biological activity [1]. They are attractive compounds for drug discovery that exhibit a wide range of biological and pharmaceutical activities such as anti-inflammatories and anti-tumor [2]. From the coordination chemistry point of view, malonamides are interesting ligands, as they are expected to exhibit interesting ligating possibilities in several ways [3]. The presence of the $-CH_2-$ group between the two amide functions increases the size of the chelate rings that can be formed [4]. The above considerations prompted us to begin a systematic study of the coordination chemistry of malonamides.

Experimental:

N',N^3 -dibenzylmalonamide (LH_2) was synthesis by using a derivative of Malonic acid and benzyl amine at room temperature. Fine crystals appeared after several days, and then recrystallized with cold ethanol. Then, the hot methanolic solution of malonamide was added to Copper (II) salt in methanol, the mixture was heated with stirring for a few minutes. From the resulting blue-solution (pH approximately 8–9) filtered and cooled at room temperature, blue crystals appeared after several days.

Results and Discussion:

We optimized condition of reactions such as temperature, pH, solvents and molar-ratio for synthesis of ligands and complexes. The formation of metal complex with neutral malonamide is feasible only in solvent mixtures containing a large concentration of non-polar solvents. The rationale for this behavior originates in the weak donor strength of the neutral amide groups. The reaction between copper (II) salts and neutral malonamide is molar-ratio dependent. A final point of interest is the fact that on complexing with copper (II) in strongly alkaline media, the amide protons of LH_2 become extremely labile.

In order to ensure the proper synthesis of ligands and complexes, diffuse reflectance FT-IR spectra (FT-IR) in the range of $400-4000\text{ cm}^{-1}$ and diffuse reflectance ^1H NMR spectra, CHNS and atomic absorbance were employed. The following spectral data indicate the metal-ligand interaction.

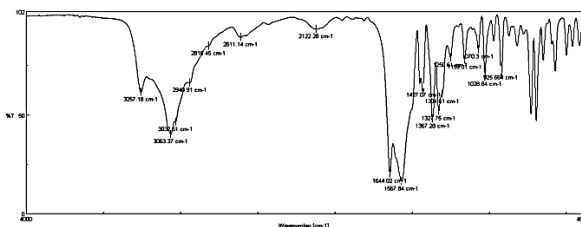


Fig.1 ligand spectrum

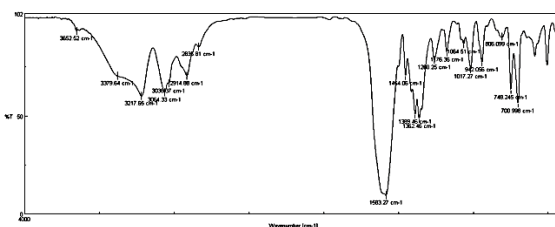


Fig.2 spectra of the copper complex

Conclusion:

In this study, We have developed a general and efficient method for the synthesis of novel N^1,N^3 -dibenzylmalonamide and other malonamidic ligands in excellent yield by using a derivative of Malonic acid at ambient temperature. Then, we studied interaction between these valuable ligands with Cu (II) and synthesized complexes. As these complexes involve Cu (II) in structures, they can be used in various fields such as biology and catalytic activities.

References:

- [1] Islam, M. S.; Barakat, A.; Al-Majid, A. M.; Ghabbour, H. A.; Rahman, A. M.; Javaid, K.; Choudhary, M. I. *Bioorg. Med. Chem.* **2016**, *24*, 1675-1682.
- [2] Rahmati, A.; *Tetrahedron Letters*, **2010**, *51*, 2967-2970.
- [3] Rodríguez-Martín, Y.; Luis, P. A. L.; Ruiz-Pérez, C. *Inorg. Chim. Acta*, **2002**, *328*, 169-178.
- [4] Raman, N.; Sakthivel, A.; Jeyamurugan, R. J. *Coord. Chem.* **2009**, *62*, 3969-3985.

Alternative way for antioxidant activity forecasting of plants according to their ATR-FT-IR fingerprints

Parisa Izadiyan^{a,d}, Bahram Hemmateenejad^{a,b,*}, Mahsa Izadiyan^c, S. Mohsen Taghavi^c

^aMedicinal and Natural Products Chemistry Research Center, Shiraz University of Medical Sciences, Shiraz, Iran

^bDepartment of Chemistry, Shiraz University, Shiraz, Iran

^cDepartment of Plant Protection, College of Agriculture, Shiraz University, Shiraz, Iran

^dStudent Research Committee, Shiraz University of Medical Sciences, Shiraz, Iran

*hemmatb@sums.ac.ir

Introduction:

Traditional medicine has been applying *Thymus* plants for many centuries. Within the *Lamiaceae* family, *Thymus* is one of the eight most important genera regarding the number of species included [1]. According to Flora Iranica [1], there are 17 *Thymus* species grown wild in Iran. *Thymus* species are currently used as culinary herbs, as well as for ornamental, aromatizing and traditional medicinal purposes in Iran country. However, herbal material can show considerable variability. The chemical constituents and their amounts in a herb can be different, due to growing conditions, such as climate and soil, the drying process, the harvest season, etc. Therefore, the quality control of herbal medicines is indispensable. FT-IR fingerprinting [2] has been recommended as a potential and reliable methodology for the identification and quality control of herbal medicines. In this study, antioxidant activity of 22 *Thymus* plant samples including 6 different species was assessed by DPPH antioxidant assay [3] and their chemical contents were also depicted by ATR-FT-IR fingerprinting.

Experimental: Fingerprints were recorded in the range of 400–4000 cm^{-1} and with a 4- cm^{-1} interval of spectral resolution (Figure 1). The correlation of the antioxidant activities (expressed as IC_{50} ($\mu\text{g/ml}$)) with the fingerprint data was investigated with different chemometrics modeling methods to find the most effective FT-IR region responsible for the antioxidant activities. The model was generated from FT-IR spectra data. The FT-IR spectra data was considered as the X variable, and the DPPH antioxidant activity measured as IC_{50} represented Y variable. Amongst the evaluated modeling methods, a PLS model with a 6 latent variables appeared to be the best model with the R squared of 0.8 and RMSE of 0.2.

Results and Discussion: Large PLS-regression coefficient reveals that a variable may be important for the modeling of Y. By inspection into the PLS results, it was revealed that two ranges of 1000-1500 and 2000-2500 are the most influencing regions that play a key role for modeling of the antioxidant activity. The first part is a sub-part of the fingerprint region (400-1500 cm^{-1}) in FT-IR spectra which help to discriminate different samples based on their antioxidant activity.

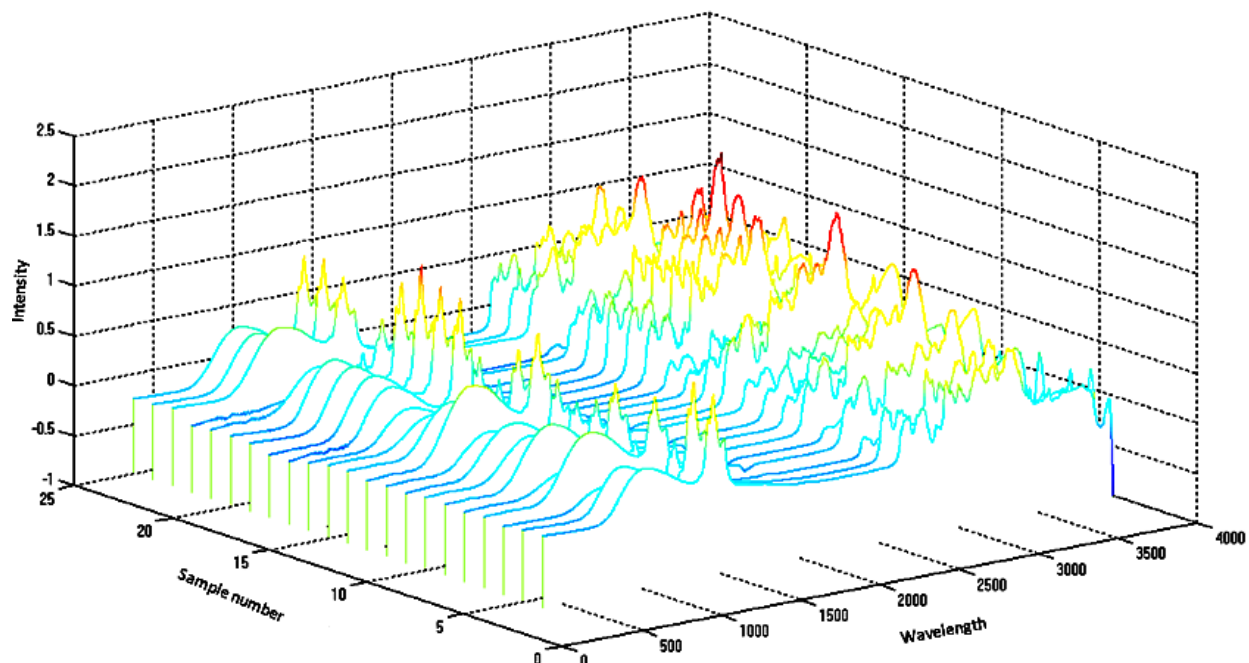


Figure 1. Overlay of ATR-FT-IR spectra of analyzed samples.

Conclusion: The constructed model could be used as an alternative to antioxidant assays where feasible. Moreover, ccombinatorial use of fingerprinting with IR and data mining with chemometrics could be considered as a useful selection method for the early quality evaluation of the *Thymus* species. Such methods could be replaced instead of expensive analysis methods such as HPLC or GC-MS chromatographic techniques. Further investigations with more samples are in progress to improve the modeling accuracy.

References

- [1] Elisabeth Stahl-Biskup; Francisco Saez. Thyme: the genus *Thymus*, *CRC Press*, **2003**.
- [2] Hans Krüger; Hartwig Schulz. *Stewart Postharvest Review*, **2007**, 3 , 1-12.
- [3] Om P. Sharma; Tej K. Bhat. *Food Chemistry*, **2009**, 113, 1202-1205.

Elucidation of the bioactive compounds of *Salvia officinalis* based on its chemical profile

Parisa Izadiyan^{a,d}, Bahram Hemmateenejad^{a,b*}

^a Medicinal and Natural Products Chemistry Research Center, Shiraz University of Medical Sciences, Shiraz, Iran

^b Department of Chemistry, Shiraz University, Shiraz, Iran

^d Student Research Committee, Shiraz University of Medical Sciences, Shiraz, Iran

***hemmath@sums.ac.ir**

Introduction: Sage Herb (*Salvia Officinalis*) is a culinary medicinal plant with the longest histories of use from ancient Egypt to present era. Sage had been reported to show some promising effects in clinical studies. Besides its reputation for curing typhoid fever and liver complaints, it is considered as a rich source of natural antioxidants and phenolic compounds [1]. Here with the application of chemometrics algorithms [2] we tried to correlate the chemical profile of sage to its antioxidant activity and total phenolic content.

Experimentals: Twenty sage herbs from different parts of Iran were collected in varied seasons based on their availability. The aerial parts were air dried and powdered by a grinder instrument. Total phenolic content (TPC) of the methanolic extracts were determined colorimetrically using Folin-Ciocalteu method [3]. TPC in extracts was expressed in terms of gallic acid equivalent (mg GA/g extract). Values were expressed as the corresponding dry weight of plant extract. All measurements were replicated three times. Antioxidant activities were also measured by DPPH antioxidant assay. Percentage inhibition was calculated and IC₅₀ values were estimated from the % inhibition versus concentration plot, using a regression algorithm. Chromatographic profiles were recorded in the range of 190–400 nm with a HPLC instrument equipped with a PDA detector (Figure 1).

Results and Discussion: The obtained values for antioxidant activity examined with DPPH radical are in the range of 17.08 to 138.46 µg/ml. The relation between antioxidant activity, TPC and HPLC-PDA chromatographic data was evaluated with PLS, PCR and ECVA chemometric methods. Amongst the evaluated modeling methods for antioxidant activity, PLS model with a 4 latent variables and PCR with 6 PCs appeared to be the best model with the R squared of 0.91 and 0.8 and also RMSE of 0.2 and 0.26, respectively. However, TPC values modeling results were not as significant as those of antioxidant activity. According to the regression results, several compounds were identified to be responsible for antioxidant activity of the analyzed sage samples. Further investigations such as LC-MS analysis are in progress for identification of the marked compounds (Figure 1).

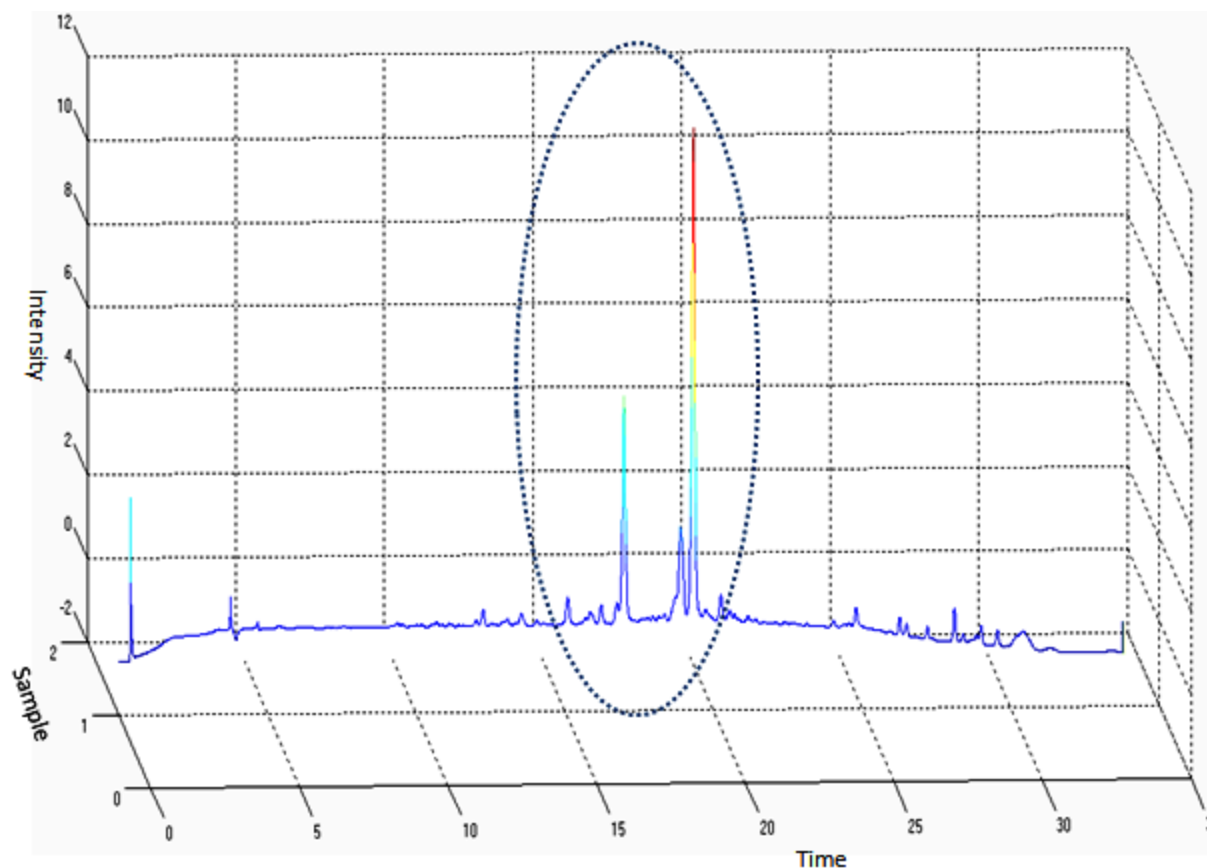


Figure 1. Chromatogram of chemical composition of *Salvia officinalis*

Conclusion: Investigation of different plant extracts from sage (*Lamiaceae*) showed high concentration of total phenols and antioxidant compounds. Phenols are very important plant constituents because of their scavenging ability on free radicals due to their hydroxyl groups. This study also confirmed that simultaneous use of chemical profiling and chemometrics is a useful and rapid method for quality control of medicinal plants and is worth being applied for standardization in food industries.

References

- [1] M.H.H. Roby; M.A. Sarhan; K.A.-H. Selim; K.I. Khalel. *Industrial Crops and Products*, **2013**, 43, 827-831.
- [2] B.K. Lavine; J. Workman. *Analytical chemistry*. **2012**, 85, 705-714.
- [3] M. Khanavi; M. Hajimahmoodi; M. Cheraghi-Niroomand; Z. Kargar; Y. Ajani; A. Hadjiakhoondi; M.R. Oreisi. *African Journal of Biotechnology*. **2009**, 8, 1143-47

Silane-Modified Bone Particles/PHBV Nanocomposites: An Efficient Tool for Enhanced Bone Regeneration

Mehdi Sadat-Shojai*, [Hassanali Moghaddas](#)

Department of Chemistry, College of Sciences, Shiraz University, Shiraz, Iran

* Email address: ms.shojai@shirazu.ac.ir

Introduction

Polyhydroxyalkanoates (PHAs) with their beneficial characteristics have been introduced as structural scaffolds for treatment of non-healing bone defects [1,2]. However, PHAs lack an effective osteoconductivity and a sufficient strength, failing to create a suitable scaffold for tissue regeneration [3]. Therefore, with the aim of improving the filler-matrix interface and bioactivity of the scaffolds, this study was tried to fabricate new fibrous architectures based on a model PHA in conjugation with nanoscopic crystals treated with organic silane modifiers. As the fabricated constructs have a close similarity to the natural fibrillar microstructures, they can be a promising candidate for bone regeneration applications.

Experimental

In brief, calcium phosphate (CaP) nanoparticles which were synthesized according to an optimized procedure [4] were modified using propyltrimethoxysilane diluted with toluene under refluxing conditions. After the grafting process, modified nanoparticles were separated from the reaction mixture and washed to remove the physically adsorbed silanes. A solution/dispersion of the modified nanoparticles and poly(3-hydroxybutyrate-co-3-hydroxyvalerate) (PHBV) in 1,1,1,3,3,3-Hexafluoro-2-propanol was then electrospun on a dynamic cylindrical collector at a rate of 2 mL/h, voltage of 25 kV and working distance of 15 cm.

Results and Discussion

In this study, CaP nanoparticles were synthesized and then modified with silane modifier to create a hybrid nanostructure with improved reinforcing properties. The chemical structure of the modified particles was characterized using Fourier transform infrared spectroscopy (FTIR) as shown in Fig.1.

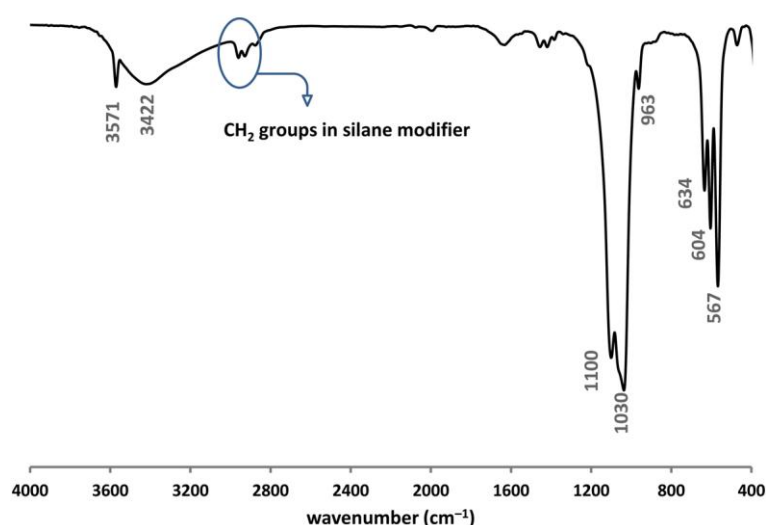


Fig. 1. FTIR spectrum of CaP nanoparticles after the grafting reaction.

According to Fig. 1, all characteristic IR bands corresponding to phosphate (1100, 1030, 963, 604, 567, and 471 cm^{-1}) and hydroxyl groups (3571 and 634 cm^{-1}) similar to bone minerals could be identified. The covalent bonding of silane molecules with nanoparticles was clearly confirmed by the characteristic peaks of CH_2 groups in the silane at the region of 2800–3000 cm^{-1} . In addition, morphological analysis by scanning electron microscopy (SEM) showed that the as-synthesized particles have nanoscopic dimensions with a uniform morphology (data not shown).

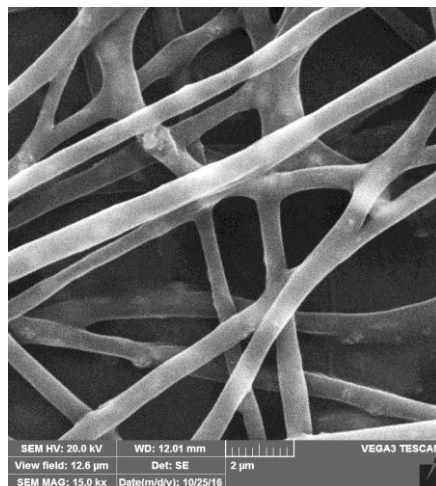


Fig. 2. Representative SEM micrograph of silane-modified nanoparticles/PHBV fibers.

As indicated by the representative SEM micrograph of Fig. 2, the as-synthesized silane-modified nanoparticles can be effectively conjugated with PHBV in the fibrous form while the fiber diameter is as small as 500 nm. These ultrafine fibers were bead-free with synergistic properties, and hence can provide opportunities to produce complex scaffolds for reconstruction of bone defects.

Conclusion

In conclusion, this study represented a successful attempt to fabricate porous PHBV nanocomposite in conjugation with silane-modified bone-like particles. It was found that ultrafine and bead-free fibers with a diameter less than 500 nm can be fabricated under the selected electrospinning conditions. Given the high structural similarity of the fabricated fibers with the natural extracellular matrix, they are expected to be a versatile candidate for orthopedic applications in the future.

References

- [1] K-hasuwan, P.-r.; Pavasant, P.; Supaphol, P. *Langmuir*, **2011**, 27, 10938–10946.
- [2] Chen, G.-Q.; Wu, Q. *Biomaterials*, **2005**, 26, 6565–6578.
- [3] Misra, S.K.; Nazhat, S.N.; Valappil, S.P.; Moshrefi-Torbati, M.; Wood, R.J.; Roy, I.; Boccaccini, A.R. *Biomacromolecules*, **2007**, 8, 2112–2119.
- [4] Sadat-Shojai, M.; Khorasani, M.-T.; Jamshidi, A.; Irani, S. *Mater. Sci. Eng. C*, **2013**, 33, 2776–2787.

Facile magnetization of metal–organic framework TMU-6 for magnetic solid-phase extraction of organophosphorus pesticides in water samples

Mehzrad Shakorian^a, Yadollah Yamini^{a*}, Meysam Safari^a

^a Department of Chemistry, Faculty of Sciences, Tarbiat Modares University, P.O. Box 14115-175, Tehran, Iran

E-mail: yyamini@modares.ac.ir (Y. Yamani).

Introduction: Organophosphorus pesticide compounds are being used in agriculture as substitutes for organochlorine and carbamate insecticides [1]. Chlorpyrifos, profenofos and phosalone are organophosphate chemicals commonly used as an insecticide. These pesticides are account for about 38% of the total pesticides used worldwide [2]. Therefore, the development of facile, recyclable and accurate methods for the determination of OP is highly desirable to report them.

MOF materials represent a tunable class of hybrid solid-state materials consisting of metal nodes or metal clusters coordinated to multifunctional organic linkers [3]. MOFs have been successfully explored as sorbents for sampling, solid-phase extraction, and solid-phase microextraction [4].

Methods/Experimental: According to the MSPE procedure, 2 mg of the sorbent were added to 25 mL of aqueous solution of organophosphorus. The mixture was stirred at 900 rpm for 30 min. Thereafter, the sorbent was collected from the resulting solution with an external magnet. The supernatant was decanted and adsorbed organophosphorus was eluted from the adsorbent surface with 100 μL of 1-butanol. Finally, 20 μL of the eluate was drawn out by a Hamilton syringe and directly injected into the HPLC-UV injection for analysis.

Results and discussion: Several factors affecting the extraction efficiency of the organophosphorus pesticide were optimized. The optimized experimental conditions were pH, 7; ionic strength, 0%; extraction time, 30 min; desorption time, 2 min; eluent type, 1-butanol; and amount of sorbent, 2 mg. Under the optimal conditions, Calibration curves were found to be linear in the range of 7.5-75 $\mu\text{g L}^{-1}$, 10-100 $\mu\text{g L}^{-1}$, and 10-150 $\mu\text{g L}^{-1}$ for phosalone, chlorpyrifos, and profenofos in water samples, respectively. The LODs, based on a signal-to-noise ratio (S/N) of 3, were 0.5, 2, and 0.5 $\mu\text{g L}^{-1}$ for phosalone, chlorpyrifos, and profenofos in water samples, respectively. The other figure of merit will be reported. The validated method was successfully applied for analysis of phosalone, chlorpyrifos, and profenofos in soil samples.

Conclusion: In the present study, a new sorbent of $\text{Fe}_3\text{O}_4\text{@TMU-6}$ MOF was synthesized and applied for MSPE of pesticides. The cage-like structure of the MOF can cause the fast and selective adsorption of OP. The mentioned MOF showed high tolerance to interferences from the matrix pesticide. The important features of the proposed method were its high adsorption capacity, good preconcentration factor, and low detection limit which is distinctive among other MSPE.

References:

- [1] M. Yadav, A. K. Shukla, N. Srivastva, S. N. Upadhyay and S. K. Dubey, *Critical reviews in biotechnology*, **2016**, 36, 727-742.
- [2] H. Zhang, C. Yang, Q. Zhao and C. Qiao, *Bioresource technology*, **2009**, 100, 3199-3204.

- [3] A. Cadiou, K. Adil, P. Bhatt, Y. Belmabkhout and M. Eddaoudi, *Science* **2016**, 353, 137-140.
- [4] E. Tahmasebi, M. Y. Masoomi, Y. Yamini and A. Morsali, *Inorganic Chemistry* **2015**, 54(2), 16863-16866 .

Trialkylamine/tetrabutylammonium bromide as a catalytic system for the highly efficient synthesis of alkyl 3-aryloxypropanoate

Farough Nasiri¹, Davood Malakutikhah²

¹Department of Applied Chemistry, Faculty of Science, University of Mohaghegh Ardabili, Po Box 56199-11367, Ardabil, Iran

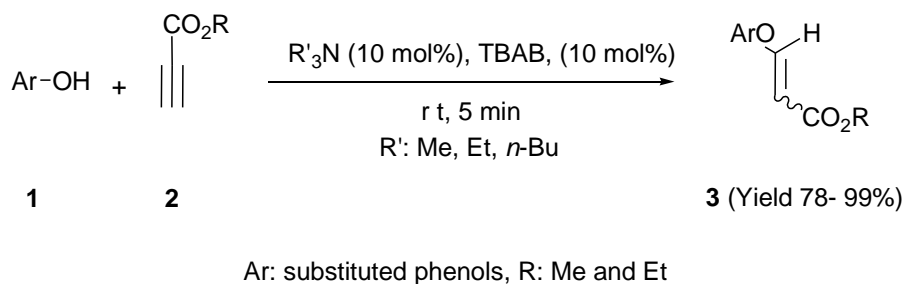
²Department of Chemistry, Faculty of Science, University of Kurdistan, Sanandaj, Iran

E-mail: nasiri@uma.ac.ir

Introduction: Vinyl ethers of phenols and alcohols are important intermediates in organic synthesis and several methods developed for the synthesis of these molecules [1, 2]. In the last two decades, the use of ionic liquids as solvent and catalyst has attracted much attention in organic synthesis and tetra-*n*-butylammonium bromide (TBAB) has been used as a very useful catalyst in various organic transformations. In continuation of our work on the reaction of phenols and electron deficient acetylenic esters [3, 4] in this work we wish to report nucleophilic conjugate addition of various substituted phenols to alkyl propiolates in the presence of a catalytic amount of TBAB and trialkylamines.

Experimental: To a stirred mixture of trimethylamine (0.025 g, 0.2 mmol), TBAB (0.06 g, 0.2 mmol), and phenol 0.19 g (2 mmol) was added drop wise 0.17 g of methyl propiolate (2 mmol) at room temperature. After 5 min, the reaction mixture was taken up in dichloromethane (15 mL) and the solution washed three times with water. The organic phase was dried and the solvent was removed, and the residue was separated by silica gel column chromatography using *n*-hexane-EtOAc as eluent.

Results and Discussion: The reaction of substituted phenols **1** with alkyl acetylenecarboxylates **2** in the presence of a catalytic amount of TBAB and trialkylamines such as trimethylamine, triethylamine, or tributylamine at room temperature leads to alkyl 3-aryloxypropanoate within 5 min. ¹H and ¹³C NMR spectra of the crude product clearly indicated the formation of two isomeric *E* and *Z* alkyl 3-phenoxy-2-propanoates **3** in good to excellent yields. The ratio of *E/Z* isomers were detected by ¹H NMR spectroscopy. The ¹H NMR spectral data of the products exhibited two isomers and both of them displayed characteristic resonance pattern with appropriate chemical shift.



The ^1H NMR spectrum of (*E*)-form isomers displayed two doublets with $^3J_{\text{HH}} = 12.3\text{-}12.5$ Hz for the two olefinic protons, while the chemical shift of the (*Z*)-forms appeared with $^3J_{\text{HH}} = 6.7\text{-}7.0$ Hz. It was in agreement with the proposed (*E*)- and (*Z*)-isomers, respectively. For example, the ^1H NMR spectrum of **3a** (Ar: Ph, R: Me) showed one single sharp line at 3.75 ppm for methoxy group and two doublets with $^3J_{\text{HH}} = 7.0$ Hz at 5.17 and 6.85 ppm for the olefinic protons in the (*Z*)-isomer and one singlet at 3.73 ppm for the methoxy group and two doublets with $^3J_{\text{HH}} = 12.3$ Hz at 5.56 and 7.81 ppm for the olefinic protons in the (*E*)-isomer.

Conclusion: In conclusion, we have described a convenient route to alkyl 3-phenoxypropanoates through nucleophilic addition of phenols to alkyl propiolates in the presence of a catalytic amount of TBAB and trialkylamine at room temperature within 5 min. The simplicity of the present procedure and high yields of products makes it an interesting alternative to other approaches.

References:

- [1] V. Potapov, M. Musalov, S. Amosova, E. Kurkutov, *Russ. J. Org. Chem.* **2011**, 47, 1594-1595.
- [2] C. Chen, R. F. Jordan, *J. Am. Chem. Soc.* **2010**, 132, 10254-10255.
- [3] I. Yavari, S. Sourì, M. Sirouspour, H. Djahaniani, F. Nasiri, *Synthesis*, **2005**, 11, 1761-1764.
- [4] F. Nasiri, B. Atashkar, *Monatsh. Chem.*, **2008**, 139, 1223-1227.
- [5] F. Nasiri, D. Malakutikhah, *Monatsh. Chem.*, 2011, 142, 807-812.

Synthesis and characterization of new chalcone complexes of Zinc and study of the interaction of this compound with DNA.

Mohammad Reza Iravani*, Hossein Loghmani, Neda Pakizehkar.

Faculty of Chemistry, University of Isfahan, Isfahan, Iran.

m.r.iravani@sci.ui.ac.ir

Introduction:

Chalcones are 1, 3-diphenyl-2-propene-1-on in which two aromatic rings are linked by a three carbon α , β - unsaturated carbonyl system or α , β -unsaturated ketones [1, 2]. Though structurally simple, they have displayed an impressive array of biological activities including antimalarial, anti-oxidant, antibacterial, antifungal, anti-inflammatory, cytotoxic and anticancer [3].

From the reaction between chalcones and metals, metal complexes obtained. Metal chelates of chalcones are effective anticancer, antitumor, anti-tuberculosis, antipyretic [4].

In this study, we have synthesized new derivative o chalcones, and then the synthesis of zinc complexes with this ligand. Then, we studied the biological properties of the product thus obtained.

Experimental:

The main method for the synthesis of chalcones is the classical Claisen-Schmidt condensation in the presence of aqueous alkaline bases. Therefore, based on this method, chalcone (1E,4E)-1,5-Bis(4-aminophenyl) penta-1,4-dien-3-one were synthesized from acetone and 4-nitrobenzaldehyde.

The substituted chalcones transition metal complex was derived from the reaction on ethanolic solution of metal salt. The chalcone ligand was reacted with zinc acetate and the transition metal-ligands 1:2 complex isolated in the solid state.

Results and Discussion:

The synthesized chalcone and its complex with zinc metal characterized by the FTIR and ^1H -NMR spectral techniques and elemental analysis. The newly chalcone ligand and its complex are stable at room temperature and pressure. The complex is insoluble in organic solvents such as methanol, ethanol while soluble in coordinating solvents such as DMSO.

The elemental analysis of zinc complex can be seen in the table below. The data indicate the formation of a complex with a molar ratio of 1:2 metals to ligand is given.

Predicted Molecular Formula: C ₃₄ H ₃₄ N ₄ O ₂ Zn				
Element	C	H	N	S
Theoretical Percent	68.51	5.75	2.40	---
Experimental Percent*	69.31	6.91	7.15	---
Standard Deviation (%)	0.01	0.02	0.05	---

*Average

FT-IR spectrum of zinc complex, different vibrations to show that coordinated ligand. The complex displayed IR peak at 1619.91 cm^{-1} and 619.038 cm^{-1} , assigned to coordinated $\nu(\text{CO})$ and $\nu(\text{Zn-O})$ vibration respectively. It showed that $\nu(\text{CO})$ vibration of free ligand 1627.63 cm^{-1} shifted to lower wavenumber owing to its coordination with Zn (II) metal center.

In recent years, the synthesis of drugs based on metal complexes with organic ligands drug and study their interaction with DNA in order to study their anticancer activity has found many applications in Pharmaceutical Sciences. In interaction drug combinations with the DNA, the structure and form of the compound are changes.

Conclusion:

We have synthesized a new complex of zinc with chalcone ligands. FT-IR and ^1H -NMR spectral data and elemental analysis results of this ligand with Zn (II) show that this complex is well prepared. Absorption spectra and fluorescence spectra data indicates that this chalcone complex has reacted well with DNA.

References:

- [1] Rajendran, M.; Thiruppathi, M. *J. Chem. Biophys. Sci.*, **2013**, 4, 38-52.
- [2] Patil, C. B.; Mahajan, S. K.; Katti, S. A. *J. Pharm. Sci. Res.* **2009**, 1, 11-22.
- [3] Aly, M. R. E. S.; Fodah, H. H. A. E. R.; Saleh, S. Y. *Eur. J. Med. Chem.*, **2014**, 76, 517-530.
- [4] Kumar, M. S.; Meenakshi, J. *J. Atoms and Molecules*, **2014**, 4, 726–733.

Molecular Dynamics Simulation of HSP90 Inhibitors Assembly at Water/Octanol Interface

Amin Reza Zolghadr*, Samaneh Boroomand

Department of Chemistry, Shiraz University, Shiraz 71946-84795, Iran

Email address: arzolghadr@shirazu.ac.ir

Introduction: Drug absorption at an acceptable dose depends on the pair of solubility and permeability. There are many potent therapeutics that are not active in vivo, presumably due to the lack of capability to cross the cell membrane. Molecular dynamics simulation of radicicol, diol-radicalol, cyclopropane-radicalol and 17-DMAG were performed at water/octanol interface to suggest interfacial activity as a physico-chemical characteristic of these heat shock protein 90 (HSP90) inhibitors. We have observed that orally active HSP90 inhibitors form aggregates at the water/octanol and DPPC-lipid/water interfaces by starting from an initial configuration with HSP90 inhibitors embedded in the water matrix.

Methods: We have used DL_POLY package for MD simulations of octanol/HSP90 inhibitors/water systems [1]. The force field is in the form of explicit flexible all-atom force field. The intramolecular and vdW potential energies of octanol and drug molecules were obtained from the General Amber Force Field (GAFF) [2]. 24 HSP90 inhibitors were added to both sides of octanol slab surface. 1500 water molecules were added randomly to fill the box.

Results and Discussion: The density of water molecules is almost vanishing in the octanol phase, followed by a steep rise to the bulk value (see Fig. 1). Fig. 1A clearly shows that radicicol molecules in the interfacial region are located mainly in the octanol side of the interface. Interestingly, Figs. 1B and 1C show that a significant amount of diol-radicalol and cyclopropane-radicalol penetrates in the octanol phase, while only a small amount is transferred into the interfacial region. Fig. 1D shows that the interfacial density of 17-DMAG increases substantially in comparison to what was observed for the densities of radicicol and its analogous while the initial amount of these HSP90 inhibitors were the same. This implies that 17-DMAG tends to be similarly partitioned between octanol and water at the octanol/water interface. Therefore, active

HSP90 inhibitors form an interfacial layer at the water/octanol interface by starting from an initial ensemble with HSP90 inhibitors inserted in the aqueous phase. In other words, as simulation progressed the inhibitor molecules very quickly aggregated and migrated toward the octanol phase and reached the interface within 1 ns. Our results show that the aggregated molecules equilibrated at octanol side of the interface within 6 ns, and remain there until the end of the simulation (24 ns). The corresponding snapshots of initial and final configurations of octanol/17-DMAG/water system are shown in Fig. 2, respectively. Fig. 2B illustrate that the location of the assembled 17-DMAG molecules remains in the vicinity of the water/octanol interface after 24 ns.

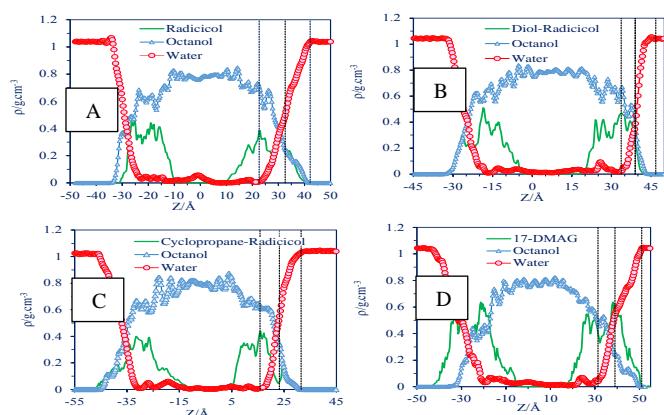


Fig. 1 The total density profiles of (A) octanol/radicol/water, (B) octanol/diol-radicol/water, (C) octanol/cyclopropane-radicol/water, and (D) octanol/17-DMAG/water, systems.

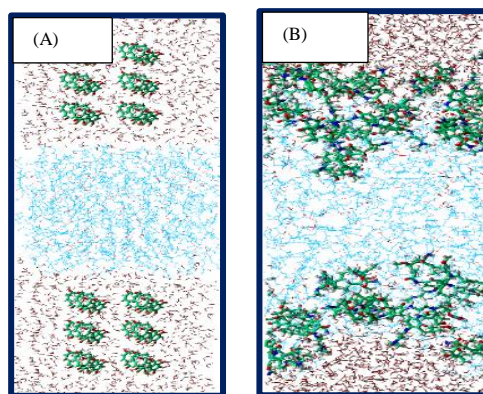


Fig. 2 Snapshots of the (A) initial configuration, and (B) the simulated 17-DMAG system after 6ns.

Conclusion: Molecular dynamics simulations of HSP90 inhibitors self-assembly at the water/octanol interface were carried out for various HSP90 inhibitors. The calculated density profiles showed that HSP90 inhibitors tend to aggregate at the liquid/liquid interface. 17-DMAG molecules are partitioned similarly between octanol and water phases while the radicol derivatives tend toward octanol phase. Our results revealed that this self-assembly is due to the hydrogen bonding interactions between inhibitor molecules and liquid phases. Interestingly, the compound with higher in vivo activity shows higher interfacial assembly.

References:

[1] Forester, T. R.; Smith, W. DLPOLY, CCP5 Program Library; Daresbury Lab.: U.K., **2001**.

[2] Wang, J.; Wolf, R. M.; Caldwell, J. W.; Kollman, P. A.; Case, D. A. *Journal of computational chemistry*, **2004**, 25, 1157-1174.

Ab Initio Study of the Intermolecular Potential Energy Surface for CO-O₂ System

Saeedeh Tashakor^{*}, Mohammad R. Noorbala, and Mansoor Namazian

Yazd University, Department of Chemistry

Email address: tashakor.s@gmail.com

Introduction: Carbon monoxide is not only hazardous and toxic, but also very flammable. It is produced from incomplete combustion due to lack of oxygen. It is produced on a large scale in industry, in combination with hydrogen, by reforming hydrocarbons, generally natural gas. It is used in large quantities to produce various intermediary organic chemicals, such as isocyanates, formic acid, acetic acids, and also certain polymers such as polycarbonates and polyketones. [1] Hence, there is a great interest in obtaining an accurate intermolecular interaction potential for modelling its structure and properties and in predicting its phase transitions.

Method: Dunning's correlation consistent basis sets (aug-cc-pVXZ, x=D,T) were used and basis set superposition error (BSSE) was corrected for all calculations using Boys and Bernardi's standard counterpoise (CP) method.[2] The interaction energy has been obtained by a supermolecular approach. Considering the supermolecular approach and counterpoise method the interaction energy between A and B molecules at a given level of theory is calculated by the following equation:

$$E_{\text{int}} = E_{\text{AB}} - E_{\text{A}} - E_{\text{B}} + \Delta E_{\text{BSSE}} \quad (1)$$

Where E_{int} is the corrected intermolecular potential energy, E_{AB} is the energy of the complex, E_{A} and E_{B} are the energies of the monomers A and B, respectively. ΔE_{BSSE} is the difference between corrected and uncorrected energies.

Results and Discussion: Incompleteness of basis set is one the source of error that limits the ultimate accuracy of the result. According to our knowledge, the best and the latest the CBS extrapolation scheme has been proposed by Okoshi et al. [3]. In this model for the DZ-level correlation energy, a factor s has been introduced to scale the cardinal number. The CBS limit correlation energy is given as follows:

$$E_{\text{CBS}}(s) = \frac{s^3 E_2 - 3^3 E_3}{s^3 - 3^3} \quad (2)$$

For each combination of the method and basis set, the optimal value of s has been determined. [3] We have shown the CBS limit obtained by this technique as OAN(C). As demonstrated in Figure . 1, with increasing the size of basis set from cc-pVDZ to OAN(C) basis set, the depth of the potential curve increases and the position of the minimum of curve shifts to a shorter intermolecular distance and also calculations better discover the attractive interaction. Therefore, the potential energy curves calculated by OAN(C) scheme predict the interaction energies better than the other basis sets in this figure.

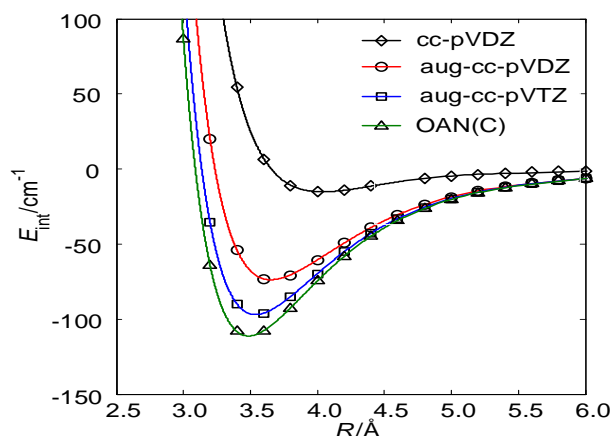


Figure 1. Calculated CCSD(T) interaction energies of CO-O₂ system using three different basis sets with changing the distance between two monomers.

Conclusions: It was demonstrated that the small basis sets such as aug-cc-pVDZ basis set leads to lower interaction energy, in comparison with those obtained using aug-cc-pVTZ especially at lower intermolecular distances. The latest extrapolation scheme was used to estimate the CBS limit. It is evident that the option OAN(C) basis set provides the best compromise between the accuracy and computational cost.

References:

- [1] M. Abbaspour; Goharshadi, E. K. *Chem Phys* **2006**, *330*, 313-325.
- [2] S. F. Boys; Bernardi, F. d. *Mol Phys* **1970**, *19*, 553-566.
- [3] 43. M. Okoshi; Atsumi, T.; Nakai, H. *J Comput Chem* **2015**, *36*, 1075-1082.

Catecholato Cobalt(III) Bis(phenolate) diamine Complexes as Models for Enzyme–substrate Adducts of Catechol dioxygenases

Yalda Sheybani pour^a, Elham Safaei^{a*}

^a *Department of Chemistry, College of Sciences, Shiraz University, Shiraz, 71454, Iran*

E-mail: e.safaei@shirazu.ac.ir

Introduction: Catechol dioxygenases are mononuclear non-heme metalloenzymes of soil bacteria which catalyze the oxidative cleavage of toxic environmental catechol substrates with concomitant insertion of molecular oxygen into their aromatic ring production of aliphatic acids. Catechol dioxygenases subdivided into two classes on the basis of the site of aromatic ring cleavage: The intradiol catechol dioxygenases, utilize mononuclear metal centers to catalyze the oxidative cleavage of the carbon–carbon bond between the two phenolic hydroxyl groups, while the extradiol-type enzymes, cleave the adjacent carbon-carbon bond [1-3]. Herein, synthesis and characterization of new mononuclear cobalt(III) complexes of di-amine bis(phenolate) H_2L^{NEX} and 3,5-di-tert-butylcatechol (3,5-DTBC) mixed ligands have been reported.

Method: Triethylamine was added to a solution of H_2L^{NEX} in methanol, and then $Co(OAc)_2$ was added under continuous stirring. After 30 minutes, a methanol solution of 3,5-DTBC and triethylamine was added to the reaction mixture. Reaction mixture was then stirred for 6 h at room temperature. Crystals suitable for X-ray diffraction were obtained by the slow evaporation of dichloromethane/methanol mixture.

Results: $CoL^{NEX}(3,5-DTBC)$ complexes were characterized by IR, UV-vis, X-ray, elemental analysis and magnetic measurements. X-ray structure analysis of complexes has revealed that the cobalt(III) core in the model compounds is a distorted octahedral coordination sphere and surrounded by two phenolate oxygen atoms, two amine nitrogens and two oxygen atoms of 3,5-DTBC (figure1). Magnetic measurement confirms the monomer character of complexes.

Conclusion: Some mononuclear cobalt(III) complexes of H_2L^{NEX} and 3,5-DTBC mixed ligands were synthesized as the enzyme/catechol adduct formation in oxygenative enzymic mechanisms.

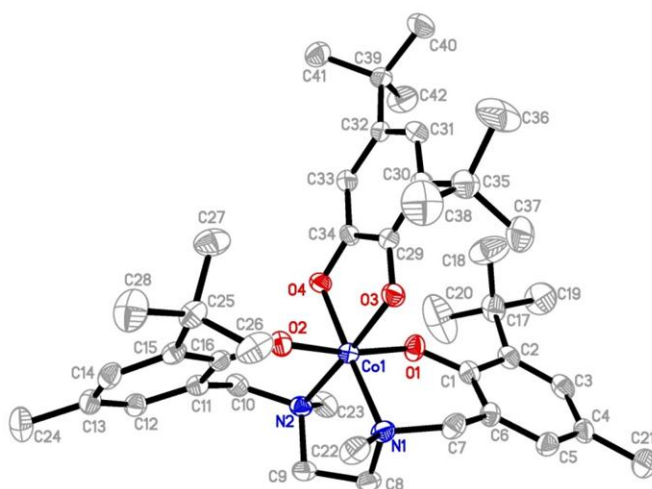


Figure1: Molecular structure of $\text{CoL}^{\text{NEBM}}(3,5\text{-DTBC})$

References:

1. Kurahashi, T; Kobayashi, Y; Nagatomo, S; Tosha, T; Kitagawa, T; Fujii, H. *Inorg.Chem*, **2005**, *44*, 8156-8166.
2. Hasan, K; Fowler, C; Kwong, P; Crane, A. K; Collins, J. L; Kozak, C. M. *Dalton. Trans*, **2008**, 2991-2998.
3. John, A; Shaikh, M. M; Butcher, R. J; Ghosh, P. *Dalton. Trans*, **2010**, *39*, 7353-7363.

Separation and determination trace amounts of glycyrrhizic acid with using UPLC

Zahra Afzali^{a, b *} Alireza Mohaddsi^c

^aDepartment of Chemistry, Payamenoor University, Tehran, Iran

^b Graduate University of Advanced Technology

zahra.afzali@yahoo.com

^c Department of Chemistry, Payamenoor University, Tehran, Iran

zahra.afzali@yahoo.com

Introduction:.

Glycyrrhizic acid is known to have anti-inflammatory, anti-viral, anti- allergic, antioxidant, gastro- protective, anti-ulcer anti – hepatotoxic and anti- cancerous properties. There are several methods, such as liquid–liquid extraction, membrane filtration, available in the literature for the enrichment and separation of it [1]. High performance liquid chromatography (HPLC) techniques are more economical and time efficient when derivatization of the sample is not required prior to analysis Due to good sensitivity and detection limit, HPLC is a very good choice for the glycyrrhizic acid quantification in different real samples [2].

Method:

In the present study, a fast, simple and sensitive vortex-assisted dispersive liquid–liquid microextraction method was developed for extraction and preconcentration of trace amounts of glycyrrhizic acid in Licorice root samples. The extraction conditions were optimized as extraction solvent, chloroform; volume of extracting, 200.0 μ L; and vortex time, 120 s. The high performance liquid chromatography (UPLC) was used to identify and quantitatively determine the amount of extract GA. The contents of Glycyrrhizic UHPLC under condition as follows: Diamonsil C18 (50mm \times 2mm) column , mobile phase: A:water-acetic acid 2%, B :acetonitrile, isocratic mode ,A:40% and B:60%;flow rate 0.2ml/min and detection wavelength of 280 nm.

Results and Discussion:

For VADLLME, a solution containing 500.0 ng glycyrrhizic acid and 400 μ L acetonitrile was adjusted to pH 7 and placed into a 10 mL screw tube. Then 200.0 μ L of chloroform (extracting solvent) was rapidly injected into the sample solution using syringe and vortex for 2 min glycyrrhizic acid was extracted into fine droplets of CHCl_3 from the resulting cloudy solution. The solution was centrifuged at 3000 rpm for 3 min. After removing the aqueous

phase, 10.0 μL of sediment phase was injected into UPLC column, and the analysis time, was 1.04 min per sample. The linear range of glycyrrhizic acid is 0.1-10.0 $\mu\text{g mL}^{-1}$, and, detection limit was 0.03 $\mu\text{g mL}^{-1}$

Conclusion:

This study presents a novel approach based on the VADLLME method coupled to UPLC for the determination of glycyrrhizic acid. The proposed method is a simple and rapid extraction technique with a large enrichment factors and low detection limit for glycyrrhizic acid determination. Influence variables such as pH, extraction solvent type and volume, salt addition, vortex and centrifuging time were optimized.

References

- [1] W. Shan, Y. Min , C. Xin , W. Qui- Rong , C. Jun. Chinese journal of natural medicine, **2015**, 13, 232-240.
- [2] Mohamad A. Shabkhiz, Mohamad H. Eikani, Zeinolabedin Bashiri Sadr , Fereshteh Golmohammad , Food Chemistry, **2016** , 210 , 396- 401

Metabolic Profiling of *Satureja khuzistanica* and as a new source of caffeice acid compounds

Mansoorreh Davoodi^{a*}, Samad Nejad Ebrahimi^b, Abdolhossein Rustaiyan^a

^aDepartment of Chemistry, Science & Research Branch, Islamic Azad University, P.O. Box 14515 775, Tehran, Iran.

^bDepartment of Phytochemistry, Medicinal Plants and Drugs research Institute, Shahid Beheshti University, Tehran, Iran

m_davoodi67@yahoo.com

Introduction: *Satureja* belong to family Labiate in Iran is collectively known as “Marze”. The genus *Satureja L.* contains over 30 species, distributed in the Mediterranean area, Middle East, and North Africa and central Asia. Fourteen species grow wild in the northern, western, and southern parts of Iran [1-3]. Except essential oil analysis the phytochemical profiling of *Satureja* are rarely studied. In continue of our project on phytochemical profiling of Iranian plants we investigated the methanolic extract of *Satureja khuzistanica* Jamzad.

Methods / Experimental: 800 g of dry leaves of plant material was ground and extracted by successive percolation with CH₂Cl₂, EtOAc and MeOH (3*5 L each). After evaporation to dryness under reduced pressure, 60 g of MeOH extract was obtained. The extract was dissolved in distilled water (1L). The aqueous solution was passed through HP-20 diaion resin to give 15.0 g polyphenol enriched material. The obtained material dissolved in 100 ml MeOH and after filtration subjected to gel chromatography on Sephadex LH-20 column. The major compounds of fraction was characterized by extensive chromatographic techniques using on-line HPLC-PDA-MSn, and off-line microprobe NMR.

Results and Discussion: The phytochemical analysis of methanolic extract of *S. khuzistanica* aerials part led us for identification of various secondary metabolites including flavonoids, monoterpene glycosides, and phenylpropanoids. The structure of isolated compounds elucidated using 1D and 2D NMR and high resolution MS spectrometry. Structure elucidation of **1-17** was achieved by a combination of 1D and 2D NMR, HRMS, and UV spectroscopy, and by comparison with published data. Compounds were identified as erigeroside (**1**), zataroside A (**2**), zataroside B (**3**), ponciretin (**4**), 5,6-dihydroxy-4',7-dimethoxyflavone (**5**), 5,6-dihydroxy-3',4',7-trimethoxyflavone (**6**), 3',4'-di-O-methyl-luteolin 7-β-neohesperidoside (**7**), linarin (**8**), acacetin 7-glucuronide (**9**), keshonin (**10**), rosmarinic acid (**11**), methyl rosmarinic acid (**12**), melitric acid A (**13**), methyl melitirinate (**14**), lycopic acid C (**15**), clinopodic acid (**16**), and diosmetin 7-rutinoside (**17**).

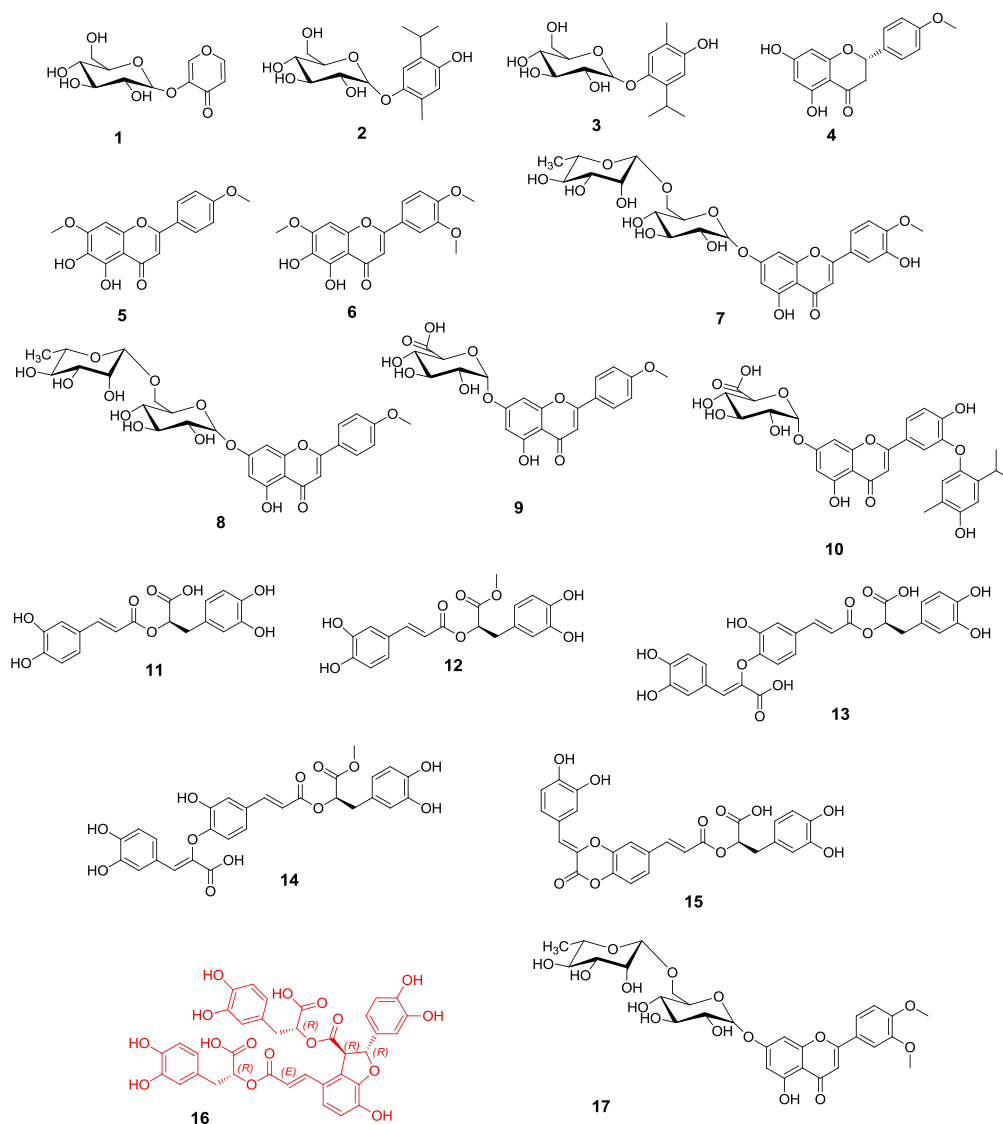


Figure 1: Structures of compounds 1-17

Conclusion: Considering the high prevalence of flavonoids and caffeic acid derivatives found in *S. khuzistanica* extract, this results introduce plant as rich source of polyphenols and this may explain some traditional therapeutic uses of this medicinal plant as antioxidant, anti-inflammatory as well as anti-diabetic agent.

References

- [1] Hadian, J., M. Hossein Mirjalili, M. Reza Kanani, A. Salehnia and P. Ganjipoor. Chemistry & biodiversity, 2011, 8(5): 902-915.
- [2] Mahboubi, M. and N. Kazempour , Journal de Mycologie Médicale / Journal of Medical Mycology 2016,26(1): e6-e10.
- [3] Moghaddam, F. M., M. M. Farimani, S. Salahvarzi and G. Amin , Evidence-Based Complementary and Alternative Medicine,2007, 4(1): 95-98)..

DNA biosensor paper for molecular detection of sickle cell disorder

Sevedeh Zohreh Azarshin^a, Hamid Galehdari^{a*}, Hooshang Parham^b, Mohammad Shafeei^a

^aDepartment of Genetics, College of Science, Shahid Chamran University, Ahvaz, Iran

^bDepartment of Chemistry, College of Science, Shahid Chamran University, Ahvaz, Iran

E-mail address: galehdari187@yahoo.com

Introduction:

Hemoglobinopathies are the most common inherited hemoglobin disorders around the world. Sickle cell state refers to the sickling changes in red cell shape. Patients with sickle cell show increased adhesiveness to the vascular endothelium, chronic hemolytic anemia, splenic sequestration crises and abdominal crises. It occurs by a point mutation in the HBB gene. At present, Most of clinical diagnostic methods are based on polymerase chain reaction (PCR) and agarose gel electrophoresis analysis. Therefore, due to the benefits of prenatal genetic screening, the use of sensitive, low cost, rapid methods for the clinical diagnostic is valuable [1, 2].

Methods:

The purpose of this study is developed method for Simultaneous detection wildtype and mutant genes in sickle cell patients. The technique is based on color changes and the naked eye detection upon enzymatic activity after hybridization target DNA with the Specific probes on nylon paper. The effect of important parameters, such as concentration of probe, Incubation time and temperature, type and volume of buffer were investigated and optimized.

Results and Discussion:

This method due to design specific probe, have high selectivity and no signal background, false positive and false negative signal. Under the optimum conditions, detection limit was 55 ng genome per sample. The method was successfully applied to diagnosis of sickle cell mutation in blood, amniotic fluid and Chorionic villus samples.

Conclusion:

This paper proposes fast and reliable diagnostic method for prenatal screening.

Keywords: DNA biosensor, sickle cell, enzymatic activity

[1] S. Noronh; S. Sadreamel; J. Strouse. *southern medical journal*, **2016**,109, 495-502

[2] G. Clarke; T. Higgins. *Clinical Chemistry*, **2000**, 46, 1284-1290

The Effect of Solvent on the stability of Nicotine - Carbon Nanotubes System Using Density Functional Study

Monir Teymoori Oghaz^{a*} and Ali Morsali^a

^a Department of Chemistry, Faculty of Science, Islamic Azad University, Mashhad Branch, Mashhad, Iran

*Corresponding author Email: Teymoori.mr@gmail.com

Introduction

The discovery of new carbon forms such as fullerenes, carbon nanotubes and graphene have brought a big interest of the scientific community because these materials exhibit remarkable properties with high potential to be applied in several technological areas [1]. In particular, carbon nanotubes (both multi-walled (MWCNT) and single walled (SWCNT)) are promising materials for several applications such as high performance composites [2], components in water filters [3], environmental sensors [4], drug delivers [5], among others. Cigarette smoke contains several toxic and carcinogenic compounds including various polycyclic aromatic hydrocarbons (collectively called tar), nicotine, among others [6]. Nicotine (Fig. 1), one of the hazardous compounds, is a major pharmacologically active component of tobacco smoke and is generally regarded as a primary risk factor in the development of cardiovascular disorders, pulmonary disease and lung cancer [7].

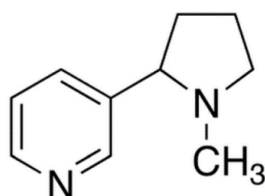


Fig. 1. The structure of nicotine

Through tobacco and others related compounds, nicotine is addictive drug used heavily by humans. Because of their psychoactive effects, nicotine could have positive effects. For example, nicotine appears to enhance concentration and memory due to the increase of acetylcholine [8]. The interaction between carbon nanotubes and some of these hazardous molecules is the subject of several experimental and theoretical studies in the literature [9]. The goal of this study is to investigate the interaction process of nicotine with the SWCNT surface and understand the influence of the nicotine position in the adsorption energy. Our calculations have been performed in both gas phase and the presence of solvent. Depending on the position of nicotine molecule in beside of carbon nanotubes the binding energy was different.

Computational Method

All calculations have been performed with the Gaussian 09 [10] program. It is well-known that DFT method [11] seems to be an excellent compromise between computational cost and accuracy of the computational results. It has been established that hybrid functional are generally accurate enough to describe the complexes involving strongly ionic hydrogen bonds [12]. Considering the wide existence of ionic hydrogen bonds in ILs, calculations carried out by using the Becke-three-parameter-Lee-Yang-Parr (B3LYP) functional with 6-31G** basis set for all atoms.

Results and Discussion

In the present study, five conformers are suggestion in the gas phase and five conformers in the solution phase (water), respectively. The conformers in the gas phase were named as G1, G2, G3, G4, and G5 and in the solution phase S1, S2, S3, S4, and S5. The BE between the nicotine and SWNT was calculated according to the following equation:

$$\Delta E = E_{conformer} - (E_{nicotine} + E_{SWNT})$$

where $E_{nicotine}$ and E_{SWNT} are the energies of the isolated molecules, respectively and $E_{conformer}$ is the energy of the nicotine-SWNT system. The ΔE for present conformers, are summarized in Table (1). Our

results show that in the gas phase, the present conformers are more stable than conformers in the solution phase. The obtained results were found to be in a reasonable agreement with those reported in the literature for SWNT complex drug delivery [13].

Table 1. Calculated the total binding energy (ΔE) of nicotine-SWNT system conformers, at B3LYP/6-31G** level.

Conformers	$E_{conformer}$	$E_{Nicotine}$	$E_{Nanotube}$	BE (H)*	BE	BE	*H=Ha rtree
					(kcal/mol)	(kj/mol)	
G1	-3927.390341	-498.995213	-3428.47056	0.0754	47.33	198.05	A mong other confor mers in the gas phase G4 is
G2	-3927.472249	-498.995213	-3428.47056	-0.0065	-4.06	-17.00	
G3	-3927.471650	-498.995213	-3428.47056	-0.0059	-3.69	-15.43	
G4	-3927.472316	-498.995213	-3428.47056	-0.0065	-4.11	-17.18	
G5	-3927.472123	-498.995213	-3428.47056	-0.0063	-3.98	-16.67	
S1	-3927.472283	-499.001086	-3428.47009	-0.0011	-0.69	-2.88	
S2	-3927.472249	-499.001086	-3428.47009	-0.0010	-0.67	-2.81	
S3	-3927.471650	-499.001086	-3428.47009	-0.0005	-0.28	-1.24	
S4	-3927.472316	-499.001086	-3428.47009	-0.0012	-0.71	-2.98	
S5	-3927.472123	-499.001086	-3428.47009	-0.0009	-0.59	-2.48	

most stable conformer. The optimized structures of the most stable conformer, G4 and S4, are represented in Fig. 2.

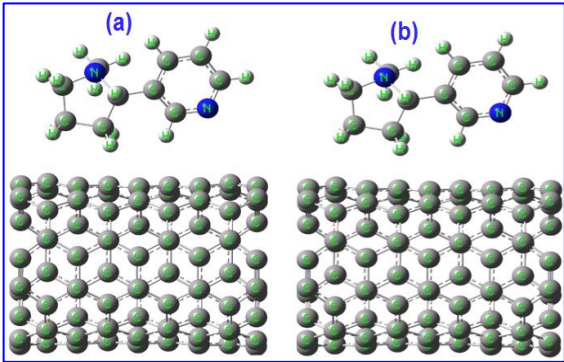


Fig. 2. Optimized geometries of the a) most stable conformer of nicotine-SWNT system in the gas phase, and b) most stable conformer of nicotine-SWNT system in the solution phase.

The position of nicotine and SWNT in G4 conformer leads formation of more interactions between the two fragments, so that this conformer is most stable. Also, in the solution phase the S4 is the most stable than others conformers. According to this tables, the relative stabilities among the ten conformers changed base the following order:

$$G4 > G2 > G5 > G3 > S4 > S1 > S2 > S5 > S\ 3> G1$$

According this order, the G1 and G4 conformers has the most unstable and most stable among all given conformers, respectively.

Conclusion

In this investigation, the interaction of nicotine and single wall carbon nanotubes using quantum mechanics, have been studied. All of the calculations have been performed using a hybrid density functional method (B3LYP) in gas and solution phases. The stability of nicotine-SWNT system were examined by binding energy. It was found that binding of nicotine and SWNT in gas phase is thermodynamically favorable.

References

[1] A. Jorio, M.S. Dresselhaus, G. Dresselhaus, Springer-Verlag, Berlin, 2008.
 [2] R.H. Baughman, A.A. Zakhidov, W.A. de Heer, Science 297 (2002) 787–792.
 [3] M.S. Mauter, M. Elimelech, Environmental Science & Technology 42 (2008) 5843–5859.
 [4] C. Hierold, A. Jungen, C. Stampfer, T. Helbling, Sensors and Actuators A: Physical 136 (2007) 51–61.
 [5]N.W.S.Kam, M.OConnell,J.A.Wisdom,H.J.Dai,Proceedings of the National Academy of Sciences of the United States of America 102 (2005)11600–11605.
 [6] Y. Xu, J.H. Zhu, L.L. Ma, J.A. An, Y.L. Wei, X.Y. Shang, Microporous and Mesoporous Materials 60 (2003) 125–138.
 [7] N.L. Benowitz, N. Engl. J. Med. 319 (1988) 1318–1330.
 [8] J. Rusted, L. Graupner, N. O’Connell, C. Nicholls, Psychopharmacology 115 (1994) 547.
 [9] F. Tournus, J.C. Charlier, Physical Review B 71 (2005) 165421.

- [10] G.W.T. M.J. Frisch et al., Gaussian Inc, Wallingford, CT, (2009).
- [11] M.C.H. W. Koch, A Chemist's Guide to Density Functional Theory, Wiley-VCH, 2000.
- [12] A. Milet, T. Korona, R. Moszynski, E. Kochanski, Journal of Chemical Physics, 111 (1999) 7727.
- [13] A. Mansoorinasab, A. Morsali, M. M. Heravi, and S. A. Beyramabadi, J. Comput. Theor. Nanosci. 12, 4935 (2015).

Fluorometric and Colorimetric Determination of Sulfide ion based on quenching effect of Copper (II) Sulfate on the Copper Nanocluster

Z.Shojaeifard^a, B.Hemmateenejd^{a,*}, M.Shamsipur^b, R.Ahmadi^a

^a Department of Chemistry, Shiraz University, Shiraz, Iran

^b Department of Chemistry, Razi University, Kermanshah, Iran

hemmatb@shirazu.ac.ir (B. Hemmateenejad)

Introduction: Sulfide is a widely existent pollutant with harmful influence on aquatic ecosystems and human health [1]. Due to the high toxicity of these species, developing a simple, cost-effective, sensitive, and selective method for monitoring total sulfide in water samples has drawn considerable attention among scientific community [2]. Among various analytical methods [1,3], fluorometric and colorimetric methods as an appealing technique have been selected for determination of sulfide. In this work, this technique was used for determination of sulfide by a turn off fluorescent property of tannic acid capped CuNCs (TA-CuNCs) in the presence of copper ion (Cu^{2+}) and sulfide.

Experimental: TA-CuNCs were synthesized as described elsewhere with minor modification [4]. The typical detection measurements were carried out as follows. 200 μL of TA-CuNCs from its stock solution was diluted to 2 mL using Tris-HCl buffered solution (0.15 M, pH 7.5). The suitable volume of Cu^{2+} ion stock solutions (20 μL of 0.2 M) was added gradually to generate the metal-ion-mediated TA-CuNCs fluorescence probes. The excitation wavelength was fixed at 360 nm and emission spectra were collected from 350 to 600 nm.

Results and Discussion: In the presence of sulfide ion, the fluorescence of TA-CuNCs/ Cu^{2+} probe significantly quenched based on the inner filter effect (IFE) of the produced CuS particles, while, sulfide ion itself cause only a slight change in the fluorescence intensity of TA-CuNCs. This probe allowed detection of sulfide over the range of 0.7-10.0 μM and 10.0- 80.0 μM with a detection limit of 0.1 μM .

CuS formation is associated with the distinct color changes from Cu^{2+} with blue color to CuS with brown species. Accordingly, CuS formation leading variation of visible color of TA-CuNCs/ Cu^{2+} sensor from blue to brown by increasing concentration of sulfide ion. Owing to the advantages of colorimetric and naked eye detection of analytes [5], color

variations of TA-CuNCs/Cu²⁺ solution in the presence of sulfide ion was used for colorimetric sulfide determination. A calibration graph was created by plotting (RGB₀ – RGB) values versus concentration of sulfide as shown in Figure 1 (RGB₀ belongs to RGB of TA-CuNCs/Cu²⁺ in the absence of sulfide ion). It was found that color changes versus sulfide concentration was linear in the range of 6–130 µM with a limit of detection of 2.0 µM that is lower than the reported permitted value by WHO.

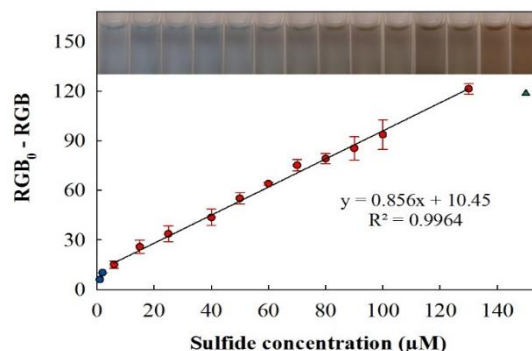


Figure1 Plot of change in the color of the TA-CuNCs/Cu²⁺ as a function of sulfide ion concentrations. RGB₀- RGB variations show the changes in the probe colors in the absence and presence of different concentrations of sulfide anion, respectively. (Inset: Changes in visible colors of the probe upon exposure to different concentrations of sulfide in Tris-HCl buffer solution (0.15 M pH 7.5).)

Conclusion: In summary, an indirect sensing method was proposed by considering the high affinity of Cu²⁺ with sulfide ion. Ensemble of TA-CuNCs with suitable concentration of Cu²⁺ can serve as a highly sensitive and selective probe for the determination of sulfide anion. In addition, the prepared TA-CuNCs/Cu²⁺ probe also exhibits visible color changes of the probe from blue to brown that can be applied for the determination of sulfide ion.

References

- [1] A. V. Péter Nagy , Zoltán Pálinkás , Attila Nagy , Barna Budai , Imre Tóth, *Biochim. Biophys. Acta* **2013**, 1840, 876.
- [2] A. Safavi, A. Abi, *IEEE Sens. J.* **2015**, 15, 3507.
- [3] J. Ma, P. Chen, H. Chang, *Nanotechnology* **2014**, 25, 195502.
- [4] H. Cao, Z. Chen, H. Zheng, Y. Huang, *Biosens. Bioelectron.* **2014**, 62, 189.
- [5] T. Gunnlaugsson, P. E. Kruger, P. Jensen, J. Tierney, H. D. P. Ali, G. M. Hussey, *J. Org. Chem.* **2005**, 70, 10875.

A simple and sensitive fluorimetric aptasensor for the ultrasensitive detection of arsenic(III) based on cysteamine stabilized CdTe/ZnS quantum dots aggregation

A. A. Ensafi*, N. Kazemifard

Department of Chemistry, Isfahan University of Technology, Isfahan 84156-83111, Iran

*Ensafi@cc.iut.ac.ir

Introduction:

Arsenic is one of the heavy metals that even in low concentration are danger to human health [1]. The adverse effects of drinking arsenic-contaminated water are skin damage, disruption of the circulation system and death, in extreme cases [2]. Aptamers are oligonucleotide molecules that bind to a specific target such as molecules or metallic ions via different bonding [3]. Quantum dots (QDs) have unique advantages for example narrow emission, size-dependent optical characters and resistance to light bleaching [4]. In This work a new aptasensor to determination of As(III) using aggregation of positively charged QDs is reported.

Methods / Experimental:

First aptamer solution was mixed with an appropriate amount of As(III) and diluted to 3.0 mL with phosphate buffer after 5 min, QDs was added into the above solution. Then, the fluorescence intensity of the prepared solution was recorded. The value of $F-F_0$ was calculated as a response function, to evaluate As(III) concentration, where F and F_0 correspond to the fluorescence intensities at 530 nm in the presence and absence of As(III), respectively.

Results and Discussion:

QDs have positive surface charge in neutral environment. The electrostatic interaction between QDs and aptamer produces neutralized surface charges of QDs. When the surface charges of QDs were neutralized the repulsion between the quantum dots was reduced and QDs were aggregated. After As(III) addition the fluorescence of QDs was enhanced upon de-aggregation. The effect of pH on the fluorescence intensity of QDs and mole ratio of the aptamer to QDs was investigated. The best response was obtained in the mol ratio of aptamer/QDs as 12.0 and at pH 7.0. At the higher pH, the electrostatic repulsion between QDs decreased as the result QDs were aggregated and insoluble. The higher mol ratio of the aptamer to QDs reduced the sensor sensitivity because the aptamer linked with cystamine and instead of decreasing, enhancement in the fluorescence was accrued and sensing mechanism was disrupted. The fluorescence spectra of QDs under different amount of As(III) were recorded. Under the optimum conditions, the linear range for As(III) measurement was obtained in the wide range of 1.0×10^{-11} to 1.0×10^{-6} mol L⁻¹ with the limit of detection as 1.3 pmol L⁻¹.

Conclusion:

A novel fluorimetric aptasensor is introduced for As(III) detection. The aptamer and As(III) form a complex, as the result de-aggregation of the quantum dots was accrued. The fluorescence intensity of QDs was enhanced upon de-aggregation of the quantum dots, which depends on the concentration of As(III). The proposed method is selective aptasensor for As(III) detection. The present assay was successfully applied for the determination of As(III) in several water samples.

References

- [1] Zhan, S., Yu, M., Lv, J., Wang, L., Zhou, P., *Aust. J. Chem.*, **2014**, 67, 813-818.
- [2] Flanagan, S.V., Johnston, R.B., Zheng, Y., *Bull. World Health Organ.* **2012**, 90, 839-846.
- [3] Jeon, W., Lee, S., Manjunatha, D.H., Ban, C., *Anal. Biochem.* **2013**, 439, 11-16.
- [4] Ensafi, A.A., Kazemifard, N., Rezaei, B., *Biosens. Bioelectron.* **2015**, 71, 243-248

Copper nanoparticles embedded hydrogel matrix as a robust catalyst for the reduction of nitro compounds

Roya Jahanshahi^a, Batool Akhlaghinia^{a,*}

^a Department of Chemistry, Faculty of Sciences, Ferdowsi University of Mashhad, P. O. Box 9177948974, Mashhad, Iran.

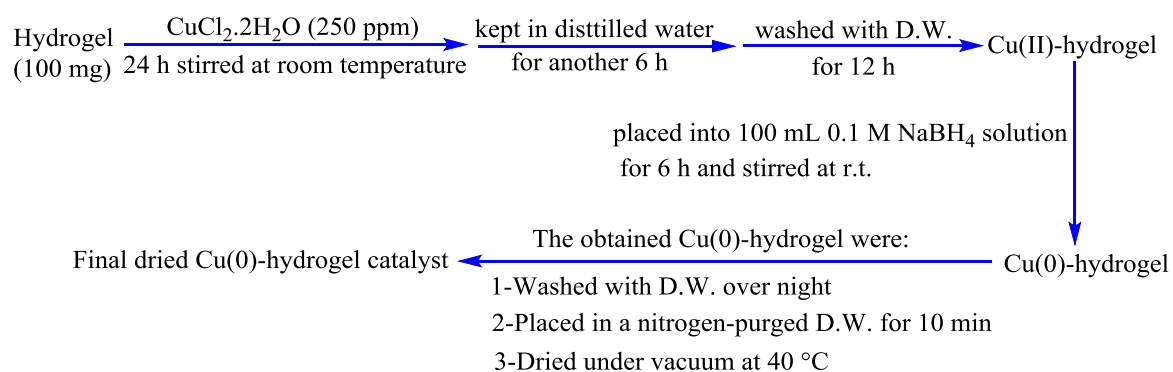
Email address: akhlaghinia@um.ac.ir

Introduction:

Aromatic nitro compounds are recognized as one of the most toxic organic pollutants, which have raised concerns regarding to human health and plant life [1]. So, converting nitro aromatic compounds to the corresponding more environment-friendly amines has paramount significance. For this purpose, mainly metal nanocatalysts are used in the presence of a reducing agent [2,3]. Herein, the chemically stable polymeric matrix of hydrogel was used as a reactor for the *in situ* preparation of Cu NPs. The generated Cu-hydrogel demonstrated a superior catalytic efficiency towards the reduction of nitroarens to their corresponding amines with NaBH₄ under mild aqueous condition.

Experimental:

Preparation of Cu-hydrogel catalyst: According to the pathway shown in Scheme 1, Cu-hydrogel was synthesized as an efficient and reusable heterogeneous catalyst.



Scheme 1. Preparation of copper nanoparticles embedded hydrogel matrix (Cu-hydrogel).

General procedure for catalytic reduction of nitro compounds: To the 0.01 M solution of nitro compound (5 mL), NaBH₄ (0.4 M, 0.075 g) was added at room temperature. Then, Cu-hydrogel (0.015 g) was added to initiate the reduction of nitro compounds. The progress of the reaction was monitored by TLC.

Results and Discussion: The newly synthesized catalyst was characterized by different techniques such as TEM and XRD. As shown in Fig. 1a, the size of Cu nanoparticles embedded in the hydrogel matrix was about 14.5 nm. XRD measurement was also used to identify the crystalline structure of Cu-hydrogel catalyst. As presented in Fig. 1b, all the

peaks which can be indexed to (1 1 0), (1 1 1), (2 0 0), (2 1 1), (2 2 0), (3 1 0) and (3 1 1) reflections, agree well with the cubic structure of cuprite (Cu_2O) (JCPDS file no. 05-0667).

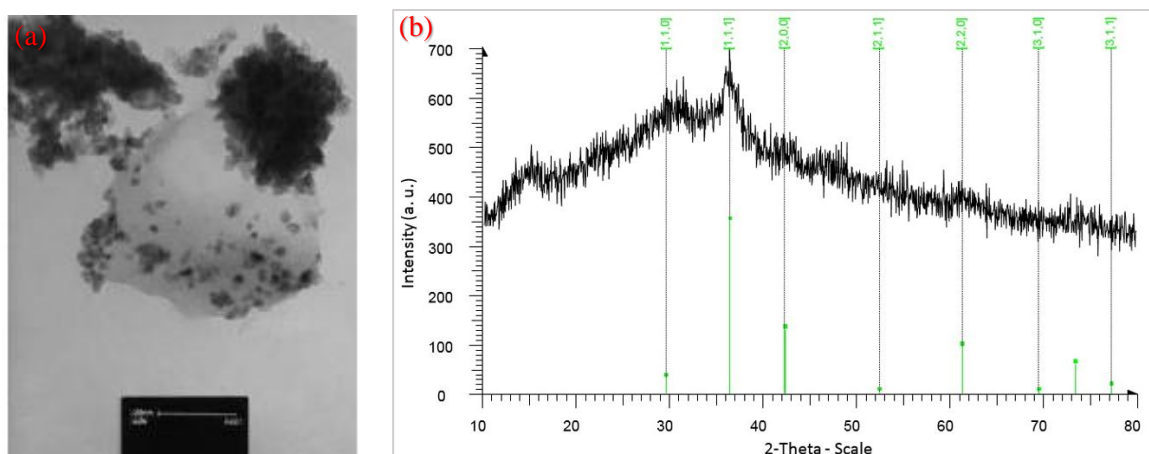
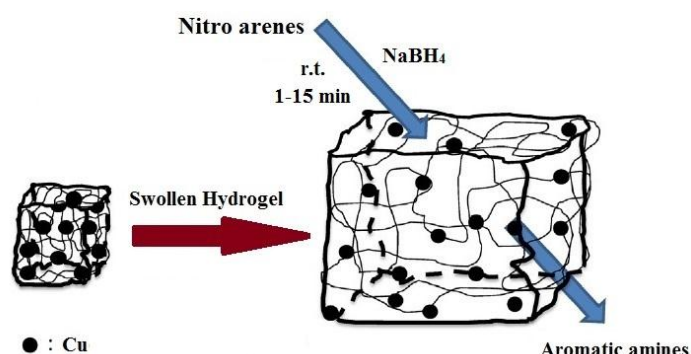


Fig. 1. (a) TEM image of Cu-hydrogel; (b) XRD pattern of Cu-hydrogel.

After the successful preparation and characterization of Cu-hydrogel, its catalytic activity was examined for the reduction of aromatic nitro compounds. The optimized reaction conditions was employed for the conversion of nitro aromatic compounds with various functional groups into their corresponding amino analogous (Scheme 2). The obtained results indicated that Cu-hydrogel is an excellent catalyst for such a transformation. In all cases, the reduction process was completed in a short time (1-15 min) and the resulting amino derivatives were isolated in good to excellent yields.



Scheme 2. Cu-hydrogel catalyst as a reactor for reduction of aromatic nitro compounds.

Conclusion:

Conclusively, the preparation and characterization of new heterogeneous designed Cu-hydrogel catalyst was demonstrated. This catalyst reveals an excellent catalytic performance in the reduction of aromatic nitro compounds. Mildness of the reaction conditions, experimental simplicity, compatibility with a wide range of substrates, high yields of the products, short reaction times, and reusability of the catalyst make this protocol very attractive and environmentally benign for the reduction of aromatic nitro compounds.

References

- [1] Sahiner. N. *Prog. Polym. Sci.*, **2013**, 38, 1329-1356.
- [2] Sahiner N.; Kaynak A.; Butun S. *J. Non-Cryst. Solids*, **2012**, 358, 758-764.
- [3] Lu Y.; Spyra P.; Mei Y.; Ballauff M. *Macromol. Chem. Phys.* **2007**, 208, 254-261.

Synthesis and characterization of Fe(III)POM/(Ni/Al)LDH/GO nanocomposite and its catalytic application in the oxidation of sulfides

Ali Dadashgholi Niatouri^a, Bahram Yadollahi^{a,*}

^a Department of Chemistry, University of Isfahan, Isfahan 81746-73441, Iran

Email address: yadollahi@chem.ui.ac.ir

Introduction:

As environment is so important in human life, paying attention to its troubles is one of the main concerns in recent years. Sulfur compounds are one of the main pollutants and because of its dangerous effects, trying to find effective solutions to protect the environment is one of the most valuable activities in catalytic investigations [1].

Polyoxometalates (POMs) as inorganic clusters have been used in various catalytic organic reactions such as oxidation of sulfides. Diverse structures of these compounds with different chemical and physical properties, easy preparation methods, sustainability and environment safety caused them to be so valuable in catalyst chemistry [2].

Methods / Experiments:

Transition metal substituted polyoxometalates (TMSPOM) have been shown good to excellent results in the oxidation of sulfides. To improve the catalytic properties of these TMSPOMs, they composed with layered double hydroxides (LDH) and graphene oxide (GO) according to the literatures [3-4].

Appropriate amounts of LDH and GO were added to TMSPOM and to gain the final composite, the mixture was stirred at reflux and afterwards it was filtered and washed several times with water and dried.

The synthesized nanocomposite was used in the oxidation of sulfides and the optimum reaction conditions were obtained by changing different reaction parameters such as the type and amount of catalyst, oxidant and solvent.

Results and discussion:

The structure and stability of synthesized nanocomposites were characterized by different methods such as XRD, UV-vis, FE-SEM, FT-IR and so on. All of the characteristic techniques approved the synthesis of nanocomposite.

The best TMSPOM/LDH/GO nanocomposites for the oxidation of sulfides was chosen among different transition metals of the first series. In this regard, the best results was obtained for Fe(III)POM/(Ni/Al)LDH/GO nanocomposite. Investigation on the effect of various LDHs was also done and (Ni/Al) LDH gave the optimal results.

Afterward, the catalytic activity of Fe(III)POM/(Ni/Al)LDH/GO nanocomposite in the oxidation of different sulfides was checked. The best reaction conditions were obtained by varying some of the reaction parameters such as solvent, amount of the catalyst and H₂O₂. Results were shown that between polar and nonpolar solvents such as ethanol, methanol, dichloromethane, *n*-hexane, THF and water, ethanol had the best results. Various amounts of the catalyst and H₂O₂ have been checked and respectively 0.005 mmol and 0.5 mL of each parameter were chosen. Reusability of the prepared nanocomposite in the oxidation of sulfide was examined and results showed no decreasing in its catalytic ability after five times.

Conclusion:

Fe(III)POM/(Ni/Al) LDH/GO nanocomposite was successfully prepared and characterized by different methods. High to excellent yields were obtained in the oxidation of different sulfides by the prepared nanocomposite. Additionally, Fe(III)POM/(Ni/Al) LDH/GO nanocomposite showed very good reusability in this catalytic system.

References

- [1] Backvall L. *Edu.*, **2004**, *17*, 24-27.
- [2] Pope, M. T.; Jeannin, Y., *Chem. Rev.*, **1983**, *8*, 109-111.
- [3] AlHazmi, F.S.; AlGhamdi, A.A.; Beall, G.; Bronstein, L. *Physicochem. Eng. Aspects*, **2015**, *7*, 723-727.
- [4] Daniela C.; Dmitry V.; Jacob M. B.; Alexander S.; Zhengzong S., *ACS Nano*, **2010**, *4*, 4806-4814.

Adsorption of Indole-3-acetic acid from Aqueous Samples by Magnetic Fe₃O₄@graphene Nanocomposite

A. Najibi^a, S. Kamran^{b*}, S.Y. Mousavi^b

^aDepartment of Chemistry, Shiraz Payame Noor University, Shiraz, Iran

^bDepartment of Chemistry, Shiraz Payame Noor University, Shiraz, Iran

^cDepartment of Anesthesia, Shahid Chamran Hospital, Shiraz, Iran

*E-mail: kamran_ss5@yahoo.com

1. Introduction

Auxins are a class of small-molecule growth hormones that are involved in a wide variety of biological processes in plants [1]. Indole-3-acetic acid (IAA) is a crucial phytohormone for precise control of growth and development of plants. Due to its low concentration in plant tissues which are rich in interfering substances, the accurate determination of this auxin remains challenge. Recently, magnetic solid-phase extraction (MSPE) [2,3] has gained increasing research interest due to its advantages over traditional SPE. Magnetite/reduced graphene oxide (MRGO) nanocomposites are excellent adsorbents for MSPE. The combination of graphene sheets and magnetic Fe₃O₄ particles offers MRGO distinguished properties such as good dispersity, large surface area, strong superparamagnetism and excellent extraction ability. In this paper, MRGO nanocomposite was used as the adsorbent for adsorption of IAA from aqueous sample. Adsorption isotherms, kinetic of adsorption and thermodynamic parameters were also characterized and reported.

2. Methods / Experimentals

Aliquots of 5 mL of the hormone solutions with initial concentrations of 0.2–0.7 mg ml⁻¹ in the pH range of 2.0–7.0 were prepared and transferred into individual beaker. A known dosage of MRGO in the range of 10–50 mg was added to each solution and the suspension was immediately shaken for a predefined period of time (1–30 minute). After the mixing time elapsed, the MRGO nanoparticles were magnetically separated and the solution was spectrophotometrically analyzed for the residual hormone.

3. Results and Discussion

The mean size and the surface morphology of the MRGO nanocomposite were characterized by TEM, XRD and FTIR techniques. Adsorption studies of IAA was performed under different experimental conditions, such as nanoparticle amount, IAA concentration, pH of the solution, ionic strength, and contact time. The equilibrium adsorption data for IAA was analyzed using Freundlich and Langmuir models. Table 1 summarizes the models constants and the correlation coefficients. As shown in Table 1, the R² of the Langmuir isotherm was higher than Freundlich isotherm for the adsorption of IAA. This indicates that the adsorption of IAA onto MRGO nanoparticles is better described by the Langmuir model than the Freundlich model.

Table 1. Adsorption isotherm parameters of IAA onto the MRGO nanoparticles.

	Langmuir model			Freundlich model		
	Q_{\max}	b	R^2	K_F	n	R^2
IAA	(mg g ⁻¹)	(L mg ⁻¹)		(mg g ⁻¹)	(g L ⁻¹)	
	22.94	24.21	0.999	3.3752	1.8929	0.979

The applicability of two kinetic models including pseudo-first order and pseudo-second order models was estimated. Adsorption process follows to pseudo-second-order kinetic model. Furthermore, the thermodynamic parameters were calculated. Adsorption process was exothermic. The calculated values of ΔG at studied temperatures indicate that the adsorption process is spontaneous. The positive value of ΔS indicates that the hormone have got lower order by being adsorbed onto the surface.

4. Conclusion

In this study MRGO nanocomposite was prepared by coprecipitation method. The mean size and the surface morphology of MRGO nanocomposite were characterized by TEM, XRD and FTIR techniques. Adsorption studies of IAA were performed under different experimental conditions in batch technique. The adsorption isotherms of IAA showed that the adsorption by MRGO was mono-layer. The adsorption kinetics of hormone on MRGO followed the pseudo-second-order model. Short contact time, high adsorption capacity, stability and reusability are advantages of MRGO nanoparticles as adsorbent.

References

- [1] E. Epstein, J. Ludwig-Müller, *Physiol. Plant* 88 (1993) 382-389.
- [2] L. Wang, X. Xu, Z. Zang, Green Sample clean-up based on magnetic multiwalled carbon nanotubes for the determination of lamivudine by high performance liquid chromatography, *RSC Adv.* 5(2015)22022-22030.
- [3] H. Abdolmohammad-Zadeh, Z. Talleb, Magnetic solid phase extraction of gemfibrozil from human serum and pharmaceutical waste water samples utilizing a beta-cyclodextrin grafted graphene oxide-magnetite nano-hybrid, *Talanta* 134(2015)387-393.

Development a New Colorimetric Sensor Array based on Functionalized Nanoparticles for Identification of Antioxidants

Mohammad Mahdi Bordbar, Javad Tashkhourian*, Bahram Hemmateenejad*

Chemistry Department, Shiraz University, Shiraz, 71454, Iran

Tashkhourian@susc.ac.ir

Hemmatb@shirazu.ac.ir

Introduction

Today, demands for ready- to-eat product including unsaturated fatty acids have increased. These foods are susceptible to attack by a variety of oxidizing agent [1]. Addition of antioxidant compounds is the best strategy for significantly delaying the oxidation mechanism [2]. The amount of antioxidant in the media must be in balance with oxidizing molecules and disrupting this balance causes destructive process called oxidative stress that plays an important role in the pathogenesis of several human diseases [2]. In addition, excessive amount of antioxidant in food has carcinogenic effects on body tissues [3]. Therefore, designing efficient methods for sensitive and selective detection of antioxidants are urgently required.

Experimental

We presented a novel colorimetric sensor array constructed by twelve functionalized metal nanoparticles consist of gold and silver nanoparticles synthesized with six different reducing agents. This sensor array used to discriminate twenty antioxidants belonging to six antioxidant families including phenolic, flavonoid, poly ol, citric acid, synthetic and bio antioxidants. Changing in color sensing elements is based on aggregation or destruction of nanoparticles. Changing in absorbance of each sensor was recorded with multimode plate reader. The discrimination ability was evaluated by linear discriminant analysis (LDA).

Results and discussion

The responses of the designed sensor array to some studied antioxidants are given in Fig. 1. The color change profiles are individual fingerprints for each specific analytes and are distinguished excellently by eye. The array responses were obtained in the optimized conditions. The discrimination ability was proven by LDA with good sensitivity, specificity, precision and accuracy which are equal to 0.95, 0.97, 0.93 and 0.89, respectively.

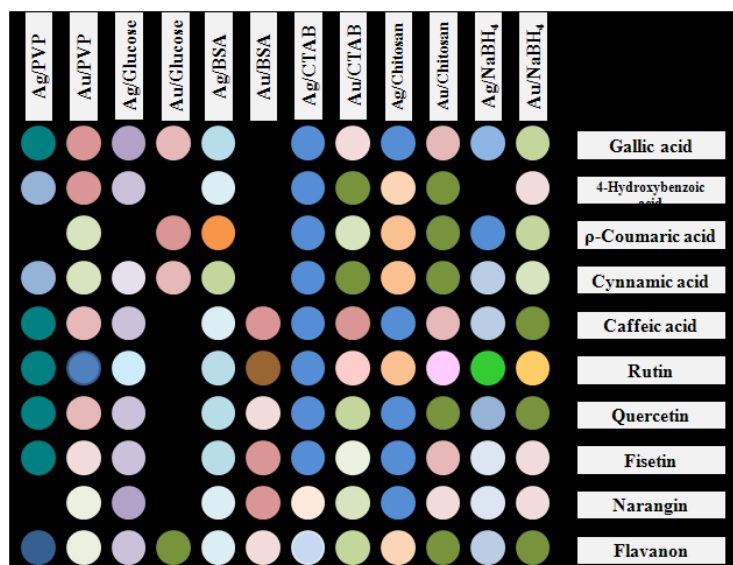


Fig. 1. Color difference maps of 10 antioxidants.

Conclusion

In summary, twelve functionalized metal nanoparticles were employed as sensing elements of a colorimetric sensor array for the detection and discrimination of 20 antioxidants. The variety of chemical constituents in antioxidant structures cause the aggregation or destruction of nanoparticles which lead to changing in color of each nanoparticles. The generated colors of sensor elements were specific for each antioxidant. The responses data was analyzed with LDA and successfully data classification was achieved.

References

- [1] I. Gülçin, *Archives of Toxicology*, **2012**, 86, 345–391.
- [2] A.M. Descalzo, A.M. Sancho, *Meat Science*, **2008**, 79, 423–436.
- [3] K. Le Gal, M.X. Ibrahim, C. Wiel, V.I. Sayin, M.K. Akula, C. Karlsson, *Science Translational Medicine*, **2015**, 7, 1–8.

Design and synthesis of new derivatives of 3-acetylthiocoumarin as 15-lipoxygenase inhibitors

Sara Zerang Nasrabad ^a, Seyed Mohamad Seyedi ^{b*}, Hamid Sadeghian ^c, Atena Jabari ^e

^a Department of Chemistry, School of Sciences, Ferdowsi University of Mashhad, Mashhad, Iran

^b Department of Chemistry, School of Sciences, Ferdowsi University of Mashhad, Mashhad, Iran

^c Department of Biology, Faculty of Sciences, Ferdowsi University of Mashhad, Iran

^d Department of Chemistry, School of Sciences, Ferdowsi University of Mashhad, Mashhad, Iran

Email address : smseyedi@um.ac.ir

Introduction:

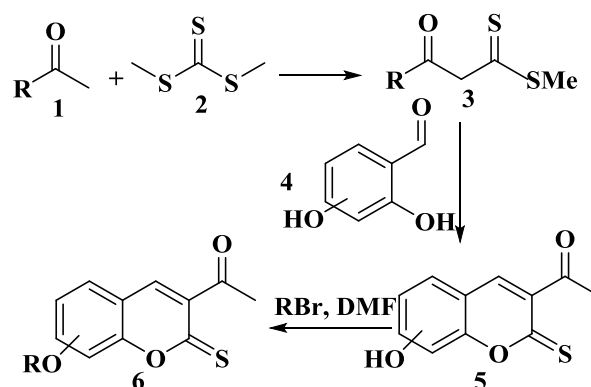
Lipoxygenases (LOs) are a main group of the non-heme iron containing proteins in lipid metabolism unsaturated fatty acids include arachidonic acid and linoleic acid convert to related metabolites by lipoxygenases and they are classified based on the position of the oxygenation of arachidonic acid (carbon number). Hydroperoxydation at 5 or 15 carbon position of the arachidonic acid respectively were converted to leukotrienes and lipoxines and eoxines in the next section, leukotrienes are released by white blood cells and play a major role in the development of inflammatory disease of the respiratory system. Research indicate these enzyme play a significant role in human disease such as cancer. In this research, with design and synthesize coumarin derivatives, we intend to revealed the chromophore groups in coumarin structure also study effect of increasing the length of prenyloxy chains in different position of coumarin ring on inhibitory activity of 15-lipoxygenase [1].

Methods / Experimentals:

In the first step the appropriate ketone 1 was added to dimethyl trithiocarbonate compound 2 the mixture stirred for 30 min at room temperature and then refluxed for 2 hours for preparation of intended β -Oxodithioesters 3. In the second step salicylaldehyde/ substituted salicylaldehyde 4 and β -Oxodithioesters that prepared in previous step, were heated and stirred for 1-2 hour. then the progress of the reactions was monitored by thin layer chromatography after completion of the reaction, water was added and the product was extracted with ethyl acetate [2]. The next step with using prenyl bromide compounds the corresponding derivatives 6 were synthesized.

Results and Discussion:

Based on scheme 1 O-Prenylated derivatives 6 were obtained from prenyl bromide in DMF in presence of base, after synthesis 3-acetyl-2-thiocoumarin compound 5 that was prepared from reaction of β -Oxodithioesters with intended benzaldehyde. The inhibitory activity of the synthetic compounds against soybean 15-LOX was determined utilizing modified catalytic oxidative coupling of 3-methyl-2-benzothiazolinone (MBTH) with 3-(dimethylamino) benzoic acid (DMAB) as reported in previous studies. In this method, the basis for the determination of lipoxygenase activity is the measurement of peroxide concentration. Among the synthetic O-prenylated compounds, 5-farnesyl had the best result on the soybean 15-LOX. Bonding affinity of the designed molecular structures toward soybean 15-LOX was studied. Docked conformers were generated in AutoDockTools (ADT) software. In docking process, flexible side chain of the active site pocket residues of soybean 15-LOX were allowed to be To perform better analysis on docking results, the average K_i (estimated inhibitory constant) of the most populated cluster (K_{iMPC}), average of all the lowest K_i from each cluster (K_{iLEC}), average K_i of all the conformers (K_{iAC}) and average K_i of a cluster in which lactone portion of thiocoumarin directed towards Fe-OH core (K_{iLFC}), were calculated for each compound. Among the four clusters, there was only an acceptable convergence between K_{iLFC} and IC_{50} results. This convergence was significantly observed for farnesyl and geranyl derivatives. In the earlier mentioned cluster (LFC), most of the conformers have hydrogen bonds with Fe-OH core through their acetyl groups and their prenyl portion are covered by side chain of some of amino acids in active site. In addition, the ability of the prenyl portion of the compounds to fill the lipophilic pocket which is formed by Ile663, Ala404, Arg403 (butyl portion), Ile400, Ile173 and Phe167 side chains can explain the direct relationship between lipoxygenase inhibition potency and prenyl length chain [3,4].



Scheme 1

Conclusion:

In this research, compound of 3-acetylthiocoumarin was synthesized and derivated by combination of prenyl bromide. These derivatives are reviewed by using the molecular docking techniques and their tension of inhibition are surveyed on 15-lipoxygenase enzyme. In the following, these mentioned compound were compered with prenyled coumarin deravitives in terms of inhibitory activity against on 15-lipoxygenase enzyme , There was a direct relationship between lipoxygenase inhibitory potency and prenyl length chain. generally, 5-O-prenyled compounds [1] were shown to have a better effect on 15-LOX.

References:

- [1] M. Iranshahi et al. / European Journal of Medicinal Chemistry 57 (2012) 134-142
- [2] O.M. Singh et al. / European Journal of Medicinal Chemistry 45 (2010) 2250–2257
- [3] L. Toledo, L. Masgrau, J.D. Mare´chal, J.M.. Lluch, A. Gonza´lez-Lafont, Insights into the Mechanism of Binding of Arachidonic Acid to Mammalian 15-Lipoxygenases, J. Phys. Chem. B. 114 (2010) 7037–7046.
- [4] J. Choi, J.K. Chon, S. Kim, W. Shin, Conformational flexibility in mammalian 15S-lipoxygenase: Reinterpretation of the crystallographic data, Proteins. 70 (2008) 1023–1032.

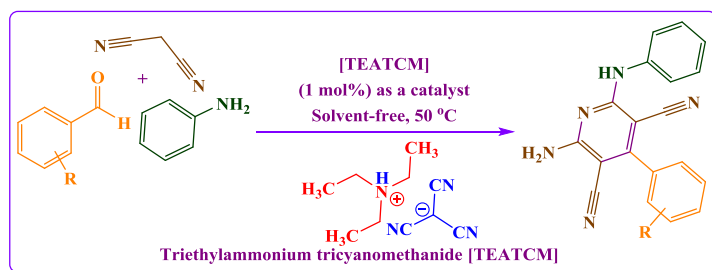
A convenient method for the synthesis of 2-amino-4-aryl-6-(arylamino)pyridine-3,5-dicarbonitriles *via* anomeric based oxidation

Maryam Khosravi, Saeed Baghery, Mohammad Ali Zolfigol*

Department of Chemistry, Faculty of Chemistry, Bu-Ali Sina University, Hamedan 6517838683, Iran

E-mail: zolfi@basu.ac.ir and mzolfigol@yahoo.com (M.A. Zolfigol).

Introduction: Pyridine derivatives are of attention because of the occurrence of their saturated and partially saturated derivatives in biologically active compounds and natural products such as pyridoxol or vitamin B₆, NAD nucleotides and pyridine alkaloids [1]. In this regard, we investigated a one-pot three-component reaction between numerous aldehydes, malononitrile and aniline at 50 °C under solvent-free condition for the synthesis of 2-amino-4-aryl-6-(arylamino)pyridine-3,5-dicarbonitriles catalyzed by triethylammonium tricyanomethanide [TEATCM] as a nanostructured molten salt (Scheme 1).



Scheme 1. The synthesis of 2-amino-4-aryl-6-(arylamino)pyridine-3,5-dicarbonitriles catalyzed by [TEATCM] as a NMS.

Experimental: [TEATCM] as a NMS catalyst (1 mol%; 0.0019) was added to a mixture of aldehyde (1 mmol), malononitrile (1 mmol; 0.066 g) and anilines (1 mmol; 0.093 g) under solvent-free condition at 50 °C for the appropriate time. At the end of reaction monitored by TLC, the resulting mixture was washed with water (10 mL) and filtered to separate catalyst from the other materials. The water was removed and the crude product was purified by recrystallization from ethanol (95%) to yield pure products.

Results and discussion: With the identical conditions in hand, the limitations and scope of this reaction was investigated by providing a series of 2-amino-4-aryl-6-(arylamino)pyridine-3,5-dicarbonitriles from the reaction between a good range of aldehydes, malononitrile and aniline using of 1 mol% of [TEATCM] at 50 °C under solvent-free condition (Table 1).

Table 1. Synthesis of 2-amino-4-aryl-6-(arylamino)pyridine-3,5-dicarbonitriles using 1 mol% of [TEATCM] as a catalyst under solvent-free condition at 50 °C.^a

Entry	Aldehyde	Time (min)	Yield (%) ^b	M.p (°C) (color)
1	Benzaldehyde	30	88	256-258 (Brown solid)
2	4-Chlorobenzaldehyde	20	91	238-240 (Yellow solid)
3	4-Methoxybenzaldehyde	15	93	230-232 (Yellow solid)
4	3-Nitrobenzaldehyde	20	91	247-249 (Yellow solid)
5	4-Nitrobenzaldehyde	30	89	258-260 (Yellow solid)
6	2,5-Dimethoxybenzaldehyde	25	89	251-253 (Yellow solid)

Reaction condition: ^aAldehyde (1 mmol), malononitrile (1 mmol), aniline (1 mmol), [TEATCM] (1 mol%); ^bIsolated yield.

Conclusion: In summary, the present investigation was presented the using of triethylammonium tricyanomethanide [TEATCM] as a nanostructured molten salt catalyst for the one-pot three-component reaction between numerous aldehydes, malononitrile and aniline in the synthesis of 2-amino-4-aryl-6-(arylamino)pyridine-3,5-dicarbonitriles at 50 °C under solvent-free condition. As abovementioned, the catalyst was recovered by easy filtration and reused for six cycles without significant loss its catalytic activity.

References:

- [1] Balasubramanian, M.; Keay, J. G. *In Comprehensive Heterocyclic Chemistry II*; Katritzky, A. R.; Rees, C. W.; Scriven, E. V. F.; Eds.; Pergamon Press: London, 1996, Vol. 5, Chapter 6, pp 245-300.

(2E,2'E)-2,2'-(pentane-2,4-diylidene)bis(1-(2,4-dinitrophenyl)hydrazine) as an efficient and versatile auxiliary ligand in Cu(II) catalyzed Buchwald-Hartwig and C-N bond formation reactions

Jasem Aboonajmi^a, Hashem Sharghi^{a,*}, Pezhman Shiri^a, Mahdi Aberi^a

^a *Department of Chemistry, Shiraz University, Shiraz, 71454, I.R.Iran, E-mail: shashem@susc.ac.ir*

Introduction

One possible choice to accelerate the metal catalyzed organic reactions especially Cu and Pd catalyzed reactions would be to use auxiliary ligands [1-2]. Although some of them could proceed smoothly on their own, several ligands have disclosed to promote rate enhancement of the metal catalyzed organic reactions without elevating metal concentrations.

In this respect, the acceleratory effect of some ligands including 7,8-dihydroxy-4-methylcoumarin, homogeneous dinuclear copper catalysts, tris(triazolyl)methane ligands, simple diamine ligands (such as trans-cyclohexane-1,2-diamine, trans-N,N'-dimethylcyclohexane-1,2-diamine, and N,N'-dimethylethylenediamine), ethyl 2-oxocyclohexanecarboxylate, and metformin have been investigated in copper-catalyzed C–N bond-forming reactions [3-4].

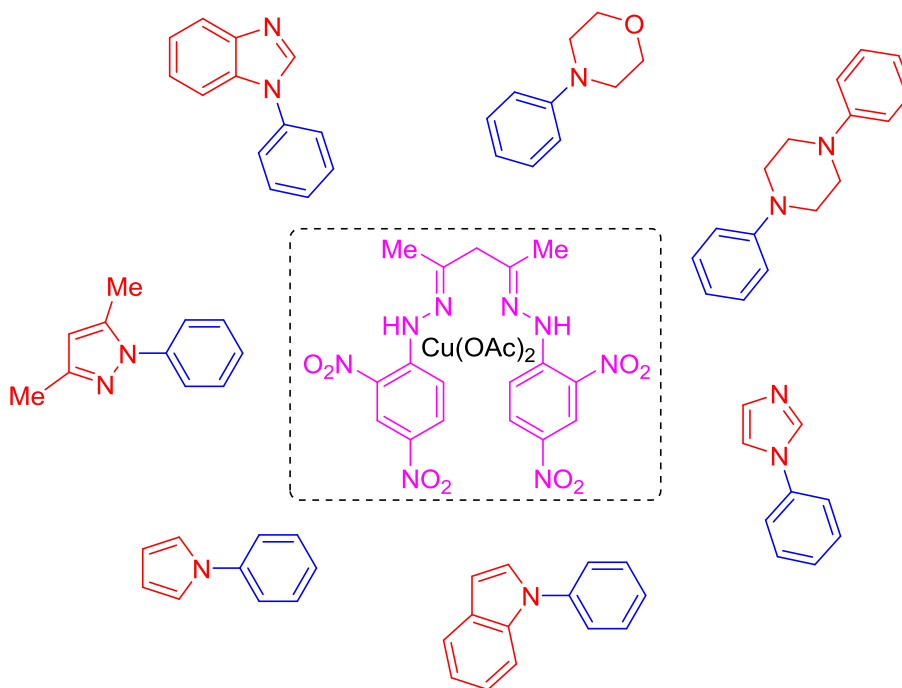
Methods/Experimentals

To a solution of the catalyst (5.0 mol%) in DMSO (0.3 ml), a mixture of N-unsubstituted compounds (1.0 mmol), aryl halides (1.2 mmol), and K₂CO₃ (1.5 mmol) was added. The mixture was stirred at 120 °C. The mixture was washed with EtOAc; after removal of the solvent, the residue was purified by column chromatography to produce N-substituted compounds.

Results and Discussion

In this work, we decided to study the effect of (2E,2'E)-2,2'-(pentane-2,4-diylidene)bis(1-(2,4-dinitrophenyl)hydrazine) (**L**) as an highly efficient auxiliary ligand on copper(II)-catalyzed C-N bond formation reactions. It can be easily prepared and no purification was required. Initial experiments were performed to examine **L** via N-substituted formation reaction of N-unsubstituted compounds (1.0 mmol) and aryl halides (1.2 mmol). After the optimization of the reaction conditions, all reactions were performed in the presence of DMSO (0.3 ml), K₂CO₃ (1.5 mmol) as base, **L** (5.0 mol%) as ligand, and Cu(OAc)₂ (5.0 mol%) as the source of copper. We were pleased to find that a wide range of N-heterocyclic compounds (such as 1H-benzo[d]imidazole, 1H-imidazole, 3,5-dimethyl-1H-pyrazole, 1H-pyrrole, 1H-indole, 2-methyl-1H-indole, 4-phenylmorpholine, 1,4-diphenylpiperazine and *etc*) can efficiently produce the corresponding products (Scheme 1). Different organic halides were also checked under the reaction conditions. In all cases, C-N cross coupling reactions were completed in a reasonable time and N-substituted compounds were isolated in good to excellent yields (**Scheme 1**). All

known products reported previously in the literature were characterized by comparison of IR and NMR spectra with those of authentic samples.



Scheme 1. Buchwald-Hartwig reaction of various structurally diverse N-unsubstituted compounds (1.0 mmol) and aryl halides (1.2 mmol) in the presence of K_2CO_3 (1.5 mmol) and copper (II)-L as a catalytic system (5.0 mol % and 5.0 mol % respectively) in DMSO (0.3 ml).

Conclusion

An extremely efficient and inexpensive ligand was prepared. Diverse N-substituted compounds were synthesized using (2E,2'E)-2,2'-(pentane-2,4-diylidene)bis(1-(2,4-dinitrophenyl)hydrazine) as a versatile auxiliary ligand in Cu(II) catalyzed C-N bond formation reactions. This method not only offers substantial improvements in the reaction yields and rates, but also avoids or reduces the use of toxic solvents and expensive catalysts which are, in terms of costs and environmental reasons.

References

- [1] Ruiz-Castillo, P.; Buchwald, S. L. *Chem. Rev.* **2016**, *116*, 12564-12649.
- [2] Arrechea, P. L.; Buchwald, S. L. *J. Am. Chem. Soc.* **2016**, *138*, 12486-12493.
- [3] Sharghi, H.; Shiri, P. *Synthesis* **2015**, *26*, 1131-1146.
- [4] Presolski, S. I.; Hong, V.; Cho, S.-H.; Finn, M. G. *J. Am. Chem. Soc.* **2010**, *132*, 14570-14576.

Application of triphenylammonium tricyanomethanide $[\text{Ph}_3\text{NH}][\text{C}(\text{CN})_3]$ as a nanostructured molten salt for the synthesis of 3-iminoaryl-imidazo[1,2-a]pyridines

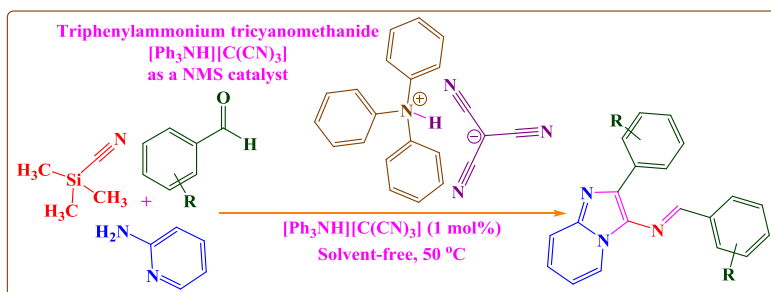
Saeed Baghery^a, Mohammad Ali Zolfigol^{a,*}, Romana Schirhagl^b, Masoumeh Hasani^a

^aDepartment of Chemistry, Faculty of Chemistry, Bu-Ali Sina University, Hamedan 6517838683, Iran

^bGroningen University, University Medical Center Groningen, Antonius Deusinglaan 1, 9713 AV, Groningen, Netherlands

E-mail: zolfigol@basu.ac.ir and mzolfigol@yahoo.com (M.A. Zolfigol).

Introduction: Among nitrogen-fused azoles, imidazo[1,2-a]pyridines have a main role in the paper because of their wide range of usages in several disciplines like medicinal chemistry, organometallics and material science [1-3]. Herein we wish to investigate the synthesis of 3-iminoaryl-imidazo[1,2-a]pyridines *via* reaction between numerous aldehydes, trimethylsilyl cyanide and 2-aminopyridine using triphenylammonium tricyanomethanide $[\text{Ph}_3\text{NH}][\text{C}(\text{CN})_3]$ as a recyclable NMS catalyst under solvent-free condition at 50 °C (Scheme 1).



Scheme 1. The synthesis of 3-iminoaryl-imidazo[1,2-a]pyridines catalyzed by $[\text{Ph}_3\text{NH}][\text{C}(\text{CN})_3]$ as a NMS.

Experimental: $[\text{Ph}_3\text{NH}][\text{C}(\text{CN})_3]$ as a NMS catalyst (1 mol%) was added to a mixture of aldehydes (2 mmol), TMSCN (2 mmol) and 2-aminopyridine (1 mmol) under solvent-free condition at 50 °C for the suitable time. After completion of the reaction monitored by TLC, the resulting mixture was washed with water (10 mL) and filtered off for isolating catalyst from the other materials. The solvent was removed and the crude product was purified by recrystallization from ethanol/water (10:1) to yield pure products.

Results and discussion: After optimization of reaction conditions, we tested the generality of this process for other substrates using aldehydes, TMSCN and 2-aminopyridine. To study the generality of the process, several aldehydes substituted with electron-donating and electron-withdrawing substituents were reacted so that the good to excellent results were achieved (Table 1).

Table 1. Synthesis of 3-iminoaryl-imidazo[1,2-a]pyridines using 1 mol% of $[\text{Ph}_3\text{NH}][\text{C}(\text{CN})_3]$ as a NMS catalyst under solvent-free conditions at 50 °C.^a

Entry	Aldehyde	Time (min)	Yield (%) ^b	M.p (°C) (color)
1	4-Methylbenzaldehyde	20	91	158-160 (Yellow solid)
2	4-Chlorobenzaldehyde	15	93	168-170 (Yellow solid)
3	4-Methoxybenzaldehyde	20	91	178-180 (Yellow solid)
4	3-Nitrobenzaldehyde	15	93	297-299 (Orange solid)
5	4-Nitrobenzaldehyde	10	95	163-165 (Brown solid)
6	3,4-Dimethoxybenzaldehyde	25	89	101-103 (Brown solid)

Reaction condition: ^aAldehyde (2 mmol), TMSCN (1 mmol), 2-aminopyridine (1 mmol), $[\text{Ph}_3\text{NH}][\text{C}(\text{CN})_3]$ (1 mol%); ^bIsolated yield.

Conclusion: Triphenylammonium tricyanomethanide $[\text{Ph}_3\text{NH}][\text{C}(\text{CN})_3]$ was found to be a recyclable NMS catalyst for the one-pot three-component condensation reaction between aldehydes, TMSCN and 2-aminopyridine, giving 3-iminoaryl-imidazo[1,2-a]pyridines under solvent-free condition at 50 °C in good to excellent yields. Also, the catalysts could be simply recovered by easy filtration and reused for numerous cycles without important loss its catalytic activity.

References:

- [1] Wan, J.; Zheng, C. J.; Fung, M. K.; Liu, X. K.; Lee, C. S.; Zhang, X. H. *J. Mater. Chem.*, **2012**, 22, 4502-4510.
- [2] Song, G.; Zhang, Y.; Li, X. *Organometallics*, **2008**, 27, 1936-1943.
- [3] Enguehard-Gueiffier, C.; Gueiffier, A. *Mini-Rev. Med. Chem.*, **2007**, 7, 888-899.

Synthesis, characterization and emission properties of the new bis(cyclometalated)platinum complexes and their thallium derivatives

Sirous Jamali,^{a*} Sheida Rajabi,^a Shahriar Kermanshahian,^a Soroush Naseri,^a Hamidreza Samouie,^b

^aChemistry Department, Sharif University of Technology, Azadi Ave., Tehran, Iran.

^bDepartment of Chemistry, Texas A&M University, PO Box 30012, College Station, TX 77842-3012.

Email address: sjamali@sharif.ir

Introduction

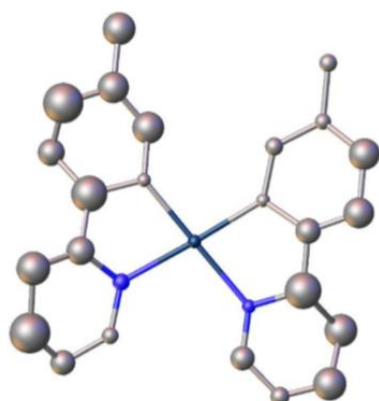
Cyclometalated complexes have recently found widespread interest as species with promising properties in various fields. The original method for preparing metallocycles is the spontaneous deprotonation of a C-H group in a suitable position. Such compounds, with C^N aromatic cycles, show interesting photochemical and photophysical properties [1] and have applications in many research field such as photo-catalysts [2], chemical sensors [3] and the light-emitting diodes [4].

Experimental

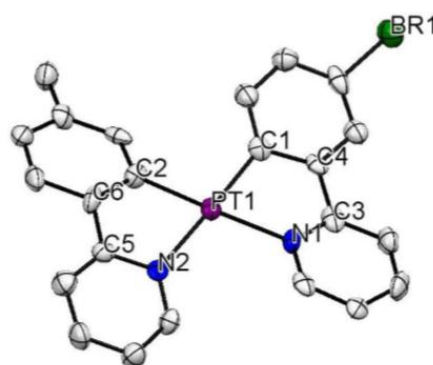
The new bis(cyclometalated) platinum(II) complexes of the type [Pt(ppy)(ppy')], in which ppy = ppy' = 2-(*p*-tolyl)pyridine, **1**; ppy = 2-(3-bromophenyl)pyridine, ppy' = 2-(*p*-tolyl)pyridine, **2**; ppy = ppy' = 2-(2,4-difluorophenyl)pyridine, **3**, have been prepared. Reaction of **1** with one equiv. TlPF₆ gave the heterobinuclear complex {Pt[(*p*-tolyl)pyridine]₂Tl}, **4**.

Results and Discussion

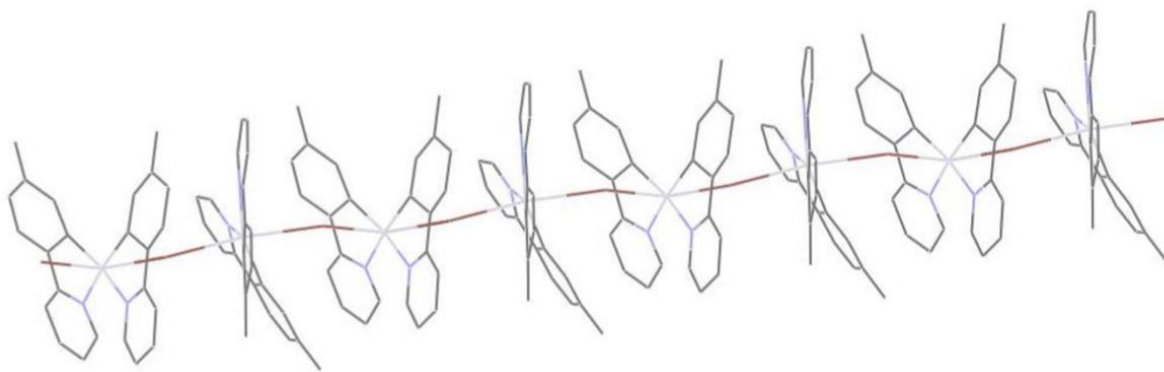
The bis(cyclometalated) platinum(II) complexes **1-4**, characterised by multinuclear NMR spectroscopy. The solid state structure of **1**, **2** and **4** determined using X-ray Crystallography. A view of the molecular structure of **1**, **2** and **4** shown in figure 1. The molecular structure of **4** has a chain polymer shape produced by Pt^{II}-Tl^I dative bonds.



1



2



4

Figure 1: Molecular structure of complexes **1**, **2** and **4**

Conclusion

In summary, a series of bis(cyclometalated) platinum(II) complexes were prepared, that show good emissive properties in solid state due to metal-metal and π - π , interaction. Emission properties of these complexes investigated at room and low temperature.

References

- [1] von Zelewsky, A. *Inorg. Chem.* **1996**, 35, 4883-4888.
- [2] Feng, K.; Zhang, R. Y.; Wu, L. Z.; Peng, M. L.; Zhang, L. P.; Tung, C. H.. *Am. Chem. Soc.* **2006**, 128, 14685-14690.
- [3] Zhao, Q.; Cao, T.; Li, F.; Li, X.; Jing, H.; Yi, T.; Huang, C. A. *Organometallics*, **2007**, 26, 2077.
- [4] a) Dixon, I. M.; Collin, J. P.; Sauvage, J. P.; Flamigni, L.; Encinas, S.; Barigelletti, F. *Chem. Soc. Rev.* **2000**, 29, 385. b) Williams, J. A. G. *Chem. Soc. Rev.* **2009**, 38, 1783.

Efficient Chloride Removal from Natural Gas Condensate by Nanoemulsion-Based Liquid-Liquid Extraction

Zohre Banan khorsheed, Mohammad Mahdi Doroodmand*

Department of Chemistry, College of Sciences, Shiraz University, Shiraz 71454, Iran

Email address: doroodmand@shirazu.ac.ir

Introduction:

Chloride ions accelerate the localized corrosion of pipeline and process equipment material of "Neutral Gas Condensate" (NGC). For chloride removal from different aqueous media, several alternative methods have been proposed such as using Bismuth-based adsorbents [1], magnesium–aluminum oxide [1], ultra-high lime ZnAl-NO₃ layered double hydroxides (as anion-exchange) [2, 3], etc. But based on immiscibility of water and NGC, probability the efficiency of chloride removal in NGC media would not be very good or maybe be ineffective, while these methods often need long time. Also some of these methods need to be acidified the NGC media that increase corrosion which is in disagreement with aim of this work. In this study, a novel nanoemulsion system was introduced to chloride removal from the NGC. Extraction efficiency is estimated to be quantitative.

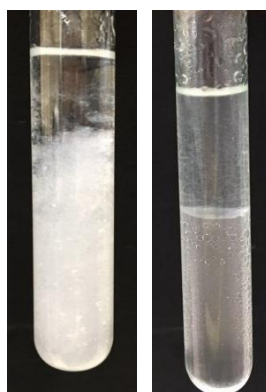
Experimental:

To synthesize nanoemulsion, sweet crude oil was used as nonpolar phase, H₂O as polar phase and also suitable disperser was used and Cu²⁺ was selected as the extractant cationic species. To perform liquid-liquid extraction, 5.0 mL extractant medium (nanoemulsion) was mixed with 5.0 mL NGC during vigorous shaking for at least 2.0 min inside a plastic or glass falcon (Volume: 13.0 mL). Then the falcon was placed inside a centrifuge for 5.0 min at 5000 rpm. Then 4.0 mL NGC was mixed with 4.0 mL aqueous Ag⁺ solution (excess concentration) with vigorous shaking for about 1 min inside another falcon. Therefore, formation of AgCl particles with white color revealed the qualitative extraction efficiency. Also the NGC was analyzed by ion-exchange chromatography to know quantitative efficiency of chloride removal.

Results and Discussion:

The extraction process was achieved based on the liquid/liquid extraction technique using nanoemulsion as extracting phase and NGC as feeding phase at standard temperature and pressure (STP) condition. It was focused on the neutral conditions in extraction step, and to prevent NGC contamination, no buffer addition was used. Effect of the presence of different cations in the synthesized nanoemulsion media were studied individually; only Cu²⁺ and Ag⁺ had good effect but Cu²⁺ was selected because 1) Cu²⁺ salts are more cheaper than Ag⁺ salts, 2) Cu²⁺ salts are more accessible than Ag⁺ salts, 3) Cu²⁺ have less effect on Fe corrosion based on reduced standard potentials [4], 4) some AgCl particles remain in NGC after using Ag⁺ solution,

consequently reduce its quality, 5) aqueous phase after extraction with Cu^{2+} can be converted to useful product ($\text{Cu}_2(\text{OH})_3\text{Cl}$) and 6) important reasons was that, chloride removal with introduced nanoemulsion/ Cu^{2+} was more than 99.5%, compared to about 45% during using Ag^+ solution. By increasing oil concentration in nanoemulsion synthesizing, needed Cu^{2+} concentration was decreased. Formation a lot of AgCl particles with white color by mixing NGC (before extraction) and aqueous Ag^+ solution showed chloride presence in NGC (Fig. 1(A)); and absence of AgCl particles after mixing NGC (after performing extraction) and aqueous Ag^+ solution revealed efficient chloride removal from the NGC (Fig. 1(B)). These qualitative results were in good agreement with ion-exchange chromatographic results.



A. **B.**
Fig. 1 A) AgCl formation **B)** absence of AgCl particles

Conclusion:

A new nanoemulsion was introduced to remove chloride ions from the NGC by liquid-liquid extraction process, and Cu^{2+} was used as extractant cation. Removal efficiency was quantitative (about 100%). Removed chloride ions in nanoemulsion (after performing liquid-liquid extraction process) will be converted to useful product i.e. $\text{Cu}_2(\text{OH})_3\text{Cl}$ Nanoparticles.

References:

- [1] Vaidya B, Watson SW, Coldiron SJ, Porter MD. Reduction of chloride ion interference in chemical oxygen demand (COD) determinations using bismuth-based adsorbents. *Analytica Chimica Acta* 1997;357:167-75.
- [2] Abdel-Wahab A, Batchelor B. Chloride removal from recycled cooling water using ultra-high lime with aluminum process. *Proceedings of the Water Environment Federation* 2001;2001:1-14.
- [3] Lv L, Sun P, Gu Z, Du H, Pang X, Tao X, et al. Removal of chloride ion from aqueous solution by ZnAl-NO 3 layered double hydroxides as anion-exchanger. *Journal of Hazardous Materials* 2009;161:1444-9.
- [4] Ives D, Rawson A. Copper corrosion I. Thermodynamic aspects. *Journal of The Electrochemical Society* 1962;109:447-51.

Design of a chemosensor for the detection and determination of Glutamic acid in some real samples

Habibollah Khajehsharifi^{1,*}, Fatemeh Heydari¹

Department of Chemistry, Yasouj University, Yasouj, Iran

E-mail address: khajeh_h@yahoo.com

Introduction

Glutamic acid or glutamate (GLA) is one of the 20 most common natural amino acids. It possesses a carboxylic acid component to its side chain. Glutamic acid is critical for proper cell function, but is not considered an essential nutrient in humans because the body can manufacture it from simpler compounds.. Instead, it is converted into L-glutamine, which the brain uses for fuel and protein synthesis. So. The determination of Glutamic acid is important. A simple and selective colorimetric method for the naked-eye detection and determination of Glutamic Acid (GLA) using Chrome Azurol S (CAS) complexed with Cu^{2+} ions as an indicator displacement assay (IDA) is described [1].

Adding GLA to a solution of the CAS-Cu^{2+} complex resulted in a ligand exchange reaction between CAS and GLA ,accompanied by a color change of the solution from blue to yellow at $\text{pH}=7.00$ [2].

The association constant for the binding of CAS to Cu^{2+} was determined by a colorimetric titration of $\log K = 4.02$ and that for the binding of GLA to Cu^{2+} was found to be $\log K = 7.87$ [3-4].

Experimentals

All chemicals were of analytical grade and used without further purification. All solutions were prepared using doubly distilled water. All natural amino acids were purchased from Merck Company. The stock solutions of amino acids with a concentration of 1.0 mM were prepared with distilled water daily. Diluted solutions were prepared from stock solutions. To prepare borate buffer, the appropriate amount of boric acid (Merck) was dissolved in distilled water and the pH was adjusted with 7.0 M solution of NaOH.

Results and Discussion

Design of an indicator displacement assay for detection and determination of Gly.

Considering the high tendency of amino acids to bind with Cu^{2+} , the Cu^{2+} ions is a suitable candidate for molecular recognition and binding of functional groups containing amino acids. So, we designed a simple and selective chemosensor based on indicator-displacement assay. For an IDA to be applicable, a suitable indicator must be able to reversibly bind to the host and signal the binding through a change in a spectroscopic signal[5] .

Conclusion

The chemosensor was used for the determination of GLA in some real samples and obtained the results indicates that this method could be applied for the determination of GLA in real samples.

References

- [1] A. Buryak; K. Severin. *J. Am. Chem.Soc*, 2005,127,3700-3701.
- [2] R. Liu; L. Li; Y. Tian. *Spectrochimica Acta Part A: Molecular and Biomolecular Spectroscopy* , 2008, 71, 1021-1026.
- [3] A. Semb;F. J. Langmyhr. *Anal. Chem. Acta*, 1966, 35,286-292.
- [4] S. A. Sajadi.*Natural Science*, 2010, 2,85-89.
- [5] G. J. Park ;S. A. Lee; Y.S. Kim . *RSC Advances* , 2015,5,31179-31188.

Triazoles Synthesis Catalyzed by Silica supported Copper(II) Complex

Pezhman Shiri^a, Hashem Sharghi^{a,*}, Mahdi Aberi^a, Jasem Aboonajmi^a

^a *Department of Chemistry, Shiraz University, Shiraz, 71454, I.R.Iran, E-mail: shashem@susc.ac.ir*

Introduction

Five-membered nitrogen heterocycles are important blocks, on account of a wide range of applications in biological systems. This type of molecules with high chemical stability to oxidation, reduction and hydrolysis have constituted one of the fascinating areas of research for producing drugs and fluorescence chemosensors. Among them, triazoles are pivotal building scaffolds; they show a broad spectrum of biological activities [1-3].

By immobilizing active ligated metals onto the suitable supports, the catalyst can be recovered and reused. According to the nature of complexes, some of them affect the rate of the reaction to produce the product in high yield.

Methods/Experimentals

To a solution of the catalyst (1.0 mol%) in water (1.0 ml), a mixture of organic halide or organic epoxide (1.0 mmol), terminal alkyne (1.0 mmol), and NaN₃ (1.2 mmol) was added. The mixture was stirred for the time given in Scheme 1. The mixture was washed with EtOAc; after removal of the solvent, the residue was purified by column chromatography.

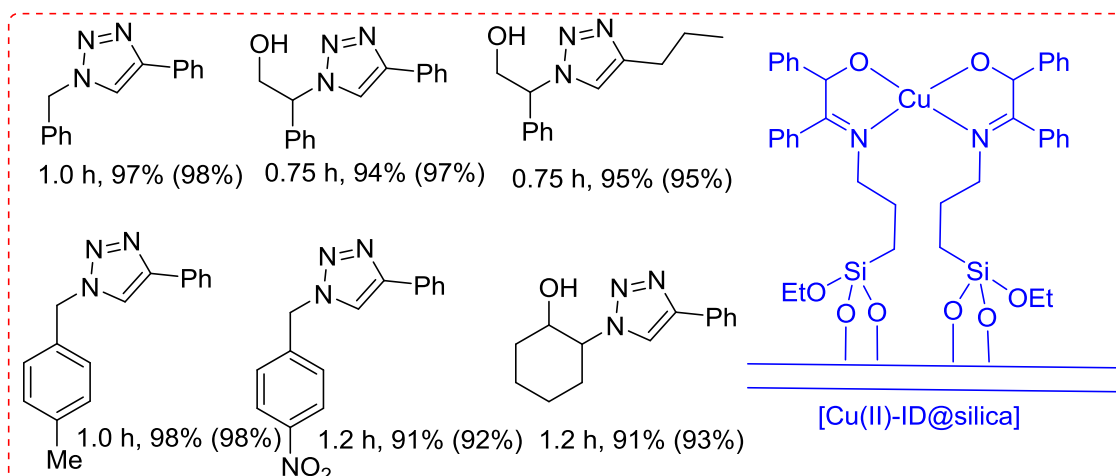
The amino functionalized silica was added to 2-hydroxy-1,2-diphenylethan-1-one in thanol, then the Cu(OAc)₂ was added at reflux condition to create [Cu(II)-ID@silica].

Results and Discussion

Initial experiments were performed to examine heterogeneous [Cu(II)-ID@silica] via triazole formation reaction of different benzyl halides or epoxides, alkynes, and sodium azide.

According to the green chemistry, the choice of green solvent such as water is crucial, so it was chosen. It was found that 25 °C for 40-90 min was the best conditions for coupling/cyclization of benzyl bromides, sodium azide, and acetylenes in a 1:1.2:1 molar ratio to substituted triazol using 1 mol% catalyst (Scheme 1).

Recycling of the heterogeneous [Cu(II)-ID@silica] was also checked through the reaction of phenyl acetylene, benzyl bromide, and sodium azide for twelve runs. The yields of desired functionalized triazole in further runs were almost the same as the first run. In every case, the heterogeneous [Cu(II)-ID@silica] were reused by simple centrifugation from the reaction mixture by washing with ethyl acetate. This organic phase was also washed with water, and purified by silica gel column chromatography employing n-hexane/ethyl acetate as eluent.



Scheme 1. Regioelective synthesis of 1,2,3-triazoles by way of a three-component reaction using 1 mol% heterogeneous [Cu(II)-ID@silica] at room temperature. (Isolated yield of product using heterogeneous catalyst; the numbers in parentheses is isolated yield of product using homogenous catalyst.)

Conclusion

In summary, we have successfully developed a novel, efficient, inexpensive, reusable silica supported Cu(II)-complex as catalyst for synthesis of divers azole products in water conditions in good to excellent yields. Moreover, this operationally simple protocol does not require the using toxic organic solvents and reagents. It is noted that this protocol provides novel, efficient, one-pot catalytic processes that enables the three-component synthetic route to triazols and β -hydroxy-triazoles, while displaying good tolerance with diverse functional groups.

References

- [1] Sharghi, H.; Shiri, P.; Aberi, M. *Mol. Divers.* **2014**, *18*, 559-575.
- [2] Sharghi, H.; Shiri, P.; Aberi, M. *Synthesis* **2014**, *46*, 2489-2498.
- [3] Sharghi, H.; Shiri, P. *Synthesis* **2015**, *26*, 1131-1146.

Electrochemical behavior of an anticancer drug 5- fluorouracil at modified glassy carbon electrode by graphene- PEDOT:PSS

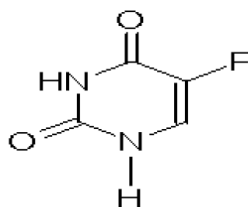
M .Mazloun-Ardakani, M. Haghshenas*, A. Khoshroo

Department of Chemistry, Faculty of Science, Yazd University, Yazd, 89195-741, Iran
Mahnoosh.Haghshenas@gmail.com

Introduction:

In this paper, nanocomposite graphene-poly(3,4-ethylenedioxythiophene) polystyrene sulfonate (RGO/PEDOT:PSS) or (RGO/P), was prepared and used to modification of glassy carbon electrode (RGO/P/GCE) for determination of anticancer drug (5-Fluorouracil).

Purine and pyrimidine bases, nucleosides and nucleotides are essential constituents of nucleic acids and enzyme cofactors required for the proper functioning of cells, tissues and organs. A variety of uracil derivatives have been reported as anti-tumour or anti-viral agents or both. Among them, 5-Fluorouracil (5-Fluoro-1H-pyrimidine-2,4-dione) (5-FU) (scheme 1) is particularly very important. As an anti-neoplastic agent, it has been used for the treatment of solid tumours of the breast and rectum [1].



Schem 1. Structure of 5-Fluorouracil

Methods / Experimentals:

The voltammetric oxidation of 5-Fluorouracil was investigated at RGO/P/GCE electrode using cyclic voltammetry (CV), differential pulse voltammetry (DPV), chronoamperometry (CA) and electrochemical impedance spectroscopy (EIS). The morphology of nanomaterial was characterized using scanning electron microscopy (SEM).

Results and Discussion:

Fig. 1 shows the CVs behaviors of the bare GCE and RGO/P/GCE in the absence and presence of 1.0 mM 5-FU at potential scan rate of 100 mVs⁻¹. Both of GCE and GCE/P did not show any peak in the working potential range in Fig. 1, however, RGO/P/GCE showed a significant current peak at about 1.1 V in the presence of 1.0 mM FU.

Therefore, there was a significant increase in the anodic peak current in the presence of 1.0 mM FU (Fig. 1), which can be related to the strong effect of conjugated polymer that can intensify currents, the excellent electro conductivity of PEDOT:PSS promoting fast electron transfer between the electrolyte and the substrate electrode [2].

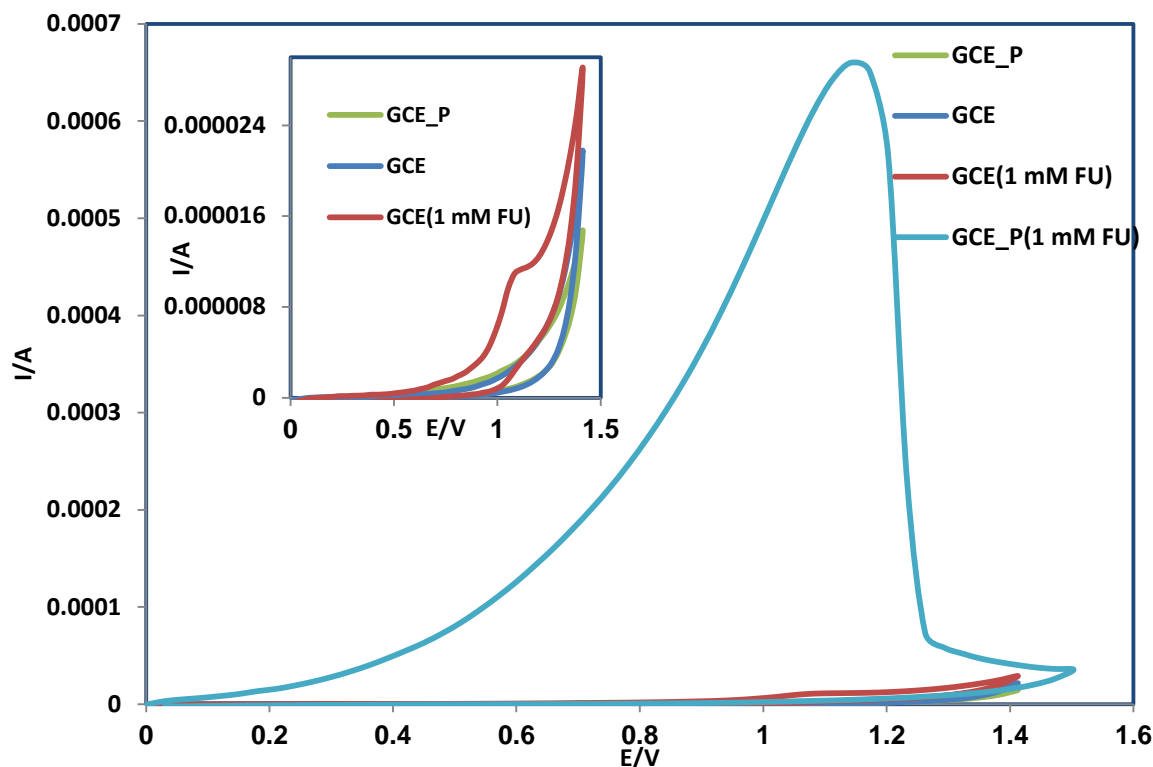


FIG. 1. Successive cyclic voltammograms of bare GCE and RGO/P/GCE in the absence and presence of 1.0 mM 5-FU at a potential scan rate of 0.1 Vs^{-1} ; phosphate buffer with pH 9.0.

The DPV technique was employed for preparation of calibration graph. Linear dynamic range was 0.5×10^{-6} to $1.6 \times 10^{-3} \text{ M}$, with detection limit of 75 nM. The proposed method was successfully applied to 5-Flurouracil determination in blood serum samples. The modified electrode showed good stability and repeatability.

Conclusion:

The voltammetric oxidation of 5-FU at graphene-PEDOT:PSS electrode in phosphate buffer solution under optimum condition, pH=9.0 has been investigated. The peak current was linear to 5-FU concentrations over a certain range, under the selected conditions. This helps in voltammetric determination of selected analyte as low as 75 nM and can be used successfully to assay the drug in pharmaceutical dosage form as well as in spiked blood serum samples.

References

- (1) Heidelberger, C. ; Ansfield, F.J. Cancer Res. **1963** , 23, 1226-1243.
- (2) Nilsson, D.; Chen, M.; Kugler, T.; Remonen, T.; Armgarth, M.; Berggren, M. Adv. Mater. **2002**, 14, 51.

Application of NZVI/ACF Nanocomposite for Removal of Nitrate and Nitrite Ions and Kinetic Study of this Process

Azam Seifi^{*a}, Soheil Aber^b, Alireza Khataee^c

^a Department of Applied Chemistry, Faculty of Chemistry, University of Tabriz, Tabriz, Iran

*a.seifi_88@yahoo.com

Introduction: Purification of water and removal of its pollutants have been among the biggest challenges for the humans from past till now. Two of these hazardous pollutants are nitrate and nitrite anions [1]. Different methods have been applied for removal of these poisonous anions from water like reverse osmosis [2], ion exchange [3] and electrodialysis [4]. Nowadays, application of nanozero-valent iron particles (NZVI) has attracted a great attention. In this research NZVI was immobilized on activated carbon fibers (ACF) and characteristics of the prepared nanocomposite were determined using XRD, SEM analysis. NZVI/ACF was applied for removal of nitrate and nitrite anions from water.

Methods / Experiments: In this study the ACF was prepared through a physicochemical method using natural Kenaf fibers as a precursor [5]. As oxidizing chemical and oxidizing gas, K_2HPO_4 and CO_2 were applied respectively. Then, NZVI particles were stabilized on the ACF using a reduction method, applying $NaBH_4$ as the reductant solution. The obtained NZVI/ACF was applied for water treatment. The influence of 4 factors was investigated on the removal process. The kinetics of the denitrification process was also investigated in this research.

Results and Discussion: The prepared nanocomposite was used to nitrate and nitrite removal from water. For increasing the removal efficiency of the nanocomposite, first the desired ratio of Fe^{2+} /ACF was determined and in the rest of the experiments this ratio was applied. The experimental results showed that the nanocomposite prepared with the Fe^{2+} /ACF ratio of $\frac{1}{2}$ had the highest removal efficiency. Moreover, the effect of the initial concentration of the solution, its pH and the nanocomposite amount on the removal efficiency was investigated. The results showed that the removal percentage reached its highest level at the lower concentrations of nitrate, acidic pHs and higher amounts of nanocomposite. For evaluating the nanocomposite efficiency, its nitrate and nitrite removal percentage was compared to that of the same amounts of its components. The results indicated that at the same experimental conditions the removal efficiency of the NZVI/ACF nanocomposite (%64.54) was higher than the sum of the removal efficiencies of NZVI (%30.42) and ACF (%21.74). According to the experimental results, the

nitrate and nitrite removal process using NZVI/ACF nanocomposite followed a pseudo-second order reaction. The obtained k_{obs} showed good compatibility with the theoretical k_{obs} .

Conclusion: The results proved the high efficiency of the prepared composite in nitrate and nitrite removal. The removal percentages were over 85%. By applying this composite nitrate concentration decreased under the WHO's regulatory limits.

Acknowledgement

Authors thank the University of Tabriz for the support provided.

References:

- [1] Burow, K. R., Nolan, B. T., Rupert, M. G., Dubrovsky, N. M., Environmental Science & Technology, **2010**, Vol. 44, 4988-4997.
- [2] Schoeman, J. J., Steyn, A., Desalination, **2003**, Vol. 155: 15-26.
- [3] Milmlie, S. N., Pande, J. V., Karmakar, Sh., Bansiwale, A., Chakrabarti, T., Biniwale, R. B., Desalination, **2011**, Vol. 276: 38-44.
- [4] Menkouchi Sahli, M. A., Tahaikt, M., Achary, I., Taky, M., Elhanouni, F., Hafsi, M., Elmghari, M., Elmidaoui, A., Desalination, **2006**, Vol. 189: 200–208.
- [5] Aber, S., Khataee, A., Sheydaei, M., Bioresource Technology, **2009**, Vol. 100: 6586-659.

Multi-component synthesis of quinoline derivatives in a mixture of graphite and methanesulfonic acid (GMA)

Mahdi Aberi^a, Hashem Sharghi^{a,*}, Jasem Aboonajmi^a, Pezhman Shiri^a

^a Department of Chemistry, Shiraz University, Shiraz, 71454, I.R.Iran, E-mail: shashem@susc.ac.ir

Introduction

Quinolines and their derivatives are important scaffolds because of their wide spectrum of biological activities and they have played an important role in medicinal chemistry due to their pharmacological properties [1-2].

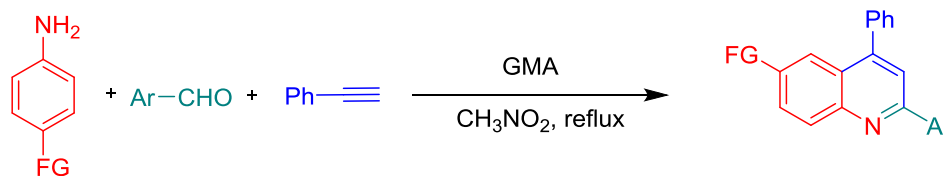
H. sharghi and coworkers reported that a mixture of CH₃SO₃H/graphite (GMA) is an effective and inexpensive reagent for regioselective acylation of aromatic ethers with carboxylic acids [3], acylation of phenol and naphthol derivatives [4] and sulfonylation of phenols and *tina-fries* rearrangement of aryl sulfonates [5] in good yields and with high selectivity.

Methods/Experimentals

A mixture of aldehyde (1.0 mmol), amine (1.0 mmol) and phenylacetylene (1.2 mmol) was added to CH₃SO₃H (0.2 ml) and graphite (0.2 g) in 5 mL CH₃NO₂ under reflux. After completion, the mixture was filtered and washed with ethyl acetate, and then the mixture was poured into H₂O. The filtrate was extracted with ethyl acetate. The organic layer was washed with NaHCO₃. The solvent was removed, which was purified by silica gel column chromatography employing *n*-hexane/ethyl acetate (10:1) as eluent.

Results and Discussion

In this work, under the optimized conditions, the reaction of aromatic aldehydes, amines and phenylacetylene was carried out in the presence of GMA *via* one-pot multi-component reaction in CH₃NO₂ under reflux (Scheme 1). Various aromatic aldehydes with substituents such as Me, OMe, Cl and isopropyl were treated with amines and phenylacetylene under identical reaction conditions. Additionally, heteroaryl aldehydes like pyridine-2-carboxaldehyde were well tolerated under the optimal reaction conditions. The present method was also examined for various anilines such as *p*-chloroaniline, *p*-toluidine and *p*-anisidine with varying aromatic aldehydes and phenylacetylene, where the desired quinoline derivatives were obtained in excellent yields. The products were characterized by its melting point, IR, ¹H NMR, ¹³C NMR, mass spectroscopic.



Scheme 1. One-pot synthesis of quinoline derivatives using GMA

Conclusion

In conclusion, we have demonstrated that an inexpensive and readily available reagent, graphite/methanesulfonic acid (GMA), is very effective for the preparation of quinoline derivatives. Cheapness, readily available starting materials, easy and quick isolation of products, high yields and operational simplicity can make this procedure a useful and attractive method for the synthesis of quinoline derivatives from aromatic amine, aldehyde and non-activated terminal alkynes.

References

- [1] Zhang, Y.; Wang, M.; Li, P.; Wang, L. *Org. Lett.* **2012**, *14*, 2206-2209.
- [2] Sawada, W.; Kayakiri, H.; Abe, Y.; Imai, K.; Katayama, A.; Oku, T.; Tanaka, H. *J. Med.Chem.* **2004**, *47*, 1617-1630.
- [3] Hosseini Sarvari, M.; Sharghi, H. *Synthesis* **2004**, 2165-2168.
- [4] Sharghi, H.; Hosseini Sarvari, M.; Eskandari, R. *Synthesis* **2006**, 2047- 2052.
- [5] Sharghi, H.; Shahsavari-Fard, Z. *Helv. Chim. Acta.* **2005**, *88*, 42-52.

Laccase-catalyzed synthesis of arylsulfonyl benzenediols, sulfonamides and sulfoxides in aqueous media at room temperature

Amin Rostami^{a,*}, Davood Habibi^b, Abdollah Rahimi^b, Sirvan Moradi^a

^aDepartment of Chemistry, Faculty of Sciences, University of Kurdistan, Sanandaj 6617715143, Iran

^bDepartment of Organic Chemistry, Faculty of Chemistry, Bu-Ali Sina University, Hamedan 6517838683, Iran

Email address of corresponding author: a.rostami@uok.ac.ir

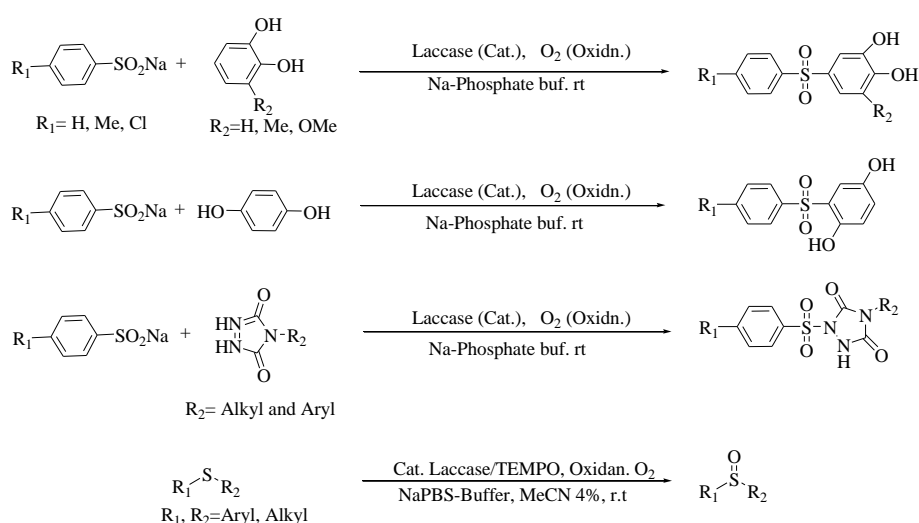
Introduction: Laccase (benzenediol:oxygenoxidoreductase, EC 1.10.3.2), a multi-copper-containing oxidoreductase enzyme, is one of the enzymes that is being studied as a biocatalyst in organic synthesis due to its ability to catalyze the oxidation of various substrates, specifically, phenols, *o*- and *p*-diphenols and lignin derivatives. This oxidation is accompanied by the reduction of dioxygen to water [1].

Sulfoxides and sulfones are valuable intermediates for the synthesis of fine chemicals and biologically active compounds [2].

Sulfonamides are widely used to treat many kinds of infection caused by bacteria and certain other microorganism [3].

Methods/Experimental: Initially, in order to optimization of the reactions conditions, the effect of solvent, temperature, and amount of catalyst on the model reactions were investigated. Next, with optimal conditions in hand, the generality and the applicability of these methods were further examined. Finally, the products were characterized by IR, and NMR spectra.

Results and Discussion: In continuation of our studies on the application of laccase as a biocatalyst in the aerobic oxidation of alcohols [4], herein, we have synthesized arylsulfonyl benzenediols and sulfonamide derivatives *via* aerobic oxidation of benzenediols and urazoles, respectively catalyzed by laccase in the presence of sodium arylsulfonates as nucleophile in phosphate buffer solution in good to high yields at room temperature. Also, the aerobic oxidation of sulfides to sulfoxides was investigated in the presence of catalytic amount of laccase and TEMPO as a mediator in Na-phosphate buffer (0.1M, pH 6)/MeCN (25:1) at room temperature (Scheme 1).



Scheme 1

Conclusion: In this research, the synthesis of valuable compounds using O₂ as an oxidant in the presence of laccase as green biocatalyst in the phosphate buffer solution as an environmentally friendly solvent at room temperature is described. The methods conform to several of the guiding principles of green chemistry.

References

- [1] M. Mogharabi; M. A. Faramarzi; *Adv. Synth. Catal.* **2014**, 356, 897- 927.
- [2] I. Frenanez; N. Khair; *Chem. Rev.* **2003**, 103, 3651-3706.
- [3] <http://medical-dictionary.thefreedictionary.com/sulfonamide>
- [4] S. Rouhani; A. Rostami; A. Salimi; *RSC Adv.*, **2016**, 6, 26709-26718.

Affinity of a Cycloplatinated(II) Complex to Bovine Serum Albumin: A Spectroscopic Approach

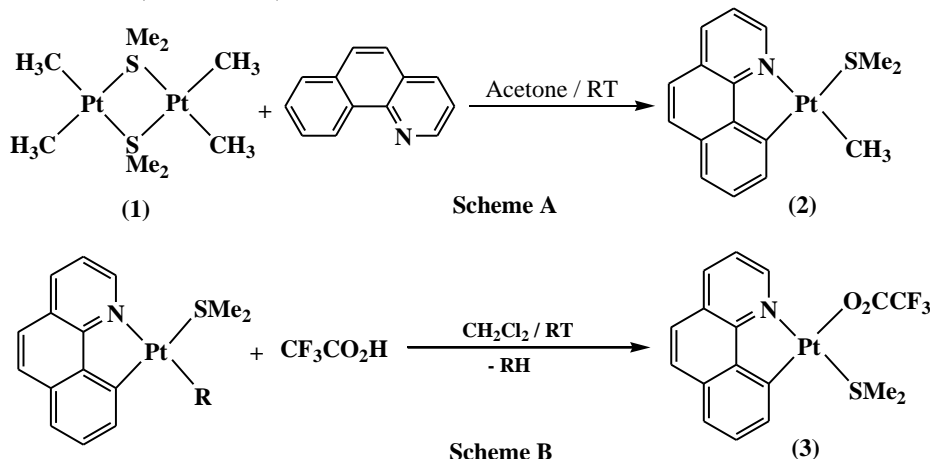
Parisa Negaresh, Marzieh Dadkhah Aseman, S. Masoud Nabavizadeh, Mehdi Rashidi*

Department of Chemistry, College of Sciences, Shiraz University, Shiraz, Iran

rashidi@chem.susc.ac.ir

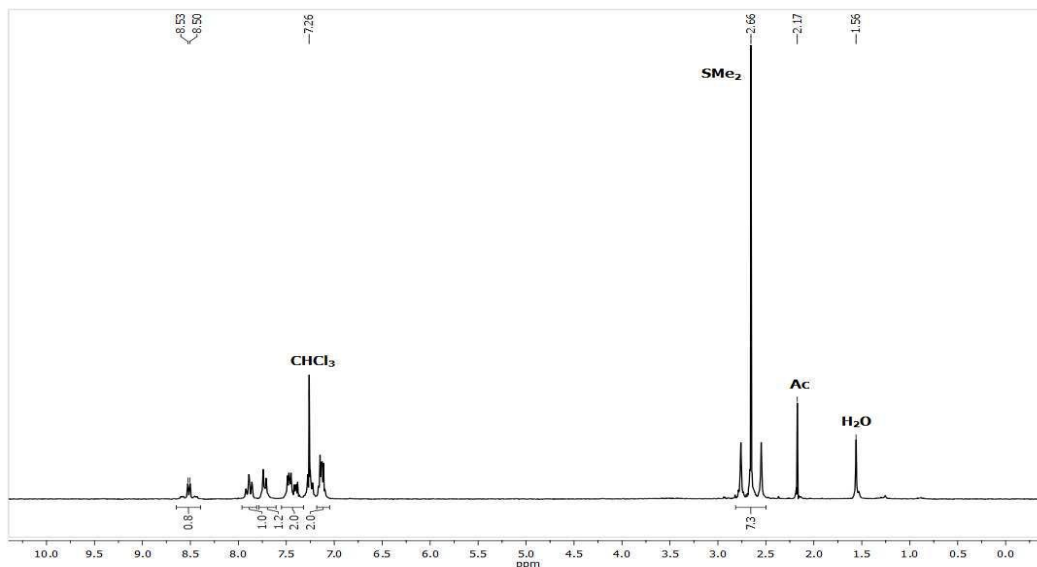
Introduction: Studies on the interaction between a drug and protein are very important in biological, biomedical and pharmaceutical sciences [1]. Among investigated proteins, Bovine serum albumin (BSA) is the most abundant carrier protein on blood stream with high affinity for a wide variety of ligands such as metabolites and drugs [2,3]. The important physiological functions of this protein are the storage and transport of wide range of endogenous and exogenous compounds such as fatty acids, hormones, bilirubin, drugs, etc, as well as, the maintenance of osmotic pressure and pH of the blood plasma [3]. The crystallographic analysis of BSA revealed that this protein contains a single chain of 585 residues with a molecular mass of 66.4 kDa. Although DNA is known as the final molecular target of platinum based drugs, their anticancer activity is also resulting of many other events, including their interaction with plasma proteins [4]. The interaction between Pt compounds and serum albumin is important on the basis of both drug delivery and possible development of acquired resistance/side effect. Therefore, the mechanism underlying Pt complex-albumin interaction seems essential for extending the knowledge of their therapeutic efficacy at the molecular level [4]. Notice that the type of ligand around the metal center can affect various properties of platinum based complexes, including their solubility, reactivity, electronic and steric properties, as well as, geometry of the metal center. In this work the four-coordinated Pt (II) complex with two labile ligands was used to study its interaction with BSA. We believe that the presents of two labile ligands at *cis* position on Pt(II) center can increase affinity of cycloplatinaited complexes to Bovine serum albumin.

Methods / Experimentals: In the present work, the known reaction of the organoplatinum(II) dimmeric complex $[Pt_2Me_2(SMe)_4]$, 1, with 2 equivalent benzo[h]quinoline, bhq, in acetone at room temperature to give the cycloplatinated(II) complex $[PtMe(bhq)(SMe)_2]$, 2, was performed (Scheme A) [5]. Reaction of the complex 2 with 1 equivalent trifluoroacetic acid (CF_3CO_2H) in dichloromethane gave the complex $[Pt(bhq)(CF_3CO_2)(SMe)_2]$, 3, by displacement of methyl ligand with CF_3CO_2 , (Scheme B) [5].



The interaction of [Pt(bhq)(CF₃CO₂)(SMe)], **3**, with Bovine serum albumin (BSA) was studied by different spectroscopic techniques, including UV-vis and fluorescence spectroscopy.

Results and Discussion: The reaction of organoplatinum (II) precursor [Pt(Me)(bhq)(SMe)], with 1 equivalent of CF₃CO₂H, trifluoroacetic acid, in dichloromethane gave [Pt(bhq)(CF₃CO₂)(SMe)], by displacement of Methyl group. A pure sample of **3** was obtained for biological studies. The ¹H-NMR spectrum of [Pt(bhq)(CF₃CO₂)(SMe)], in CDCl₃ is shown in Figure 1. The protons of SMe ligand were observed at δ = 2.6 ppm as a singlet signal with ³J (PtH) = 0.6 Hz. A doublet at δ = 1.9 ppm with ³J (PtH) = 36.0 Hz and ³J (HH) = 0.3 Hz was



assigned to the H_A proton of bhq.

Figure 1. ¹H-NMR spectrum of the complex [Pt(bhq)(CF₃CO₂)(SMe)], **3**, in CDCl₃.

Conclusion: The BSA protein's ability for binding to the complex **3**, using UV-vis and fluorescence spectroscopy, was investigated in an attempt to assess denaturing properties of this complex against serum albumin. We found that this complex having two adjacent leaving groups at Pt center has a high affinity to bind to BSA. Further investigations are underway.

References:

- [1] E. I. Montero, B.T. Benedetti, J. B. Mangrum, M.J. Oehlsen, Y. Qu, N.P. Farrell, *Dalton Trans.* 2007, 493, 4938.
- [2] T. Wang, B. Xiang, Y. Wang, C. Chen, Y. Dong, H. Fang, M. Wang, *Biointerfaces* 2008, 70, 113.
- [3] B.X. Huang, H.Y. Kim, C. Dass, *J. Am. Soc. Mass Spectrom.*, 2004, 15, 1237.
- [4] J. J. Wilson, S. J. Lippard, *JACS*, 2014, 136, 8790.
- [5] M. G Haghighi, S. M Nabavizadeh, M. Rashidi, M. Kubicki, *Dalton Transactions*, 2013, 42,

Constructing a Uric Acid Sensor Based on Electrodeposition of Silver Hexacyanoferrate Nanoparticles on a Glassy Carbon Electrode Modified with Carbon Quantum Dots

Hamed Tavakkoli , Morteza Akhond* ,Ghodratollah Absalan

Professor Massoumi Laboratory, Department of Chemistry, College of Sciences, Shiraz University, Shiraz 71454, Iran

*akhond@chem.susc.ac.ir

Introduction: Recently, the use of carbon quantum dots (CQDs) has been reported for electrode surface modification [1, 2]. The CQDs have significantly attracted the attention of the research communities due to their fascinating properties including their size and inexpensive nature. Transition metal hexacyanoferrates, an important kind of multicore inorganic polymers, have also attracted considerable attention due to their open zeolite-like structure and attractive magnetic, optical, and electroactive characteristics. They are widely used in many fields, such as sensing, electroanalysis and electrochromic devices [3]. In this study, a novel electrochemical sensing system based on electrodeposition of silver hexacyanoferrate nanoparticles on a CQD-modified glassy carbon electrode (CQDs/GCE) has been developed for the sensitive determination of uric acid.

Experimentals: Generally, the electrolyte solutions were deoxygenated with pure nitrogen gas (99.999%) bubbling before each experiment and all tests were performed under nitrogen atmosphere at room temperature. The chemicals were of analytical reagent grade and the solutions were freshly prepared with doubly distilled water. The electrochemical measurements were carried out using a computer-controlled autolab electrochemical system equipped with a three-electrode configuration: an Ag/AgCl/KCl (3 M) reference electrode, a platinum disk as a counter electrode. All electrodes were inserted into a 20-mL glass cell.

Results and Discussion: The electrochemical impedance spectroscopy (EIS) was performed to observe the impedance changes of electrode surface during the modification process. As shown in Fig. 1, on the bare GCE (curve A), there was a very small semicircle domain, implying very low electron transfer resistance to the redox-probe dissolved in the electrolyte solution. There was a big semicircle appeared in the high frequency range at the CQDs/GCE (curve B), indicating that CQDs formed a barrier repelling the electron transfer between the bare electrode and the electrolyte. The semicircle was disappeared after electrodepositing nano-silver hexacyanoferrate (AgHCF) on the CQDs/GCE surface (curve C). This suggested a synergistic effect after functionalization of carbon quantum dots with nano-silver hexacyanoferrate which decreased the resistance of electron transfer. During the evaluation of electrocatalytic properties of the modified electrode, it was found that the prepared electrode oxidized UA in well-defined peaks with enhanced oxidation current responses. The electrocatalytic peak currents of UA at the surface of AgHCF/CQDs/GCE were linearly dependent on their concentration. These peak currents were linear up to $3.4 \times 10^{-6} - 7.6 \times 10^{-4} \text{ mol L}^{-1}$. Examination of Fig. 2 showed that the peak current of UA increased with an increase in UA concentration.

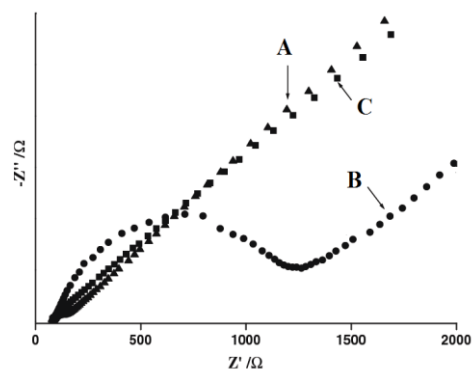


Fig. 1 The EIS of (A) bare GCE, (B) CQDs/GCE and (C) nano-AgHCF/CQDs/GCE recorded in 0.1 M KCl solution containing 2.5 mM $\text{Fe}(\text{CN})_6^{3-}$ and 2.5 mM $\text{Fe}(\text{CN})_6^{4-}$.

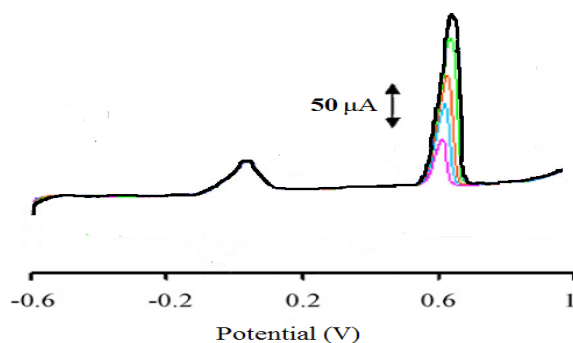


Fig. 2 The LSVs for different concentrations of UA at the AgHCF/CQDs/GCE modified electrode

Conclusion: A sensor for uric acid has been fabricated based on the functionalization of carbon quantum dots with nano-silver hexacyanoferrate. The AgHCF/CQDs nanocomposites were prepared by electrodeposition. Finally, the AgHCF/CQD/GCE was used as an electrochemical biosensor for the sensitive determination of uric acid. The electrode has many advantages such as excellent stability, rapid response, ease of construction and use, good sensitivity and selectivity for the determination of uric acid.

References

- [1] Nguyen, H. V.; Richtera, L.; Moulick, A.; Xhaxhiu, K.; Kudr, J.; Cernei, N.; Polanska, H.; Heger, Z.; Masarik, b, d Pavel Kopel, M.; Stiborova, M.; Eckschlager, T.; Adam, V. , Kizek R.; *Analyst*, **2016**, *141*, 2665-2675.
- [2] Martín-Yerga, D.; Costa Rama, E.; Costa-García, A.; *Analytical Chemistry*, **2016**, *88*, 3739–3746.
- [3] Yang S. ; Li, G.; Wang, G.; Zhao, J.; Qiao, Z.; Qu, L.; *Sensors and Actuators B: Chemical*, **2015**, *206*, 126–132.

Synthesis, characterization and emission properties of the new bis(cyclometalated)platinum complexes and their gold derivatives

Sirous Jamali,^{a*} Sheida Rajabi,^a Shahriar Kermanshahian,^a Niyaz Alizadeh,^a Hamidreza Samouie,^b

^aChemistry Department, Sharif University of Technology, Azadi Ave., Tehran, Iran.

^bDepartment of Chemistry, Texas A&M University, PO Box 30012, College Station, TX 77842-3012.

Email address: sjamali@sharif.ir

Introduction

Luminescent platinum(II) complexes are attracting much attention because of their extensive photochemical and photophysical properties [1–3]. Among all the numerous applications in the area of materials science, the platinum(II) complexes are especially appealing because of their potential use in the development of new tunable optoelectronic molecular devices and dye-sensitized solar cells, as well as in sensor manufacturing and as imaging reagents for biomolecules.[4]

Experimental

The new bis(cyclometalated) platinum(II) complex [Pt(ppy)(ppy')], **1**, in which ppy = 2-(2,4-difluorophenyl) pyridine and ppy' = 2-(*p*-tolyl) pyridine, has been prepared. Reaction of **1** with one equiv. of [Au (PPh₃)]⁺ gave the heterobinuclear complex {Pt[(*p*-tolyl) pyridine][2-(2,4-difluorophenyl)pyridine](AuPPh₃)}, **2**.

Results and Discussion

The bis(cyclometalated) platinum(II) complexes **1** and its gold derivative, **2**, characterised by multinuclear NMR spectroscopy. The solid state structure of **1** further determined using X-ray crystallography. The metal-metal interaction between gold and platinum centres result in red emissive complex **2** that its photophysical properties is under investigation.

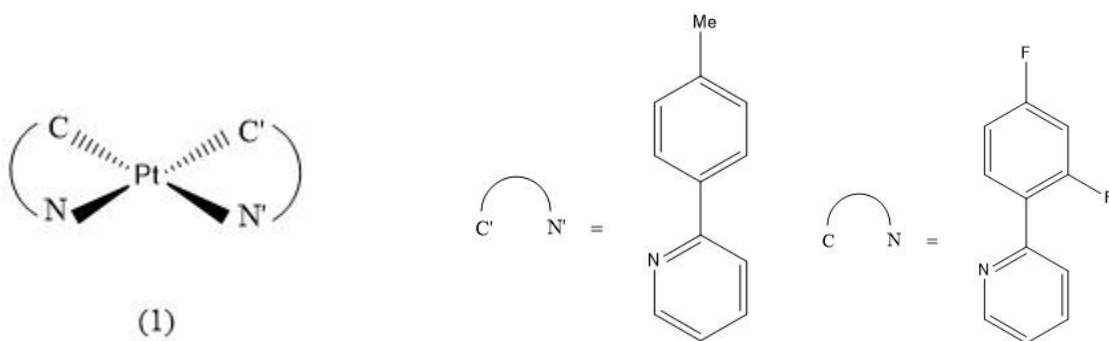


Figure 1. Bis(cyclometalated) platinum(II) complex

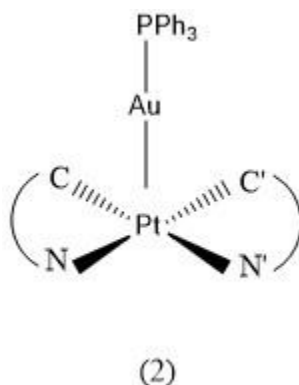


Figure 2. Platinum(II)-gold(I) complex

Conclusion

In summary, the platinum(II) complex, **1** and the platinum(II)-gold(I) complex **2** were prepared, that show good emissive properties in solid state due to metal-metal and π - π , interactions. Complex **1** and **2** are supposed to have remarkable luminescence properties which are under investigations.

References

- [1] Williams, J. A. G. *Top. Curr. Chem.* **2007**, 281, 205–268.
- [2] Maestri, M.; Deuschel-Cornioley, C.; von Zelewsky, A. *Coord. Chem. Rev.* **1991**, 111, 117–123.
- [3] Balashev, K. P.; Puzyk, M. V.; Kotlyar, V. S.; Kulikova, M. V. *Coord. Chem. Rev.* 1997, 159, 109–120.
- [4] Gareth Williams, J. A.; Develay, S.; Rochester, D. L.; Murphy, L. *Coord. Chem. Rev.* **2008**, 252, 2596–2611.

Chemometrics Investigation of the Fluorescence-enhanced Sensing Mechanism of BSA- Gold-nanoclusters to Silver(I) Ions in Aqueous Solutions

Fayezeh Samari^{a,*}, Bahram Hemmateenejad^b, Mojtaba Shamsipur^c

^a Department of Chemistry, College of Sciences, University of Hormozgan, Bandar Abbas, Iran

^b Department of Chemistry, Shiraz University, Shiraz, Iran

^c Department of Chemistry, Razi University, Kermanshah, Iran

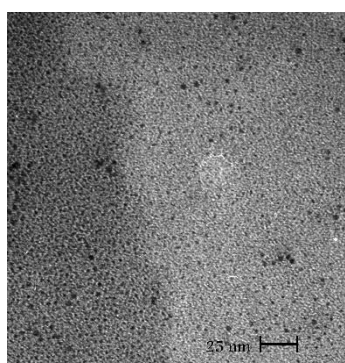
Email address: fsamari@hormozgan.ac.ir, fayezehsamari@gmail.com

Introduction: The study of few-atom metal clusters have become an attractive field as they are the bridge to study the evolution of materials properties from isolated atoms to nanoparticles [1,2]. A recent report [3] showed that when the size of gold or silver particles, possibly being extended to other metals, the reducing activity can be greatly strengthened. And especially, they found that silver ions can be reduced by Au₂₅, and the gold atoms in Au₂₅ were replaced by silver. This reductive phenomenon study encourage us to investigate the mechanism of the enhancing response of BSA- gold-nanoclusters (AuNCs@BSA) toward of silver (I) ions (Ag⁺). The fluorescence emission of AuNCs@BSA was obviously quenched with blue-shifted and then, enhanced in the presence of Ag⁺, while no such changes were observed upon the addition of other metal ions. Then, we aimed to employ well-established MCR–ALS technique [4] coupled with simple fluorescence spectroscopy to explore fluorescence-enhanced sensing mechanism of AuNCs@BSA to Ag⁺ in aqueous solutions.

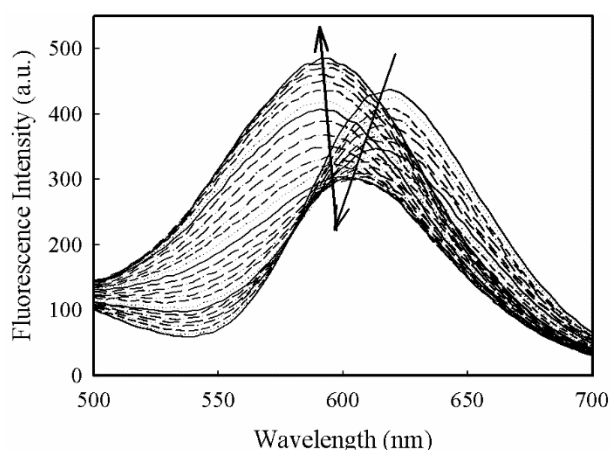
Methods / Experimentals: The AuNCs@BSA were synthesized according to the reported method [5]. Two solutions of AuNCs@BSA with different concentration were prepared in phosphate buffer solution of pH 7.4. Then each solution was titrated manually by successive additions of Ag⁺ solution, followed by fluorescence intensity measurement of solution 5 min after each addition. The total fluorescence profiles obtained in two different solution were arranged in column-wise manner to form an augmented data matrix D. MCR–ALS was employed in order to resolve concentration and pure spectral profiles of involved species.

Results and Discussion: Fig. 1 shows the TEM images of the AuNCs@BSA. Upon excitation at 370 nm, AuNCs@BSA exhibited an emission band at 619 nm, after addition of Ag⁺ the emission band shifted to 604nm with a decrease in intensity and then the emission band shifted to 594nm with an enhancement in intensity (Fig. 2). For chemometrics study, the augmented matrix D was subjected to factor analysis (FA) in order to determine number of independent species involving in this process and we considered 3 principal components for further MCR–ALS analysis. Evolving factor analysis (EFA) was then employed to obtain an

initial estimate of concentration profile. For MCR-ALS, non-negativity constraint was applied to both concentration and spectral profiles. Also, unimodality and closure constraints were applied on concentration profiles. In addition, an increase of NaCl solution to the solution containing Ag^+ + AuNCs@BSA did not show any precipitation while the addition of NaCl to Ag^+ solution causes the turbidity of the solution. The evidences prove that the AuNCs act as reductant to reduce Ag^+ to Ag^0 and finally incorporate to form hybrid Au@AgNCs.



TEM images of BSA-AuNCs. Scale bar is 25 nm.



Fluorescence spectra of the BSA-AuNCs in the presence of increasing concentrations of Ag^+ . The arrows indicate the signal changes by increasing analyte concentrations as, $0 - 4.4 \times 10^{-5}$ M

Conclusion: In summary, we investigated the interaction mechanism of BSA-protected small gold-nanoclusters with silver (I) ions. It is revealed by using fluorescence spectra and chemometrics. The MCR-ALS Analysis of the fluorescence data matrix revealed the presence of 3 chemical species. Also, the results showed that the AuNCs act as reductant to reduce Ag^+ to Ag^0 and finally incorporate to form hybrid Au@AgNCs. Hence, the 3 chemical species revealed by MCR-ALS could be attributed to AuNCs@BSA, Au@AgNCs and an intermediate.

References

- [1] Diez, I.; Ras, R. H. A. *Nanoscale*, **2011**, 3, 1963–1970.
- [2] Shang, L.; Dong, S.; Nienhaus, G. U. *Nano Today* **2011**, 6, 401–418.
- [3] Wu, Z. *Angew. Chem., Int. Ed.* **2012**, 51, 2934–2938.
- [4] Jaumot, J.; Piña, B.; Tauler, R. *Chemometr. Intell. Lab. Syst.* **2010**, 104, 53–64.
- [5] Xie, J.; Zheng, Y.; Ying, J. Y. *J. Am. Chem. Soc.* **2009**, 131, 888–889.

Synthesis of new β -lactams via the Staudinger reaction

Nafiseh kamali nezhad ^{*a}, Mohammad Reza Islami ^b, Behjat Bananezhad, Mahnoosh Rashidi

Department of Chemistry, Shahid Bahonar University of Kerman, Kerman 76169, Iran

n.kamali35@gmail.com

Introduction

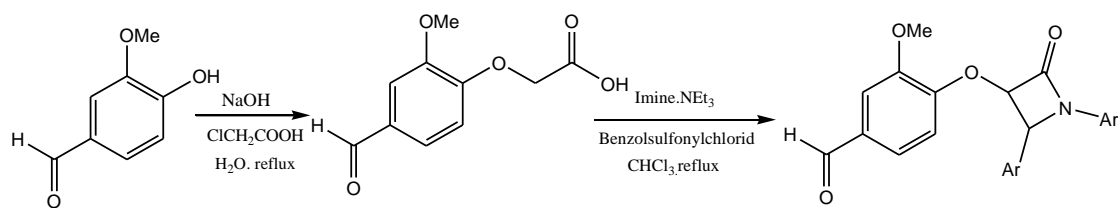
Of the diverse compounds that display antibacterial activities, β -lactams are still considered valuable antibiotics. Monocyclic β -lactams are known to exhibit unique physical and chemical properties due to their structural features. The first synthetic β -lactam was prepared by Hermann Staudinger in 1907 by reaction of the Schiff base of aniline and benzaldehyde with diphenylketene in a [2+2] cycloaddition [1,2].

One of the most important methods for the synthesis of β -lactam is the use of ketenes. Ketenes are highly reactive species in many organic reactions and are usually used in organic synthesis to prepare four- and six-membered rings [3,4].

Vanillin is a phenolic aldehyde, which is an organic compound with the molecular formula $C_8H_8O_3$. Its functional groups include aldehyde, hydroxyl, and ether. It is the primary component of the extract of the vanilla bean. Synthetic vanillin is now used more often than natural vanilla extract as a flavoring agent in foods, beverages, and pharmaceuticals [5].

Experimental

(4-formyl-2-methoxy-phenoxy)-acetic acid was mixed with Benzolsulfonylchlorid, imine and dry Et_3N in anhyd $CHCl_3$ under a nitrogen atmosphere at reflux, and the reaction mixture was stirred overnight. The solution was washed with 8% aq HCl and then with H_2O . The organic layer was filtered, and the solvent removed under reduced pressure. The product was purified by column chromatography using *n*-hexane–EtOAc (10:1 v/v) as eluent. New β -lactams was obtained as sole product.



Scheme 1 Synthesis of the β -lactam compound from (4-formyl-2-methoxy-phenoxy)-acetic acid

Results

The structures of synthesized compounds were established on the basis of their spectral data. Spectral data of compounds were in full agreement with proposed structures. The spectra showed a singlet at $\delta = 3.89$ ppm corresponding to OCH_3 group; two doublet at $\delta = 5.1$ and 5.2 ppm for vicinal methine protons along with a multiplet at $\delta = 6.9\text{--}7.42$ ppm for phenyl ring protons, a singlet at $\delta = 9.89$ ppm corresponding to H of aldehyde. Characteristic ^{13}C NMR signals were shown due to two carbonyl groups at $\delta = 161$ and 191 ppm signals at $\delta = 63.11$ and 55.9 ppm for two methine and signals at $\delta = 63$ ppm for methoxy group. The IR spectra of these compounds showed absorption bands due to the carbonyl group at $1643\text{--}1763\text{ cm}^{-1}$.

[1] [Hermann Staudinger](#). "Zur Kenntniss der Ketene. Diphenylketen". Justus Liebigs Ann. Chem. 1907 **356** (1-2): 51–12

[2] Fisher, J. F.; Meroueh, S. O.; Mobashery, S. *Chem. Rev.* 2005, 105, 395–424

[3] Leung-Toung, R.; Wentrup, C. J. *Org. Chem.* 1992, 57, 4850–4858.

[4] Allen, A. D.; Lai, W. Y.; Ma, J.; Tidwell, T. T. J. *Am. Chem. Soc.* 1994, 116, 2625–2626.

[5] Brenes, Manuel; Aranzazu García; Pedro García; José J. Rios; Antonio Garrido. *Journal of Agricultural and Food Chemistry*. 1999 **47**(9): 3535–3540

Electrochemical determination of glutathione in hemolysed erythrocyte by modified glassy carbon electrode

M .Mazloun-Ardakani , Z. Tavakolian- ardakani*, A. Khoshroo

Department of Chemistry, Faculty of Science, Yazd University, Yazd, 89195-741, Iran

tavakolianz@yahoo.com

Introduction:

Glutathione (GSH) is a biological compound widely distributed in living cells from microbes to higher organisms. It is found mainly in its reduced form being the most abundant nonprotein sulfhydryl compound in cells [1]. The level of glutathione in blood may reflect glutathione status in less accessible tissues. Thus, measurement of (GSH) in blood is essential and can be used as an indicator of disease risks in humans [2].

In this paper, was determinated GSH by multiwall carbon nanotubes (MWCNT_s) - modified glassy carbon electrode (GCE). (2Z,4E) -3-(3,4- dihydroxy phenyl) -1,5-bis(2,4-dinitrophenyl) formazon (DPBDF) used as a mediator between the analyte and electrode surface.

Methods / Experimentals:

The electrocatalytic oxidation of GSH was investigated at the surface of modified electrode using cyclic voltammetry (CV), differential pulse voltammetry (DPV) and chronoamperometry. The morphology of nanomaterial was characterized using scanning electron microscopy (SEM).

Results and Discussion:

The electrocatalytic behavior of DPBDF was investigated Its quasi-reversible behavior revealed. The pH range studied (pH 3-10) and exhibited a diffusion-controlled behavior. Fig. 1 shows the CVs behaviors of the bare GCE and MWCNT-DPBDF-GCE in the absence and presence of 2.0 mM GSH at a potential scan rate of 30 mVs⁻¹. The anodic peak at about 0.3 V was appeared.

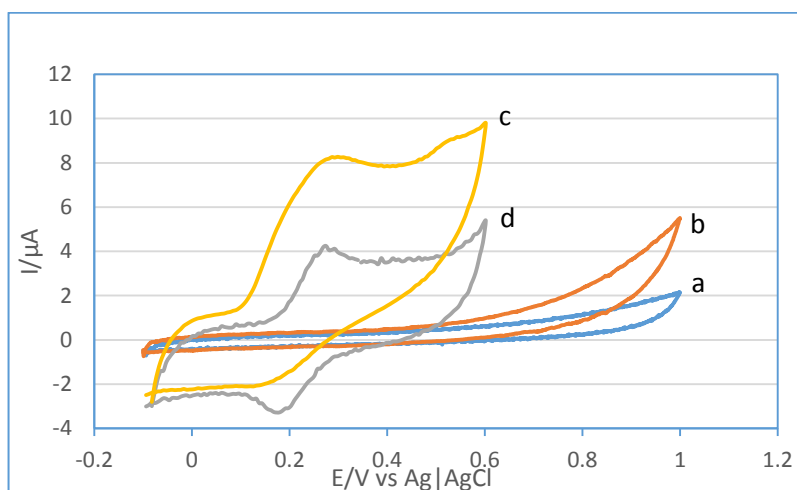


Fig.1. Cyclic voltammograms (a) in the absence and (b) presence of 2.0 mM GSH in phosphate buffer solution (pH 7.0) at the surface of GCE at scan rate 30 mVs⁻¹. (c) as (b) and (d) as (a) at the surface of modified MCNT- GCE

The influence of some GSH metabolites and structurally related substances of common blood components on the assay were also examined, since this electrode is to be applied in erythrocyte samples. The results showed that l-ascorbic acid produced a slight increase in the sensor response. A slight interference from cysteine was also observed, due to the structural similarity between this compound and the GSH molecule. Although both l-ascorbic acid and cysteine showed slight interferences, they are normally not present at a significant levels in erythrocyte samples [3]. The other interfering compounds (glutamic acid, glucose, glycine, , ...) did not show significant interferences on the sensor response.

DPV was used for determination and quantitation of GSH in three different hemolysed erythrocyte samples by the standard addition method. Calibration curve was obtained by using DPV technique. Linear dynamic range was between 0.05 and 100.00 μM . The modified electrode showed good stability and repeatability.

Conclusion:

The novel voltammetric sensor is developed for the determination of GSH. It can be used for real sample analysis. This mediator shows excellent catalytic effects on the oxidation of GSH. It has been found that with CV the oxidation of GSH occurs at a potential of about +0.3V. The method is rapid, reproducible, selective, and sensitive for the determination of GSH.

References:

- (1) Ohmori S, Kawase T, Higashiura M, Chisaka Y, Nakata K, Yamasaki Y. High-performance liquid chromatographic method to analyze picomole levels of glutathione, cysteine and cysteinylglycine and its application to pre-cancerous rat livers. *J Chromatogr B* 2001;762:25–32.
- (2) Pastore A, Feredici G, Bertini E, Piemonte F. Analysis of glutathione: implication in redox and detoxification. *Clin Chim Acta* 2003;333: 19–39.
- (3) P. Calvo-Marzal, K.Y. Chumbimuni-Torres, N.F. Hoehr, L.T. Kubota, *Clin. Chim. Acta* 371 (2006) 152.

Comparative investigation on the effective role of patch-clamp techniques during following the interaction between stem-cell and ionic species: Effective role of voltammetry

Sajedeh Karami, Mohamad Mehdi Doroodmand,*

Department of Analytical Chemistry, Shiraz University, Shiraz, Iran

*E-mail: doroodmand@shirazu.ac.ir.

Introduction:

The patch clamp technique was first used by Neher and Sakmann (1976) to resolve currents through single acetylcholine-activated channels in cell-attached patches of membrane of frog skeletal muscle. The method they used and subsequent refinements have led to techniques for high resolution recording of current in excised membrane patches in addition to those that remain cell-attached. Single channel recording yields information about unitary conductance and kinetic behavior of ionic channels already partly investigated by classical voltage clamping and by noise analysis; it is also leading to the discovery of new classes of ion channel [1]. Neuronal activity is dominated by synaptic inputs from excitatory or inhibitory neural circuits. With the development of *in vivo* patch-clamp recording, especially *in vivo* voltage-clamp recording, researchers can not only directly measure neuronal activity, such as spiking responses or membrane potential dynamics, but also quantify synaptic inputs from excitatory and inhibitory circuits in living animals. This approach enables researchers to directly unravel different synaptic components and to understand their underlying roles in particular brain functions [2].

Methods / Experimental:

Margrie et al. firstly systematically introduced the *in vivo* blind-patch procedure in 2002. In blind patch mode, the recording pipette is moved forward to hunt for cells without visual guidance. Electrophysiological signals read from the pipette tip can provide helpful information. A change in seal resistance reflects the distance between the pipette tip and nearby neurons. An increase in pipette resistance and the occurrence of tiny spikes and pulsation-like waveforms may indicate that the pipette is approaching a nearby cell. The recorded spike shapes can provide helpful clues to identify the cell type of the recorded neuron (presumably). For example, excitatory pyramidal cells usually have a longer trough-to-peak interval than parvalbumin expressing (PV+) inhibitory interneurons.

Results and Discussion:

In most cases, *in vivo* patch-clamp recordings are performed in superficial regions. *In vivo* whole-cell recording from neurons 2~5 mm below the brain surface, such as in the hippocampus or thalamus has also been reported. There is no clear limitation of recording depth for *in vivo* patch-clamp recording. But the pipette tip is more easily contaminated when penetrating into

deeper nuclei. One possible solution is to use a “guiding tube” to create a clean path for the recording pipette. There are also other methods (Fig. 1), such as the removal of superficial tissue to expose the recording area. It remains more difficult to perform patch-clamp in deeper nuclei such as the basal ganglia **in vivo**, so experimenters have chosen different ways, such as ex-vivo patch-clamp.

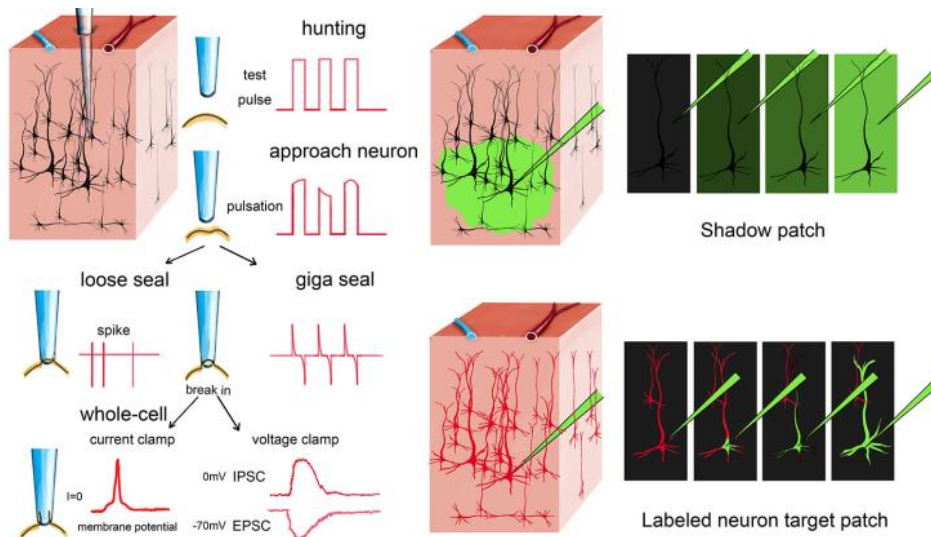


Fig. 1. Effective role of stem-cell during interaction with ionic species [1].

Conclusion:

In this study, we present an optimized cell application protocol minimizing the amount of cells required for an automated patch clamp system, the Patchliner. We demonstrate that this procedure is applicable to hIPS cell-derived neurons and Hg^{+2} playing a particular role in screening, as well as primary pancreatic islet cells. Our protocol makes automated patch clamp recordings compatible with the study of expensive cells and low-yield primary cell preparations. We think that this optimization will substantially enhance the efficiency and applicability of automated patch clamp in drug development and safety screening.

References:

- [1] Boyden, E.S. & Raymond, J.L. Neuron 39, 1031–1042 (2003).
- [2] Chow, B.Y. et al. Nature 463, 98–102 (2010)

Design and synthesis of new derivatives of 2-Thiocoumarin as 15-lipoxygenase inhibitors

Elahe Khavari Moghadam^a, Seyed Mohamad Seyedi^{b*}, Mostafa Gholizade^c, Hamid Sadeghian^d, Atena Jabari^e

^a Department of Chemistry, School of Sciences, Ferdowsi University of Mashhad, Mashhad, Iran

^b Department of Chemistry, School of Sciences, Ferdowsi University of Mashhad, Mashhad, Iran

^c Department of Chemistry, School of Sciences, Ferdowsi University of Mashhad, Mashhad, Iran

^d Department of Biology, Faculty of Sciences, Ferdowsi University of Mashhad, Mashhad, Iran

^e Department of Chemistry, School of Sciences, Ferdowsi University of Mashhad, Mashhad, Iran

Email address : smseyedi@um.ac.ir

Introduction:

15-Lipoxygenases are a family of iron-containing proteins that have the capability for unsaturated fatty acid peroxidation in animals and plants. Human lipoxygenase can be set in two Subgroup 15-LO-1 and 15-LO-2. In terms of tissue distribution or enzyme properties, 15-LO-1 is converted linoleic acid and arachidonic acid to related metabolites. Studies show that 15-LO-1 can be affect process of developing coronary artery disease. Therefore, strong efforts is taken seeking and synthesis of specific and appropriate inhibitors of enzymes that is involved in fatty acid oxidation of arachidonic. In this research, with design and synthesis thiocoumarin derivatives, we intend to find the chromophore groups in coumarin structure for example thio group. Also with synthesize prenyloxy thiocourin derivatives SAR study had been done.

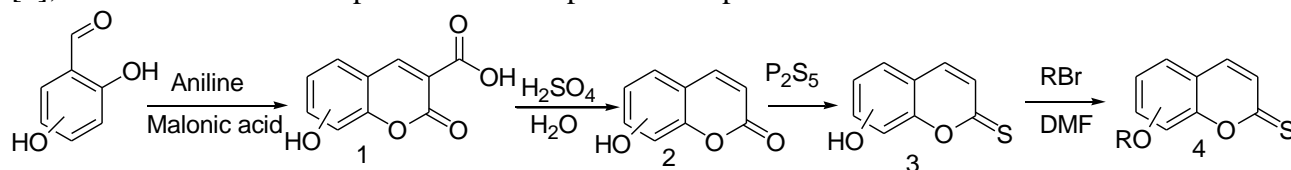
Methods / Experimentals:

In the first step, by using malonic acid, aniline and suitable benzaldehyde in reflux condition, 3-carboxylic coumarin (compound 1) was produced. In the second step, from hydrolysis of product that prepared in the previous reaction in reflux, in present of concentration sulfuric acid and H₂O with accompanied by the emission of CO₂. The next step involved adding Phosphorus pentasulfide and produced intended thiocoumarin which in continue with using prenyl bromide compound 4 has been synthesized [1].

Results and Discussion:

According to scheme 1, after hydrolysis of 3-carboxylic coumarin and making 2-thiocoumarin, the intended derivatives obtained by reaction of prenyl bromids and base in DMF. The inhibitory activity of the synthetic compounds against soybean 15-LOX was determined utilizing modified catalytic oxidative coupling of 3-methyl-2-benzothiazolinone (MBTH) with 3-(dimethylamino) benzoic acid (DMAB) as reported in previous studies. In this method, the basis for the determination of lipoxygenase activity is the measurement of peroxide concentration. Among the synthetic O-prenylated compounds, 5-farnesyloxy had the best result on the soybean 15-LOX. Bonding affinity of the designed molecular structures toward soybean 15-LOX was studied. Docked conformers were generated in AutoDockTools (ADT) software. This convergence was significantly observed for farnesyl and geranyl derivatives. In the earlier mentioned cluster (LFC), most of the conformers have hydrogen bonds with Fe-OH core through their thio groups and their prenyl portion are covered by side chain of some of amino acids in active side. In addition, the ability of the prenyl portion of the compounds to fill the lipophilic pocket which is formed by Ile663, Ala404, Arg403 (butyl portion), Ile400, Ile173 and Phe167 side chains can

explain the direct relationship between lipoxygenase inhibition potency and prenyl length chain. To find the effect of thio group on inhibitory potency, lipoxygenase inhibition of the synthetic compounds was also compared to the related analogs with no thio group substituent. For this purpose, lipoxygenase inhibitory of O-farnesyl derivatives of 5-, 6-, 7-, and 8-hydroxythiocoumarin, and their inhibitory activity against 15-LOX reported in previous study [3], were measured in comparison with the present compounds.



Scheme 1

Conclusion :

All of the favorite mono prenyloxythiocoumarins were synthesized and their inhibitory potency against SLO were evaluated. The SAR studies showed the importance of prenyl length in SLO inhibition. It was also found that for farnesyl derivatives the role of thiocoumarin substitution site in SLO inhibition is very predominant. The observed inhibition differences between the mentioned enzymes originated from chemical nature and hydrophobic property of their active side pocket residues [3].

References:

- [1] Rafat M; El-Khatib. Indian Journal of Chemistry, **2002**, 41A, 1575- 1579.
- [2] L. Toledo; L. Masgrau; J.D. Marechal; J.M. Lluch; A. González-Lafont. The Journal of Physical Chemistry, **2010**, 114, 7037–7046.
- [3] M. Iranshahi; A. Jabbari; A. Orafaie; A. Mehri; R.S. Zeraatkar; T. Ahmadi; M. Alimardani; H. Sadeghian. European Journal of Medicinal Chemistry, **2012**, 57, 134–142.

Degradation kinetics study of Rhodanin in the presence of nanostructured TiO₂

Shiva Joohari^a and Morteza Montazerzohori

^aDepartment of Basic Sciences, Yasooj Branch, Islamic Azad University, Yasooj, Iran

^bDepartment of Chemistry, Faculty of Sciences, Yasouj University, Yasouj, Iran

Corresponding author Email: Shjoohari@yahoo.com

1. Introduction

Organic dyes as one important class of pollutants insert toxicity and carcinogenic agents into wastewaters. Therefore, there are many attentions for removal from wastewater before its discharge into environment. Photocatalytic process as a clean method is able to decolorize and to remove organic dye from wastewater by high oxidant species such as hydroxyl radicals[1-5]. Titanium dioxide is the most common semiconductor that well photocatalytically catalyze degradation of many pollutants. In this work, kinetic study of photocatalytic degradation of rhodanin using titanium dioxide nanoparticles with average size of 15 nm is described.

Keywords: kinetics, degradation, nanostructure.

2. Experimental

Chemical reagent for preparation were provided from Merck, Fluka and/or Sigma-Aldrich companies and used without further purification. rhodanin was purchased from Merck. Nano-titanium dioxide (99.9%) in anatase phase with particle sizes of 15 nm was used as photocatalyst. A photoreactor system equipped with 400W high pressure mercury lamp was applied for photodegradation processes. A UV-visible instrument was applied for following of dye concentration. At each experiment the photocatalyst was removed from irradiated suspension by a centrifuge. F60 pH-meter was applied for check of pH after preparation of each medium.

3. Result and discussion

Various amounts of photocatalyst were loaded under the same photocatalytic process at each pH to achieve the optimum amount of photocatalyst. The results of this investigation are observable as residual concentration- catalyst amount plots that were obtained after 1 hour irradiation of suspensions in figure 1.

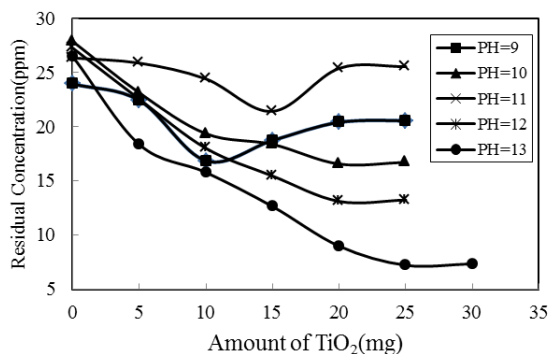


Fig. 1. Effect of photocatalyst amount on the residual concentration after 1 hour irradiation.

Kinetic behaviors of dye photocatalytic removal was found to obey from pseudo-first-order model because the plots of $\ln(C_0/C_t)$ of dye versus irradiation time as exhibited in figure 2 (in which, C_0 and C_t are concentration at time =0 and t) are linear with good linear regression coefficients (R).

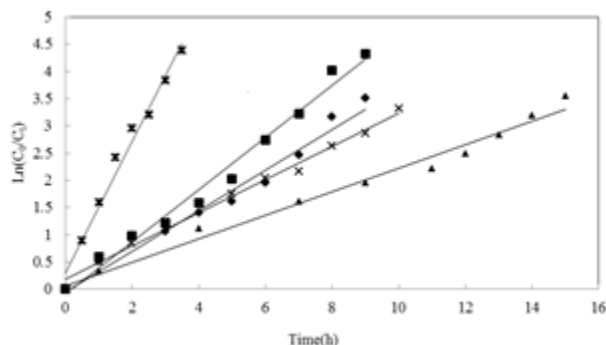


Fig. 2. $\ln(C_0/C_t)$ of dye versus times plots at various buffer pHs (pH=9 (♦), pH=10(■), pH=11(▲), pH=12(×) and pH=13(*)).

Conclusion

In this research, photocatalytic degradation kinetics of rhodanin by use of titanium dioxide nano particles with average size of 15 nm under high pressure mercury lamp (400 W) irradiation was performed. Kinetic behaviors of photocatalyt process were well fitted into Langumuir-Hinshelwood kinetic model. K_{obs} and k_r were evaluated in the range of 0.215- 1.116 h^{-1} and 19.61-500.00 $mg \cdot L^{-1} \cdot h^{-1}$ respectively.

References

- [1] Ahmed S., Rasul M.G., Brown R., Hashi M.A., . Environ. Manag., 92(3) (2011) 311–330.
- [2] Al-Rasheed R., Cardin D. J., Appl. Catal. A, 246(1) (2003) 39–48.
- [3] Alkan M., Demirbaş O., Dogan M., Fresenius Environ. Bull., 13(11a) (2004) 1112-1121.
- [4] Aquino J. M., Rocha-Filho R. C., Bocchi N., Biaggio S. R., J. Appl. Electrochem., 40(10) (2010) 1751-1757.
- [5] Allen N. S., Edge M., Sandoval G., Verran J., Stratton J., Maltby J., *Photochem. .Photobiol.*, 81(2005) 279–290.
- [6] Montazerozohori M., Habibi M. H., Joohari S., Khodadostan, V., Annali Dichimica, 97(10) (2007) 1015-1026.
- [7] Montazerozohori M., Nasr-Esfahani M., Nezami S., Mojahedi S., Fresenius Environ. Bull., 20(2011) 1836-1840.

Theoretical study of Structure and Electronic Properties of Adamantane and its Si-doped structures

Forough Kalantari Fotooh^{1a*}, Mehdi Atashparvar^a

^aDepartment of chemistry, Yazd branch, Islamic Azad University, Yazd, Iran.

Email address: f_kalanrtari_f@iauyazd.ac.ir

Introduction: Diamondoids have major applications in nanotechnology, drug delivery and medicine due to their six or more linking groups and their special physical and chemical properties [1-3]. The smallest possible of these polycyclic diamondoids is adamantane (C_6H_{12}) with unique physical and chemical properties. DFT calculations for adamantane show that they are nonreactive, and interact weakly with each other [2]. Substituting H and C-H groups with different atoms and functional groups like N, Na, B and O atoms changes its electronic properties such as, the HOMO-LUMO gap, conductance and binding energy [3-5].. A recent report by Ficher, Baumgartner and Marschner (FBM) of synthesis of sila-adamantane is a breakthrough in the synthesis of sila-adamantane [6]. Followed by this report, electronic structure of $C_{24}Si_{14}H_{72}$ within Perdew- Burke- Ernzerh of density functional model was reported [7]. In this paper, we have doped one to ten carbon atoms of adamantane with Si atoms and investigated their structure and electronic properties using density functional theory.

Computational method: Our calculations are based on the ab initio density functional theory (DFT) within three parameter B3LYP/6-31+G** functional. The natural bond orbital (NBO) calculations and all calculations of HOMO-LUMO gaps were also performed at the same level of theory. Gaussian03 package was used for all calculations.

Results and discussion: Figure 1 shows the optimized structure 1-10 sila- adamantane together with their isosurfaces plot of HOMO and LUMO states. The C-C bond length in adamantane is 1.54Å. C/Si doping in adamantane increase the C-C bond lengths to 1.56 Å.

The Si-C bond lengths are about 1.90 Å and the Si-Si bond lengths are 2.36 Å. It can be observed from isosurfaces plot of HOMO and LUMO states in figure 1, HOMO of adamantane is mostly related to C(1)-H bond, while its LUMO isosurface is diffused over hydrogen atoms. It can be also seen from figure 1 that HOMO state of 1-sila adamantane is not concentrated on Si-H bond. The same orbital distribution can be observed for 2 to 5-sila adamantane. The LUMO of 6-10 sila adamantane is related to Si-H bond with an anti-bonding character. 10-sila adamantane has a low energy gap about 6.3 eV. According to figure 1, HOMO state of this particle is nearly localized over Si-C bonds.

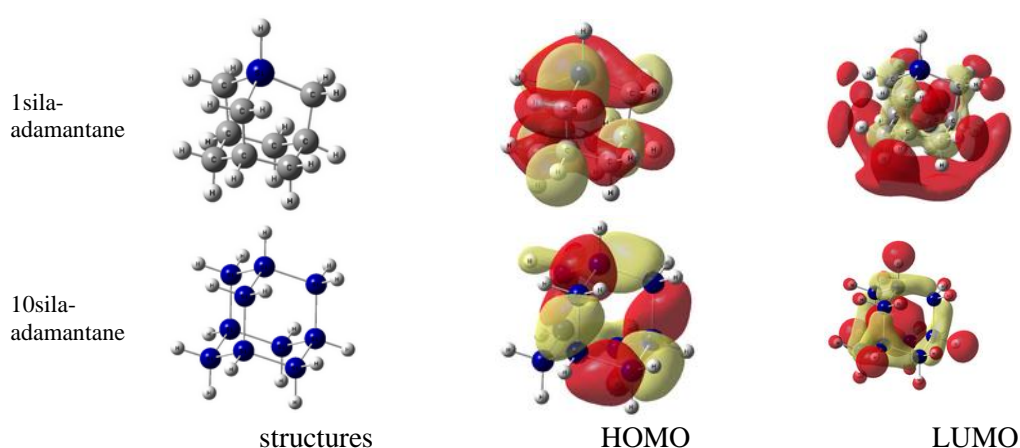


Figure 1: Optimized structure of 1,10 Si-doped adamantane and their isosurfaces plot.

Conclusion: The structural results show that X(1)-H sites of adamantane and sila-adamantane is the most favorable site for doping. Doping with silicon atoms lowers the energy gap in most structures. Any way 6-Sila adamantane show the highest energy gap among all structures.

Refrencess:

- [1] Mansoori G.A. Diamondoid Molecules. *Advances in Chemical Physics*: John Wiley & Sons, Inc.; **2008**, P 207-258.
- [2] McIntosh G.C., Yoon M., Berber S., Tománek D. *Physical Review B*. **2004** 70, 045401.
- [3] Xue Y., Mansoori G.A., *Int J Mol Sci*. **2010** 11, 288-303.
- [4] Hamadani M., Khoshnevisan B., Fotooh F.K. *THEOCHEM*. **2010** 961, 48- 54.
- [5] Bibek A., Maria F. *Nanotechnology*. **2015** 26, 035701.
- [6] Fischer J., Baumgartner J., Marschner C. S. *science*. **2005** 310, 825-825.
- [7] Pichierri F. *Chemical Physics Letters*. **2006** 421, 319-323.

Synthesis of 4-phenylthiophene-3-carbonitrile derivatives via one-pot Gewald reaction

Parinaz Vakiliyan^a, Atefeh Hadizadeh^a, M. Saeed Abaee^{a,*}, Mohammad M. Mojtahedi^a

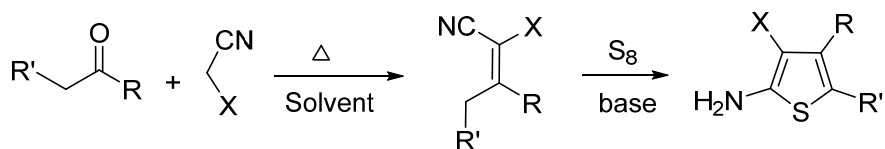
^aChemistry and Chemical Engineering Research Center of Iran, Tehran, Iran.

Email: abaee@ccerci.ac.ir.

Introduction

The Gewald reaction is an organic reaction involving the condensation of a ketone or an aldehyde with an activated nitrile and elemental sulfur in the presence of a suitable base to give substituted 2-amino-thiophenes [1]. The first step of the Gewald reaction is usually a Knoevenagel condensation producing an acrylonitrile which then undergoes nucleophilic addition with sulfur [2]. The 2-aminothiophene derivatives are important heterocycles with diverse applications in dye industry, pharmacy and agriculture [3].

There are many articles reported under microwave irradiation, heating and sonication in this regard [4-5]. In this context, we described new conditions for both the Knoevenagel and Gewald reactions and their application in the synthesis (Scheme 1). The high efficiency and ease of product isolation persuaded us to investigate the Gewald reaction of acetophenone derivatives under thermal and ultrasonic conditions.



Scheme 1. 2-aminothiophene synthesis via Gewald reaction

Experimental

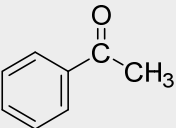
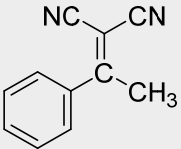
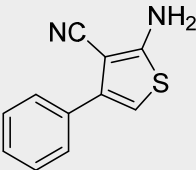
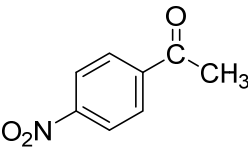
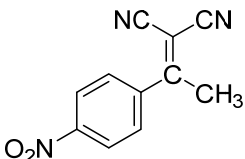
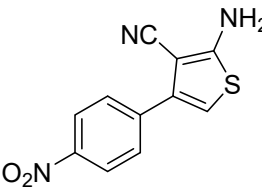
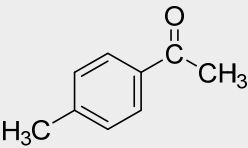
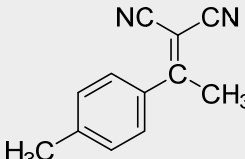
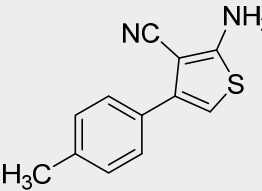
Ketone (2 mmol) was mixed with activated nitrile (2 mmol) in solvent (H₂O/EtOH) (4 ml) at 80 °C. When TLC showed completion of the first step (formation of desired Knoevenagel product), to this mixture were added sulfur (2 mmol) and trimethylamine (2 mmol). The reaction was monitored by TLC experiments. After 4 hours the mixture was diluted with CH₂Cl₂ and washed with water. The organic phase dried over Na₂SO₄. Upon concentration, the mixture solidified, and the solid was recrystallized by means of petroleum ether to obtain the final product.

Results and Discussion

In continuation of the previous studies and to develop green chemistry, we decided to evaluate Gewald reaction. We first investigated a model reaction by reacting acetophenone with malononitrile and elemental sulfur in water as solvent (Table 1, entry 1). To show the generality of the method, the optimized conditions for other ketones were used. Therefore, derivative bearing electron donating (Table 1, entry 2) and electron withdrawing (Table 1, entry 3) substituents of acetophenone underwent reactions.

It was concluded, the use of water as the solvent, gave high yields of products in shorter times than ethanol. It is notable that acetophenone with electron-donating substituent obtained less yields than acetophenone with electrone withdrawing substituent.

Table 1

Entry	Ketone	Knoevenagel product	Gewald product	Time (h)	Yield (%) ^a
1				7	88
2				7	81
3				7	54

^a GC yields.

Conclusion

In this study, we described a new methodology for the synthesis of 2-aminothiophenes via sonication or conventional heating in aqueous media in good yields.

References

- [1] Puterová, Z.; Krutošiková, A.; Véghe, D. *Arkivoc*, **2010**, 206-246.
- [2] Huang, Y.; Dömling, A. *Mol. Divers.*, **2011**, *15*, 3-33.
- [3] Barnes, D. M.; Haight, A. R.; Hameury, T.; McLaughlin, M. A.; Mei, J.; Tedrowy, J. S.; Riva Toma, J. *Tetrahedron*, **2006**, *62*, 11311-11319.
- [4] Sridhar, M.; Rao, R. M.; Baba, N. H. K.; Kumbhare, R. M. *Tetrahedron*, **2007**, *48*, 3171-3172.
- [5] Liang, C.; Lei, D.; Wang, X.; Zhang, Q.; Yao, Q. *J. Sulfur Chem.*, **2013**, *34*, 458-463.

Conformational Analysis and Intramolecular Hydrogen Bonding in 4-Butylmino-3-Penten-2-One

Ali Reza Berenji^{a,*}, Samira Soltani^b, Mohammad Vakili^c

^aAcademic Center for Education, Culture, and Research (ACECR), Mashhad 91779, Iran

^bDepartment of Chemistry, Ferdowsi University of Mashhad, International Campus, Mashhad 91779, Iran

^cDepartment of Chemistry, Ferdowsi University of Mashhad, Mashhad 91779, Iran

Email address: aberenji@gmail.com

Introduction: β -Enaminones are a group of compounds which form an intramolecular hydrogen bonded system assisted by resonance [1]. This special hydrogen bonding makes them to play the role of a good ligand to provide useful complexes. To identify the structure and stability of these complexes, the structure and intramolecular hydrogen bond strength of these ligands should be investigated.

In this study, all theoretically possible conformers of 4-butylamino-3-penten-2-one (BPO), a β -ketoamine, are optimized using density functional theory (DFT) to identify the stable conformers. The hydrogen bond strength in all stable structures is estimated by considering the geometrical parameters obtained from the DFT calculations and also by calculating the hydrogen bond energies using Bader's atoms in molecules (AIM) theory.

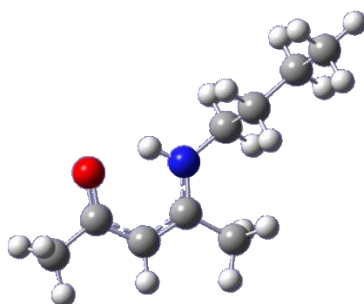


Fig.1. One of the stable conformers of 4-butylmino-3-penten-2-one

Methods: All calculations have been performed at the B3LYP/6-311++G** level of theory, using Gaussian 09 program [2]. To obtain the stable conformers of the titled molecule, the different conformers were considered by rotating the molecule about its bonds (Fig. 1). The vibrational wavenumbers were calculated to confirm the optimization process. The electron densities, Laplacian of the critical point of $\text{NH}\cdots\text{O}$ bond, and the hydrogen bond energies were calculated by AIM2000 program [3].

Results and Discussion: According to our calculations, 2 stable conformers were obtained. They were the same and the difference between them is the location of butyl group above or below the surface of the molecule. The $\text{N}\cdots\text{O}$ distance is 2.664 Å. It confirms that the hydrogen bond in this molecule is slightly stronger than that in 4-amino-3-penten-2-one (APO) [4]. The corresponding value is 2.671 Å. The difference between the studied compound and APO is the substitution of the $-\text{NH}_2$ group by the

–NHC₄H₉ group in APO. According to our study, two factors are responsible for this interesting bond strength, i.e., steric effect and inductive effect. The results obtained from AIM and NBO calculations also confirm the above conclusion.

Conclusion: The molecular structure and the intramolecular hydrogen bond strength of BPO were predicted using DFT calculations (B3LYP/6-311++G(d,p)). The results were in good agreement with the AIM results. All theoretical results indicate that substitution of a n-butyl group with a hydrogen atom adjacent to the nitrogen atom, slightly strengthens the intramolecular hydrogen bond in comparison with APO.

References

- [1] S. Soltani-Ghoshkhaneh; M. Vakili; S.F. Tayyari; A.R. Berenji. *J. Mol. Struct.*, **2016**, 1103, 35.
- [2] M. J. Frisch; et al., Gaussian 09, Revision A.02, Gaussian, Inc., Wallingford CT, **2009**.
- [3] F. Biegler-König; J. Schönbohm; D. Bayles. *J. Comp. Chem.*, **2001**, 22, 545.
- [4] A.R. Berenji; S.F. Tayyari; M. Rahimizadeh; H. Eshghi; M. Vakili; A. Shiri. in: A. Afkhami (Ed.). *Book of Abstracts of 15th Iranian Chemistry Congress*, Bu-Ali Sina University, Hamedan, **2011**, p. 1065.

Cyclocondensation of 2-Aminobenzimidazole with Dimedone and its Benzaldehyde derivatives

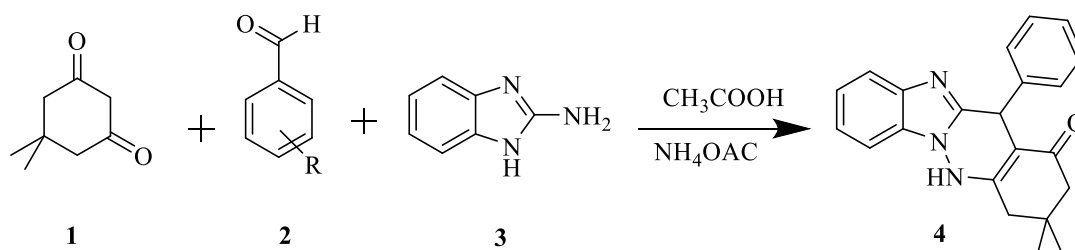
Hossein Mehrabi ^a and Anita Azizian-Broojen ^{a*}

^a Department of Chemistry, Faculty of Science, Vali-e-Asr University of Rafsanjan, Rafsanjan 77176
(E-mail: aziziananita@yahoo.com).

Introduction: Regiodirectivity in the cyclizations of α -amino azoles with carbonyl 1,3-biselectrophiles is the subject of a series of studies [1-5]. However, work in this area has not lost current interest because of the many reagents used in similar reactions.

Experimental: A mixture of 5,5-dimethylcyclohexane-1,3-dione **1** (0.28 g, 2 mmol), benzaldehydes **2** (0.2 ml, 2 mmol) with one drop of acetic acid in solvent-free in 100 °C for appropriate time, in following, 2-aminobenzimidazole **3** (0.133 g, 1 mmol) in acetic acid (3 ml) and ammonium acetate (0.08 g) was heated for 24 h in 100 °C. The completion reaction was identified by TLC, the mixture was cooled, precipitated was filtered and residue with chloroform produce yellow solid, and compound **4** was filtered off and recrystallized from ethanol.

Results and Discussion: In this work, we demonstrate study of the reaction of 2-aminobenzimidazole **3** in acetic acid as solvent with the substituted benzaldehydes **2** and dimedone **1**, for the produce of the intermolecular condensation of 3,3-dimethyl-12-phenyl-3,4,5,12-tetrahydrobenzo [4,5] imidazo[1,2-b] cinnolin-1(2H)-ones. Our study indicated that the initial compaction of benzaldehydes and dimedone occurred, in the preceding the attack of nitrogen ring of aminobenzimidazole at carbon in attach of benzene of intermediate and cyclization at the carbonyl position of dimedone (Scheme 1).



Scheme 1: Reaction of dimedone, substituted benzaldehydes and 2 aminobenzimidazole

Conclusion: In conclusion, the synthesis of 3,3-dimethyl-12-phenyl-3,4,5,12-tetrahydrobenzo [4,5] imidazo[1,2-b] cinnolin-1(2H)-ones from the reactions of 2-aminobenzimidazole with substituted benzaldehydes and dimedone have been studied.

References

- [1] Kost, A. N., *Khim Geterotsikl. Soedin*, **1980**, 1200.
- [2] Fisher, G. *Adv. Heterocycl. Chem.*, **1993**, 57, 81.
- [3] Yamashkin, S. A; Kucherenko, N. Ya; Yurovskaya, M. A. *Khim. Geterotsikl. Soedin.*, **1997**, 579.
- [4] Desenko, S. M; Orlov, V. D; Estrada, Kh. *Khim. Geterotsikl. Soedin.*, **1990**, 999.
- [5] Lipson, V. V; Desenko, S. M; Shishkina, S. V; Shirobokova, M. G; Shishkin, O. V; Orlov, V. D. *Chemistry of Heterocyclic Compounds*, **2003**, 39, 1041.

Preconcentration and spectrofluorimetric determination of valsartan in biological samples

Fatemeh golshani sabet^a, Tayyebah madrakian^{b,*}, Abbas afkhami^c

^{a,b,c} Faculty of Chemistry, Bu-Ali Sina University, Hamedan, Iran

Email: Madrakian@gmail.com

1.Introduction:

Valsartan is a potent, orally active nonpeptide tetrazole derivative which causes reduction in blood pressure and is used in treatment of hypertension. Valsartan is 3-methyl-2-[pentanoyl-[4-[2-(2*H*-tetrazoyl-5yl) phenyl] phenyl] methyl] amino] butanoic acid, with empirical formula C₂₄H₂₉N₅O₃. Valsartan is not extensively metabolized and is mainly excreted by non-renal routes [1]. Several methods like thin-layer chromatography-densitometric method [2], liquid chromatographic system with fluorescence detection [3] and capillary electrophoresis [4], have been reported for determination of valsartan in biological systems. But these methods are expensive and not economically. In this study, we report a novel spectrofluorimetric method for the determination of Valsartan by magnetic nanoparticle.

2.Methods/ Experimental:

Magnetic nanoparticles (MNSs) were synthesized by the solvothermal reduction method with minor modifications [5]. Then, these MNSs were used to prepare silica coated magnetite nanospheres (SCMNSs). Finally the surface of SCMNSs was modified by 3-aminopropyltriethoxysilane as amine functional groups. The resultant product (NH₂-SCMNSs) was collected.

2.1 general procedure

The interaction of valsartan and NH₂-SCMNSs was followed spectrofluorimetrically by monitoring the change in the fluorescence intensity of valsartan after adsorption on the surface of NH₂-SCMNSs and desorption of the nanoparticles surface in optimum conditions.

3.Results and Discussion:

Prepared NH₂-SCMNSs were characterized by TEM, XRD and FT-IR measurement. Solution pH important parameter that affects adsorption process of valsartan. The solution pH would affect both aqueous chemistry and surface binding-sites of the adsorbent. The effects of pH were tested in the range 2.0-10.0 using Britton-Robinson buffer with ultrasonication time of 15 min and nanospheres dosage of 3.50 mg . in this condition we reached maximum signal at pH 4.0. In order to optimize the use of NH₂-SCMNSs , it is important to establish the most appropriate adsorption isotherm. Langmuir, Freundlich, and Redilch–Peterson equations were used to analysis the experimental. Calibration curve in the range of 4.0×10^{-3} to 0.3 ng mL⁻¹ was linear and the calibration equation of $A = 1069.5 C + 50.2$ with a correlation coefficient of 0.9934 of (n =13) was achieved. The detection limit for the valsartan was 0.001 mg.L⁻¹ and the relative standard deviation (RSD) for determination of 8.0×10^{-3} and 0.2 mg mL⁻¹ of valsartan was 1.97% (n=10), and 0.76% (n=10), respectively.

4.Conclusion:

In this study, we report a novel spectrofluorimetric method for the determination of Valsartan by magnetic nanoparticle. The method was applied to the trace valsartan determination and preconcentration in healthy and infected human urine samples. The developed approach was responsiveness for valsartan determination with 4.0×10^{-3} to 0.3 mg.L⁻¹ linear rang and showed a selective response to valsartan.

5.References:

- [1] Siddiqui. N; Husain. A; Chaudhry. L; Alam. sh; Mitra. M. Journal of Applied Pharmaceutical Science, 2011, 01 (04); 12-19.
- [2] Tsvetkova1. D; Obreshkova1. D; Petkova. V. Journal of Pharmacy and Pharmaceutical Sciences, 2015, 4, 01-11.
- [3] del Rosario Brunettoa. M; Contrerasa. Y; S. Journal of Pharmaceutical and Biomedical Analysis, 2009, 50, 194-199.
- [4] Ran Lee. K; Thi Nguyen. N; Jae Lee. Y. Archives of Pharmacal Research,2015,38,826-833.
- [5] M.Ahmadi; T.Madrakian; A.Afkhami. Sensor Actuat B-Chem, 2015, 210,439-445.

An ultrasound enhanced dispersive liquid-liquid microextraction for simultaneous determination of five drugs by gas-chromatography-flame ionization detector & selected ion monitoring-mass spectrometry in biological real samples using chemometrics methodology

Amir Ismailzadeh^a, Mahboubeh Masrournia^{b,*}

^aYoung Researchers and Elite Club, Mashhad Branch, Islamic Azad University, Mashhad, Iran

^bDepartment of Chemistry, Mashhad Branch, Islamic Azad University, Mashhad, Iran

*Corresponding author: Email:masrour@mshdiau.ac.ir

1. Introduction:

The dispersive liquid-liquid microextraction (DLLME) method was firstly proposed by Assadi and co-workers in 2002, offers a prominent method to overcome many sample preparation difficulties. The DLLME procedure is commonly established in a ternary solvent mixture including extractor solvent, disperser solvent and an aqueous sample comprising the objective analytes [1, 2]. When the solution mixture containing extractor and disperser solvent is syringed promptly into sample, a cloudy solution swiftly appears owing to the co-solvency of disperser solvent with the two different phases; so the extraction equilibrium is occurred almost immediately among the aqueous solution and the finely divided droplets of extractor solvent, resulting in large contact surface area and leading to analytes transfer into the extractor solvent [3]. The goal of this study was to develop an efficient extraction method in order to achieve the maximum enrichment factors (EFs) and low limit of detections (LODs) for all target analytes. In this study, a sensitive analytical method is proposed based on extraction and preconcentration of five Psychotherapeutic drugs (Caffeine, Lidocaine, Tramadol, Venlafaxine & Chlorpromazine) by DLLME using ultrasound irradiation.

2. Experimental:

1 mL of sample solution with pH 11 was transferred into a 10-mL glass test tube. 0.5 mL methanol (as disperser) containing 50 µL octanol (as extraction solvent) was rapidly injected into solution using a 1-mL syringe. A cloudy solution (water, methanol and octanol) was formed which was stable for a long time. After spending 30 seconds in the ultrasound bath, the mixture was centrifuged for 5 minutes at 3000 rpm. Organic solvent (octanol) was gathered on the surface of aqueous phase as a small drop. A portion of the collected organic phase is removed by a micro-tube. An amount of 1 µL of organic phase was removed using a 10-µL GC microsyringe and injected into the GC injector port for analysis. All experiments were performed in triplicates and mean of the results was used in plotting of graphs and preparation of tables.

3. Result and Discussion:

In this paper an efficient, robust, simple, sensitive and rapid analytical method based on DLLME followed by gas chromatography-flame ionization detector (GC-FID) and mass spectrometry-selected ion monitoring (GC-MS-SIM) has been proposed for the extraction and simultaneous determination of five Psychotherapeutic drugs in human urine and breast-milk samples. The influence of several parameters was studied using multivariate experimental design and the main factors that potentially affecting the procedure were optimized by a screening (two level factorial) design followed by response surface (central composite) design and desirability functions in order to optimize the efficiency of the process. The optimal conditions were 1 mL of initial sample volume, 0.5 mL of methanol as disperser solvent, 0.5 mL of octanol as extractor solvent, 30 sec of ultrasounds stirring and extraction pH 11. Under optimized conditions, the proposed method showed good separation of neuromusculars in 2 & 3 min, good linearity in the range of 0.1-1000 µg.L⁻¹ & 0.01-0.5 µg.L⁻¹, limits of detection 0.1-0.5 µg.L⁻¹ & 0.01-0.05 µg.L⁻¹ and determination coefficients higher than 0.996 for GC-FID and GC-MS-SIM respectively. The

method precision ($n=6$) was evaluated showing relative standard deviations lower than 4% (breast milk) & 4.5% (urine). The average extraction recoveries & enrichment factors ranged from 89 to 106% & 268 to 319 respectively.

4. Conclusion:

Basically the presence of disperser solvent in DLLME, increases the solubility of lipophilic analytes into the aqueous sample solution due to its relatively nonpolar behavior in the aquatic environment which causes to relatively little extraction yield. To modify the extraction efficiency, some smart strategies have been developed using ultrasound irradiation, vortex shaking, sample preheating and air aspiration. Until now, the DLLME method has been extensively used for the analysis of several compounds in environmental aqueous samples, consisting aromatic hydrocarbons, chlorophenols, pesticides, phthalate esters, etc. Furthermore, its usage has been developed in trace elemental analysis [4].

References

- [1]. Liang, P., J. Xu, and Q. Li. *Analytica Chimica Acta*, 2008. 609(1): p. 53-58.
- [2]. Moinfar, S. and M.-R.M. Hosseini. 169(1-3): p. 907-911.
- [3]. Rezaee, M., et al. *Journal of Chromatography A*, 2009. 1216(9): p. 1511-1514.
- [4]. García-López, M., I. Rodríguez, and R. Cela. *Journal of Chromatography A*, 2007. 1166(1-2): p. 9-15.

Potentiometric biosensor for determination of lactose using kefir grains modified on multi-walled carbon nanotubes/casein composite

Farideh Zare, Mohammad Mahdi Doroodmand*

Department of Chemistry, College of Sciences, Shiraz University, Shiraz 71454, Iran.

Email address: doroodmand@shirazu.ac.ir

Introduction:

The dairy industry has made several attempts to improve the quality and the nutrient contents of milk-based formula. In order to develop special products for specific people, some ingredients have been added to the milk powder [1]. For example, calcium is added to prevent osteoporosis that frequently affects old people, while some vitamins and minerals are used in the formulae for pregnant women [1]. Recently enriched milk with carbohydrates and carbohydrate-reduced production has been existed.

Lactose is the main carbohydrate in the dairy products and is considered as the only saccharide synthesized by mammals at a concentration of 4–5% (w/v) in cow and other mammals, and ~8% in the human milk [1, 2]. This disaccharide is catabolized into glucose and galactose monosaccharides by the enzyme lactase [1, 3]. Lactose has many important physiological functions. For instance, it takes part in metabolism of calcium to help the absorption of calcium in human body [4]. It also plays an important role in the formation of the neural system and the growth of skin (texture), bone skeleton and cartilage in infants and so it can prevent rickets and saprodonia [1]. This compound is able to develop the producing of bacillus in babies' bowels too. In this study for the first time a novel method has been introduced for rapid detection and determination of lactose in the milk samples by potentiometry using Kefir grains as alive micro-organisms.

Experimental:

In this study, a simple and selective biosensor has been introduced for determination of lactose by potentiometric method based on the catalytic behavior of kefir grains via modification with multi-walled carbon nanotubes (MWCNTs)/casein composite as indicator electrode and sat'd Ag/AgCl as reference electrode. To fabricate the indicator electrode, kefir grains were initially dried using a freeze dryer during 48 h time and powdered with an electronic grinder. Then ~ 0.15 g kefir powder as optimum value was physically mixed with MWCNTs/casein with optimized weight ratio of 0.005/0.3 (w/w) and mixed with ~ 150 μ L nujol oil. The generated paste was then packed inside a Teflon tube (i.d: 10 mm, height: 100 mm) and adopted as indicator electrode. Maximum potentiometric response was also observed at pH 7.0 and 0.51 M ionic strength, controlled using phosphate buffer (0.01 M) and NaCl (0.5 M), respectively. The linear dynamic range during lactose determination was ranged between 1.0×10^{-12} - 1.0×10^{-4} M with detection limit of 3.0×10^{-14} M based on extrapolation definition. The response time based on the 90% of maximum response (t_{90}) was estimated to be ~2 min. The validity as well as the application of this method were evaluated via determination of lactose in some various types of milk samples.

This method was considered as reliable, rapid and sensitive sensor for selective detection and determination of lactose.

Results and Discussion:

A novel dissolved and gaseous oxygen electro-optical sensor was fabricated based on the dependency of the fluorescence intensity of a synthesized nitrogen-doped carbon nanodots (N-CDots) during the amperometric reduction of O₂ at potential of -0.55 V (vs. Ag/AgCl) for about 20s using a three-electrode system including gold rod as working electrode, platinum rod as counter electrode and Ag/AgCl (3.0 M Cl⁻) as reference electrode, followed by measuring the fluorescence intensity at excitation wavelength of 350 nm. Under optimized condition, i.e. 5.0 µg mL⁻¹ of N-CDots, ionic strength of 0.5 M and room temperature, the linear range was estimated to be between 0.11-22 µg mL⁻¹ with detection limit of 0.07 µg mL⁻¹ (n=4). And for gaseous oxygen the linear dynamic range was between 3.0 to 48.0 % with the limit of detection of 0.95 % (n=4). The response time (*t*₉₀) of the sensor was estimated to be 20 s. No interfering effect was observed during analysis of at least 200-fold excess (vs. 2.0 µg mL⁻¹ dissolved oxygen) of organic and inorganic species such as, K₂SO₄, KNO₃, MgCl₂, MnCl₂, NaClO₄, NaF, NH₄Cl, CaCl₂ and Na₃PO₄. Except NaNO₂ and NaHCO₃ which has interfered for respectively 12-fold and 75-fold excess. The reliability of the method was also evaluated via analyses of waste and industrial samples.

Conclusion:

In this work, a sensitive and reproducible biosensor has been introduced for lactose determination based on the catalytic behavior of kefir grains. This technique has revealed some beneficial aspects such as more simplicity, high selectivity, fast response time and acceptable detection limit.

References:

- [1] W. Xinmin, Z. Ruili, L. Zhihua, W. Yuanhong and J. Tingfu, Determination of glucosamine and lactose in milk-based formulae by high-performance liquid chromatography, J. Food Composition Anal., 21 (2008) 255-258.
- [2] S.R. Hertzler and S.M. Clancy, Kefir improves lactose digestion and tolerance in adults with lactose maldigestion, J. Am. Diet. Assoc., 103 (2003) 582-587.
- [3] K. Venema, Intestinal fermentation of lactose and prebiotic lactose derivatives, including human milk oligosaccharides, Int. Dairy J., 22 (2012) 123-140.

[4] Y.N. Ni, Y.R. Wang and S. Kokot, Osteryoung square wave voltammetric determination of lactose in food samples by a derivative procedure, *Chin. Chem. Lett.*, 19 (2008) 1491-1494.

Carbon Paste Modified Electrode with Layered Co(OH)₂ Deposited Polymeric Carbon Nitrides for High-Performance Nonenzymatic Glucose Sensing

S. F. Nami-Ana¹, J. Tashkhourian*¹, M. Shamsipur*²

¹Department of Chemistry, College of Sciences, Shiraz University, Shiraz 71456, Iran

²Department of Chemistry, Razi University, Kermanshah, Iran

E-mail: Tashkhourian@susc.ac.ir

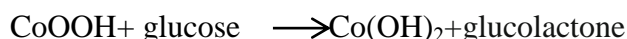
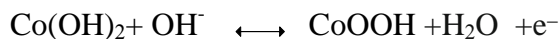
Introduction: Enzyme-based glucose sensors exhibit high sensitivity and selectivity for glucose. However, such biosensors require complicated immobilization procedures and exhibit poor long-term stability [1]. As a result, increasing attempts have been undertaken to develop nonenzymatic glucose biosensors based on noble metals, oxides, and their composites with CNT or graphene[2]. Cobalt ion-based materials have received much attention because of their stability in alkaline conditions, electrocatalytic activity, and interchange ability between various valence states[3].

Carbon nitrides(C₃N₄) are a class of polymeric materials consisting mainly of carbon and nitrogen has rich surface properties that are attractive for many applications, including catalysis, due to the presence of basic surface sites[4].

Methods/Experimentals: Bulk -C₃N₄ was prepared by a traditional thermal polymerization of Guanidine in a crucible at 550 °C. The final yellow powder was then collected. The hybridized materials were obtained as follow. 1 g of as-prepared g-C₃N₄ was immersed into 5.0 mL aqueous solutions containing different amounts of Co(NO₃)·6H₂O. Thereafter, 1.0 mL of aqueous ammonia was added drop wise into the above solution, and a green precipitate was immediately formed and dried in an oven at 80 °C for 12 h. The modified carbon paste electrode (Co(OH)₂-C₃N₄/CPE) was prepared by hand mixing. Electrochemical oxidation of glucose was investigated by cyclic voltammetry and amperometry in the electrolyte solution include 0.1M KOH.

Result and Discussion: Physicochemical characterization of synthesized nanocomposite was done by CHN, XRD,FT-IR, and TEM analysis that well illustrates the successful fabrication of layered Co(OH)₂ nanocrystals on the surface of the C₃N₄ semiconductor with a layered polymeric structure. The synthesized nanocomposite was used for modified carbon paste electrode and applied to catalyze electrochemical oxidation of glucose.

The cyclic voltammograms at the surface of modified electrode in the electrolyte solution including 0.1 M KOH showed a good reversible peak that is attributed to the redox reaction of immobilized Co(OH)₂/CoOOH. electrocatalytic mechanism is as follows:



Obvious changes of the peak currents were observed after the addition of glucose, indicating obvious electrochemical catalysis of the modified electrodes to the oxidation of glucose. The bare electrode did not show any changes by adding different concentration of glucose. At the same time, both the cathodic and anodic peak potentials shifted positively, ascribing to the diffusion limitation of glucose in the catalytic process. Electrochemical behavior of the modified electrode containing different concentration of glucose is shown in Fig. 1. The

linear range for glucose determination by this modified electrode was obtained 1×10^{-6} to 1×10^{-3} M with the detection limit of 5×10^{-7} M.

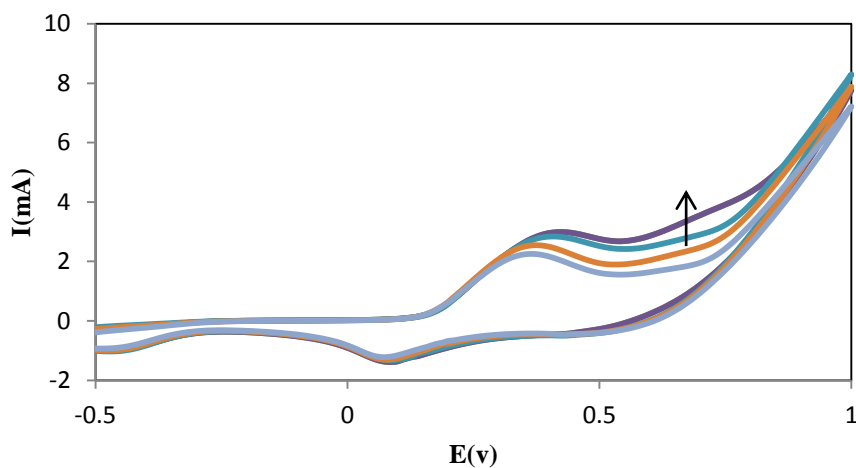


Fig.1

Conclusion: Herein, a nonenzymatic glucose sensor based a novel nanocomposite of Co(OH)_2 deposited polymeric carbon nitrides- carbon paste modified electrode was introduced as an excellent platform to electrocatalyze glucose oxidation. The sensor showed high electrocatalytic ability to glucose oxidation with a low detection limit and a short response time in amperometric detection of glucose. The morphology of Co(OH)_2 provided abundant active sites and shows a novel synergy with C_3N_4 could improve the electrochemical behavior toward glucose.

References

1. Park, S; Boo, H; Chung, T. D. *Anal. Chim. Acta*, **2006**, 556, 46–57.
2. Bai, L. J; Yuan, R.; Chai, Y. Q; Zhuo, Y; Yuan, Y. L; Wang, Y. *Biomaterials*, **2012**, 33, 1090–1096.
3. I.G. Casella, M. Gatta, *J. Electroanal. Chem.* **2002** 534, 31.
4. Wang, X. C.; Maeda, K.; Thomas, A.; Takanabe, K.; Xin, G.; Carlsson, J. M.; Domen, K.; Antonietti, M. *Nat. Mater.* **2009**, 8, 76–82.

The evaluation of synthesized Ni-Cr-LDH nanostructure as a biosensor

Parvaneh Dalir kheirollahi nezhad^a, Kamelia Nejati^a, Nasrin Amiri^a

^a *Department of Chemistry, Payam-e-Noor University, P.O. Box, 19395-3697 Tehran, Iran*

Abstract

In this research, measurement and determination of 2-nitro phenol concentration that exist in the wastewater of refineries or paint manufacturing factories obtained using nano structure of nickel chromium layered double hydroxides (LDH) as biosensor. High sensitivity and accuracy are the advantages of nanoscaled biosensors. In this regard, synthesizing nano particles of nickel chromium layered double hydroxides must be ensured. Thus, with a view to this purpose, the method of electrochemical precipitation of carbon glass electrodes was used. In order to investigate the manner of obtained electrochemical electrode and its ability to be a sensor, the voltametric method was applied in various pHs. Based on the experiments of this study, pH=13 was determined as optimum pH. Meanwhile, it is worth saying that the structure of nickel chromium hydroxides is in a layered form. Based on the drawn voltagrams the synthesized electrode proved the possibility of using nickel chromium layered double hydroxides as sensor. In this study, it was observed that the synthesized biosensor can determine the 2-nitro phenol concentration with high exactness.

Keywords: nickel, chromium, 2-nitrophenol, carbon's glass, cyclic voltametry, biosensor.

Introduction

Development of analytical methods with biosensors are available for detection of these compounds [1]. The increasing interest in LDH as host matrix has been enhanced because of their versatile properties in terms of chemical composition of both layer and interlayer, their high and tune able layer charge density resulting in adaptable anion exchange capacity [2]. So, the intrinsic LDH properties make them very desirable to confine negatively charged biomolecules such as amino acids, DNA and etc [3, 4]. Instead of a simple physical mixture, the incorporation of compound within LDH was rather carried out during the LDH synthesis [5]. In this paper, we displayed that Ni-Cr-LDH as a biosensor could be benefit for assaying nitric compounds.

Methods / Experimentals

To synthesize Ni-Cr-LDH nanostructure, by electrochemical method 0.12 mmol NiCl₂ (0.03 gr) and 0.04 mmol (0.12 gr) CrCl₃ and 0.15 mmol (0.01 gr) KCl were decanted into cell. 50 ml of deionized and dicarbonated water as solvent were added to them. Depositing LDH on electrode was performed by Chronoamperometry method and by applying constant potential of -0.9 on electrode in three-electrode system (working electrode (GC), the auxiliary electrode (Pt) and the Control electrode (Calomel)) which deposition time in different times was assumed 5 seconds. In the upper pH, depositing was performed in times of 15, 30, 60, 90, and 120 seconds.

Results and Discussion

In Fig. 3.1, SEM picture shows that the synthesized sample is sheet, and structure nanoparticles are in one dimension not in all dimensions.

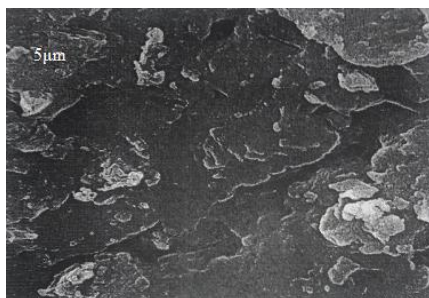


Fig. 3.1. SEM image of Ni-Cr-LDH

XRD pattern of Ni-Cr LDH nanostructure shows that nanostructure has high crystallinity and No characteristic peaks from any other impurity were observed (Fig. 3.2). The average crystallite size of LDHs indirections a and c were determined by employing Scherrer's formula, with λ being the wavelength of the X-ray ($\text{CuK}\alpha$), β the full width at half-maximum of the diffraction peak in radian units, K the Scherrer constant (0.89), and θ the Bragg's angle in degree unit. The size of these nanostructure has been determined 4.1 nm. According to results of X-Ray Diffraction patterns, it can be concluded that all of synthesized samples have high purity. But Ni-Cr-LDH in presence of water solvent, 2-propanol and surfactant with a metal ratio of 3:1 in 60 °C temperature, has high crystallinity.

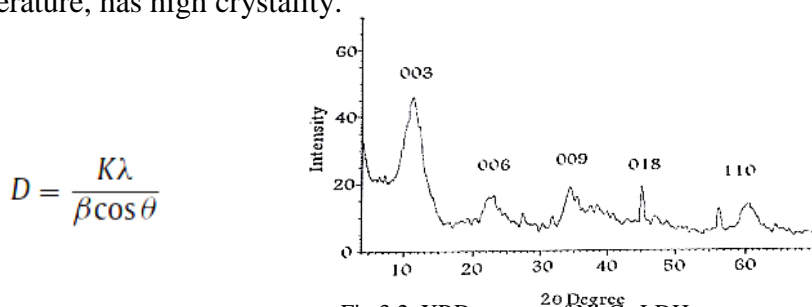


Fig 3.2. XRD pattern of Ni-Cr-LDH

Conclusion

In this study, we could synthesize Ni-Cr LDH nanostructure in the low temperature (60 °C) , molar ratio of 3:1 and solvents that everywhere are available. The size of these nanostructure has been determined 4.1 nm by employing Scherrer's formula. Ni-Cr-LDH was characterized with PXRD, FT-IR and SEM.

References

- [1] U. Bilitewski, A.P.F. Turner (Eds.), *Biosensors for Environmental Monitoring*, Harwood Academic Publishers, **2000**.
- [2] C. Forano, S. Vial, C. Mousty, *Nanohybrid enzymes – layered double hydroxides: potential applications*, *Curr. NanoSci.*, **2006**, vol. 2, pp. 283–294.
- [3] E. Ruiz-Hitzky, M. Darder, P. Aranda, *Functional biopolymer nanocomposite based on layered solids*, *J. Mater. Chem.*, **2005**, vol. 15, pp. 3650–3662.
- [4] J.H. Choy, S.J. Choi, J.M. Oh, T. Park, *Clay minerals and layered double hydroxides for novel biological applications*, *Appl. Clay Sci.*, **2006**, vol. 36, pp. 122–132.
- [5] F. Leroux, J. Gachon, J.-P. Besse, *Biopolymer immobilization during the cristalline growth of layered double hydroxide*, *J. Solid State Chem.*, **2004**, vol.177, pp. 245–250.

How Do Neuroprotective Drugs Prevent Membrane Disruption?

Amin Reza Zolghadr*, Maryam Heydari Dokoochaki

Department of Chemistry, Shiraz University, Shiraz 71946-84795, Iran

Email address: arzolghadr@shirazu.ac.ir

Introduction: Alzheimer's disease (AD), the most common form of dementia, is a progressive neurodegenerative disorder that is associated with daily living through anxiety, depression, apathy, psychosis, memory loss and cognitive impairment [1]. A critical event in the pathogenesis of AD is self-aggregation of A β peptides into toxic soluble protofibrils or oligomers [2]. In this study, the primary goal is to understand in details the mechanism of cell membranes damage and cell death in AD. To this aim, the effect of interactions between A β oligomers and model membrane are illustrated. Simulations of A β oligomer in a model dipalmitoylphosphatidylcholine (DPPC) bilayer environment can provide the resolution necessary to explain how the protein interacts with the surrounding lipids and disrupt the membrane. Also, the partitioning and aggregation of carbazolium-based small drug, P7C3, at phospholipid membranes/ionic aqueous solution is presented.

Methods: The structure and topology of P7C3 was generated by the small molecule topology generator PRODRG [3]. The partial atomic charges are calculated by using natural population analysis as implemented in Gaussian 09 program. Simulations were carried out with the GROMACS 4.5.3 program suite using the GROMOS96 53a6 force field under constant number, pressure, and temperature (NPT) conditions for all our systems, aiming to provide some molecular insights into the interactions of amyloid oligomer with bio-membranes to provide some guidance for pathogenic and treatment of AD.

Results and Discussion:

The aim of this study is the investigation of P7C3 effects on the neural cells that are attacked by A β fibrils. Figure 1 depicts the snapshots of A β stack interacting with membrane/P7C3 enriched aqueous ionic solutions. At the start of the simulations the drug molecules were distributed in the water phase and separated from each other by about 2 nm in the initial configuration. As simulation proceeded, the P7C3 molecules very quickly migrated toward the membrane phase and reached the interface within 200 ns (close snapshots are shown). During this process the drug

molecules are aggregated and stable self-assemblies are formed right where the protein is located in membrane. These snapshots confirm that although small amounts of water pass through the membrane, the A β protein tilting and ion channel formation is postponed. Figure 2 shows the membrane/aqueous ionic solutions enriched with 48 molecules of P7C3 and A β stack at $t = 200$ ns. This figure illustrate that drug molecules self-aggregated at the interface of water and membrane. This aggregation prevents A β oligomers from entering into the cell membrane and inhibits their damaging effects. In this way, P7C3 molecule protects newborn neurons from apoptotic cell death.

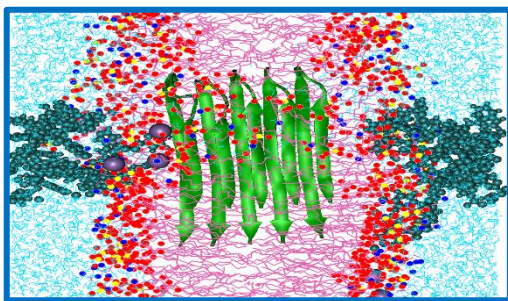


Figure 1. Snapshots of the A β stack interacting with membrane/P7C3 enriched aqueous ionic solutions.

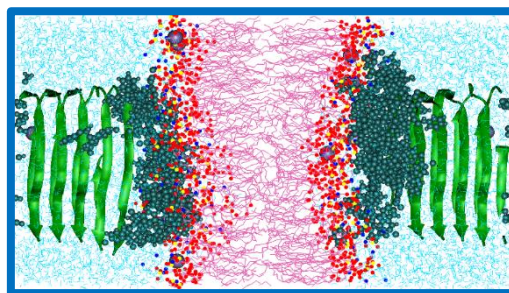


Figure 2. Snapshots of the membrane/aqueous ionic solutions enriched with 48 molecules of P7C3 and A β stack.

Conclusion: We have performed a systematic study of the DPPC membrane perturbation by A β_{42} fibril in the presence of P7C3 neuroprotective drugs using molecular dynamics simulation. To study the effect of A β_{42} fibrils on the membrane we placed the A β_{42} stack in the center of the DPPC bilayer membrane. These and more detailed investigations indicate that the membrane sustain substantial structural changes when A β_{42} peptides are added. The hydrophobic mismatch between fibrils and peptides leads to the tilting of A β_{42} stack and formation of an ion channel. An important result from our simulations is the self-assembly of P7C3 molecules at the water/membrane interface and prevention of A β_{42} precipitation in to the membrane.

References:

-
- [1] Palmer, A. M. *Trends Pharmacol. Sci.*, **2002**, 23, 426-433.
 - [2] Selkoe, D. J. *Neuron*, **1991**, 6, 487–498.
 - [3] SchuÈttelkopf, A. W., & Van Aalten, D. M. *Acta Crystallographica Section D: Biological Crystallography*, **2004**, 60, 1355-1363.

Extraction and determination of precious metals by means of a novel nanocomposite made from polypyrrole-polythiophene copolymer coated on the surface of graphene oxide/magnetite

Niloofar Jalilian, Homeira Ebrahimzadeh*, Ali Akbar Asgharinezhad

Faculty of Chemistry, Shahid Beheshti University, G.C., Evin, Tehran, Iran

Email address: h-ebrahim@sbu.ac.ir

Introduction: Removal and recovery of expensive heavy metals from wastewater and mineral samples are of a great importance due to health and environmental reasons and economic motivations to reuse and recycle [1]. SPE is the most common technique for routine analysis of samples with complex matrices because of its simplicity, rapidity, high pre-concentration factors, low cost, and low consumption of organic solvent. Graphene oxide (GO) has attracted tremendous attention as a potential sorbent for the separation and preconcentration [2]. Combining the excellent properties of magnetic GO and conducting polymers, made it possible to design and develop advanced nanosorbents with some unique features.

Methods / Experimental: At first, GO sheets were decorated with magnetite nanoparticles via a facile one-step chemical reaction strategy, which were then grafted by a silica layer to obtain high stability in acidic solutions. Afterwards, the surface of mGO@SiO₂ was coated by polypyrrole-polythiophene copolymer via oxidative polymerization of pyrrole and thiophene.

Results and Discussion: In order to explore the composition of prepared mGO@SiO₂@PPy-PTh nanosorbent, SEM, TEM, VSM, FT-IR, and TGA analysis were employed to characterize the nanocomposite.

Design of experiments approach was employed in order to optimize the extraction conditions. The highest D value (0.9998) in sorption step was obtained under the operational condition of: pH of sample 4.8; sorption time, 6.3 min; mGO@SiO₂@PPy-PTh amount, 19 mg. The optimum extraction recovery and the highest D value (1.000) in elution step was obtained by selecting the

following conditions: an elution time of 15.5 min and by using 6 mL 1.5 mol L⁻¹ thiourea in 1.0 mol L⁻¹ HCl as an eluent.

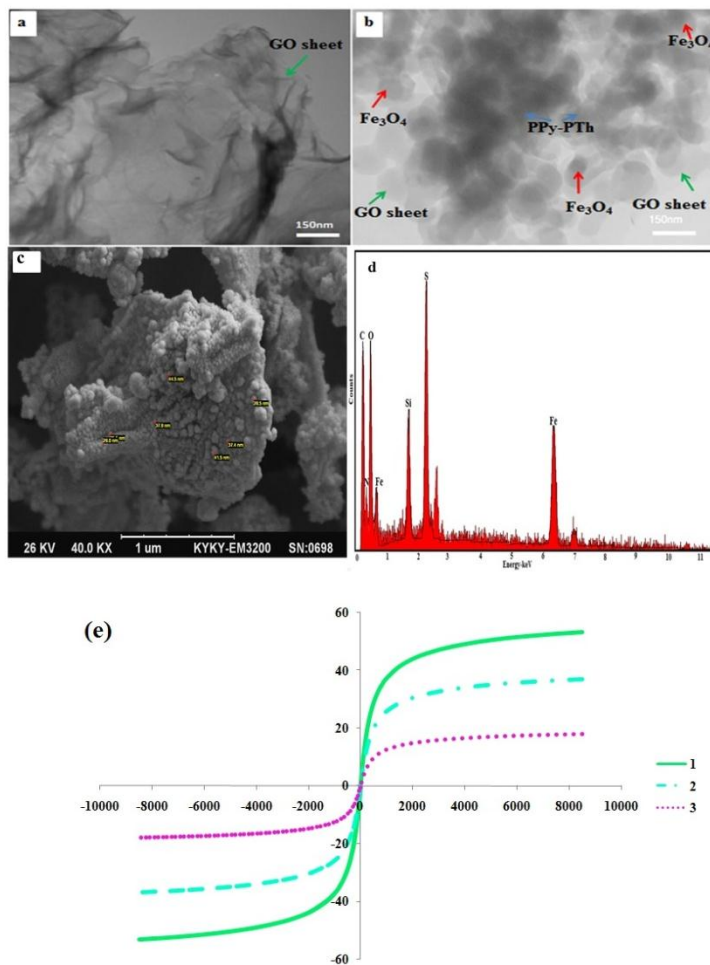


Fig. 1: TEM images of (a) GO and (b) mGO@SiO₂@PPy-PTh nanocomposite, (c) SEM image of mGO@SiO₂@PPy-PTh nanocomposite, (d) EDX analysis of mGO@SiO₂@PPy-PTh nanocomposite and (e) VSM curves of (1) mGO, (2) mGO@SiO₂ and (3) mGO@SiO₂@PPy-PTh nanocomposite.

Conclusion: Herein, a novel nanocomposite made from SiO₂-coated magnetic graphene oxide and polypyrrole-polythiophene copolymer, was synthesized by a facial method and employed as a sorbent for the extraction of precious metal ions.

References

- [1] Lifshitz E, Brumer M, Kigel A, Sashchiuk A, Bashouti M, Sirota M, Galun E, Burshtein Z, AQLQ, Ledoux-Rak I, Zyss J, J Phys Chem B, 2006, 110: 25356-25365.
- [2] Asgharinezhad AA, Ebrahimzadeh H, J Chromatogr A, 2016, 1435: 18-29.

A novel metal enhanced fluorescence bio probe based on poly vinyl alcohol-borax hydrogel platform functionalized by Ag dots for insulin determination

Matineh Ghomi^a, Nahid Pourreza^{b*}

^{a, b} Department of Chemistry, Faculty of Science, Shahid Chamran University of Ahvaz, Ahvaz

Email address: npourreza@yahoo.com

Introduction: Herein we have developed a novel metal enhanced fluorescence (MEF) bio-probe based on simultaneous synthesis and embedding of Ag dots into biocompatible poly vinyl alcohol-borax hydrogel (AgD@PBH) that can determine insulin hormone. The great feature of this bio-probe is in situ preparation of PBH with simultaneous synthesis and embedding of uniform, highly stable AgDs into PBH without adding any reducing agent. Hydrogels can be composed of natural or synthetic polymers. This three-dimensional polymeric network [1] has a unique property as result of their ability to absorb/retain large quantities of water [2]. Insulin is a natural and most important regulatory polypeptide hormone which is made of 51 amino acids linked by disulphide bond [3]. Therefore insulin was selected as analyte to acquire a straightforward strategy of bio-probe.

Methods / Experimentals: The PBH@AgD was synthesized by mixing PVA, borax and silver nitrate solution. To plan 'on' fluorescence bio- assay, the appropriate amounts of bio-probe, NaCl electrolyte, Britton–Robinson buffer and different concentration of insulin solution was transferred into a volumetric flask. It was vortex and the fluorescence intensity of the sol PBH@AgD was recorded. The blank intensity was measured similar to recommended procedure with the exception that no insulin solution was added.

Results and Discussion: Comparing the UV-Vis spectrum of PBH alone and in the presence of Ag dots shows the appearance of an absorption peak with a maximum at 422 nm for PBH@AgD bed which can also confirm the functionalization of PB hydrogel bed with AgDs. To approve the synthesis of Ag dots in the PBH platform, energy dispersive X-ray microanalysis, the average particle size and TEM images of functionalized hydrogel was taken. Effect of different parameters such as pH variation, concentration of borax and etc. was investigated. Under the approved condition, the linear detection range was validated over the concentration of 5 to 220 ng mL⁻¹. The Limit of detection was 0.02 mg L⁻¹. The relative standard deviation for 60 and 140 mg L⁻¹ was 0.42 and 0.13 % (ten replicate measurements), respectively. The developed probe was successfully applied for insulin detection in plasma with acceptable result and good fluorescence recovery.

Conclusion: In summary, we have introduced a novel PBH@AgD bio-sensor platform for convenient, fast and precise insulin determination. This bio-probe was easily synthesized and in situ AgDs were loaded inside its network. This strategy has been successfully employed to quantify insulin in healthy and diabetic serum samples.

References

- [1] Z. P. Zhou; H. D. Huang; Y. Chen; F. Liu; C. Z. Huang; N. Li. Biosens. Bioelectron. **2014**, 52,367–373.
- [2] C. D. Geddes; A. Parfenov; I. Gryczynski; J. Malicka; D. Roll; J.R. Lakowicz. Journal of Fluorescence, **2003**, 13, 119–122.
- [3] K. Aslan; C.D. Geddes, Analytical Chemistry, **2005**, 77, 8057–8067.

Design, synthesis and evaluation of TiO₂ nanocomposite by ionic liquid assisted sol-gel method for hollow fiber solid-phase microextraction of celecoxib in human plasma and drug formulation using spectrofluorimetry experimental design

Maliheh Saghravani¹, Mahmoud Ebrahimi^{2,*}, Zarrin Es'haghi³

¹Young Researchers and Elite Club, Mashhad Branch, Islamic Azad University, Mashhad, Iran

²Department of Chemistry, Mashhad Branch, Islamic Azad University, Mashhad, Iran

³Department of Chemistry, Payame Noor University (PNU), ۱۹۳۹۲-۴۶۹۷, I.R. of Iran

*Corresponding author: Email: M.ebrahimi@mshdiau.ac.ir

Introduction: Celecoxib (CEL), ۴-[۲-(۴-methylphenyl)-۳-(trifluoromethyl)-۱H-pyrazol-۱-yl] benzenesulfonamide, is a selective cyclooxygenase-۲ (COX-۲) inhibitor and nonsteroidal anti-inflammatory drug (NSAID) that applied for the treatment of rheumatoid arthritis, osteoarthritis [۱] and also for the relief of inflammation and pain[۲]. Spectrofluorimetry has been widely used in the determination of pharmaceutical compounds [۳, ۴]. This method due to high sensitivity, much selectivity, economic and easy operation is appropriate.

In this paper, we reported the new method for determination of celecoxib in trace amounts by sol-gel technique with combination nano-TiO₂ and ionic liquid (IL) into hollow fiber. Combination nano-particle and IL increased sensitivity, intensity fluorescence peak and reduced limit of method detection. The influences factors on the efficiency of method were investigated by multivariate methods such as Placket-Burman design (PBD) and central composite design (CCD).

Methods /Experimental:

All computations were performed on a computer with ۸ GB memory and an Intel Pentium ۷ ۳.۰۷ GHz CPU. The Minitab ۱۷ and Design Expert ۷ software of were used for experimental designs, statistical evaluation, and model fitting in this work.

Results and Discussion:

Some of factors such as type of nano particle, amount of nanoparticle and type of desorption solvent optimized by one variable at the time method and others factors optimized by experimental design. A Placket-Burman design was carried out for eight factors (pH, volume of aqueous solution, volume of organic solvent, adsorption time, desorption time, amount of surfactant, stirring rate, determination of temperature) containing ۱۷ run.

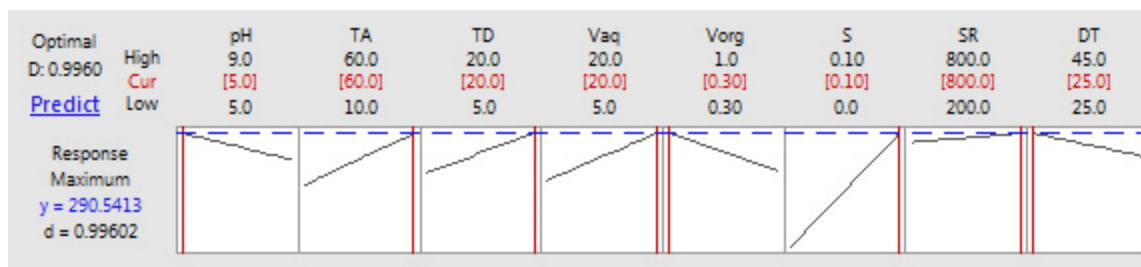


Figure 1. The optimal chart gained from PBD

The next of analysis of responses, the significant factors identified and optimized by central composite design in 16 run. This design consists of a small factorial design (2^3 hypercube points, 2×2 axial points, and 2 replicates of center points). By using regression analysis on experimental data, the results of CCD were fitted with a polynomial equation for each response. The cubic model expressed an empirical relationship between response and input variables in uncoded values. The R^2 and R^2 -(adj.) for the models were obtained 97.27% and 82.91%. In order to achieve the maximum response, the obtained equation was solved and the amount of optimized were calculated in maximum desirability.

Conclusion:

For the first time, HF-SPME method with sol-gel technique based on TiO_2 -IL composite were used for extraction and determination celecoxib. This method has advantages such as simplicity, least utilization of organic solvent, suitable repeatedly, relatively good accuracy and precision. The first stage for optimization, by manual methods were optimized three factors. The next stage, eight factors were investigated by using Plackett-Burman design. Significant parameters were optimized by CCD.

References

- [1] Srinivasu M; Rao D S ; Reddy G O. *J. Pharm. Biomed. Anal.*, 2002, 28, 293-300.
- [2] Rose M; Woolf E ; Matuszewski B. *J. Chromatogr. B: Biomed. Sci. Appl.*, 2000, 738, 377-380.
- [3] Manzoori J L ; Amjadi M. *Spectrochim. Acta, Part A*, 2003, 59, 99-116.

[4] Xiliang G;Yu Y, Guoyan Z; Guomei Z; Jianbin C ; Shaomin S. *Spectrochim. Acta, Part,*
2003, 59, 3379-3386.

One-pot Synthesis of 2-(2-hydroxyphenyl)benzo[d]thiazol Derivatives Under solvent-free reaction conditions

Hoorieh Djahaniani*

Department of Chemistry, Collage of basic Science, East Tehran Branch, Islamic Azad University,

PO Box 33955-163, Tehran, Iran

E-mail: jahanbani.ho@gmail.com

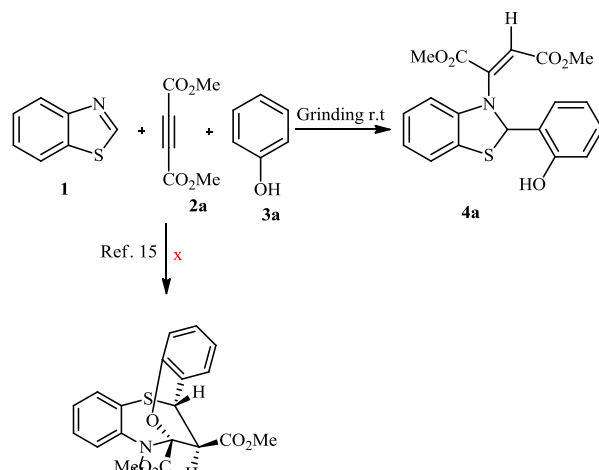
Introduction: Due to biological activity of a significant number of compounds containing benzothiazole ring system and in continuation of our interest in developing new environmentally benign methods for the synthesis of heterocyclic compounds by MCRs [1-2], herein we wish to report an efficient three-component from BTA, acetylenic esters and hydroxyl aromatics compounds to synthesize of 2- benzothiazole derivatives in high yield (Scheme 1).

Method / Experimental: All chemicals used in this work purchased from Merck or Aldrich and used without further purification. Melting points measured on an Electrothermal 9100 apparatus and were uncorrected. IR spectra were obtained on an ABB 53 FT-IR (FTLA 2000) spectrometer. ^1H NMR and ^{13}C NMR spectra were obtained on Bruker DRX-400 AVANCE at 400 MHz, using TMS as internal standard and at room temperature in CDCl_3 as solvent. Elemental analyses were carried out using a Heraeus CHN–O– Rapid analyzer rapid analyzer. The X-ray diffraction measurement was made on a STOE IPDS-II diffractometer.

A mixture of benzothiazole (0.22 g, 2.0 mmol), dimethyl acetylenedicarboxylate (0.28 g, 2.0 mmol) and phenol (0.094 g, 2.0 mmol) were placed in a mortar. The mixture was ground with a mortar and pestle at room temperature for 12 min. After completion of the reaction, as indicated by TLC (ethyl acetate: *n*-hexane, 1: 3), the product was recrystallized from diethyl ether.

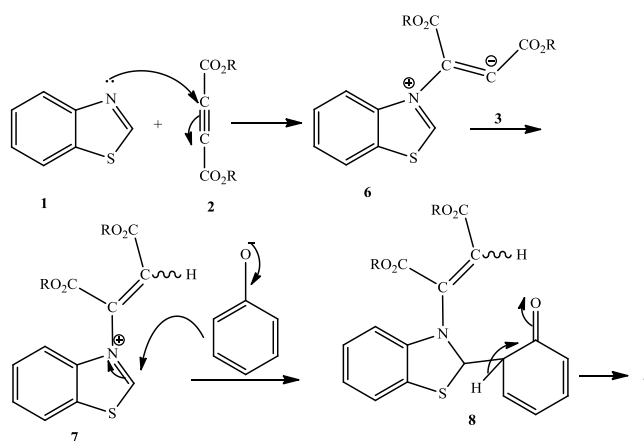
Results and discussion: The consideration of previous report encouraged us to investigate for the reaction of benzothiazole **1** and dialkyl acetylenedicarboxylates **2** in the presence of some hydroxyl aromatic compounds such as phenols, 4-hydroxy quinoline, and 8-hydroxy quinoline **3**. In this regard, we chose reaction between **1** and dimethyl acetylenedicarboxylate (DMAD) **2a** in presence of phenol **3a** in CH_2Cl_2 at room temperature. It was interesting that based on the proposed mechanisms in our recent report, the predicted product was not detected at all, while dimethyl (*E*)-2-(2-(2-hydroxyphenyl)benzo[d]thiazol-3(2H)-yl)-3-methylbut-2-enedioate **4a** was obtained (Scheme 1).

Then we continued our investigation in various solvent such as CH_2Cl_2 , CHCl_3 , H_2O , THF, and also solvent-free reaction conditions at room temperature for 12 h and also grinding at room temperature for 15 m. It was found that the reaction under grinding reaction resulted in higher yield (Scheme 1).



Scheme 1.

A reasonable mechanistic postulate for the formation of **4** is given in Scheme 2.



Scheme 2.

Conclusion: In summary, the reaction between benzothiazole and dialkyl acetylenedicarboxylates in the presence of some phenols without electron-withdraw substitution, presents a novel, one-pot, clean, convenient, simple and inexpensive approach into the synthesis of 2-benzothiazole derivatives of potential synthetic and pharmacologically interest. This procedure carries significant advantages because of the minimization of labor, time, and cost. Noteworthy, our work introduces a very easy and simple one-pot multicomponent reaction under the solvent-free grinding conditions, without any catalyst, activation or modification.

References

1. Djahaniani, H.; Aghdashi-Abhari, L.; Mohtat, B., *J. Serb. Chem. Soc.* **2015**, *80*, 459–464.
2. Djahaniani, H.; Fatemi, F.; Ektefa, F.; Mohtat, B.; Notash, B. Water: *Combinatorial Chemistry & High Throughput Screening*, **2015**, *18*, 990-999.

Optimization of Dried Blood Spot Sample Preparation Steps to Determine the Amino Acid Biomarkers in Infants Using High Performance Liquid Chromatography

Maryam Alsadat Mousavi, Zahra Talebpour^{a*}, Ahmad Mani^b, Kambiz Gilany^c

^a Department of Chemistry, Faculty of Physics & Chemistry, Alzahra University, Vanak, Tehran, 1993891176, Iran

^b Department of Chemistry, Faculty of Basic Sciences Tarbiat Modares University, Jalal Al Ahmad, Tehran, 14115-335, Iran

^c Department of Embryology and Andrology, Shahid Beheshti University, Evin, Tehran, 19615-1177, Iran

*e-mail: ztalebpour@alzahra.ac.ir

Introduction

Metabolic disorders are caused by the accumulation of toxic metabolites in the body that lead to irreversible physiological effects. Phenylketonuria (PKU) and maple syrup urine disease (MSUD) are one of the most common inborn errors of metabolism. Screening for these disorders is typically performed on a dried blood spot samples (DBSs)[1,2]. Due to the nature of the sample and small quantities of metabolites, it is necessary to determine the optimum conditions for the extraction[3]. Many factors such as type of solvent, the volume of solvent, temperature of thermal stabilization step, time of shaking and vortex, among others, may significantly influence the extraction efficacy.

Experimental

Stock solutions were prepared and DBS specimens were collected from one healthy adult volunteers. A pre-column o-phthaldialdehyde-3-mercaptopropionic acid derivatization is then followed by analysis of the amino acids by RP-HPLC. The chromatographic separation was carried out at a flow rate of 1 mL/min with a gradient in mobile phase composition at a wavelength of 338 nm. A central composite design (CCD) was used to investigate the effects of four independent mentioned variables. A 6.18 mm diameter disk was punched from each DBSs and extracted with various condition.

Result

In this study, the optimum conditions for the extraction of amino acids from DBSs were determined using response surface methodology (RSM) and reverse phase high performance liquid chromatography (RP-HPLC) with a UV detector, with pre- column derivatization. A separation of 21 amino acid was performed by changes in chromatographic conditions. The mobile phase consisted of solvent A, 100 Mm sodium acetate buffer (pH 6.8), and solvent B, acetonitrile-methanol-water (45:45:10). The obtained chromatogram was shown in Fig 1. Chromatogram of extracted amino acids from DBSs was shown in Fig 2.

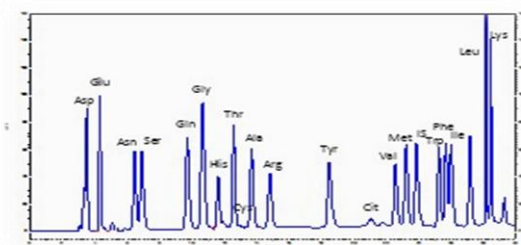


Figure 1. Chromatogram of standard solution

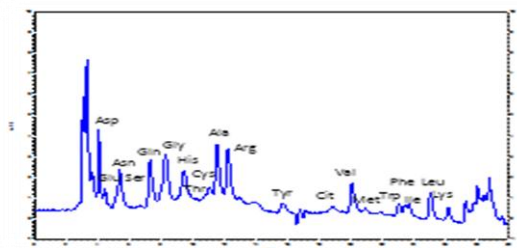


Figure 2. Chromatogram of DBS sample

For extraction of DBS, MeOH:H₂O (50:50 v/v), ACN:H₂O (50:50 v/v), sodium tetra borate buffer, TCA 1% (w/v), TCA 10% (w/v), TFA 1% (v/v), TFA 10%(v/v), HCl 1mM, HClO₄ 5% (v/v) as a extraction solvents were used. From these solvents four of them have the best response. Among these four solvents, MeOH:H₂O (50:50 v/v) has the best response for the desired amino acids. Extracted amino acids level for each solvent was shown in Fig 3.

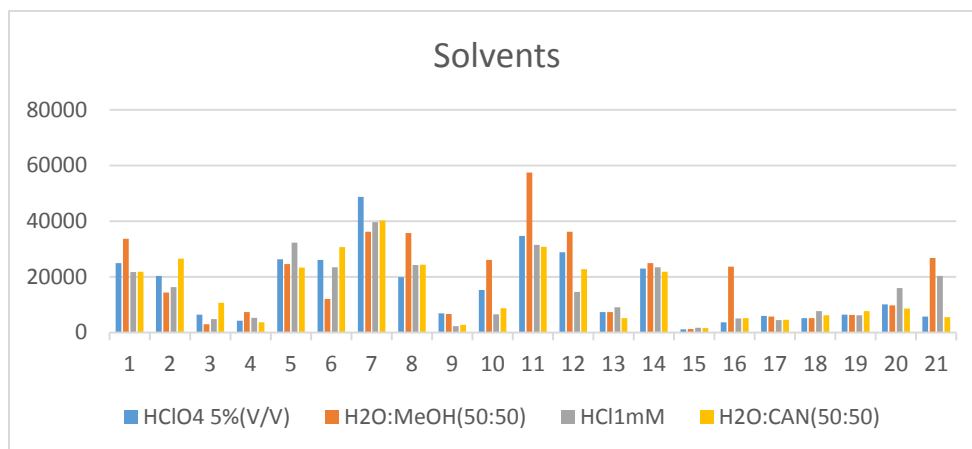


Figure3. Extracted amino acids level for each solvent

Based on the result of CCD, vortex time does not have a significant impact on the extraction efficacy. Intra-assay and inter-assay coefficients of variation were respectively 15.45% and 11.10%.

Conclusion

A simple and rapid method for the extraction and quantization of 21 amino acids from DBSs was introduced in this study. This study provide extraction procedure that have a maximum response for all basic amino acids. This method can be used for specialized investigation metabolic disorders to minimize false positive results. This method is highly accurate newborn screening and follow up for PKU and MSUD.

References

- [1] N.H.Kim, J.S.Jeong, H.J.Kwon, Y.M.Lee, H.R.Yoon, K.R.Lee, S.P.Hong, Simultaneous diagnostic method for phenylketonuria and galactosemia from dried blood spots using high-performance liquid chromatography-pulsed amperometric detection, *J. Chromatogr. B Anal. Technol. Biomed. Life Sci.* 878 (2010) 1860–1864. doi:10.1016/j.jchromb.2010.04.038.
- [2] R.Pecce, E.Scolamiero, L.Ingenito, G.Parenti, M.Ruoppolo, Optimization of an HPLC method for phenylalanine and tyrosine quantization in dried blood spot, *Clin. Biochem.* 46 (2013) 1892–1895. doi:10.1016/j.clinbiochem.2013.08.022.
- [3] V.Houbart, G.Cobraiville, A.Servais, A.Napp, M.Merville, M.Fillet, Hepcidin determination in dried blood by microfluidic LC-MS/MS: comparison of DBS and volumetric absorptive microsampling for matrix effect and recovery, *Bioanalysis.* 7 (2015) 2789–99. doi:10.4155/bio.15.181.

Facile Synthesis, Characterization and Biological Evaluation of Various Oxygen and Nitrogen Containing Heterocycles as α -Glucosidase Inhibitors

Maryam Nourisefat * ^{a,b,d}, Massoud Amanlou ^c, Farhad Panahi ^e Ali Khalafi-Nezhad ^d and Ali Akbar Moosavi-Movahedi ^{a,b}

a) *Institute of Biochemistry and Biophysics, University of Tehran, Tehran, Iran*

b) *UNESCO Chair on Interdisciplinary Research in Diabetes, University of Tehran, Tehran, Iran*

c) *Department of Medicinal Chemistry, Tehran University of Medical Sciences, Tehran, Iran*

d) *Department of Chemistry, College of Sciences, Shiraz University, Shiraz 71454, Iran*

e) *Department of Polymer Engineering and Color Technology, Amirkabir University of Technology, Tehran, Iran*

* Corresponding author: Tel: +98 21-61113381, E-mail: m.nourisefat@ut.ac.ir

Introduction :

As a serious global health crisis, diabetes mellitus commonly referred to as diabetes is a common metabolic diseases, characterizing by abnormally high blood sugar level [1]. Therefore, avoiding wide fluctuations in blood glucose levels by inhibition of the carbohydrate-hydrolyzing enzymes is critical for treatment for glycemic control [2-3]. Therefore, beside the commercial inhibitors of α -Glucosidase which are widely in use for the treatment of diabetes, it is necessary to develop more tolerable α -Glucosidase inhibitors with less unfavorable side effects. The object of this study was to synthesize some heterocyclic compounds [4] to access their inhibitory properties against α -Gucosidase as antidiabetic inhibitors.

Methods / Experimentals :

The importance of this project is to application of new strategies for synthesis of different class of oxygen and nitrogen containing heterocyclic compounds using a multi-component reaction in a single-step process. Then rational virtual screening was employed over almost Two-hundred compounds. Here the inhibitory effects of the selected compounds against α -Glucosidase were evaluated, spectroscopically. The interactions between enzyme and the heterocyclic compounds have been also investigated by computational study including docking and molecular dynamic.

Results and Discussion:

In this project new scaffolds containing substructures such as pyrimidine-fused heterocycle ring including amino acid moiety, indole containing xanthene and chromene derivatives, benzoxazole and benzothiazol including poly hydroxyl groups and other heterocyclic compounds were introduced. The selected compounds revealed interesting inhibitory enzymatic activity against α -Glucosidase. In structure of this set of compounds, the biological activity changed by only alternation of subunit although the significant role of substructures were stable. Therefore, it is possible to modulate their α -Glucosidase inhibitory action, and find the quantitative structure–activity relationship models (QSAR). So the synthetic compounds were compared for their enzyme inhibitory action, IC_{50} value, the inhibition parameter, K_i and other kinetic parameters of the enzyme was obtained. According to the type of inhibition of each compound, the computational study can help to verify the mechanistic effect of the synthetic compounds on enzyme. Also infrared and fluorescence spectroscopy

were applied to study of the structural changes of the α -glucosidase enzyme via the interactions with the selected aforementioned compounds.

Conclusion:

This study may suggest an easy access to new and diversified class of synthetic heterocyclic compounds as the novel molecular templates with a range of inhibitory properties against α -Glucosidase. Therefore, considering inhibitory properties of the synthetic compounds against this carbohydrate-hydrolyzing enzyme and simplicity of their preparation procedures, makes it possible to synthesis safer anti-diabetic drugs by selection of appreciate starting materials in the multi-component reaction.

References

- [1] S. Christudas, L. Gopalakrishnan, P. Mohanraj, K. Kalyamoorthy, P. Agastian, *Int. J. Integr Biol*, **2009**, 6, 41–45.
- [2] C.M. Renders, G.D. Valk, S.J. Griffin, E.H. Wagner, W.J.J. Assendelft, *Diabetes Care*, **2001**, 24, 1821–1833.
- [3] H. Lebovitz, *Curr. Ther. Diabetes*, **1997**, 26, 539–551.
- [4] A. Khalafi-Nezhad, M. Nourisefat, F. Panahi, *Org. Biomol. Chem*, **2015**, 13, 7772-7779.

Heterogenization of manganese porphyrin via hydrogen bond in Zeolite Imidazolate Framework-8 matrix, a host-guest interaction

Mojtaba Bagherzadeh*, Elnaz Mesbahi

Chemistry Department, Sharif University of Technology, Tehran, Iran

Email address: bagherzadeh@sharif.edu

Introduction:

Epoxidation of olefins have been paid much attention, using modified metalloporphyrins as models for cytochrome-P450 [1]. The existence of hydrogen bonding in the active site of natural systems has been proposed as an important factor for heterolytic O–O bond cleavage, especially in peroxidase [2]. Moreover, hydrogen bonding in P450 results in high catalytic performance in consequence of a shorter Fe-S bond and greater electron donation from the axial thiolate ligand [3]. Hence, the investigation of the hydrogen bond effects is worthwhile in the catalysis researches.

In this work, Mn(por) bearing OH substituents in *ortho* and *meta* position of phenyl groups is heterogenized in Zeolite Imidazolate Framework (ZIF-8) matrix via host-guest interaction. The OH groups are capable of producing hydrogen bond with the C-H on the 2-methylimidazolate parts of the matrix in the periphery of the porphyrin. The olefine epoxidation in the presence of the heterogenized metalloporphyrin and tetra-*n*-butylammoniummonopersulfate as oxidant have been examined.

Experimentals:

Synthesis of T(2,3-OHP)PorMnOAc

5,10,15,20-tetrakis(2,3-dimethoxyphenyl)porphyrin was prepared by the Lindsey method [4]. The free-base porphyrins was metalated by corresponding salt; Mn(OAc)₂·4H₂O according to the Adler method [5]. James method with some modification in its purification was used for demethylation of the aforementioned porphyrin to the corresponding hydroxy porphyrin [6].

Synthesis of T(2,3-OHP)PorMn@ZIF-8

The template-directed strategy was performed by mixing 2-methylimidazolate (0.33 mmol) and Zn(NO₃)₂ (0.28 mmol) with T(2,3-OHP)PorMn in DMF to afford T(2,3-OHP)PorMn@ZIF-8. The mixture was transferred into Teflon-liner Parr pressure vessels. Teflon liners were placed in autoclaves, and heated to 408 K for 36 h.

Epoxidation reactions

In a 5 mL round bottom flask containing CH₂Cl₂/Methanol (1:5), the alkenes (0.2 mmol), catalyst (5 mg) and tetra-*n*-butylammonium hydrogen monopersulfate (0.4 mmol) were added. The mixture was stirred for 24 h at ambient temperature in a closed system and analyzed by GC in the end.

Results and Discussion:

Olefine epoxidations were carried out in the presence of heterogenized metalloporphyrin (T(2,3-OHP)PorMn@ZIF-8) and *n*-Bu₄NHSO₅. The results obtained through injection of the reaction solutions into GC showed an enhanced catalytic efficiency and a fairly good reusability for the aforementioned catalyst compared to the previously reported homogeneous complexes.

Conclusion:

The cooperating interplay of a kind of hydrogen bond is supported by the enhanced catalytic efficiency and fairly good reusability of the catalysis system presented.

References

- [1] Ortiz de Montellano PR. *Cytochrome P450: Structure, Mechanism, and Biochemistry*, Plenum Press: New York, 1995.
- [2] Gray HB, Lipard SJ and Valentine JF. *Bioinorganic Chemistry*, University Science Books: 2005.
- [3] Krest CM, Silakov A, Rittle J, Yosca TH, Onderko EL, Calixto J, Green MT. *Nat. Chem.* 2015, **7**, 696-702.
- [4] Lindsey JS, Hsu HC and Schreiman IC. *Tetrahedron Lett.* 1986; **27**: 4969–4970.
- [5] Adler AL, Long FR and Kampas F. *J. Inorg. Nucl. Chem.* 1970; **32**: 2443–2445.
- [6] James DA, Arnold DP and Parson PG. *Photochem. Photobiol.* 1994; **59**: 441.

A Complete Comparative Study of New Superior Green Nanobiocomposite via Common Nanosorbents

R. Moosavi^{*,#}, A. Afkhami

^aYoung Researchers and Elite Club, Shiraz Branch, Islamic Azad University, Shiraz, Iran

²Department of Chemistry, Bu-Ali Sina University

* Corresponding Author's E-mail: Raz.Moosavi@gmail.com

Introduction: Increasing human pollutions decrease the amount of water left on Earth! A main globally alarming issue is industries effluent. Wastewater if treated may be reused for various purposes. Hence it's essential to develop, cost effective and environment-friendly techniques for separating pollutants effectively [1, 2].

Magnetic separation had been interested as a preferred method because it is suitable for heterogeneous bulk systems, commands further pollution effects and serves as an easy fast method utilizing external magnetic fields [3].

But new efficient strategies for commercial wastewater treatment applications should be explored to introduce unique magnetic sorbents in an economic and eco-friendly manner.

Methods/Experimental: Synthesized magnetic nanomaterials were characterized by SEM, TEM, XRD and EDX measurements. Eventually experimental adsorption data were completely analyzed by ten different kinetic and equilibrium models, using nonlinear regression, for obtaining all the model parameters, maximum adsorption values, rate constants, correlation coefficients and four error functions. Here we used the robust design multivariate optimization in the laboratory experiments. For additional performance the antibacterial effects against both Gram-negative bacteria *E. coli* and Gram-positive bacteria *S. aureus* was proposed as well.

Results and Discussion: Firstly, Cinnamon-extract as reducing as well as capping agent [4] was used for green synthesis of Cin-Ag/Fe₃O₄ nanobiocomposite. The synthesis using plant extracts is simple, economical, requires less reaction time which results in green ultimate product [4]. Then Cin-Ag-Fe₃O₄ particles were studied as an adsorptive substrate holding regenerable properties under an external magnetic force [4]. We proposed comparative studies for all aspects of the new nanocomposite, and the adsorption of some typical organic toxins, as a large common class of environmental harmful compounds in the absence and presence of surfactant, was investigated (example of comparisons shown in Fig. 1).

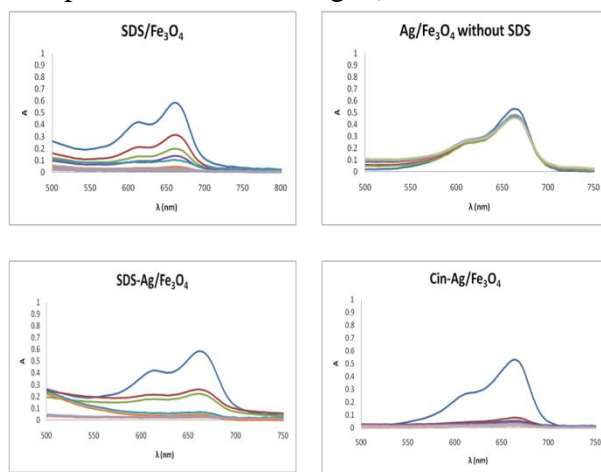


Fig. 1 The pseudo-second-order adsorption mechanism on different adsorbents

For instance Fig. 1 shows within almost 0–3 min, 84.76% removal of the whole at equilibrium was achieved for nanobiocomposite. Such a fast adsorption rate is attributed to the absence of internal diffusion.

Facts suggest that the green composite, without any surfactant, could rapidly and effectively adsorb effluent in a new way for practical usage.

The recyclable studies also showed high performance of the nanocomposite.

Noteworthy to prevent time and resource wasting on unnecessary experiments, simultaneous optimization and response surface methodology for influence factors and their interactions was used (Fig. 2). Also various isotherm and error models were employed to interpret the adsorptive behaviors.

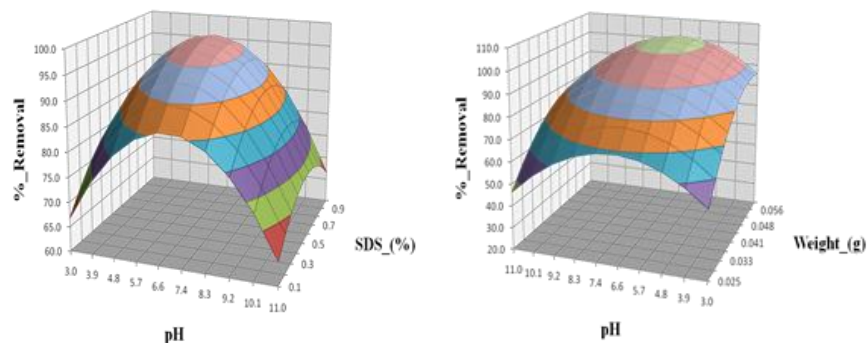


Fig. 2 Typical response surfaces of full quadratic model between removal and two variables

Conclusion: In order to address wastewater-treatment problem, an efficient cost-effective and environmentally benign nanobiocomposite was introduced in a new green manner usage. The overall comparison includes synthesis, capacities, many equilibrium and kinetic parameters besides other features were investigated. Of particular interest, the nanocomposite was bi-functional and showed both antibacterial and higher net magnetic moments. Results indicated an unprecedented adsorption at saturation over conventional adsorbents necessarily for industrial applications, and thanks to high specific surface and new capabilities, the green process lasts a few minutes.

References:

- [1] S. Patil, D. Patil, S. Renukdas, N. T. Patel, Comparative study of kinetics of adsorption of methylene blue from aqueous solutions using cinnamon plant(*Cinnamomum zeylanicum*) leaf powder and pineapple (*Ananas comosus*) peel powder, *Orbital Elec. J. Chem., Campo Grande*,4 (2012) 77-100.
- [2] M. Rafatullah, O. Sulaiman, R. Hashim, A. Ahmad, Adsorption of methylene blue on low-cost adsorbents: a review. *J. Hazard. Mater.* 177 (2010) 70-80.
- [3] A. Afkhami, R. Moosavi, Adsorptive removal of Congo red, a carcinogenic textile dye, from aqueous solutions by maghemite nanoparticles, *J. Hazard. Mater.* 174 (2010) 398–403.
- [4] R. Moosavi, S. Ramanathan, Y. Y. Lee, K. C. S. Ling, A. Afkhami, G. Archunan, S. T. Selvan, Synthesis of antibacterial and magnetic nanocomposites by decorating graphene oxide surface with metal nanoparticles. *RSC Adv.*, 5(2015) 76442-76450.

On the Dependency between Principal Components in Principal Component Analysis (PCA)

Elaheh Talebanpourbayat^a, Bahram Hemmateenejad^{*,a}, Morteza Akhund^a

^a Chemistry Department, Shiraz University, Shiraz, Iran

hemmatb@shirazu.ac.ir

Introduction: Principal component analysis (PCA) is a dimensionality reduction method in which an original data is remapped into a new coordinate system based on the variance within the data space. A mathematical procedure is applied in PCA, transforms a series of (possibly) correlated variable into a (smaller) number of uncorrelated and orthogonal factors named principal components.[1] However, the principal components are uncorrelated but might be dependent. To measure dependency, two indices including maximum information coefficient (MIC) [2] and distance correlation (DC) [3] were utilized. In this work, the dependency between principal components was investigated in the several simulation data sets in the presence of the different types of artifacts. Finally, the potential applicability of dependency concept was employed to estimate the chemical rank in the different real evolving processes which were monitored by different kinds of techniques such as spectroscopy, chromatography, and electrochemistry.

Methods / Experimental: To investigate the dependency between principal components, data sets were simulated under a wide range of conditions. For spectroscopic study, two models were selected including kinetic and equilibrium models. the concentration profiles of species involved in the evolving (kinetic and equilibrium) processes were simulated, for a given rate constant(s) and equilibrium constant, respectively. Each clean simulated data set was constructed by pre-postmultiplying of concentration profile by the multiple overlapping Gaussian absorption bands. Simulated chromatographic data set, was generated by the pure spectra and elution profile of components. Finally, to make simulated data sets resemble real data more closely, different kinds of artifacts (homoscedastic noise, heteroscedastic noise, and baseline drift) were added. Published FTIR-ATR spectroscopic, UV-Visible spectroscopic, DAD-HPLC, and chronoamperometry datasets were used as the real data sets to investigate dependency measurement.

Results and Discussion: PCA is a universal and well established exploratory technique which decomposes the original data set to a bilinear model of uncorrelated factors called principal components (PC). Any physical or chemical factors involved in the evolutionary process cause the variation in the data space influences the principal components. So, they can be considered as the factors that assess the progress of the evolutionary process and therefore, the valuable information can be extracted from them. [4] Due to importance of the PCs, the investigation of their properties has the critical importance. To address this issue, the dependency between PCs was studied.

First of all, a normally distributed random data set (100×100) was generated with zero mean and unit standard deviation. The dependency between each pair of PCs was determined by the

MIC and DC. (data not shown) ANOVA test shown no significant differences between MIC and DC obtained from the first seven PCs. So, no significant dependency was detected in random data set. In the next step, the dependency between PCs was investigated in the presence of the analyte(s) in the wide range of chemical systems and monitoring techniques which are just exemplified here by simulating a kinetic model of the two-step consecutive first order reactions of the form $A \rightarrow B \rightarrow 2c$ with signal-to-noise ratio is equal to five. The concentration profile and pure spectra, and the resulted absorbance spectra are shown in Figure 1. (a-c).

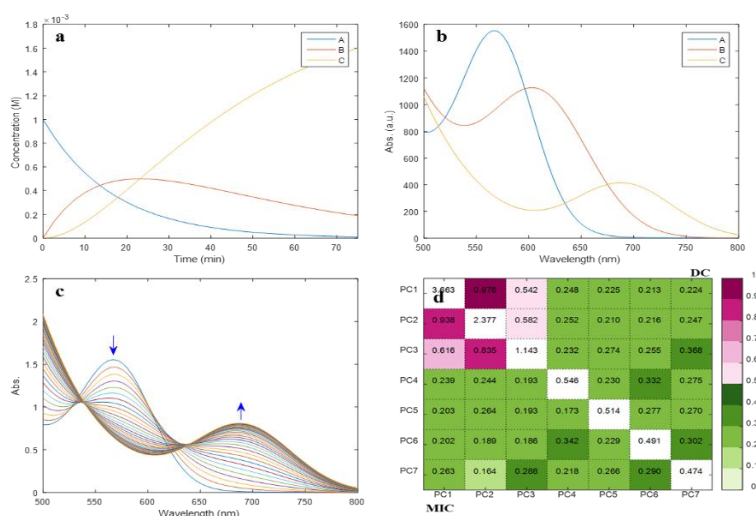


Figure1. a) Concentration profile, b) pure spectra, c) the resulted absorbance spectra of the simulated datasets for the first order two-step consecutive reaction of form $A \rightarrow B \rightarrow 2c$, and d) MIC and DC between the pairs of PCs.

As can be seen (Figure 1. d), the MIC and DC values are decreased when secondary PCs that correspond to noise PCs are introduced. The primary PCs are shown highly dependency while they are uncorrelated. On the other hands, low degree of dependency was detected between noisy PCs (the secondary PCs). This results suggest that dependency concept between PCs relate to the number of chemical rank of system. This idea was utilized to estimate chemical rank by defining of two new indices based on MIC and DC to determine number of significant PCs in ill-condition.

Conclusion: MIC and DC could easily detect mutual dependency between PCs. Primary PCs containing the systematic informations show high degree dependency between PCs while no significant dependency was detected between the secondary PCs involved noisy information. The indices were derived from the dependency between PCs, usually reports better results in real data sets.

References

- [1] de Juan, Anna; Tauler, Rom à J. Journal of Chromatography A, 2007, 1158, 184.
- [2] Reshef, David N.; Reshef, Yakir A.; Finucane, Hilary K.; Grossman, Sharon R.; McVean, Gilean; Turnbaugh, Peter J.; Lander, Eric S.; Mitzenmacher, Michael; Sabeti, Pardis C. Science, 2011, 334 (6062), 1518.
- [3] Székely, Gábor J.; Rizzo, Maria L.; Bakirov, Nail K. Annals of Statistics, 2007, 35 (6), 2769.
- [4] Thurston, Tom J.; Brereton, Richard G.; Foord, Dan J.; Escott, Richard E. A. Talanta 2004, 63 (3), 757.

Ab initio potential energy surface by modified Shepard interpolation and classical reaction dynamics for the NH + NO reaction

Marzyeh Mohammadi, Shapour Ramazani*

Department of Chemistry, Yasouj University, 75914 Yasouj, Iran.

Email: ramazani@yu.ac.ir

Introduction: The reaction of NH with NO has recently received a lot of attention in the kinetics community, because of its importance in the combustion of nitrogen containing fuels, in thermal DeNO_x, and related process. There have been several measurements of the overall rate constants for NH+NO, including room temperature studies, shock tube, and flame measurements. The rate constant is found to have values in the range $3.8\text{--}5.8 \times 10^{-11}$ cm³/s at 300 K, increasing slowly with temperature [1]. In this work, classical dynamics simulations for the NH + NO reaction have been investigated on an interpolated ab initio potential energy surface.

Method: In this study the PES has been computed as a modified Shepard interpolation over a data set of ab initio points using the Grow methodology. The energy can be expressed in terms of all the atom-atom distances. For any atomic configuration, the atom-atom distances, R_n , $n=1, \dots, N(N-1)/2$, are easily calculated from the Cartesian coordinates. We can use, $(Z_n = \frac{1}{R_n})$. The potential energy at a configuration R in the vicinity of a data point, $R(i)$, can be expanded as a Taylor series, T_i , in these inverse distances.

$$T_i(Z) = V[Z(i)] + \sum_{k=1}^{3N-6} [Z_k - Z_k(i)] \frac{\partial V}{\partial Z_k} \bigg|_{Z=Z(i)} + \frac{1}{2!} \sum_{k=1}^{3N-6} \sum_{j=1}^{3N-6} [Z_j - Z_j(i)] \times [Z_k - Z_k(i)] \frac{\partial^2 V}{\partial Z_k \partial Z_j} \bigg|_{Z=Z(i)} + \dots$$

Where $V[Z(i)]$ is the value of the potential at $Z(i)$ and the derivatives are taken with respect to inverse distance at $Z(i)$. Once the required energy and derivatives have been evaluated at some number, N_d , of molecular configurations (number of data points) through ab initio calculations, a modified Shepard interpolation gives the total potential energy at any configuration Z as a weighted average of the Taylor series about all N_d initial data points and their symmetry

equivalents:

$$E(Z) = \sum_{g \in G} \sum_{i=1}^{N_{d_{\text{aug}}}} w_{goi}(Z) T_{goi}(Z)$$

Where each T_i , has associated weight, w_i . In this expression G denotes the symmetry group of the molecule. The details of the Grow methodology have been presented previously [2-4].

Results and Discussion: As indicated in Figure 1, it was found that there were different reactive channels available depending on the orientation of the colliding fragments. Depending on the orientation of reactant molecules, complexes vw_1 and vw_2 were formed. HNO, N, NON, H, N₂H, O, N₂O, N₂, OH products, six vibrationally energized were observed.

In this work the reaction probabilities calculated for the interpolated gas-surface PES as a function of the number of data points (Figure2). The PES was interpolated using the two part weight function. All of the result will be reported in the conference, including preliminary investigations of the suitability of the grown PES for studying inelastic (non-reactive) collisions.

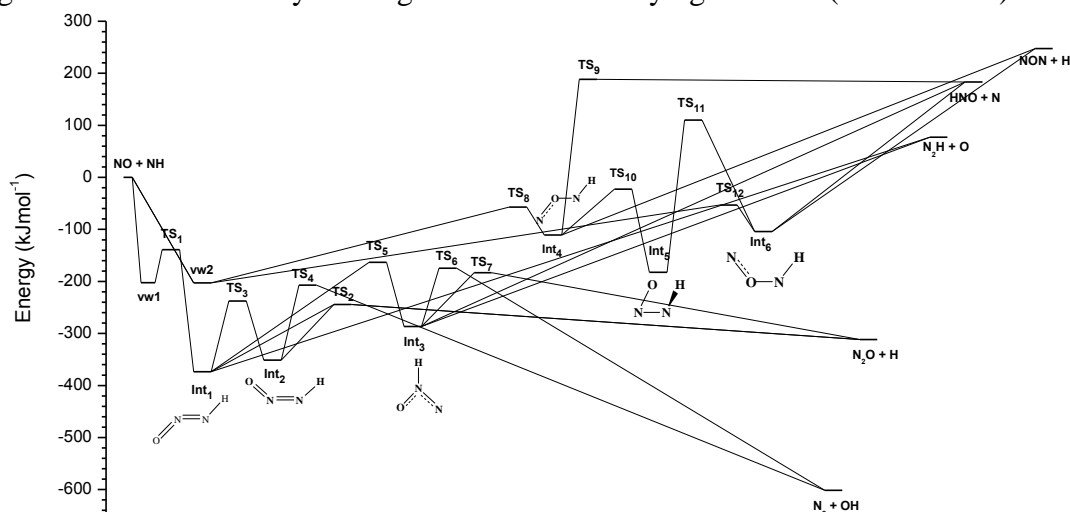


Figure 1. Relative energies of all species in the reaction $\text{NO} + \text{NH}$ at the $\text{mp2/6-311++g(d,p)//ccsd(t)/6-311+g(d)}$ level.

Conclusion: The suggested mechanism consists of includes 5 products and 12 transition states ($\text{TS}_1\text{-TS}_{12}$). $\text{N}_2 + \text{OH}$ product is more stable than the other products. Depending on the orientation of reactant molecules, complexes vw_1 and vw_2 were formed. Reaction probabilities calculated for the interpolated gas-surface PES as a function of the number of data points.

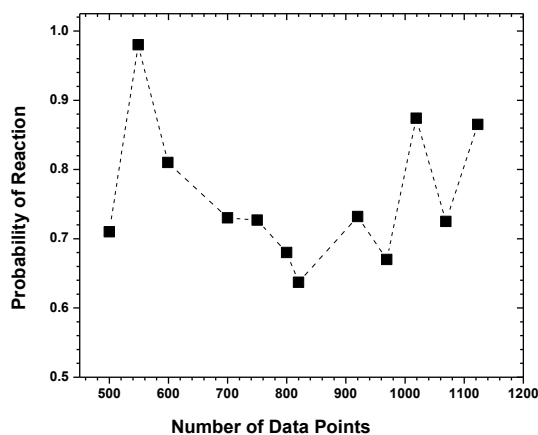


Figure 2. Reaction probability vs number of data points for a PES constructed using a two order Taylor expansion.

References

- [1] Kimberly S. Bradley; Patrick McCabe; George C. Schatz. *J. Chem. Phys.* **1995**, 102, 6696-6705.
- [2] M. A. Collins. *Theor. Chem. Acc.* **2002**, 108, 313-324.
- [3] S. Ramazani; T. J. Frankcombe; S. Andersson; M. A. Collins. *J. Chem. Phys.* **2009**, 130, 244302-9.
- [4] R. P. A. Bettens; M. A. Collins. *J. Chem. Phys.* **1999**, 111, 816.

A theoretical study on borazine structure via an anomeric based oxidation

Avat(Arman) Taherpour^{*a,b}, Mohammad Ali Zolfigol^{*c}, Mahya Kiafar^c, Meysam Yarie^c, Saber Mirzaei^a

^a Department of Organic Chemistry, Razi University, Kermanshah, P.O. Box: 67149-67346, Iran.

E-mail: avatarman.taherpour@gmail.com

^b Medical Biology Research Center, Kermanshah University of Medical Sciences, Kermanshah, Iran.

^c Department of Organic Chemistry, Faculty of Chemistry, Bu-Ali Sina University, Hamedan, P.O.

Box: 6517838683, Iran. E-mail: zolfi@basu.ac.ir, & mzolfigol@yahoo.com, Fax: +98 8138257407

Introduction:

The inorganic benzene, borazine B_6N_6 , is a textbook example of a six- σ -electron six-membered ring.[1] Compared to benzene, the cyclic delocalization of electrons in the borazine ring is reduced due to the large electronegativity difference between boron and nitrogen. The polarity of the B-N bond causes borazine to show a reactivity pattern different from that of benzene. Understandably, the chemistry of borazine is dominated by addition reactions. The electrophiles first attack at nitrogen centers and form the corresponding conjugate acid, $H_3B_3N_3H_3E^+$ (E^+ = electrophile; H^+ , CH_3^+ , etc.), similar to the benzonium ion and under basic conditions, substitution reactions occur.[2]

Methods:

The structures **1-4** were optimized at the DFT-B3LYP/6-31G* theory level.[3] All the calculations of the structures 1-4 (Figure 1) were carried out using the *Spartan '10* package.[3] The calculations on the selected structural data (bond length (Å), bond angle (°) and torsional angle (°)) of the structures 1-4 were undertaken using a DFT-B3LYP/6-31G* method. In order to evaluate the aromaticity indexes of these molecules, the nucleus-independent chemical shifts (NICS) of them have been calculated using the 6-31+G** basis set. [4] The dummy atom was placed 1 Å above the ring plane.

Results and Discussion:

Recently, we have introduced the new term entitled "anomeric based oxidation" for the first time [5]. The aims of this study is tasked-specific and knowledge based development of anomeric based oxidation and/or aromatization. This computational study will be present another piece of a practical puzzle that lead to the target molecules via anomeric based oxidation mechanism and/or aromatization. With this aim, we have chosen borazine B_6N_6 as a target molecule for its aromaticity investigations. The structures **1-4** were optimized at the DFT-B3LYP/6-31G* method. [3] In Figure 1 has shown the selected structural data (bond length (Å), bond angle (°)) of the structures **1-4**.

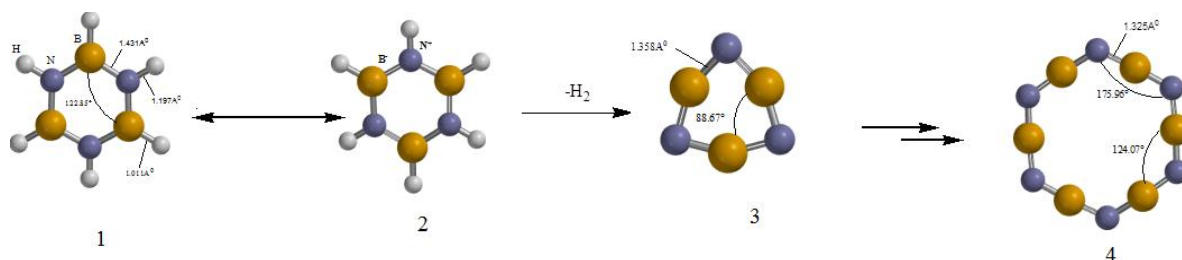


Figure 1. The structures **1-4** were optimized at the DFT-B3LYP/6-31G* method

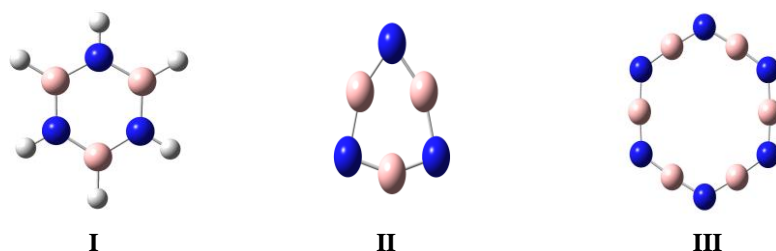


Table 2. The calculated NICSs (ppm) for the target molecules. The negative values indicate the aromaticity.

compound	Benzene	I	II	III
NICS	-10.24	-2.78	-2.43	0.99

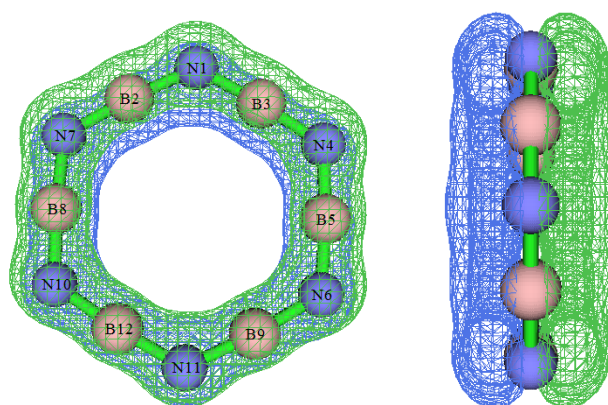


Figure 2. The up (left) and side (right) view of compound III molecular orbital (HOMO-10, Isovalue 0.035)

The results of NICS calculation are shown in table 2. For more clarity the NICS value of benzene molecule is also calculated at the same level. The compounds I and II are both aromatic. However, in comparison to the benzene, their aromaticity is significantly lower. About the compound III, the NICS value elucidates an antiaromatic compound. This molecule which is the dimer of compound II has 12 π electrons. According to the Hückel's rule ($4n+2$) this molecule should be antiaromatic which justify the outcome of NICS calculation. But, the planar structure and also the very low NICS value interested us to assess its molecular orbitals more carefully. As depicted in the figure 2, the p orbital of this system can interact with each other to generate a conjugated system. This phenomenon just has been seen for the aromatic compounds.

Conclusion:

This calculation reveals a competition between the Hückel's rule and the conjugation of the p orbitals. The aromatization stability is tends toward Hückel's rule. On the other hand the p conjugation determines the structure (planar) of this system. Thus development of anomeric based oxidation and/or aromatization mechanism lead to knowledge based designing of

biomimetic reactions in the future. We think that the obtained results from this research will be support the idea of rational designs, syntheses and applications of target molecules for the development of anomeric based oxidation and/or aromatization mechanism.

References:

- [1] Stock, A.; Pohland, E. *Chem. Ber.* **1926**, *59*, 2215.
- [2] (a) Chiavarino, B.; Crestoni, M. E.; Fornarini, S. *J. Am. Chem. Soc.* **1999**, *121*, 2619. (b) Chiavarino, B.; Crestoni, M. E.; Marzio, A. D.; Fornarini, S.; Rosi, M. *J. Am. Chem. Soc.* **1999**, *121*, 11204.
- [3] All of the calculations were performed by: *Spatran '10*-Quantum Mechanics Program: (PC/x86) 1.1.0v4. **2011**, Wavefunction Inc., USA.
- [4] NICS citation: P. V. R. Schleyer, C. Maerker, A. Dransfeld and H. Jiao, *J. Am. Chem. Soc.*, **1996**, *118*, 6317–6318.
- [5] (a) M. A. Zolfigol, F. Afsharnadery, S. Baghery, S. Salehzadeh and F. Maleki, *RSC Adv.*, 2015, **5**, 75555., (b) M. A. Zolfigol, M. Safaiee, F. Afsharnadery, N. Bahrani-Nejad, S. Baghery, S. Salehzadeh and F. Maleki *RSC Adv.*, 2015, **5**, 100546., (c) A. R. Moosavi-Zare, M. A. Zolfigol and Z. Rezanejad, *Can. J. Chem.* 2016, **94**, 1., (d) M. A. Zolfigol, M. Kiafar, M. Yarie, Avat(Arman) Taherpour and Mahdi Saeidi-Rad, *RSC Adv.*, 2016, **6**, 50100., (e) M. A. Zolfigol, A. Khazaei, S. Alaie, S. Baghery, F. Maleki, Y. Bayat and A. Asgari *RSC Adv.*, 2016, **6**, 58667., (f) M. Kiafar, M. A. Zolfigol, M. Yarie, A.(A.) Taherpour, *RSC Adv.*, 2016, **6**, 102280.

Theoretical Kinetics Study of decomposition of dichlorodifluoromethane in gas phase

Marzyeh Mohammadi, Shapour Ramazani*, Faredoon Hooshmandi

Department of Chemistry, Yasouj University, 75914 Yasouj, Iran.

Email: ramazani@yu.ac.ir

Introduction: Chlorofluoromethanes have a variety of important industrial applications. However, they are photochemical sources of C1 atoms, and it is this property that has been shown to be detrimental to stratospheric ozone concentration. In chlorine-substituted methanes, the C-Cl bond has the lowest energy, and if chlorine substitution is increased, the first C-Cl bond energy is generally lowered. Hence, dissociation to produce a C1 atom is expected to be an important dissociation channel [1]. We study the reaction decomposition of dichlorodifluoromethane in the gas phase to investigate their order of stability and study the kinetics of the reaction.

Method: The geometries of the stationary points were optimized at the MPWB1K [2] level. Calculations at the MP2/6-311++g(d,p)//CCSD(T) 6-311++g(d) [3,4] level were carried out to obtain more accurate energies for the stationary PES (Figure 1). The RRKM-TST model was used to calculate the individual rate constants [5].

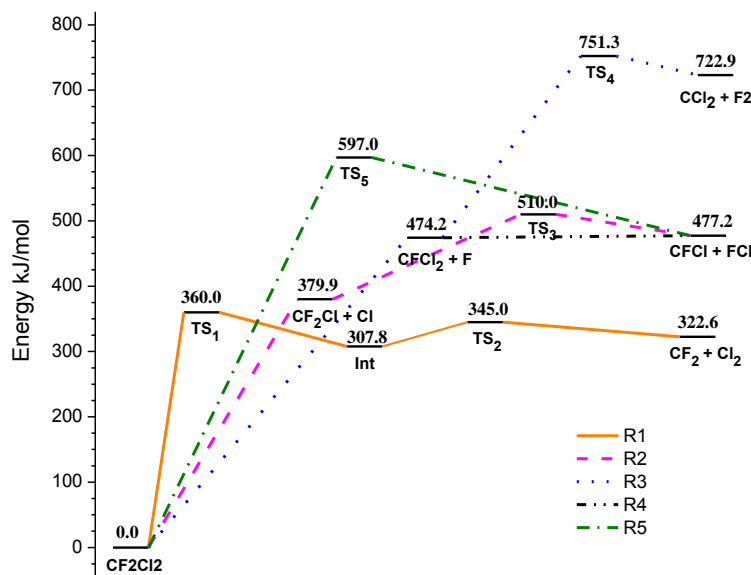


Figure 1. Relative energies of all species in the reaction of decomposition of dichlorodifluoromethane at the mp2/6-311++g(d,p)//ccsd(t)/6-311+g(d) level.

Results and Discussion: Figure 1 shows that the PES of R1 is lower than the other reactions. Separation of fluorine atoms of the molecules CF_2Cl_2 depends on a relatively high energy. Channels R2, R4, and R5 produce the products CFC1 and ClF . Theoretical study of the reaction decomposition of CF_2Cl_2 in the gas phase was considered to investigate their order of stability and study the kinetics of the reaction R1 along with the consumption of CF_2Cl_2 to

produce CF₂ and Cl₂ and a chemically-energized intermediate (Int).Figure 2 shows the effect of temperature on the calculated rate constants for channel R1.Nonlinear least-squares fitting [6] was used to calculate all rate constants at T=1000 to 2300 K Using $k = A(\frac{T}{300})^n \exp\left[-\frac{E(T+T_0)}{R(T^2+T_0^2)}\right]$

Arrhenius Equations and reported in Table 1.

Table 1. The Fitted Parameters for Reactions R in the Temperature Range T=1000- 2300 K.

Parameter	Reactions	
	(R1) _{tun}	(R1) _{notun}
A(s ⁻¹)	2.2×10 ⁵⁰	2.3×10 ⁵⁰
n	4.6	4.6
E(kJ mol ⁻¹)	477.0	477.3
T ₀ (K)	58.4	58.7

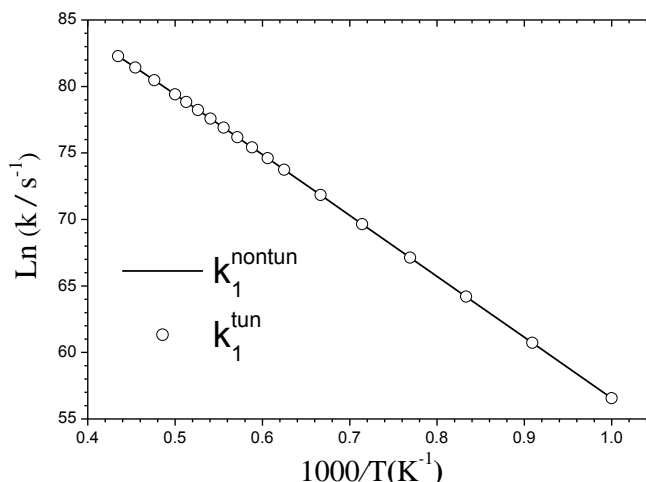


Figure 2. Arrhenius plot of the calculated rate constants for reactions R1 in which rate constants are determined.

Conclusion:CF₂Cl₂ is more stable than the other compounds. CF₂Cl₂ decomposition leads to the formation of three product groups thatCF₂+Cl₂ product is more stable than other products.Therefore,the rate constant calculations were done on R1.Tunneling effect was not effective for this reaction.

References

- [1] S. S. Kumaran; K. P. Lim; J. V. Michael; A. F. Wagner.*J. Phys.Chem.* **1995**,99, 8673-8680.
- [2] Y. Zhao; D.G. Truhlar.*J. Phys. Chem. A.* **2004**, 108, 6908-6918.
- [3] C.h. Møller; M.S. Plesset. *Phys. Rev.* **1934**,46, 618-622.
- [4] J.A. Pople; M. Head-Gordon; K. Raghavachari.*J. Chem. Phys.***1987**, 87, 5968-5975.
- [5] M. R. Berman; M. C. Lin.*J. Phys. Chem.* **1983**, 87, 3933-3942.
- [6] J. Zheng; D.G. Truhlar; *Phys. Chem. Chem. Phys.* **2010**, 12,7782-7793.

Thermal aging and triplet kinetic comparison of Ocfol explosive with different grade of HMX explosive using by DSC/TGA non isothermal methods

Hamid Sinapour, Sajjad Damiri*, Hamid Reza Pouretedal

Faculty of applied science, Malek-ashtar University of Technology, Shahin-shahr, Iran

s_damiri@mut-es.ac.ir

Introduction: Octahydro-1,3,5,7-tetranitro-1,3,5,7-tetrazocine (HMX) is one of the energetic material used for various applications. There are two grade of HMX namely A-HMX and B-HMX which contain 4-6% and below 1% of 1,3,5-Trinitro-1,3,5-triazacyclohexane (RDX) impurity respectively. To phlegm and desensitize the HMX about 5% wax was added which new composition called Ocfol [1].

Many unexpected runaway accidents had occurred due to explosives storage or transportation around the world [2]. Aging is the most serious reason of these kinds of accidents.

The goal of this work is to compare the effects of RDX impurity and wax additive on kinetic and thermal aging of HMX.

Methods: The DSC thermograms for A-HMX, B-HMX and Ocfol under Argon atmosphere and the heating rates of 4, 6, 8 and 10 °C min⁻¹ are shown in Fig. 1

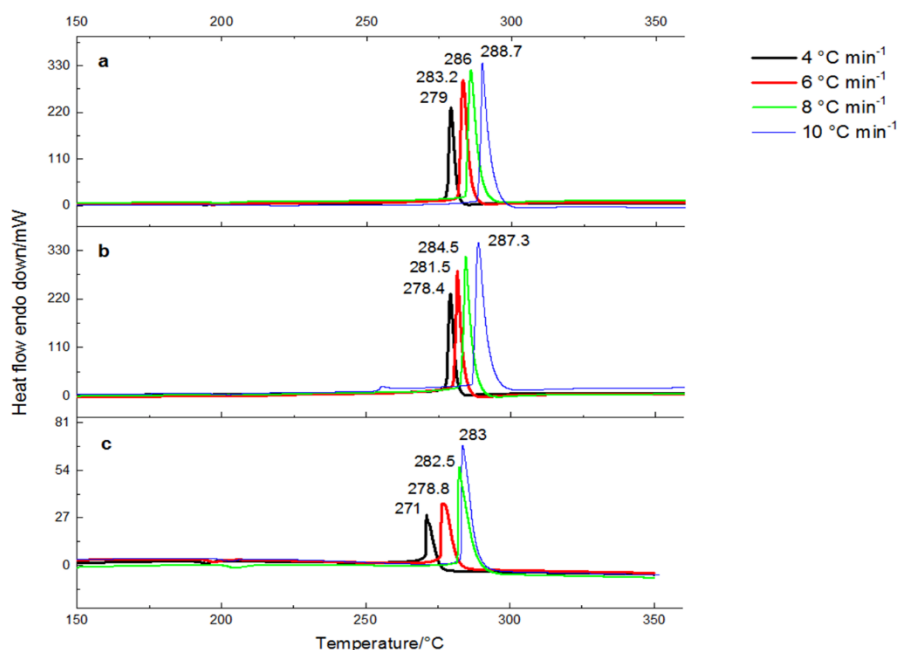


Fig 1 DSC thermograms under Ar atmosphere at different heating rates for a – B-HMX (< 1% RDX impurity), b – A-HMX (5% RDX impurity), c – W-HMX (5% wax) samples

In kinetic analysis, the rate of a solid-state reaction can be assumed a function of temperature and conversion which generally described by [3]:

$$\frac{d\alpha}{dt} = k(T)f(\alpha)$$

Results and Discussion: The KAS isoconversional method was used to obtain activation energies of 229.36, 221.05 and 267.37 kJ mol⁻¹ and then the compensation effect method was used to obtain preexponential factors of 4.345×10²⁰, 3.785×10²¹ and 5.77×10²⁵ S⁻¹ for B-HMX, A-HMX and Ocfol respectively. As there is a variety in E_a and A, the reaction model was found A2 for all of them.

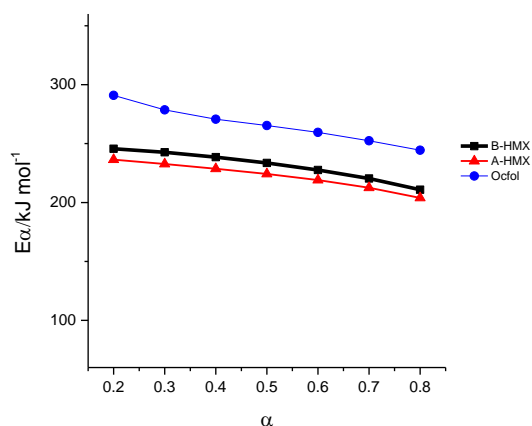


Fig. 2 Activation energy versus the extent of conversion between α= 0.2-0.8 at four heating rates of 4, 6, 8, 10 °C min⁻¹

Conclusion: The reaction models are same in all cases but decomposition temperature and activation energy were decreased in runty values in A-HMX while the preexponential factor was increased. The wax additive decreases decomposition temperature while it increases the activation energy, preexponential factor and lifetime of HMX in Ocfol sample sorely. B-HMX or pure HMX has longer lifetime and it could be stored for longer period in compare with A-HMX.

References:

- [1] S. Bulusu; R. Behrens. *Def. Sci. J.*, **1996**, 46, 347-360.
- [2] D. J. Peng; C. M. Chang; M. Chiu. *J. Hazard Mater.*, **2004**, 18, 1-13.
- [3] C.H. Bamford; C.F. Tipper. *Elsevier*, **1980**, 22.

Synthesis and characterization of high catalytic activity magnetic Fe₃O₄ supported Pd (II), as a green and efficient nanocatalyst for the Suzuki-Miyaura cross-coupling reaction in water

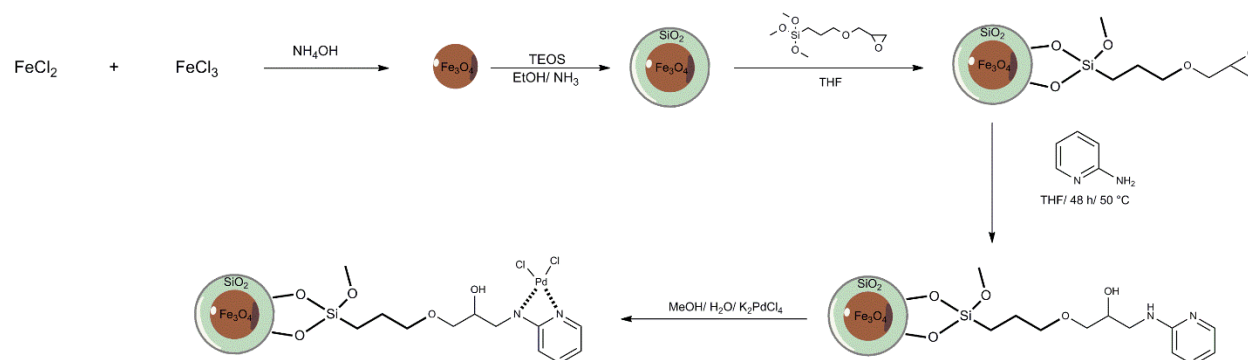
Firouz Matloubi Moghaddam^{a*}, Ashkan Karimi^a, Seyed Ebrahim Ayati^a

^aLaboratory of organic synthesis and natural products, Chemistry department, Sharif University, Tehran, Iran

matloubi@sharif.edu

Introduction: Transition metals play an essential roles in cross-coupling reactions [1]. The Suzuki reaction between aryl halides and aryl bromic acid is one of the important and widely used procedures for the synthesis of molecules containing biphenyl moiety, which is found in many fine chemicals and biologically active compounds [2], [3]. This work reports a green and high yield protocol for the Suzuki reaction. Here, a nanomagnetic catalyst based on Palladium with 2-amino pyridine ligand has been used for the Suzuki reaction at room temperature and in water. Also, a very promising result was observed for oxidation and Sonogashira reaction.

Experimental: The overall fabrication strategy is shown in Scheme 1. The silica-coated magnetic nanoparticles were synthesized according to the procedure reported elsewhere in the literature [4]. The silica-coated magnetic nanoparticles were used to synthesize [MNPs@2-aminopy][Cl] nanoparticles. The catalyst was fully characterized by FT-IR, TGA, CHN, SEM, EDX, and atomic absorption spectroscopy. Also DFT method was employed for electronic and structural studies. The synthesized catalyst was used in the synthesis of different derivatives of biphenyl systems. The optimized condition was identified by GC.



Scheme 1

Results and discussion: The surface morphology of the synthesized nanoparticles was observed by SEM. Fig. 1 shows uniform sized spherical particles with slight aggregation and a mean particle size of 20–25 nm. Atomic absorption spectroscopy (AAS) analysis of the catalyst showed the amount of palladium loaded on the magnetic nanoparticles was about 0.80 mmol g⁻¹. In addition to its recyclability, its air and moisture-stable properties other important aspects of this new heterogeneous catalysis. We evaluated optimized reaction condition at room temperature and in water. The reaction of phenyl bromic acid and para bromo toluene was fully converted after 4 hours. In general, the yields of the reactions in all cases were excellent and were completed in moderately low reaction times.

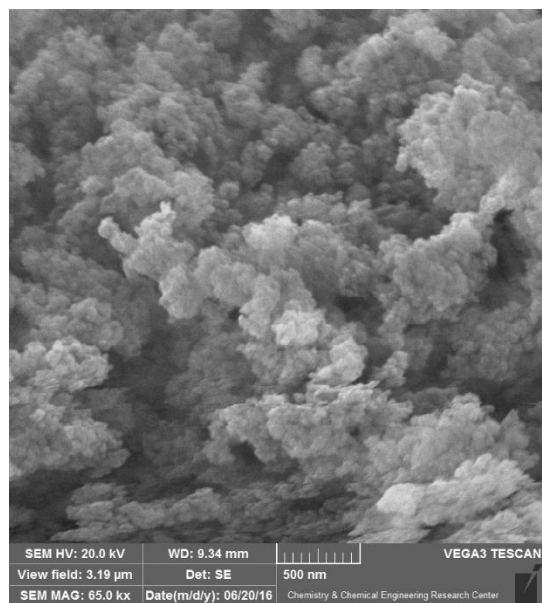


Fig. 1

Conclusion: In the present paper, we summarized the application of a nanomagnetic catalyst of Pd in the Suzuki reaction. This catalyst can not only catalyze the reaction with high yields, but also because of its function in the water, it adheres to the principles of green chemistry, and, furthermore, because of its magnetic property it can easily be separated from the reaction medium by using an external magnet.

References

- [1] T. Hayashi, M. Konishi, Y. Kobori, M. Kumada, T. Higuchi, K. Hirotsu, *J. Am. Chem. Soc.* **1984**, *106*, 158 – 163.
- [2] R. Chinchilla, C. Miyaura, Norio; Yamada, Kinji; A. Suzuki, *Tetrahedron Letters*. **1979**, *20*, 3437–3440.
- [3] A. Chatterjee, T. R. Ward, *Catalysis Letters*, **2016**, *146*, 820–840
- [4] A. Pourjavadi, S. H. Hosseini, S. T. Hosseini, S. A. Aghayee Meibody, *Catal. Commun.* **2012**, *28*, 86-89

A comprehensive study on enhanced photocatalytic activity of Nickel and Zinc oxides

Hadis derikvandi, Alireza Nezamzadeh-Ejhi^{*}

Department of Chemistry, Shahreza Branch, Islamic Azad University, P.O. Box 311-86145, Shahreza, Isfahan, Iran

The photocatalytic degradation of metronidazole was studied using ZnO–NiO/nano-clinoptilolite under UV irradiation. The clinoptilolite nano-particles (NC) were obtained via ball-mill method. The catalyst was obtained via calcinations of Ni(II)-Zn(II)-exchanged NC. The mole ratio of ZnO/NiO affected the photodegradation efficiency because activity of the coupled catalysts depends to the both e⁻/h⁺ production and electron scavenging processes. XRD, FTIR, SEM-EDX, X-ray mapping, DRS, TEM and BET techniques were used for characterization of the samples. The experimental parameters which influenced degradation process were optimized as 1.2 g L⁻¹ of NiO_{0.7}–ZnO_{4.3}/NC catalyst, 2 mg/L metronidazole at pH 3. The degradation/ mineralization extents were confirmed by COD and HPLC.

Keywords: photocatalytic photodegradation, Clinoptilolite nano-particles, Calcination, temperature, Metronidazole, NiO-ZnO, semiconductors

Introduction

Enormous research activities on the photocatalytic properties of semiconductors have been triggered all over the world. A photocatalytic mechanism [1] is based on that in an aqueous environment, the photogenerated electrons (e⁻) and holes (h⁺) can undergo reaction with dissolved molecular oxygen, surface hydroxyl groups and adsorbed water molecules to form hydroxyl (·OH) and superoxide (O₂⁻) radicals. Due to high activities of these radicals, which can easily oxidize the organic matters to H₂O, CO₂ and other inorganic substances, the technology has tremendous potential in environmental management applications. To improve the photocatalytic activities, an effective means of combining semiconductors with different band-gaps and supporting them onto a suitable support such as zeolites have been suggested. In the present work, for increasing the photocatalytic activities of ZnO and NiO towards photodegradation of Metronidazole (MNZ) their coupled system was supported onto clinoptilolite nanoparticles.

Experimental

2 g NC powder was added to solutions with different Ni(II) and Zn(II) concentrations to prepare Ni(II)-Zn(II)-NC samples (10 mL, 12 h at continuous stirring). The suspensions were centrifuged at > 5000 rpm and the ion exchanged samples were calcinated at 400 C (as optimized calcination temperature) to prepare NiO-ZnO-NC catalysts with different NiO/ZnO ratios. Ni and Zn amount of the catalysts was calculated by atomic absorption spectroscopy.

Result and discussion

XRD patterns

The XRD pattern showed in Fig. 1A belongs to NiO-ZnO/NC which presents characteristic XRD lines of clinoptilolite zeolite according to JCPDS No. 39–1383. More XRD and XRF data of the used clinoptilolite has reported in our previous work [5]. XRD lines of NiO phase were observed at 37.26° (111), 43.3° (200), 69.89 (220), 75.43° (311), 79.43 (222) which have good agreement with JCPDS No. 89–1397 and literature [6]. Typical XRD reflections of ZnO were also assigned

at 31.84 (100), 34.51 (002), 47.63 (102), 56.71 (110), 62.69 (103), 69.18 (201) which agree with JCPDS PDF No. 880287 and literature [6-7].

As shown in Fig 1B absorbance intensity of MNZ solution during the photodegradation was decreased, confirming degradation of MNZ molecules to smaller fragments. Fig. 2 shows that the best photodegradation activity NZ₃-NC catalyst, confirming mole ration of NiO/ZnO affects the degradation activity.

.....

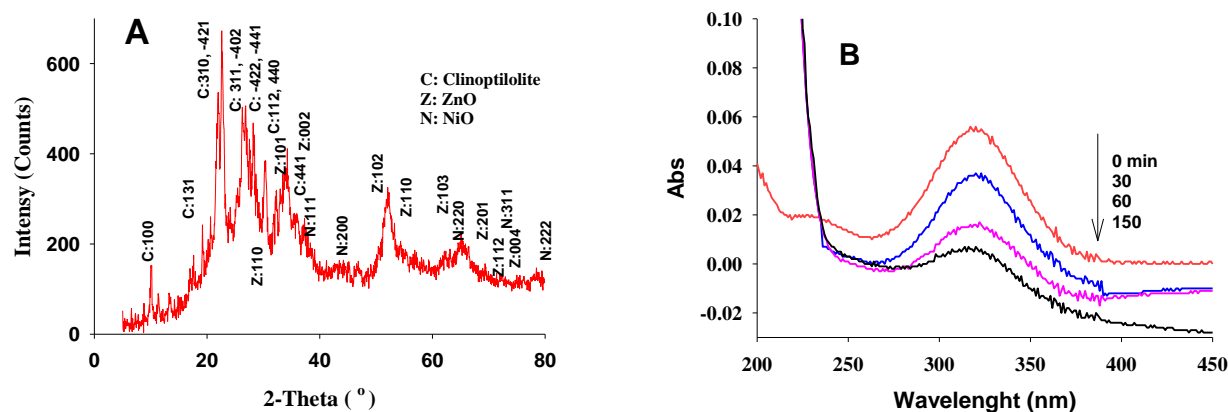


Fig. 1. A) XRD pattern of NiO-ZnO-NC; **B)** Decrease in UV-Vis absorption spectra of MNZ solution during its photodegradation by NiO-ZnO-NC; catalyst

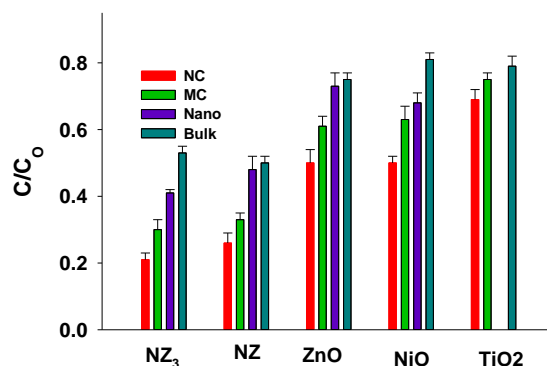


Fig. 5. Effect of supported NiO/ZnO ratio onto MC particles on photodegradation extent of MNZ

Conclusions

Based on the obtained results, both coupling and supporting of ZnO and NiO semiconductors significantly increased their photocatalytic activity. Also, particles size of the zeolitic support affected the catalytic activity of the supported semiconductors, so the best activity was obtained for the supported semiconductors onto clinoptilolite nanoparticles.

[1] M.R. Hoffmann, S.T. Martin, W.Y. Choi, D.W. Bahnemann, Environmental applications of semiconductor photocatalysis, Chem. Rev. 95 (1995) 69–96

- [2] X. Zhu, C. Yuan, Y. Bao, J. Yang, Y. Wu, Photocatalytic degradation of pesticide pyridaben on TiO_2 particles, *J. Mol. Catal. A: Chem.* 229 (2005) 95–105.
- [3] K. Tanaka, K. Padermpole, T. Hisanaga, Photocatalytic degradation of commercial azo dyes, *Water Res.* 34 (2000) 327–333.
- [4] N. Ajoudanian, A. Nezamzadeh-Ejhieh, Enhanced photocatalytic activity of Nickel oxide supported on clinoptilolite nanoparticles for the photodegradation of aqueous cephalixin, *Mater. Sci. Semicond. Proces.* 36 (2015) 162–169
- [5] A. Nezamzadeh-Ejhieh, Kh. Shirvani, CdS loaded an Iranian clinoptilolite as a heterogeneous catalyst in photodegradation of p-Aminophenol, *J. Chem.* (2013) (Article ID 541736, 11 pages).
- [6] F. Tian, Y. Liu, Synthesis of p-type NiO/n-type ZnO heterostructure and its enhanced photocatalytic activity, *Scripta Mater.* 69 (2013) 417–419.
- [7] J. Zhou, F. Zhao, Y. Wang, Y. Zhang, L. Yang, Size-controlled synthesis of ZnO nanoparticles and their photoluminescence properties, *J. Lumin.* 122–123 (2007) 195–197.

Synthesis of New Reactive Dye by Modification of CI Reactive Black 5 Dye

Fereshteh Aminrad^a, Javad Mokhtari^{b,*}, Mahdi Nouri

^a The University of Guilan, Department of Textile Engineering, Rasht, Iran

^b The University of Guilan, Department of Textile Engineering, Rasht, Iran

Email address: j.mokhtari@guilan.ac.ir

Introduction: Reactive dyes are extensively used in the textile industry because of their good properties [1]. The bisazo reactive dyes have great possibility for structural variations and the production of a wide range of reactive dyes [2]. These dyes include two azo chromophores in their molecular structure [3]. In the present work we choose sulfamerazine group to be incorporated into a commercial reactive dye structure Remazol Black B (CI Reactive Black 5) by replacing PABSES (p-aminobenzene-sulphatoethylsulphone) with sulfamerazine group resulting a modified reactive dye.

Experimentals: The PABSES was diazotized in HCl by addition of sodium nitrite at 5°C. The product was coupled with H-acid at pH 2. For diazotisation of sulfamerazine, sodium nitrite was dissolved in concentrated sulphuric acid. The temperature was up to 60°C for a short time, then reduced to 5°C and the sulfamerazine was added slowly. The diazonium salt was added to product of previous step at pH 4.5-5. The dye was precipitated by adding NaCl, filtered off and dried at 30°C.

Results and discussion: The structure characterization was studied using FTIR and ¹H-NMR spectroscopy. The infrared spectra of the synthesized dye exhibited a band at 1497cm⁻¹ due to azo group that confirmed the coupling procedure was successful. A band at 3455cm⁻¹, was assigned to the stretching vibration of N-H groups. The S=O stretching bands of the dye are located at 1139-1284 cm⁻¹. Also, the FTIR spectra of dye showed bands at 1215cm⁻¹ and 1627cm⁻¹ that corresponding the C=C and C-N groups respectively (Figure 1). The ¹H-NMR spectrum of modified dye showed a peak in the 7.95 ppm assigned to aromatic protons. The spectrum revealed two triplets at 3.61 and 4.18 ppm, each integrated to two protons, assignable to the α- and β-methylene protons of the sulphatoethylsulphone (SES) group, respectively. Two NH proton resonances were observed in 10.08 and 11.22 ppm. Additionally, the peak appeared at 2.21 ppm can be attributed to the methyl protons. NH₂ protons were observed as broad peak at 5.49-6.07 ppm (Figure 2). The dye had a maximum absorption λ_{max} (H₂O) 580 nm.

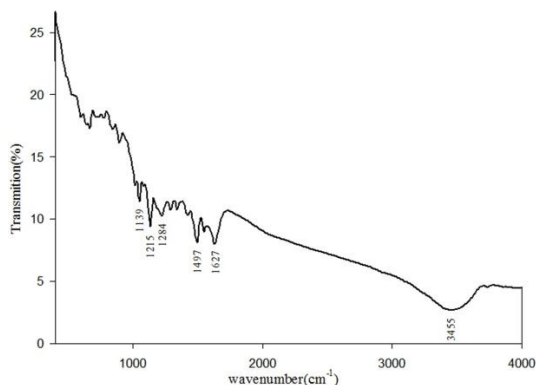


Figure 1. FTIR spectra of dye

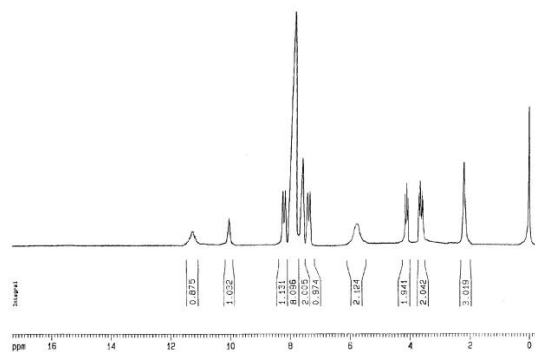


Figure 2. ¹H-NMR spectra of dye

Conclusion: Modification of a commercial reactive dye (Remazol Black B) for synthesizing a new bisazo reactive dye was carried out by replacing PABSES in the commercial dye with sulfamerazine group. Different properties of new dye analyzed by analytical methods such as FTIR, ¹H-NMR, and UV/Visible spectrometer. The spectra of the dyes confirmed the presence of sulfamerazine group.

References:

- [1] HF Rizk; SA Ibrahim; MA El-Borai. *Dyes and Pigments*, **2015**, 112, 86-92
- [2] YA Youssef; AA Mousa; R Farouk and EA El-Kharadly. *Coloration Technology*, **2005**, 121, 149-254
- [3] AO Özdemir; B Çağlar; M Tutak and O Demiryürek. *Coloration technology*, **2015**, 132, 130-134

Study of application of cucurbituril as a nanoporous adsorbent in removal of nitrophenol from wastewaters

Shaghayegh Javidnezhad , Arash Larki*,Yadollah Nikpour

Department of Marine Chemistry, Faculty of Marine Science, Khoramshahr University of Marine Science and Technology, Khoramshahr, Iran

**E-mail: Arash_larki@yahoo.com*

Introduction: Cucurbiturils (CB) are macrocyclic molecules made of glycoluril monomers linked by methylene bridges which it are particularly interesting to chemists because they are suitable hosts for an array of neutral and cationic species. The rigid structure and capability of forming stable complexes with molecules and ions also make CB attractive as a building block for the construction of supramolecular architectures [1, 2]. In this paper, we applied a specific nano cucurbituril for adsorption and removal of nitrophenol from wastewaters.

Method/ Experimentals:

The cucurbit [6]uril nonporous was synthesis by cooperation of researchers in Technology Research Institute of Ahvaz [3]. The suggested adsorbent was synthesized and characterized using powder X-ray diffraction, SEM, TEM (Fig. 1) and FT-IR spectroscopy. The removal procedure was studied in batch mode and effects of important parameters such as pH of aqueous medium, adsorbent dosage, contacting time and interfering ions on the adsorption were investigated and optimized. At the optimized conditions, the adsorption isotherms were measured and results were fitted with Langmuir, Freundlich and Temkin isotherm models.

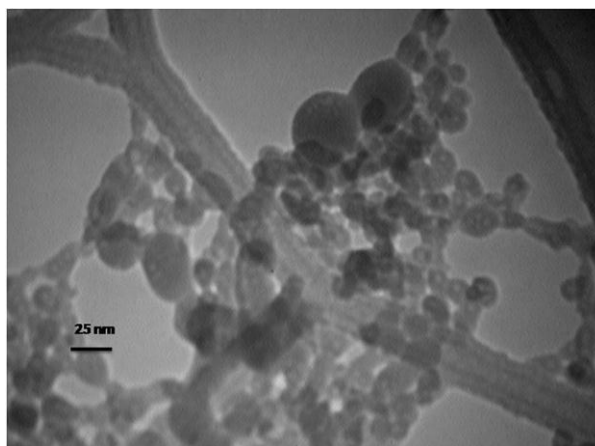


Fig. 1. TEM of CB[6].

Results and discussion: The results of investigation of solution pH show that the removal of analyte is almost constant in the pH range of 3-9. It was found that the adsorption of nitrophenol on cucurbit [6]uril were correlated well with the Freundlich equation as compared to the Langmuir and Temkin equations in the studied concentrations, and the maximum loading capacity was found upper than 50 mg g⁻¹. The pseudo-first order and pseudo-second order kinetic models for nitrophenol removal by CB[6] was investigated. The correlation coefficients for the second- order kinetic model were higher than 0.999 indicating the applicability of this kinetic model of the adsorption process of nitrophenol on CB[6].

Conclusion: The adsorption was found to be independent of pH in the range of 3-9 but it was dependant on adsorbent dosage, and contact time. Isotherm analysis of the data showed that the adsorption followed the Freundlich model well. The results showed that CB[6] has a high adsorption capacity for nitrophenol which is comparable or better than other adsorbents. Finally the removal procedure was successfully applied to the removal of nitrophenol from wastewater samples.

Keywords: Nano-cucurbituril, Nitrophenol, Removal, Batch procedure.

References:

- [1] K. I. Assaf, W. M. Nau, *Chem. Soc. Rev.*, **2015**, 44, 394-400.
- [2] S. Lim, H. Kim, N. Selvapalam, K. Kim, S. Cho, G. Seo, K. Kim, *Angew. Chem.*, **2008**, 120: 3400–3403.
- [3] S.J. Saghanezhad, Y. Nazarib, F. Davod, *RSC Adv.* **2016**, 6, 25525-25530

Theoretical study of coupling constants across N...H–F hydrogen bond in a substituted T-shaped configuration: Exploring the role of CH... π interaction in the presence of electron-donating and electron-withdrawing substituents

Hamid Reza Masoodi*, Sotoodeh Bagheri

Department of Chemistry, Faculty of Science, Vali-e-Asr University of Rafsanjan, P.O.Box77176, Rafsanjan, Iran

E-mail address: h.r.masoodi@vru.ac.ir

Introduction

The H-bonding between the aromatic rings and some other proton donors has been studied periodically by theoretical and experimental methods [1]. CH... π interactions were often regarded as the weakest class of H-bonds. Nevertheless, the nature of the CH... π interactions is significantly different from conventional H-bonds.

The T-shaped configurations can often be seen in biological systems, supramolecular chemistry and host–guest chemistry. Therefore, it would be important to understand how substituents affect the different properties of the configuration [2]. An important area of both experimental and computational research is the study of interactions in T-shaped complexes using NMR spectroscopy [3].

Methods

The geometry optimization of the complexes have also been performed at the MP2(FC)/6-311++G(d,p) level using the Gaussian 09 suite of programs. The basis set superposition error was considered by the counterpoise method in the geometry optimization.

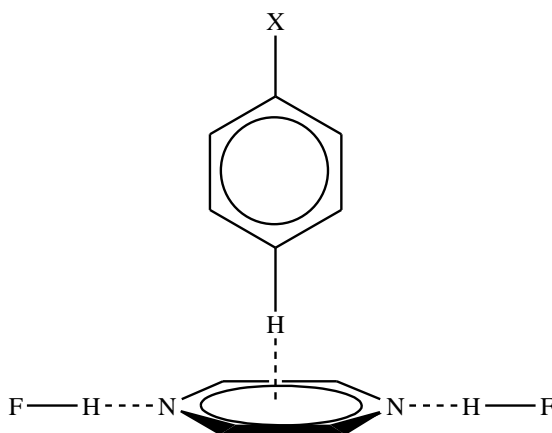
The wave functions obtained at MP2(FC)/6-311++G(d,p) level have been analyzed by the quantum theory of atoms in molecules and natural bond orbital method using AIM2000 and NBO5.0 softwares, respectively.

Herein, the NMR calculations were performed at B3LYP/6-311++G(d,p) and PBE0/6-311++G(d,p) levels using SPINSPIN keyword.

Results and discussion

In a previous work, we investigated the influence of substituents on cooperativity between CH... π and N...H H-bonds in the T-shaped configuration of X-benzene \perp (FH...pyrazine...HF) complexes [4]. Here, we theoretically examine the influence of CH... π interaction on coupling constants across $^{15}\text{N}\dots^{1}\text{H}\text{--}^{19}\text{F}$ H-bond in the substituted T-shaped complex of X-benzene \perp (FH...pyrazine...HF) (see Scheme 1).

It was observed that $^1J_{N-H} / |^2J_{N-F}|$ is diminished /amplified by increasing electron-donating power of substituents. These correlations can be explained using Hammett constants. Also, reverse / direct correlations have been found between $^1J_{N-H} / |^2J_{N-F}|$ and binding energies ($|\Delta E_{\text{quaternary}}|$). The results indicated that $|^2J_{N-F}|$ increases as cooperative and synergistic energies become more negative. This trend is reversed for $^1J_{N-H}$. AIM and NBO analyses showed that the decrease / increase in $^1J_{N-H} / |^2J_{N-F}|$ values is accompanied by increasing electron density at N...H BCP and energy value of $Lp_N \rightarrow \sigma_{H-F}^*$ interaction.



Scheme 1. The investigated complexes. X = H, F, Cl, Br, CCH, BF₂, NC, CF₃, CN, NO₂, CH₃, C(CH₃)₃, NH₂, N(CH₃)₂.

Conclusions

Meaningful relationships have been observed between the coupling constants and geometrical parameters, binding energies and topological properties of electron charge density in considered T-shaped complexes.

References

- [1] S.J. Wilkens, W.M. Westler, F. Weinhold, J.L. Markley, *J. Am. Chem. Soc.* **2002**, *124*, 1190-1191.
- [2] X. Lu, H. Shi, J. Chen, D. Ji, *Comp. Theor. Chem.* **2012**, *982*, 34-39.
- [3] J.A. Platts, K. Gkionis, *Phys. Chem. Chem. Phys.* **2009**, *11*, 10331-10339.
- [4] H.R. Masoodi, S. Bagheri, S. Saeednia, M. Mohammadi, A.R. Raeisipoor, *Struct. Chem.* **2016**, *27*, 1521-1530.

A new optode based on derivatives of isonicotinohydrazide in presence of carbon dots in PVC matrix for determination of copper ion

Seyed alireza shahamirifard^a, Mehrorang Ghaedi^{b*}

^a Department of Chemistry, Faculty of Sciences, Yasouj University, Yasouj 75918-74831, Iran

^b Department of Chemistry, Faculty of Sciences, Yasouj University, Yasouj 75918-74831, Iran

m_ghaedi@yahoo.com

Introduction

Detection and determination of copper ions is very important because it is the third largest amount of transition elements exist in our human body[1]. However copper is highly toxic and even causes wilson's and alzheimer in humans disease [2]. polyvinyl chloride (PVC) is the most widely used polymers in optical sensors [3]. In order to increase the sensitivity of the sensor response carbon dots(CDs) are a good option[19-22].the optimizing of variable performed by central composite design (CCD) because it is better than one-variable at a time (OVAT) because time and material consumption is lowed and interaction between variable is investigated[4].

Methods/ Experimentals

The ionophore synthesized by mixing of isonicotinohydrazide and dialdehyde in suitable amount and carbon dots(CDs) prepared by citric acid (CA) in sufficient condition.for preparation of membrane ionophore(X_1), ionic additive(X_2), DBP and PVC ratio(X_3) are mixed in optimum condition that it resulted of CCD according figure 1.

Results and discussion

Spectral characteristic shown in figure 2 that it is compared sensor performance in phosphate buffer solution (1) and membrane (2). the absorption spectra of free and immobilized ligand (H2L) recorded after reaching equilibrium in phosphate buffer solutions(PBS) containing various concentrations of Cu^{2+} ions. Since fluctuation of pH changed the absorbance of both the free and complexed forms of the immobilized ionophore , pH examined in range of 3 to 10. and pH 7.7 seems to be a proper choice. Curvatures response surface plots seen in figure 3 may be assigned to interaction between the variables. The response time of the optode is 5min. That it exhibits a linear range from of 6.3×10^{-6} to 3.78×10^{-5} mol L⁻¹ of Cu^{2+} ions. Regeneration of the optode membrane was investigated by various reagents and EDTA is the best. The results show that the selectivity, reproducibility and repeatability are acceptable. The applicability of this optical sensor for the valuation of Cu^{2+} ion content were certified by the analysis of real samples such as water samples is satisfactory.

Conclusion

The analytical figure of merit of proposed optode was in good level. The optode was found to be stable and dependable for Cu^{2+} ions determination in various samples

This optical sensor gives a sensitive, low cost and selective procedure for the determination of Cu^{2+} ions based on a novel optode. Optode reversibly is associated with color change from colorless to yellow.

References

[1] S. Acikgoz, M. Harma, M. Harma, G. Mungan, M. Can, S. Demirtas, *Biological trace element research*, (2006), 113, 1-8.

[2] R. Uauy, M. Olivares, M. Gonzalez, *The American journal of clinical nutrition*, 67 (1998) 952-959.

[3] M. Ghaedi, A. Shahamiri, B. Mirtamizdoust, S. Hajati, F. Taghizadeh, *Spectrochimica Acta Part A: Molecular and Biomolecular Spectroscopy*, 138 (2015) 878-884.

[4] H. Liu, Y. Liu, D. Zhu, *Journal of materials chemistry*, 21 (2011) 3335-3345.

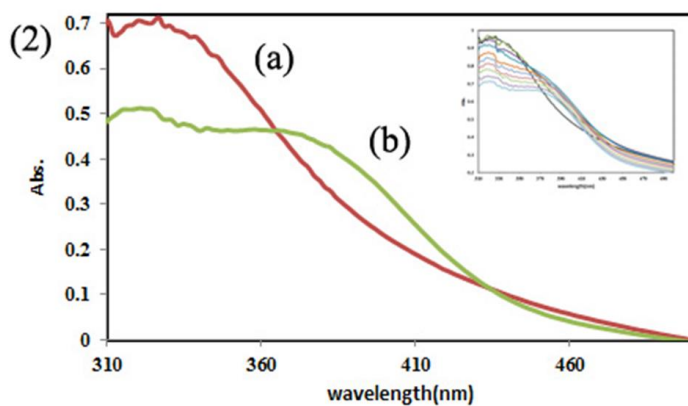
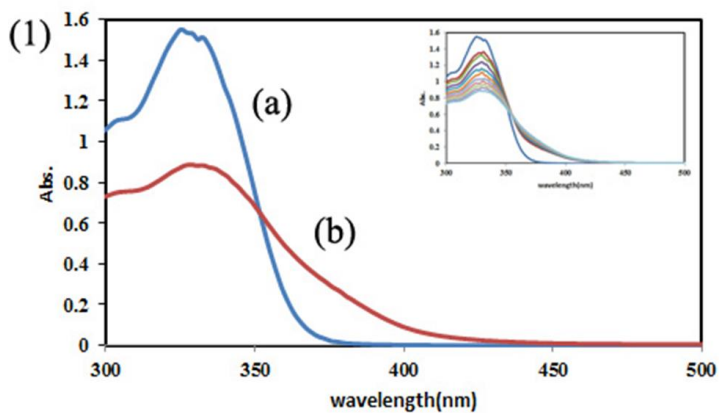
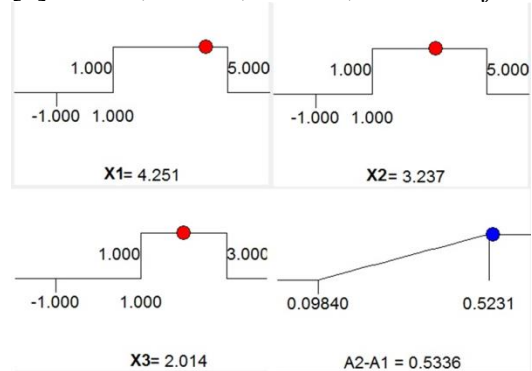


Fig. 1 result of CCD

fig. 2 Spectral characteristic

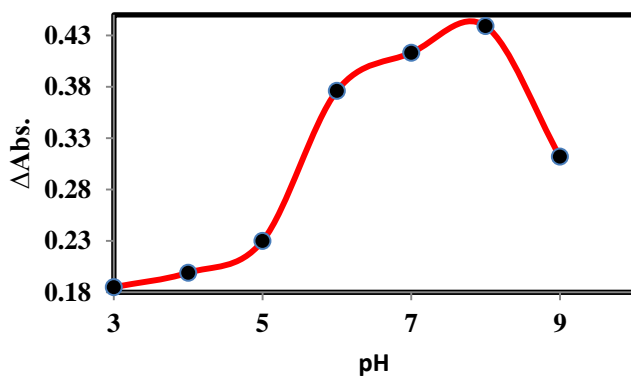


fig. 3 effect of pH

Design and construction of an ion-selective membrane electrode for potassium cation by using kryptofix 22 based on PVC

Mahboubeh Vafi, Gholam Hossein Rounaghi*, Zarrin Es'haghi

Department of Chemistry, Mashhad Branch, Islamic Azad University, Mashhad, Iran.

E-mail address: ghrounaghi@yahoo.com; rounaghi.gh@msdiau.ac.ir

Introduction: Ion-selective electrodes (ISE) are the chemical sensors with the longest and probably with the most frequent routine application. In recent years, studies in the design of selective ionophore as a sensor for ion selective electrodes have been carried out [1]. A significant number of macrocyclic ligands, have been used in the construction of polyvinyl chloride (PVC) based membrane electrodes for determination of alkali and alkaline earth metal cations in solution. The cryptand molecules are three dimensional analogues of crown ethers, but they are more selective and complex the guest ions more strongly. In contrast to the typical crown ethers, cryptands bind the guest ions by both nitrogen and oxygen donors. Their three-dimensional encapsulation mode, confers some size-selectivity. We report here the result of investigation of design and construction of an ion-selective membrane electrode for potassium cation by using kryptofix 22 based on PVC.

Methods / Experimentals: In this research project, a highly selective potassium cation electrode was prepared by using kryptofix 22 as an ionophore, o-nitrophenyl octyl ether (o-NPOE) as plasticizer, graphite as an additive and polyvinyl chloride (PVC). Dip/Dry method has been applied to coat the graphite rod with the sensing membrane. The amounts of membrane ingredient under optimal compositions were mixed and dissolved in THF. A polished graphite electrode (3 mm diameter and 10 mm length) dipped into the membrane solution, then removed and allowed to dry for 24 hour. A membrane was formed on the graphite surface as sensing layer.

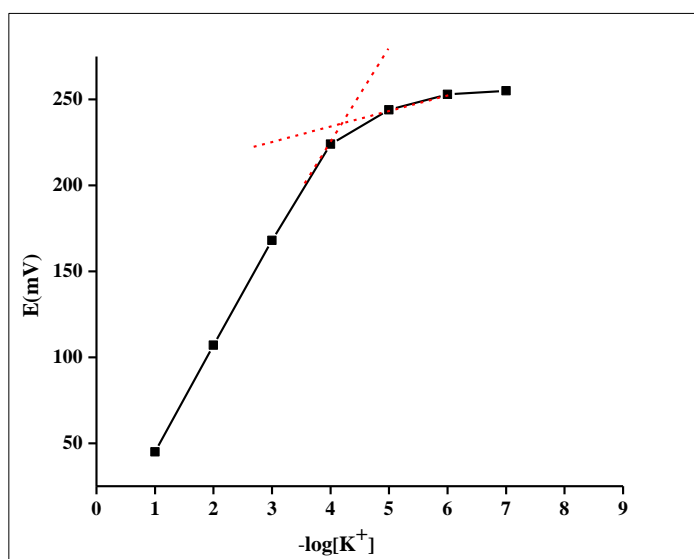
All measurements were carried out at room temperature with a cell of following type:

Ag|AgCl; KCl (satd.) || K⁺ sample solution | Ion-selective electrode | graphite bar.

The performance of the electrodes was examined by measuring the emfs of KNO₃ solutions prepared with a concentration range of 10⁻¹ to 10⁻⁶ M by successive dilution.

Results and Discussion: The influence of the membrane composition on the potentiometric response of the electrode has been investigated and optimized to improve the performance characteristics. At the first, we determined the kind of plasticizer and then we obtained the optimum composition of the membrane. The best performance was obtained with the membrane composition (W/W %) of o-nitrophenyl octyl ether (66%), PVC (24%), graphite (9.4%) and

kryptofix²² (2.5%). The electrode exhibits a Nernstian slope (59.6 ± 0.6 mV/decade) in a linear concentration range of 1.0×10^{-4} to 1.0×10^{-1} M. The electrode has a good response time of about 10 s, with a satisfactory reproducibility and relatively long life time about 4 weeks without significant drift in potential. The electrode operates in the pH range of 3.0–7.0 for 10^{-5} M solutions of K^+ cation. This electrode reveals an acceptable selectivity towards K^+ cation over a wide concentration range of heavy metal cations.



Conclusion: Ionophores for use in sensors should have rapid exchange kinetics and adequate complexation formation constants in the membrane. In addition, they should be well soluble in the membrane matrix and have a sufficient lipophilicity to prevent leaching from the membrane into the sample solution. The ionophore is selective for potassium ion, due to the good fit condition of K^+ to kryptofix²² cavity. The main advantage of the potentiometric potassium cation selective coated-membrane electrode is its simple of preparation, short conditioning time, fast response time, Nernstian behavior and improved good selectivity. The coated-membrane is long lived and chemically stable.

Reference:

[1] Fereshteh Karimian, Gholam Hossein Rounaghi, Mohammad Hossein Arbab-Zavar, Chinese Chemical Letters, 2014, 25, 809–814.

Theoretical investigation of axial strain effects on aromaticity factor in single-walled zigzag boron nitride nanotubes

Sotoodeh Bagheri* , Hamid Reza Masoodi, Ehsan Bahrani Nezhad

Department of Chemistry, Faculty of Science, Vali-e-Asr University of Rafsanjan, P.O. Box 77176, Rafsanjan, Iran

E-mail address: S.Bagheri@vru.ac.ir

Introduction: Recent studies have shown that applying strain to nanotubes will affect their property. For example, it has been reported that the band structure of carbon nanotubes can be altered by mechanical strain and by changing the CNT size, except for uniaxially strained armchair tubes [1]. We have investigated the influence of strain on structural and electronic properties of zig-zag type of boron nitride nanotubes (BNNTs) by density functional theory calculations [2]. Our results show that the effect of axial strain on the electronic and structural properties of zig-zag BNNTs depends on the diameter as well as the length of the nanotube.

Methods: The geometry of nanotubes was optimized at the B3LYP/6-31+G(d) level using the Gaussian03 suit of programs. The principal idea of the geometry-based index was based on the harmonic oscillator model of aromaticity (HOMA) [3]. To distinguish the π -electron delocalization, Raczyńska and co-authors proposed Harmonic Oscillator Model of Electron Delocalization (HOMED) [4]. In the present work, the axial strain effects on aromaticity factor in some single walled BNNTs have been studied. The HOMA and HOMED have been calculated to quantify aromaticity in terms of structural criteria.

Results and Discussion: The stoichiometry of (4,0)₃, (5,0)₃, (6,0)₃, (4,0)₅, (5,0)₅, and (6,0)₅ BNNTs are B₁₆H₈N₁₆, B₂₀H₁₀N₂₀, B₂₄H₁₂N₂₄, B₂₄H₈N₂₄, B₃₀H₁₀N₃₀, and B₃₆H₁₂N₃₆, respectively. The engineering strain in the axial direction of the BNNT is given by

$$\varepsilon_{\text{Eng}} = \frac{L - L_0}{L_0}$$

where L is the length of the BNNT in the axial direction following elongation and L₀ is the initial length. With regard to Figure 1, it can be concluded that aromaticity of zig-zag BNNT decreases

with the increase of axial strain (E_{eng}). The general trend of HOMA during tension is similar to that in HOMED in all studied nanotubes. The HOMED index is between 0.9 and -0.9 contrary to the HOMA index which varies from 0.6 to -4.0 during tension. Almost all of HOMA have strongly negative values contrary to the HOMED indices during tension.

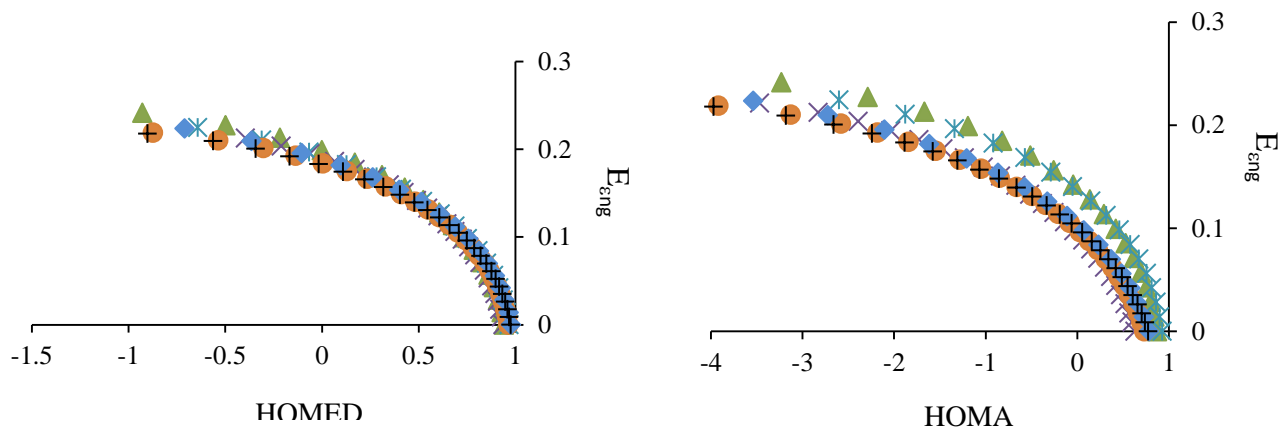


Figure 1. The relationship between HOMA, HOMED and E_{eng} in considered systems.

The cohesive energy or the binding energy (BE) per atom for BNNT was calculated according to the following formula:

$$\text{BE} = \frac{[aE_{\text{B}} + bE_{\text{N}} + cE_{\text{H}}] - [E_{\text{BaNbHc}}]}{a + b + c}$$

where a , b , and c are the number of B, N, and H atoms, respectively. E_{B} , E_{N} , and E_{H} are the ground state total energies of B, N, and H atoms, respectively, and E_{BaNbHc} is the total energy of the optimized clusters representing the nanotubes. The results indicated that the increase in BE values is accompanied with decreasing aromaticity.

Conclusion: With regard to changes of HOMA and HOMED during tension, it can be concluded that aromaticity of zig-zag BNNT decreases with the increase of axial strain.

References

- [1] AM. Rao; PC. Eklund; S. Bando; A. Thess; RE. Smalley, *Nature*, **1997**, 388, 257–259
- [2] H. Roohi; S. Bagheri, *Struct Chem*, **2013**, 24, 409–420
- [3] J. Kruszewski; T.M. Krygowski, *Tetrahedron Lett.* **1972**, 3839–3842.
- [4] E.D. Raczyńska; M. Hallman; K. Kolczyńska; T.M. Stępniewski, *Symmetry*, **2010**, 2, 1485-1509

Flame atomic absorption spectrometric determination of trace amount of cadmium and chromium after separation and preconcentration onto ion- exchange polyamide 66 coated Al_2O_3

Fereshteh Bayatiyani, Ali Asghar Amiri*, and Nooredin Goudarzian

Department of Applied Chemistry, Shiraz Branch, Islamic Azad University, Shiraz, Iran

*Corresponding author: amiri1355@gmail.com

1. Introduction

Pollution of aquatic environments by heavy metals, particularly as a result of industrialization, is increasingly being associated with public health in an urban setting, since heavy metals not only lead to contamination of aquatic life, but also cause harm to people's health, even at low concentrations. Among heavy metals, Cd (II) and Cr (III) are seriously considered to be toxic for animals and humans alike, and it is classified by the International Agency for Research on Cancer as a human carcinogen. Nevertheless, low concentrations of Cd (II) and Cr (III) ions in environmental water samples associated with high matrices effects; make the direct determination of the element a very difficult task. This way, separation and pre concentration procedures must be performed prior to the analysis. Methods based on solid phase extraction (SPE) have been increasingly used to the detriment of liquid–liquid extraction, due to their advantages including cost effectiveness, easiness of automation with flow injection analysis, environmentally friendly, faster, simpler, higher preconcentration factors and improved sensitivity. In this study, our objective is to investigate the feasibility of polyamid66 (PA)/ Al_2O_3 dispersed on solid substrate of silica matrix, prepared by sol–gel process, as a promising adsorbent for Cd (II) and Cr (III) ions and optimization of adsorption were investigated.

2. Experimental

2.1 Preparation of PA66/ Al_2O_3 : The preparation of PA66/ Al_2O_3 by sol–gel process was carried out. First of all, polyamid6 granule dissolved in small amounts of THF then the solution slowly added to the Al_2O_3 previously suspended in ethanol under a nitrogen atmosphere, and the resulting mixture was stirred at 60 °C. The solvent was slowly evaporated until gel formation. The gel obtained was ground and the remaining solvent were evaporated under vacuum, resulting in a xerogel completely dried. The resulting particles were washed with ethanol in a soxhlet extractor. Finally, the material was washed with deionized water and ethanol, and dried under vacuum and then stored.

3. Results and discussion

The adsorbent revealed characteristics of a porous material and a remarkable specific surface area. The high specific surface area reflects the good accessibility of sites provided by the adsorbent for Cd (II) and Cr (III) ions. This feature is highly desirable for the proposed application of this solid adsorbent in flow preconcentration system for the determination of metals. In addition, the high specific surface represents significant advances over resin-based ion-exchange adsorbents. A good dispersion of the Al_2O_3 on the polymer matrix is an important feature for the application of the material as a new adsorbent for trace metals. The PA66/ Al_2O_3 material exhibits excellent mechanical and chemical Resistance. The infrared spectrum of PA66/ Al_2O_3 shows signals at $\sim 3400\text{ cm}^{-1}$ which are attributed to N-H absorption and deformation modes of O–H bonds of molecularly adsorbed water ($\delta\text{O–H}$), respectively. The

absorption at $\sim 1715\text{ cm}^{-1}$ is related to stretching of the ($\nu\text{C=O}$) groups. The broad absorption centered at 3386 cm^{-1} is assigned to stretching vibration of O–H groups involved in hydrogen bonds ($\nu\text{O–H}$). The shoulders at 3250 cm^{-1} and 3650 are related to free and strongly H-bonded OH groups, respectively. The infrared spectra showed no bands that are typical of Al–O vibrations in the region between 700 and 550 cm^{-1} . The infrared spectra also indicated that the Al_2O_3 network is slightly disturbed in the presence of polymer matrix.

Determination of Cd (II) and Cr (III) in water samples and certified reference Material:

The accuracy was evaluated by addition and recovery tests on samples of tap, mineral and river waters, as well as by analysis of certified reference materials and cigarette sample. The results obtained for recovery, ranging from 99.6% to 100%, attested the accuracy of the method for water samples. Furthermore, the certified amounts of Cd (II) and Cr (III) ions in certified reference materials. The results also confirm the accuracy of the method for biological samples, which are submitted to acid digestion.

4. Conclusions

The present study reported the use of PA66 dispersed on alumina matrix as an adsorbent for Cd (II) and Cr (III) ions. The new sorbent, synthesized by sol–gel process, has shown excellent features that include homogeneous dispersion of the Al_2O_3 and PA66 and satisfactory adsorptive capacity for Cd (II) and Cr (III) ions. The adsorption process fitted to the Langmuir linear model very well. The on-line preconcentration system provided a reliable, simple and fast method to monitor Cd (II) and Cr (III) ions in natural water and potable water samples which allows a maximum level of $3.0\text{ }\mu\text{g L}^{-1}$. Additionally, the material was highly stable, considering that, throughout the study so far, only one minicolumn was used without losses of adsorption capacity. Finally, the results obtained show that studies involving porous alumina doubly modified with polymer matrix are promising materials for the development of new methods of preconcentration of metal ions and especially anionic species, depending on sample pH.

References:

- [1]. Olsen KB, Wang J, Setiadji R, Lu J., Field screening of chromium, cadmium, zinc, copper, and lead in sediments by stripping analysis, *Environmental science & technology*, **2010**;28(12):2074-9.
- [2] Lu P, Feng Q, Meng Q, Yuan T., Electrokinetic remediation of chromium- and cadmium-contaminated soil from abandoned industrial site, *Separation and purification technology*, **2012**;98:216-20.
- [3] Ghorbel-Abid I, Galai K, Trabelsi-Ayadi M., Retention of chromium (III) and cadmium (II) from aqueous solution by illitic clay as a low-cost adsorbent. *Desalination*, **2010**;256(1):190-5.

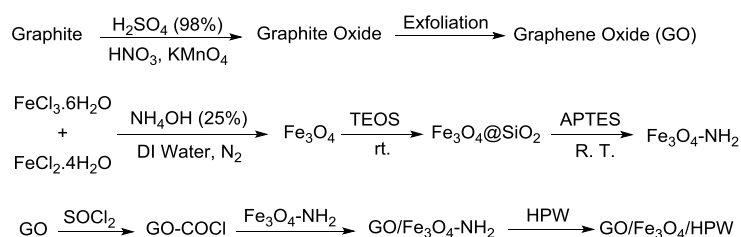
Synthesis, characterization and catalytic applications of GO/Fe₃O₄/HPW in selective oxidation of alcohols using H₂O₂ as oxidant

Kamal Amani^{a,*}, Kamran Darvishi^a

^a Department of Chemistry, Faculty of Sciences, University of Kurdistan, 6617715175, Sanandaj, Iran.
E-mail: amani_71454@yahoo.com, Tel: +98 (87) 3362 4133

Introduction: Oxidation of alcohols to their corresponding carbonyl compounds is one of the most important functional groups transformations in organic chemistry. The development of an environmentally and economically process by H₂O₂ as oxidant along with recyclability of the catalyst is a challenge [1]. Heteropoly acids (HPAs) possess interesting properties that make them useful for catalytic applications [2]. HPAs have the low surface area in nonpolar solvents and are soluble in polar solvents that reduce their recyclability [3]. Therefore, we were planning heterogenization of tungstophosphoric acid via immobilization on graphene oxide/Fe₃O₄ nanocomposite (GO/Fe₃O₄/HPW) that has high surface area, high stability and separability. As synthesized new nanocatalyst was employed for selective oxidations of alcohols to their corresponding carbonyl compounds.

Experimental: GO/Fe₃O₄ nanohybrid was prepared according to the reported methods [4, 5]. GO/Fe₃O₄/HPW nanocomposite was prepared as follow: 100 mg of the GO/Fe₃O₄ was dispersed in 5 mL of deionized water and ultrasonicated for 30 min. Then, a solution of H₃PW₁₂O₄₀.nH₂O (200 mg) in 2 mL deionized water was added dropwise into the solution and ultrasonicated for 30 min and the mixture was stirred for 24 h at RT. Finally, the catalyst was magnetically separated and washed twice with water and dried at 60 °C (Scheme 1). The alcohol oxidation reaction was carried out as follows: 1 mmol of the alcohol and 20 mg of the catalyst were charged in a 25 mL round-bottomed flask and then 3.3 mL of H₂O₂ (10%, 10 mmol) was added dropwise within a period of 5 min. The mixture was stirred at 70 °C for 1-24 h. The progress of the reaction was followed by TLC. After the completion of the reaction, the catalyst was separated using the magnet, and the product was extracted with diethyl ether (3×5 mL) and purified by column chromatography.



Scheme 1: The strategy for the synthesis of GO/Fe₃O₄/HPW nanocomposite

Results and Discussion: The obtained GO/Fe₃O₄/HPW nanocomposite was well characterized with different techniques, such as FT-IR, XRD, TEM, SEM, EDX, TGA-DTA, AGFM and BET measurements. The techniques used were showed that graphene oxide layers are well prepared and the various stages of preparation of the catalyst have been successfully completed.

To evaluate the efficiency of the catalyst, the oxidation of benzyl alcohol to benzaldehyde was selected as the probe reaction. The effect of the reaction temperature, the reaction time, and also the amounts of H₂O₂ and catalyst on benzyl alcohol oxidation are summarized in chart 1. The substitution effect was investigated and found that higher oxidation rate and yields were obtained for the primary benzyl alcohols with electron-donating groups.

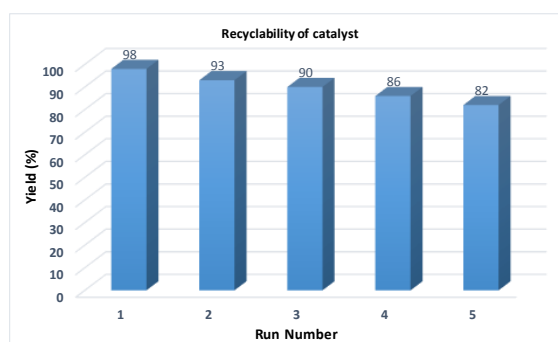
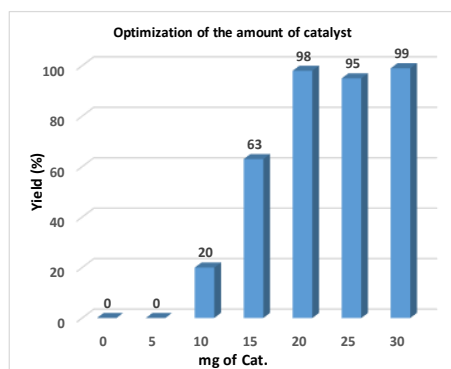
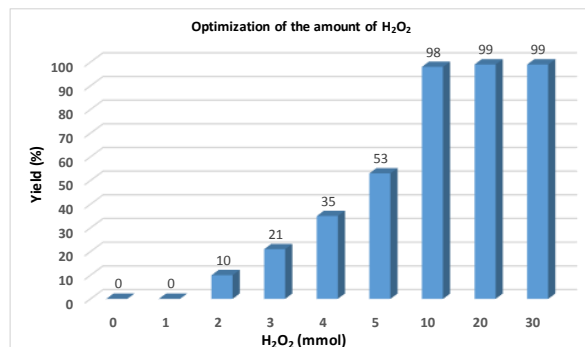
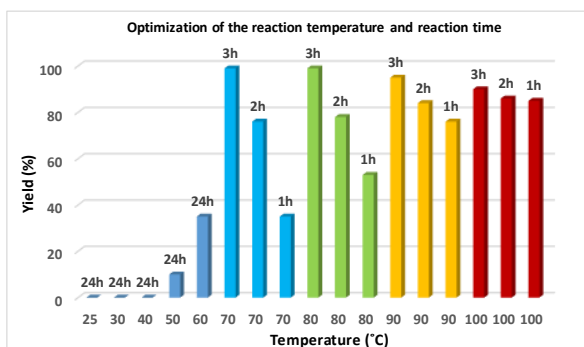


Chart 1: Optimization of reaction conditions for the oxidation reaction of benzyl alcohol, (A) the reaction temperature and the reaction time, (B) the amount of H₂O₂ as oxidant, (C) the amount of the catalyst and (D) the recyclability of the catalyst.

Conclusion: We have developed a new catalyst system as a green, safe and magnetically recoverable heterogeneous nanocatalyst. This advanced catalyst system showed catalytic activity with impressive recyclability at the oxidation of alcohols in the presence of H₂O₂. The magnetic heterogeneous nanocomposite was easily separated from the reaction mixture by using an external magnet. By using this catalytic system, the benzylic alcohols were oxidized to the corresponding aldehydes or ketones with almost 70–99% yields. The recycled catalyst was then successfully reused for at least five times with only a slight decrease in catalytic performances.

References

- [1] Li, X.; Cao, R.; Lin, Q. *Catal. Commun.*, 2015, **69**, 5–10.
- [2] Liu, R.; Li, S.; Yu, X.; Zhang, G.; Zhang, S.; Yao, J.; Keita, B.; Nadjjo, L.; Zhi, L. *small*, 2012, **8**, 1398–1406.
- [3] Kumar Saini, M.; Gupta, R.; Parbhakar, S.; Singh, S.; Hussain, F. *RSC Adv.*, 2014, **4**, 38446–38449.
- [4] Xie, G.; Xi, P.; Liu, H.; Chen, F.; Huang, L.; Shi, Y.; Hou, F.; Zeng, Z.; Shaob, C.; Wang, J. *J. Mater. Chem.*, 2012, **22**, 1033–1039.
- [5] Shahbazi, F.; Amani, K. *Catal. Commun.*, 2014, **55**, 57–64.

Biosorption of lead ion by biomass of Marshmallow

^aM. Tamimi^a, A.A. Amiri^b

^aDepartment of applied chemistry, Shiraz Branch, Islamic Azad University, Shiraz, Iran

^{*}amiri1300@gmail.com

Introduction: Heavy metals in the environment are considered as a potential risk to living organisms. Heavy metals are toxic because they can disturb some of the vital factors of human bodies at high concentrations[¹]. Not getting metabolized in the body is one of the most fundamental problems associated with heavy metals[²]. In fact, heavy metals will not be excreted from the body after entering it, in return, they will be deposited and accumulated in tissues such as fats, muscles, bones and joints. Among heavy metals, lead has a high priority for removal from aqueous solutions due to stimulation, accumulative property, Carcinogenesis, Mutagenicity and Non-Biodegradability[³].

Method/Experimentals: The study was performed on a laboratory scale. At first, some grams (amounts) of marshmallow were taken via several steps. Then the removal efficiency of metals was measured under various conditions. Finally the adsorption isotherms of metal ions on the adsorbent were evaluated based on the Langmuir and Freundlich isotherm models. After preparation of the samples, heavy metals' contents were measured by atomic absorption machine.

Effective parameters on biosorption process evaluated in this project include the solution's pH, the amount of bioadsorbent, the initial concentration of metal ion and exposure time. Desirable obtained pH value for lead biosorption is 7. Bio-absorption of metal ions increases by increasing the amount of adsorbent, and the adsorption becomes constant after the optimal amount of 3 grams. The higher the concentration of metal ion in solution, the greater bio-adsorbent ability in its removal. Langmuir isotherm model showed better proportionality with the adsorption data of metal ion. Biosorption rate of metal ion was reported to be very fast, and the best absorption percentage was at 30 minutes.

Results and Discussion: This study aimed to remove heavy metals from water samples by marshmallow biomass. Based on the results obtained in this project, marshmallow biomass can be used as effective bioadsorbent to reduce pollutions of wastewaters contaminated with heavy metal ions, particularly lead, as a result of the advantages include its low cost, high absorption capacity and the rapid rate of biosorption.

Reference:

[¹] Larson, V.J. , and Schierup , H.H, 1981 , “*The use of straw for removal of metals from waste water*” . J. Environ. Qual . , 10(2) 188-193

[²] رکنی ، ن. (1387) “*اصول بهداشت مواد غذایی*” ، چاپ سوم ، انتشارات و چاپ دانشگاه تهران ، صفحه ۱- ۱۵۴

[³]] Davis , T.A , Voleshy , b , and Vieira , R.H.S.F, (2000) “ *Sargassum seaweed as biosorbent for heavy metals*”. Water Research , 34 , (17) 4270-4278.

Investigation of Catalytic Properties of Two New Orthopalladated Complexes Supported on Montmorillonite: Synthesis, Characterization and Application in the Aerobic Oxidation of Alcohols

Sara Hashemi^a, Kazem karami^{a,*}

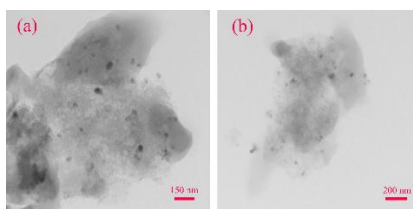
Department of Chemistry, Isfahan University of Technology, Isfahan, 84156/83111, Iran

E-mail address: karami@cc.iut.ac.ir

Introduction: Oxidation of alcohols to aldehydes or ketones has been widely studied due to its importance in production of chemicals in the chemical industry [1, 2]. MMT broadly used as a solid support for expensive or not-easily accessible reagents, organometallic complexes, nanoparticles (NPs) and provide the easy recovery and reusability of the reagents [3]. In this work, the reactions were performed in 6 h, 60 °C, and air bubbling was used instead of O₂ and H₂O₂. So, less time and energy were consumed in comparison to many other catalytic alcohol oxidation reactions. Finally, the catalyst was reusable at least four times.

Experimentals: Starting materials and solvents were purchased from Sigma-Aldrich or Alfa Aesar and used without further purification. MMT-K10 with cation-exchange capacity of 119 meq/100 g was provided by Aldrich chemical Co. The original MMT-K10 powder sample was sieved and the fraction <40mm was used as a host matrix for preparation of the Pd complexes/MMT nanohybrids.

Results and Discussion: The IR characteristic bands confirmed the presence of the complexes intercalated between the MMT layers. The remarkable shift toward lower angle in XRD patterns indicated an increase in the interlayer distances, and confirmed that intercalation and surface modification of the complex has occurred. The FE-SEM images of the corresponding hybrid that confirms the distribution of complex 1 on the clay. The corresponding TEM images reveal that the Pd complex/MMT nanohybrid was formed and Pd complex 1 well dispersed through the support surface.



TEM images of complex 1/MMT nanohybrid

We studied the ability of catalyst 1 and 2 to catalyze the aerobic oxidation of benzyl alcohol. In order to compare catalyst 1 with catalyst 2, we focused our attention on the aerobic oxidation of benzyl alcohol under optimal reaction conditions (85 °C, toluene as solvent, K₂CO₃ as base, in air). With the optimized reaction conditions recognized, the scope of aldehyde and/or ketone formation was examined with catalyst 1. To study the generality of modified clay for alcohol oxidation, some aromatic alcohols were employed. For 2-phenylethanol oxidation, 100% conversion was observed at 3 h. Substrates with electron donating groups are more reactive than those with electron withdrawing groups.

Conclusion: all reactions were performed at 60 °C with bubbling of air, and the corresponding products were obtained in good or excellent yields in the presence of low catalyst Pd-loading. This class of heterogeneous Pd catalyst allows the alcohol oxidation reactions to promote with remarkable yields. The small size of the Pd complex/MMT nanohybrid clarified the remarkably high activity of this specific catalyst.

References

- [1] T. Mallat, A. Baiker, *Chem. Rev.*, **2004**, 104, 3037.
- [2] K. Mori, T. Hara, T. Mizugaki, K. Ebitani, K. Kaneda, *J. Am. Chem. Soc.*, **2004**, 126, 10657.
- [3] B. S. Kumar, A. Dhakshinamoorthy, K. Pitchumani, *Catal. Sci. Tech.*, **2014**, 4, 2378.

Synthesis, Characterization and Catalytic Activity of Dicationic Ionic Liquids/HPA Composites as New Heterogeneous Catalysts for Alkene Oxidation with Molecular Oxygen

Fahime Nezampour^a, Mehran Ghiaci^{a,*}

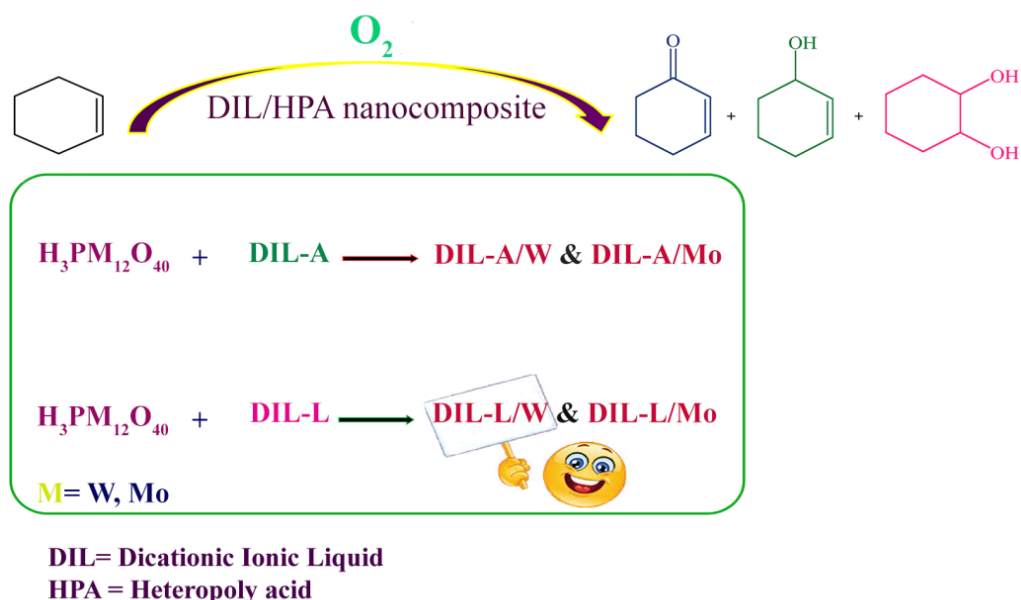
^a*Department of Chemistry, Isfahan University of Technology, Isfahan, 8415683111, Iran*

*mghiaci@cc.iut.ac.ir

Introduction: Oxidation of unsaturated hydrocarbons on the allylic and the double bond positions are very important transformations in the synthetic organic chemistry [1,2]. Cyclohexene as an important petrochemical resource, in the oxidation process could undergo provoking olefinic oxidation at the double bond in addition to allylic oxidation. Heteropoly acids (HPAs) and also ionic liquid compounds have attracted a lot of attention due to their unique features. Herein, we used dicationic ionic liquids/HPA nanocomposites for oxidation of cyclohexene in the presence of molecular oxygen, under solvent free conditions. We have tried to improve double bond oxidation over the allylic oxidation.

Methods / Experimentals: All materials and solvents used in this study were purchased from Sigma-Aldrich and Merck Company. The products were characterized by FT-IR, ¹H NMR, GC, GC-MS, FESEM-EDX, TEM, BET, ICP-OES and XRD techniques. DIL/HPA nanocomposites were prepared by the interaction of two kinds of DILs with HPAs in aqueous media. DILs consist of aliphatic (L) and aromatic (A) linkage.

Results and Discussion: To prepare our catalysts, DIL-A and DIL-L were dissolved in DI water and an aqueous solution of HPA was slowly added to them. The resulting solid was separated by filtration, dried at ambient temperature and renamed hereafter as DIL-A/W, DIL-A/Mo, DIL-L/W and DIL-L/Mo (Scheme 1). These composites were used for oxidation of cyclohexene and the best results achieved by DIL-L/W.



The products were characterized by FT-IR, ^1H NMR, GC, GC-MS, FESEM-EDX, TEM, BET, ICP-OES and XRD techniques. FT-IR spectra confirmed the incorporation of HPAs into DILs. According to FESEM-EDX images, the obtained DIL-L/W is composed of spherical nanoparticles with an average size of around 35 nm and consists of N, C, O, Br, P and W atoms.

Conclusion: On the basis of two dicationic ionic liquids and heteropoly acids, different catalysts were prepared. The catalyst, DIL-L/W was found to have a desirable catalytic activity for oxidation of cyclohexene under solvent free conditions. By considering various parameters the reaction conditions were optimized. The maximum conversion of cyclohexene was 96% and selectivity for the main product i.e., 1,2-cyclohexanediol was 86%.

References:

- [1] Yang, D.; Jiang, T.; Wu, T.; Zhang, P.; Han, H.; Han, B. *Catal. Sci. Tech.* **2016**, 6, 193-200.
- [2] Kuznetsov, M. L.; Rocha, B. G. M.; Pombeiro, A. J. L.; Shulpin, G. B. *ACS Catal.* **2015**, 5, 3823-3835.

Application of modified mica sheets as a thin film microextraction phase and optimization of ketorolac extraction condition using response surface methodology

Maryam Naghavi, Fariborz Momenbeik*

Department of chemistry, University of Isfahan, Isfahan, 81746-73441, Iran

Email: f.momen@chem.ui.ac.ir

Introduction: Sample preparation, is an essential step prior to analysis and have great influence on the reliability and accuracy of the analysis. In recent years, solid phase microextraction (SPME) has become an attractive and widely used sample preparation technique [1]. Thin film microextraction (TFME), a format of SPME technique, was developed using a sheet of flat film with high surface area-to-volume ratio as extraction phase. An important direction for TFME development is exploration of new coatings and new thin-film formats for a wide variety of applications [2]. The aim of this work is to introduce modified mica as a new extraction phase of TFME. To our knowledge, this is the first report on the use of modified mica as a sorbent for TFME. The potential application of the modified mica sheets as an extracting phase for TFME was investigated using ketorolac as model compound which determined by HPLC. The effect of different experimental parameters on the extraction efficiency of the method was studied using central composite design (CCD) and response surface methodology (RSM). Finally, the analytical performance and feasibility of the method in real sample analysis were investigated.

Methods: A stock standard solution of 1000 mg L⁻¹ of ketorolac was prepared in acetonitrile (ACN). Working standard solution of 50 mg L⁻¹ was prepared in water. The aqueous solutions were prepared daily by diluting working solution with pure water to get the desired concentration levels. The analyses were performed on an analytical reversed-phase ODS column. The mobile phase consisted of methanol and water (0.1% (v/v) acid formic) with the ratio of (70:30) at a flow rate of 1.0 mL min⁻¹. Wastewater sample was collected from Isfahan municipal wastewater treatment plant and filtered with a 0.45 µm

syringe filtration disk. The mica sheet was stirred in 1M HCl for 60 min at 50 °C and then rinsed and dried at 110 °C. Mica strips (1 cm×6 cm) was dispersed in 10 ml solution of aminopropyltriethoxysilane (APTES) in toluene and stirred for 24 h, washed with toluene and acetone and dried at 110 °C. Modified mica pieces (1 cm×1 cm) were conditioned by 200 µl methanol, dried at room temperature and then positioned inside the sample solution container. After extraction, analyte was desorbed 140 µL of acetonitrile and injected to HPLC. The statistical computer package “Design-Expert 7.1.5 Trial” was used for experimental design and multivariate optimization of TFME procedure.

Results and discussion: FT-IR spectra of the mica surface before and after modification were recorded to evaluate the modification of mica. Optimum amount of APTS was 10% and the optimum time of reaction with APTES was 6 h. 5 types of solvents were studied as desorption solvent and the best result was achieved by acetonitrile. A 32 run CCD was used for design and optimization of the effective parameters. The optimum values of factors are: 5 ml of aqueous sample with pH=6, 4 min extraction time and desorption with 140 µl ACN while sonicated for 140 S were among the best conditions for ketorolac TFME. The calibration curve was obtained under the optimized conditions and using this plot, figures of merit of the proposed method were evaluated. The proposed method presents suitable working linear ranges (1- 20 µg L⁻¹) with a good linearity ($R^2 = 0.998$), good limit of detection (0.457 µg L⁻¹), acceptable repeatability (%RSD <10) and good accuracy (recovery = 83.6%). Finally, the amount of spiked ketorolac to wastewater as a real sample was determined using this method.

Conclusion: In this project, modified mica was used as an extraction phase in TFME. The experimental results demonstrate that the chemically modified mica can be used for extracting ketorolac from aqueous solution with low LOD, wide linear range and good recovery.

References

- [1] A. Mehdinia; M. O. Aziz-Zanjani Solid-Phase Microextraction in Analytical Separation Science **2015**, 5:8, 1385–1400.

[2] R. Jiang; J. Pawliszyn *TrAC Trends Anal. Chem.* **2012**, 39, 245-253.

A Magnetic Polysulfonate for Enrichment Trace Determination of Isosorbide Dinitrate

Habibollah Eskandari^{a,*}, **Aziz Ghacemi**^a

^a*Department of Chemistry, Faculty of Basic Sciences, University of Mohaghegh Ardabili, Ardabil*

heskandari@uma.ac.ir

Introduction: Prior to assess the trace level of analytes in complex matrixes, separation and preconcentration techniques are necessary to eliminate or minimize matrix effects and to achieve high extraction efficiencies and preconcentration factors. In expanding analytical fields such as environmental, biological and material monitoring of important compounds, there is an increasing need to develop the simple, sensitive and selective analytical techniques that do not use expensive or complicate test equipments. Solid phase extraction (SPE) is one of the most reliable and convenient separation tools, which can effectively decrease the detection limit and eliminating the matrix interferences. Isosorbide dinitrate (ISDN) is a nitrate used pharmacologically as a vasodilator for angina (heart-related chest pain), congestive heart failure and esophageal spasms [1, 2]. In the viewpoint of analytical chemistry, trace determination of ISDN in environment and biological fluids is important.

Methods / Experimentals: The present work contains a methodology for preparation, characterization and application of an anionic magnetic nanoparticle material as an efficient adsorbent. 2-Acrylamido-methylpropane sulfonic acid was polymerized on the surfaces of magnetite nanoparticles in the presence of N, N'-methylenebisacrylamide as the cross-linking agent and persulfate as catalyst. The prepared magnetic adsorbent was characterized by FT-IR, SEM, XRD and TEM. The efficiency of the prepared magnetic polymer as a solid phase extractant for trace extraction-determination of ISDN was investigated. Metoclopramide was diazotized with nitrite (produced from hydrolysis of ISDN) and then was coupled with N-(1-naphthyl) ethylenediamine to prepare an azo dye. In acidic media, the azo dye was present as a cationic dye and therefore was extracted by the prepared anionic adsorbent. The dye was desorbed by a basic ethanolic solution and was monitored spectrophotometrically at 512 nm. Absorbances were measured with a 1650 PC Shimadzu spectrophotometer, equipped with a quartz cell (0.5 mL inner volume and 10 mm optical path). All chemicals used were of analytical reagent grade, also deionized water was used for preparation of the solutions.

Results and Discussion: The spectrophotometric determination method is based on a diazotization-coupling reaction after hydrolysis of ISDN at 80 °C for 60 min in a sodium hydroxide concentration of 0.05 mol L⁻¹ (optimum condition for ISDN hydrolysis).

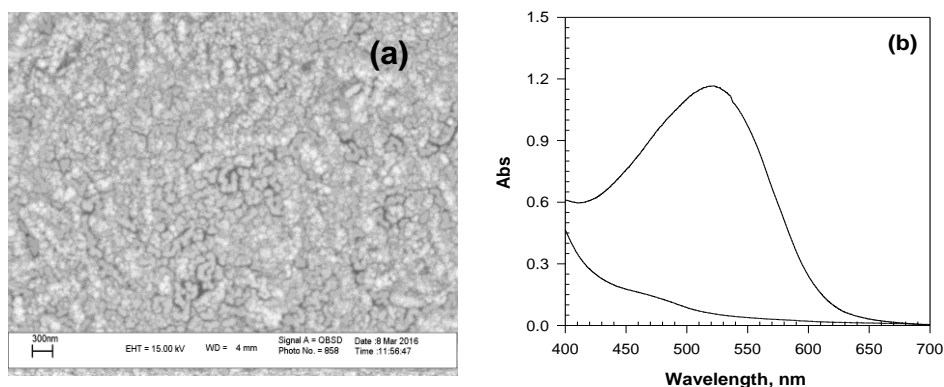


Fig. 1: (a) SEM micrograph of the magnetic polysulfonate; (b) typical UV-visible spectra of blank and sample containing ISDN after SPE-backextraction procedure.

All affecting parameters were optimized with a one at a time protocol. The optimal conditions for the hydrolysis of ISDN and for the established SPE method were applied and a calibration graph was obtained. One linear range was observed in the range of 1.0-90.0 ng mL⁻¹ of ISDN. Limit of detection was found as 0.6 ng mL⁻¹ of ISDN by 10 times blank repetitive experiments.

The selectivity of the method was also evaluated after individually addition of different concentrations of foreign species to the solutions containing ISDN as 10 ng mL⁻¹. No mild or serious interferences were found.

For examining the suitability of the presented SPE-spectrophotometric method for ISDN determination in real samples, the method was applied to various water, soil, plasma, urine and pharmaceutical formulations. In all the cases, to the samples, standard solutions of ISDN were added and accuracy and applicability of the method for ISDN determination in the sample matrices, were evaluated.

Conclusions: A new magnetic cation exchanger polymeric adsorbent was synthesized and was used for enrichment-determination of ISDN in various samples. The presented method was simple, accurate and sensitive.

References

- [1] M.J. Ahmed; M.N. Uddin. *Chemosphere*, **2007**, 67, 2020-2027.
- [2] Naeemullah; T.G. Kazi; M. Tuzen. *Food Chemistry*, **2015**, 172, 161–165.

Oxidation of Dibenzothiophene (DBT) by Proline Based Aminophenolate Tungsten Complex Supported on SBA-15

Iraj Saberikia^a, Elham Safaei^{b*}, Babak Karimi^a

^a Institute for Advanced Studies in Basic Sciences (IASBS), 45137-66731, Zanjan, Iran

^b Department of Chemistry, College of Sciences, Shiraz University, Shiraz, 71454, Iran

E-mail: e.safaei@shirazu.ac.ir

Introduction. Oxidation of sulfides are important discussion of chemicals transformations for the synthesis of various chemically and biologically significant molecules, natural products and drugs [1,2]. Tungston complexes are one of the best catalysts for the sulfides oxidation reactions since it contains the catalytic center in a variety of enzymes, e.g. acetylene hydratase. In this study, a novel tungston based catalyst has been synthesized by covalent grafting of (S)-1-(3,5-dichloro-2-hydroxybenzyl)pyrrolidine-2-carboxylic acid ligand onto functionalized ordered mesoporous silica (SBA-15) followed by complexation with tungsten oxy chloride. The immobilized catalyst was employed for the catalytic oxidation of dibenzothiophene to the corresponding sulfone. Moreover, this catalyst could be easily recovered by simple filtration and recycled for five times without loss of activity and selectivity.

Experimental methods. The catalyst was prepared by stirring a mixture of surface-bound amine, [(S)-1-(3,5-dichloro-2-hydroxybenzyl)pyrrolidine-2-carboxylic acid) L^{Pro}] and dicyclohexylcarbodiimide in dry THF at room temperature for 72 h under Ar atmosphere. The solid was filtered off and washed with ethanol using a Soxhlet apparatus to remove unreacted starting materials. Then, proline based amino phenolate tungsten complex supported on SBA-15 synthesised by complexation of surface bound ligand (SBA-15@AP-L^{Pro}) by WOCl₂ and triethylamine in ethanol at room temperature for 48 h.

Results and discussions. The process for preparing the catalyst and its intermediates was monitored by N₂ adsorption-desorption analysis Tab. 1 and Fig. 1. The nitrogen sorption analysis of SBA-15@AP-L^{Pro}-W confirms a regular and uniform mesostructure with a decrease in surface area and pore volume parameters in comparison with that of pristine SBA-15.

Tab. 1: Structural parameters of materials determined from nitrogen sorption

Sample	BET SA [m ² .g ⁻¹]	V _P [cm ³ .g ⁻¹]
SBA-15	968	1.23
SBA-15@AP-L ^{Pro} -W	372	0.57

To evaluate the general applicability of the catalyst (SBA-15@AP-L^{Pro}-W), the oxidation of various sulfides was explored. Additionally, the oxidation of dibenzothiophene (DBT) gave an overall yield of dibenzothiophene sulfone in high yields and selectivity (Table 2). We also studied the recyclability of the catalyst. The catalyst showed no significant loss of activity after five cycles.

Fig. 1: N₂ adsorption–desorption isotherm of SBA-15@AP-L^{Pro}-W

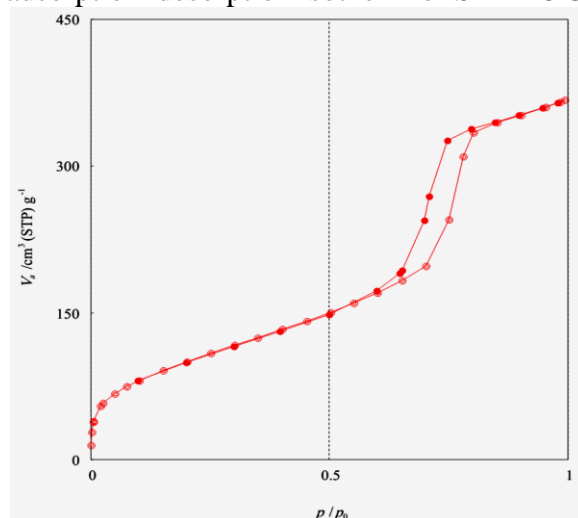
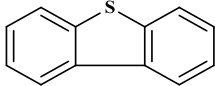
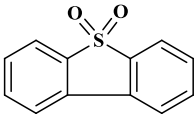


Table 2: Oxidation of dibenzothiophene (DBT) to dibenzothiophene sulfone

Substrate	Product	T °C	Solvent	H ₂ O ₂ (eq)	Con. %	Yield %	Time (min)
		70	CH ₃ CN	4 eq	96	>99	120

Conclusion. SBA-15@AP-L^{Pro}-W has been synthesized by covalently anchored tungston complex onto SBA-15. This catalyst is highly effective in the selective oxidation of sulfides by H₂O₂. The characterization results exhibit that the pore structure of SBA-15 remain intact after several synthetic procedure. It is found that SBA-15@AP-L^{Pro}-W exhibits better catalytic performance for oxidation of various sulfides at the optimized conditions.

References

1. Solladie, G. *Heteroat. Chem*, **2002**, *13*, 443-452.
2. Karimi, B.; Khorasani, M. *ACS Catalysis*, **2013**, *3*, 1657-1664.

Efficient and selective Oxidation of Alcohols Catalyzed by a Novel Iron Complex Supported on Silica coated magnetic nanoparticles

Touraj Karimpour ^a, Elham Safaei ^{b*}, Babak Karimi^a

^a *Institute for Advanced Studies in Basic Sciences (IASBS), 45137-66731, Zanjan, Iran*

^b *Department of Chemistry, College of Sciences, Shiraz University, Shiraz, 71454, Iran*

E-mail: e.safaei@shirazu.ac.ir

Introduction. Employing abundant and low price metal catalysts is one of the critical needs for sustainable chemical synthesis. According to the most potential of iron in biological system, iron catalysts are ideal for broad-scope of valuable organic transformations such as conversion of alcohols to carboxylic acids [1-3]. The separation of catalyst from the reaction mixture is complicated; therefore, the anchoring of metal complexes to high surface area solid supports can improve their catalytic performance. In this survey, we report a simple strategy for discovering a novel and highly active magnetically separable catalyst for alcohol oxidation.

Experimental methods. Using simple strategy a magnetically separable catalyst consisting of iron complex with amine bis(phenolate) ligand, covalently supported on amine functionalized silica-coated Fe₃O₄ nanoparticles was prepared. Chemical nature and structure of mentioned catalyst were confirmed by TEM, SEM, FTIR, TGA, ICP-AES, VSM, XPS, AAS, and elemental analysis (CHN) techniques.

Results and discussions. An iron complex of amine bis(phenolate) ligand was covalently anchored on magnetically separable silicate to afford an efficient system for alcohol oxidation. For indicating the eligibility of aforementioned environmentally friendly catalyst, a broad range of alcohols have been converted to the corresponding acids and ketones under optimum condition. It was worth noting that the high oxidative conversion was observed not only for primary alcohols, but also for secondary alcohols.

The result showed impressive recyclability of catalyst for six successive cycles for alcohol oxidation. The same patterns in powder x-ray diffraction of recovered catalysts and pristine catalyst, demonstrated stability of the catalyst. Moreover, stability in structure and morphology of recovered catalyst has been obviously seen in SEM and TEM images. Also, TGA and VSM analyses corroborated the catalyst stability during the reaction. All of these result confirmed that the iron complex was strongly anchored to the magnetite nanoparticles.

Conclusion. We synthesized a novel magnetically recoverable iron amine bis(phenol) ligand complex, that was immobilized on the silica coated magnetic nanoparticles by covalent linkage [Fe₃O₄@SiO₂-APTESFeL^{GDC}], and characterized by various techniques. Beside the simple separation of catalyst, achieved results, confirmed the high/excellent conversion percentage under mild conditions for high selective oxidation of broad range of alcohols to corresponding acids and ketones.

References

- [1] K. Manna, P. Ji, Z. Lin, F. X. Greene, A. Urban, N. C. Thacker and W. Lin, *Nat. Commun.* **2016**, 7, 12610.
- [2] Z. Alaji, E. Safaei, L. Chiang, R. M. Clarke, C. Mu and T. Storr, *Eur. J. Inorg. Chem.* **2014**, 2014, 6066-6074.
- [3] B. Karimi, Z. Naderi, M. Khorasani, H. M. Mirzaei and H. Vali, *ChemCatChem* **2016**, 8, 906-910

Mild and efficient method for the synthesis of dihydropyrimidinones in novel ChCl:TFA deep eutectic solvent

Adeleh Moshtaghi Zonouz*, Nasrin Babajani

Chemistry Department, Faculty of Science, Azarbaijan Shahid Madani University, Tabriz, Iran

E-mail: adelehmz@yahoo.com

Introduction

Dihydropyrimidinones (DHPMs), an important class of organic compounds, have become increasingly significant due to their therapeutic and pharmacological properties. Biginelli-type condensation reaction, which is one of the multi-component reactions (MCRs), is a very useful reaction for preparing 3,4-dihydropyrimidin-2(1*H*)-ones, their thiones analogs and other related heterocyclic compounds [1].

With the growing awareness of environmental issues and increasing need to reduce use of harmful chemicals in chemical, medicinal and industrial research in view of their effects, and the consequent risk for the human health, in recent years green chemistry has been a fascinating area of chemical research. The green chemistry aims to design environmentally benign chemical processes and synthetic methodologies in order to eliminate or reduce the use of hazardous and toxic chemicals at any stage of production in the industry or laboratory [2]. Within the framework of green chemistry, solvents occupy a strategic place. Green chemistry aims to replace the hazardous and/or harmful solvents with more environmentally friendly. A recent alternative solvent is the category of Deep Eutectic Solvents (DESs). Deep eutectic solvents, also known as deep eutectic ionic liquids (DEILs) or low-melting mixtures (LMMs) or low transition temperature mixtures (LTTMs) in the literature, have become more and more attractive in recent years due to their interesting properties and benefits, such as low cost of components, easy to prepare, tunable physicochemical properties, negligible vapor pressure, non-toxicity and biodegradability. These eutectic mixtures have been widely used as green and sustainable media as well as catalysts in many chemical processes [3]. Herein, we wish to report the utilization of novel ChCl:TFA deep eutectic solvent in the one-pot, three-component Biginelli reaction.

Experimental

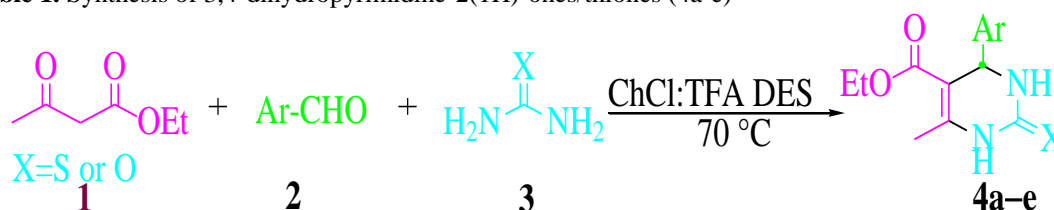
General procedure for the preparation of 3,4-dihydropyrimidin-2-(1*H*)-ones. A mixture of aromatic aldehyde (1 mmol), ethyl acetoacetate (1.3 mmol), urea or thiourea (1.5 mmol) in 3 mL ChCl:TFA DES was stirred at 70 °C for the desired time as indicated in Table. The progress of the reaction was monitored by TLC using *n*-hexane/ethyl acetate (3:2) as eluent. After completion of the reaction, water (15 mL) was added to the reaction mixture. The precipitated solid was collected by filtration to afford the corresponding pure product in excellent yield 90-96% (Table 1).

Results and discussion

Firstly, novel ChCl:TFA deep eutectic solvent was prepared and characterized in this work. Physical properties of DES, including density and viscosity were studied. In order to optimize the reaction conditions, initially, the reaction of 1 mmol benzaldehyde, 1.5 mmol urea with 1 mmol ethyl

acetoacetate in ChCl:TFA DES (3 mL) was tested in room temperature. The progress of the reaction was negligible even after 1 hr stirring. By raising temperature to 70 °C, the reaction was completed in 12 minutes and the desired product was obtained in 96% yield (Table 1, entry 1). The optimized conditions were then applied to a range of aldehyde substrates. Both electron-poor and electron-rich aldehydes were well tolerated (Table 1).

Table 1. Synthesis of 3,4-dihydropyrimidine-2(1H)-ones/thiones (4a-e)



Entry	X	Ar	Product	Time (min)	Yield (%)
1	O	C ₆ H ₅	4a	12	96
2	O	4-MeC ₆ H ₄	4b	11	94
3	O	3-O ₂ NC ₆ H ₄	4c	13	95
4	S	C ₆ H ₅	4d	24	94
5	S	3-O ₂ NC ₆ H ₄	4e	25	90

Conclusion

In summary, we have successfully developed an efficient and environmentally friendly approach for the synthesis of dihydropyrimidinone derivatives via a three-component reaction using ChCl–TFA deep eutectic solvent as a dual catalyst and environmentally benign reaction medium. The reaction showed good functional group tolerance, excellent yields, and simple product isolation without using specific purification such as chromatography. The potential uses of this route in synthetic and medicinal chemistry may be significant, since the products share structural and functional groups of biologically active molecules.

References

- [1] Bhosale, R. S.; Bhosale, S. V.; Wang, T. P.; Zubaidha, K. *Tetrahedron Lett.*, **2004**, 45, 9111-9113.
- [2] Francisco, M.; Bruinhorst, A. V. D.; Kroon, M. C. *Angew. Chem. Int. Ed.*, **2013**, 52, 3074-3085.
- [3] Liu, P.; Hao, J-W.; Mo, L-P.; Zhang, Z-H. *RSC Adv.*, **2015**, 1-54.

A Facile and Efficient Synthesis of Novel Multisubstituted Pyrroles from α -Bromoacetophenones and 2-Nitroethene-1,1-diamines

Mojikhalifeh Sanaz, Hasaninejad Alireza*

Department of Chemistry, Faculty of Sciences, Persian Gulf University, Bushehr 75169, Iran; Fax: +98-771-4545188; E-mail: a_hasaninejad@yahoo.com

Introduction: As one of the most important heterocycles, substituted pyrroles are not only found in many natural products and pharmaceuticals¹ but are also widely used in material science and supramolecular chemistry.² A variety of elegant methods for the synthesis of pyrroles have been developed in the past decades, however, a facile and efficient procedure for the synthesis of multisubstituted pyrroles remains highly desirable.

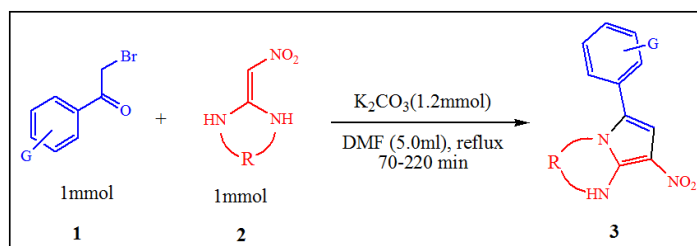
Recently, a metalfree synthesis of substituted pyrroles by the domino reaction of cyclic enamminones with halogenated nitroolefins has emerged.³

we have improved the synthetic method and developed a facile and efficient synthetic method for the synthesis of multisubstituted pyrroles from α -bromoacetophenones and 2-nitroethene-1,1-diamines.

General procedure for synthesis of multisubstituted pyrroles: α -bromoacetophenone(1mmol) and 2-nitroethene-1,1-diamine⁴, were added in a 25.0 mL roundbottomed flask contained K_2CO_3 (1.2mmol) and DMF (5.0 mL) and the resulting mixture was refluxed.

The reaction was monitored by TLC. After completion, the reaction mixture was allowed to cool down at room temperature, then saturated salt-water was added and the resulting residue was collected and purified by thin layer chromatography.

Results and Discussion: To begin our study, α -bromoacetophenone and 2-(nitromethylene)imidazolidine were chosen as model substrates to optimize the reaction conditions. After screening the various parameters such as solvent, catalyst and temperature, the optimum conditions were obtained as follows: α -bromoacetophenone (1mmol), 2-nitroethene-1,1-diamine (1mmol), K_2CO_3 (1.2mmol), DMF (5.0 mL) under reflux (Scheme1).



Scheme 1: synthesis of multisubstituted pyrroles

Under the optimized reaction conditions, we have explored the substrate scope. α -bromoacetophenone derivatives **1** and various 2-nitroethene-1,1-diamines **2** were allowed to react together. Various types of multisubstituted pyrroles were synthesized. The structures of them are shown in Figure 1.

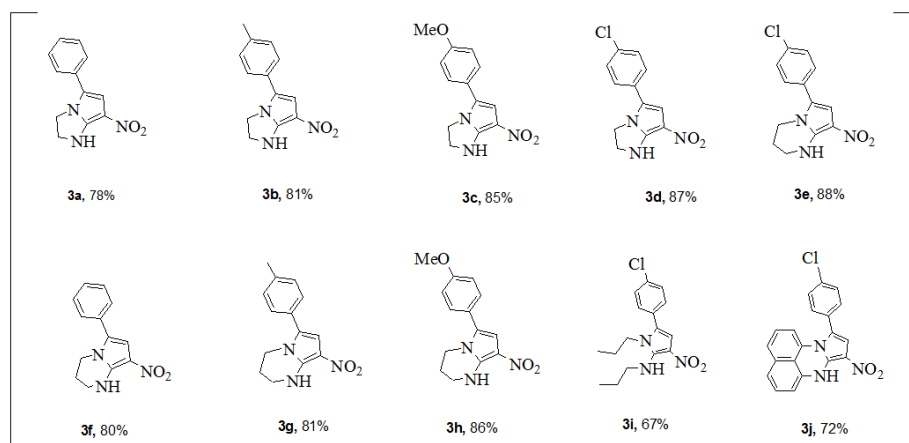


Figure 1: The structures of synthesized multisubstituted pyrroles

As shown in Figure 1, transformations displayed high functional group tolerance in high yields. α -bromoacetophenone bearing electron donating or –withdrawing substituents gave the desired multisubstituted pyrroles. (Figure 1, entries 3a-3j).

In addition, we have investigated the reactions of various 2-nitroethene-1,1-diamines with α -bromoacetophenone. Satisfactorily, the reactions afforded the corresponding pyrroles with great efficiency. In general, the aliphatic diamines show better reactivity than aromatic diamines or aliphatic amines (Figure 1, entries 3a, 3i, 3j).

Conclusion: In conclusion, we have demonstrated a facile and efficient procedure for the synthesis of multisubstituted pyrroles. This general protocol shows good functional group tolerance. Under the transition metal-free conditions, a wide variety of multisubstituted pyrroles were synthesized in good to excellent yields.

Reference

- [1] G. A. Pinna, M. M. Curzu, M. Sechi, G. Chelucci and E. Maciocco, *Farmaco*, **1999**, 54, 542;
- [2] T.A. Skotheim, R. L. Elsenbaumer, J.R. Reynolds, ed. *Handbook of Conducting Polymers*, 2nd ed.; Marcel Dekker: New York, **1998**.
- [3] M. Rueping and A. Parra, *Org. Lett.*, **2010**, 12, 5281.
- [4] D. P. Sangi; J. L. Monteiro; K. L. Vanzolini; Q. B. Cass; M. W. Paixão; A. G. Corrêa. *J. Braz. Chem. Soc.*, **2014**, 25, 1-15.

Amide Bond Formation in Deep Eutectic Solvents

Neda Manuochehri,^a Dariush Saberi,^{b,*} Khodabakhsh Niknam^{a,*}

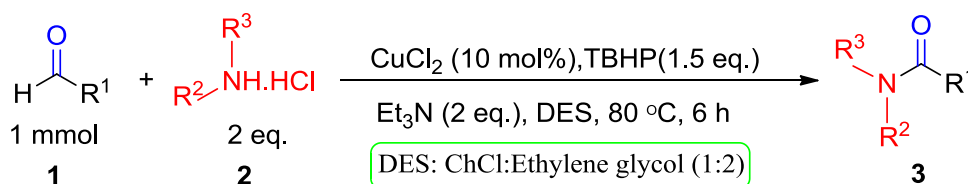
^aDepartment of Chemistry, Faculty of Sciences, Persian Gulf University, Bushehr 75169, Iran; Fax: +98-771-4545188; E-mail: niknam@pgu.ac.ir

^bFisheries and Aquaculture Department, College of Agriculture and Natural Resources, Persian Gulf University, Bushehr 75169, Iran; E-mail: saberi_d@pgu.ac.ir

Introduction: Within the framework of green chemistry, solvents occupy a strategic place. A new family of green solvents is deep eutectic solvents (DESs), a eutectic mixture with a melting point lower than 100 °C [1-2]. These DESs exhibit similar physico-chemical properties to the traditionally used ionic liquids, while being much cheaper and environmentally friendlier. Owing to these remarkable advantages, DESs are now of growing interest in many fields of research. Amide bonds have been ubiquitously found in the scaffolds of pharmaceuticals, agrochemicals, polymers, etc [3-4]. Synthesis of amides in DESs, instead of less environmentally friendly organic solvents, can be interesting since most of these solvents are not toxic and are also recyclable.

General procedure for synthesis of amides in DESs: To a mixture of catalyst (10 mol%), amine (2 mmol), and Et₃N (2 mmol) in ChCl:Ethylene glycol (1 mL) were added aldehyde (1 mmol) and TBHP (1.5 equiv.) and the mixture was stirred at 80 °C for 6 h. The reaction was monitored by TLC. After completion, the reaction mixture was allowed to cool down at room temperature. The reaction mixture was diluted with water (5 mL) and ethyl acetate (5 mL). The DES being soluble in water comes in the water layer. The combined organic layers were concentrated in vacuum and the resulting residue was purified by column chromatography.

Results and Discussion: Oxidative coupling of the benzaldehyde with ammonium chloride as the model reaction under the various conditions in order to establish the optimal conditions was investigated. After screening the various parameters such as catalyst, temperature, base, oxidant, and DES, the optimum conditions were obtained as follows: aldehyde (1 mmol), amine hydrochloride salt (2 equiv.), ChCl:Ethylene glycol (1 mL), Et₃N (2 equiv.), TBHP (1.5 equiv.), CuCl₂ (10 mol%), at 80 °C (Scheme 1).



Scheme 1: Amide bond formation in ChCl:Ethylene glycol as DES

To understand the substrate scope of this reaction, a wide range of aldehydes and amine hydrochloride salts were allowed to react together under the optimum reaction conditions. Various types of amides were synthesized in this way in moderate to good yields. The structures of some prepared amides are shown in Figure 1.

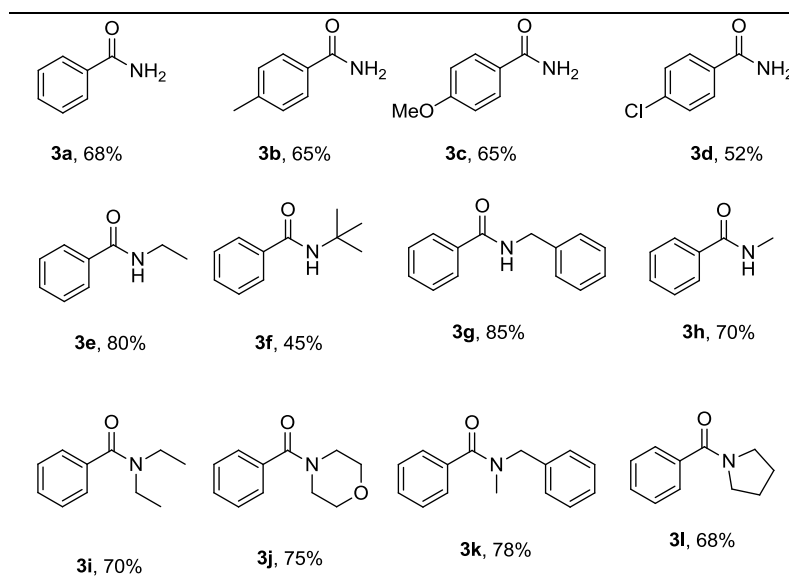


Figure 1: The structures of amides synthesized in DES

As can be seen in Figure 1, various primary, secondary, and tertiary of amides were well synthesized in ChCl:Ethylene glycol as a green solvent in acceptable yields.

Conclusion: Oxidative coupling using biodegradable ammonium deep eutectic solvent based on choline chloride and ethylene glycol provides an efficient and convenient method for the synthesis of benzamide and their derivatives. Employments of DES as an environmentally benign solvent as well as diversity in the synthesis of products are salient features of this method.

Reference

- [1] Q. Zhang; K. De O. Vigier; S. Royer; F. Jérôme. *Chem. Soc. Rev.*, **2012**, 41, 7108-7146.
- [2] M. Francisco; A. Bruinhorst; M. C. Kroon. *Angew. Chem. Int. Ed.*, **2013**, 52, 3074 -3085.
- [3] W. Wang; T. T. Yuan; D. D. Li. *Angew. Chem. Int. Ed.*, **2011**, 50, 1380-1383.
- [4] X. X. Zhang; W. T. Teo; P. W. H. Chan. *J. Organomet. Chem.*, **2011**, 696, 331-337.

Air-assisted dispersive liquid–liquid microextraction by solidifying the floating organic droplets for spectrophotometric simultaneous determination of some drugs in biological samples using chemometrics methods

Farnaz Farahmand, Bahar Ghasemzadeh and Abdolhossein Naseri *

Department of Analytical Chemistry, Faculty of Chemistry, University of Tabriz, Tabriz, Iran

Introduction: β -Adrenergic blockers represent a very important class of drugs that are used worldwide for treating various cardiac diseases[1]. Atenolol, Carvedilol, and Propranolol are β -blocker group forming antihypertensive drugs widely used to treat hypertension and some other disorders [2]. Pharmacokinetic and pharmacodynamic studies are important for the determination of the metabolism of drugs and for the design and development of safe medication. An air assisted liquid–liquid microextraction using the solidification of a floating organic droplet method (AADLLME-SFOD) coupled with a multivariate calibration method, namely partial least squares (PLS), was developed for the rapid and simple determination of Atenolol, Propranolol and Carvedilol in biological samples via a spectrophotometric approach.

Methods / Experimentals: In this method, a low-density solvent with a melting point near room temperature was used as the extraction solvent, and the emulsion was rapidly formed by pulling in and pushing out the mixture of aqueous sample solution and extraction solvent for ten times repeatedly using a 10-mL glass syringe. After centrifugation, the extractant droplet could be easily collected from the top of the aqueous samples by solidifying it at a temperature lower than the melting point. In the second step analytes were back extracted simultaneously into the acidic aqueous solution.

Results and Discussion: This method combines the advantages of AADLLME and dispersive liquid–liquid microextraction based on the solidification of floating organic droplets (DLLME-SFOD). Under the optimized conditions, calibration graphs were seen to be linear in the range of 0.3-6, 0.3-2 and 0.3-1.4 $\mu\text{g mL}^{-1}$ for ATE, CAR and PRO, respectively. Other analytical parameters were obtained as follows: enrichment factors (EFs) were found to be 11.24, 16.55 and 14.9, and limits of detection (LODs) were determined to be 0.09, 0.10 and 0.08 $\mu\text{g mL}^{-1}$ for ATE, CAR and PRO, respectively. There is a clear overlapping of the three complexes. To overcome this problem a suitable and simple technique, which presents a good recovery, is PLS regression. A mixture design was used to maximize statistically the information content in the spectra. These 27 samples were taken with concentrations of ATE, CAR and PRO varied between 0.5-2, 0.2-0.8 and 0.3-1.0 $\mu\text{g mL}^{-1}$, respectively. The compositions of the ternary mixtures used in the calibration matrices. For prediction set, five prepared mixtures that were not included in the previous set were employed as independent test to ensure that the prediction and real samples are in the subspace of training set. The spectral region between 200 and 300 nm.

Conclusion: In this study, AADLLME-SFOD method coupled with UV-vis was developed for simultaneous spectrophotometric determination of ATE, CAR and PRO in biological samples using multivariate calibration. Compared with other microextraction techniques this method was applied without the need of organic dispersive or

highly toxic chlorinated solvents. Due to the simple collection procedure applied along with the low toxicity, low density and melting point of the extraction solvent used; the proposed method can provide a good repeatability, high enrichment factor and good recovery.

References:

1. Saleem, K., et al., *Recent developments in HPLC analysis of β -blockers in biological samples*. Journal of chromatographic science, 2013; p. bmt030.
2. Prichard, B., J. Cruickshank, and B. Graham, *Beta-adrenergic blocking drugs in the treatment of hypertension*. Blood pressure, 2001. **10**(5-6): p. 366-386.

Densities And Viscosities Of Binary Mixture Methanol-Toluene

Asma sadrmousavidizaj *, and Dr Majed hamzelo

Department of Physical Chemistry, School of Chemistry, University of Tehran, Tehran, Iran

Email:asmamousavi58@gmail.com

Introduction: The density and viscosity are important basic data used in chemical engineering designs, solution theory, and molecular thermodynamics. However, a survey of the literature shows that very few measurements have been made on the physical properties of binary mixtures for methanol-toluene. Nevertheless, to our knowledge, no density and viscosity data on mixtures for methanol-toluene were previously reported in the literature. In this work, densities and viscosities for methanol-toluene mixtures have been measured under normal atmospheric pressure at temperature 298 K. From measurements of densities, the apparent volume percents of methanol-toluene were calculated. Results were fit to obtain the appropriate parameters and standard deviations between the measured and fitted values.

Methods / Experimentals: . The readings from 3 pycnometers were averaged to determine the density. the density ρ was then calculated from the relationship:

$$\rho = \frac{m}{v}$$

After thermal stability was attained, the flow times of the liquids were recorded with an electronic digital stopwatch correct to At least 3 repetitions of each datum point obtained were reproducible to the viscosity η was then calculated from the relationship:

$$\frac{\eta_{\text{solution}}}{\rho_{\text{solution}}} = \frac{\eta_{\text{solvent}}}{\rho_{\text{solvent}}} \left(\frac{t_{\text{solution}}}{t_{\text{solvent}}} \right)$$

where η_{solution} , ρ_{solution} and t_{solution} and η_{solvent} , ρ_{solvent} and t_{solvent} are the viscosities, densities, and flow time of the mixture and water, respectively .

The results for time and mass is reported in Table[1]

Table.1. Time and Mass from methanol-toluene

water	taverage=10.48 s	m =1.076 g
-------	------------------	------------

Volume percents	Timeaverage (s)	Mass (g)
Methanol 100% + Toluene 0%	09.03	0.8307
Methanol 90%+ Toluene 10%	08.76	0.8387
Methanol 80%+ Toluene 20%	08 .38	0.842
Methanol 70%+ Toluene 30%	07.90	0.8428

Methanol 60%+ Toluene 40%	07.78	0.8429
Methanol 50%+ Toluene 50%	07.76	0.8466
Methanol 40%+ Toluene 60%	07.58	0.8465
Methanol 30%+ Toluene 70%	07.42	0.8388
Methanol 20%+ Toluene 80%	07.33	0.8439
Methanol 10%+ Toluene 90%	07.25	0.8434
Methanol 0%+ Toluene 100%	07.22	0.8428

Results and Discussion: The measured densities and viscosities of methanol-toluene With literature values are included in Table [1], and it is clear from Table 1 that the experimental results show good agreement with the literature data. The experimental densities and viscosities at temperature($T^{\circ}K$) are listed in Tables[2], which showed the dependencies of density and viscosity on concentration, were plotted, respectively. It can be found that the density and viscosity increase with increasing concentration of at constant temperature and the dependence of density and viscosity concentration.

Table.2. Density and relative viscosity and Special viscosity of Methanol Toluene

volume percents	Density($\frac{g}{ml}$)	relative viscosity (mPa.s)	Special viscosity (mPa.s)
Methanol 100% + Toluene 0%	0.8428	0.5947	-0.4053
Methanol 90%+ Toluene 10%	0.8387	0.5825	-0.4175
Methanol 80%+ Toluene 20%	0.842	0.5594	-0.4406
Methanol 70%+ Toluene 30%	0.8428	0.5278	-0.4721
Methanol 60%+ Toluene 40%	0.8429	0.5199	-0.4801
Methanol 50%+ Toluene 50%	0.8466	0.5208	-0.4791
Methanol 40%+ Toluene 60%	0.8465	0.5087	-0.4913
Methanol 30%+ Toluene 70%	0.8460	0.4934	-0.5066
Methanol 20%+ Toluene 80%	0.8439	0.4904	-0.5096
Methanol 10%+ Toluene 90%	0.8434	0.4795	-0.5205
Methanol 0%+ Toluene 100%	0.8428	0.4824	-0.5176

Conclusion:The values of the apparent volume percent of in pure methanol and pure toluene have also been given in Tables 2 The apparent density increases as volume percents Toluene increases until Methanol 50%+ Toluene 50% then density decrease and relative viscosity bigning decrease then increases and decreases.

These values are important because they form thebasis for understanding molecular interactions.

References

- 1) Reilly, J.; Northman, W. *PhysioChem. Methods*, 1978, 88-90.
- (2) Krishnan, M. R. V.; Laddha, G. S. Heat of Mixing and Vapor Liquid Equilibrium Data of Binary Liquid MixturessPrediction from Viscosity Data. *Ind. Chem. Eng., Trans* 57, 1963.
- (3) Martin Contreras, S. Densities and Viscosities of Binary Mixtures of 1,4-Dioxane with 1-Propanol and 2-Propanol at (25, 30, and 40) °C. *J. Chem. Eng. Data* **2001**, 46, 1149-1152.

An Efficient Method for the Preparation of Tert-butyl peresters from Benzyl cyanide and Tert-butyl hydroperoxide

Hajar Hashemi^a, Khodabakhsh Niknam^{*a}, Dariush Saberi^{*b}

^a*Department of Chemistry, Faculty of Sciences, Persian Gulf University, Bushehr 75169, Iran;*

^b*Fisheries and Aquaculture Department, College of Agriculture and Natural Resources, Persian Gulf University, Bushehr 75169, Iran*

E-mail address of Corresponding author: niknam@pgu.ac.ir

Abstract: A novel protocol to synthesize tert-butyl peresters from benzyl cyanides and tert-butyl hydroperoxide has been successfully achieved. In the presence of tert-butyl hydroperoxide, Csp³–H bond oxidation, C–CN bond cleavage and C–O bond formation proceeded smoothly in solvent free conditions.

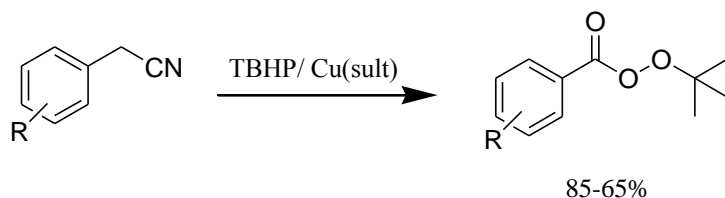
Introduction: Since C–C bond cleavage was reported, which has become attractive topic and given opportunity to utilization of starting materials to construct new chemical bonds.¹ As the substrate of a powerful building blocks, benzyl cyanide reagents represent a kind of stable obtained structures. While C–CN bond is relatively stronger because of the higher bond dissociation energy.² Thus, the cleavage of C–CN bonds is a challengeable topic.

Tert-Butyl peresters are one of the most important materials in many fields of chemistry.^{3,4} Traditionally, the synthesis of tert-butyl peresters relied on the reaction of carboxylic acids with tert-butyl hydroperoxide by apply base.⁵

Experimental: Herein, we report a new green, mild and efficient method for the synthesis of tert-butyl perester derivatives from benzyl cyanides in the present of tert-butyl hydroperoxide and cupper sult in solvent free conditions. Compared to the traditional method, our methodology is distinguished by high atom economy and free of base.

Results and Discussion: 2-phenylacetonitrile with tert-butyl hydroperoxide (TBHP) was chosen as a model reaction for optimization of the reaction conditions including the catalyst type, solvent and temperature, additive. The best conditions was when cupper sult catalyst was applied in solven free. Substituted 2-phenylacetonitrile could undergo C–CN bond cleavage by TBHP to give the corresponding perester products in high yields.

Phenylacetonitrile with electron-rich substituents like methyl ($-\text{CH}_3$) and methoxy ($-\text{OCH}_3$) reacted smoothly with TBHP to provide the corresponding peresters. Phenylacetonitrile containing electron-withdrawing groups like fluoro ($-\text{F}$) and chloro ($-\text{Cl}$), were used as substrates, could also be peresterified by TBHP to give the corresponding ester products through C–C bond activation under the optimal reaction conditions.



Conclusion: In summary, the novel oxidative of C–CN bond with TBHP and copper salt for the synthesis of tert-butyl peresters has been presented. In the present system, we achieved oxidation of $\text{sp}^3\text{C–H}$ bonds, C–C bond cleavage and C–O bond formation in short reaction time.

References:

- [1] (a) C. H. Jun. *Chem. Soc. Rev.*, **2004**, 33, 610; (b) S. E. Allen; R. R. Walvoord; R. Padilla-Salinas; M. C. Kozlowski. *Chem. Rev.*, **2013**, 113, 6234.
- [2] A. A. Zavitsas. *J. Phys. Chem. A.*, **2003**, 107, 897.
- [3] P. C. Montevecchi; A. Manetto; M. L. Navacchia; C. Chatgililoglu. *Tetrahedron*, **2004**, 60, 4303.
- [4] F. Formaggio; M. Crisma; L. Scipionato; S. Antonello; F. Maran; C. Toniolo. *Org. Lett.*, **2004**, 6, 2753
- [5] N. Milas; D. M. Surgenor. *J. Am. Chem. Soc.*, **1946**, 68, 642.

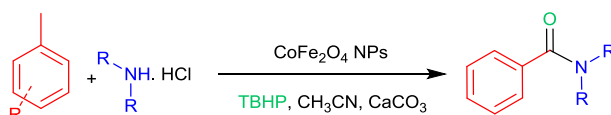
Green synthesis of primary, secondary, and tertiary amides through oxidative amidation of methyl groups with amine hydrochlorides over recyclable CoFe₂O₄ NPs

Esmail Eidi, Mohammad Zaman Kassaei*

Department of Chemistry, Tarbiat Modares University, P.O.Box 14155-175, Tehran, Iran
(kassaeem@modares.ac.ir)

Introduction

Amides are one of the most important functional groups in contemporary chemistry and this motif plays a significant role in the synthesis of natural products, polymers, pharmaceuticals, and fine chemicals. Furthermore, it has been assessed that about 25% of all synthetic pharmaceutical drugs contain an amide unit [1]. Direct oxidative amidation of methylarenes with amines is an attractive and economical method for synthesis of these compounds [2]. Here we report application of CoFe₂O₄ NPs, as a green, effective, clean, and recoverable magnetic nanocatalyst for the synthesis of important amides (Scheme 1).



Scheme 1 Oxidative amidation of methylarenes catalysed by CoFe₂O₄ NPs.

Experimental

General

All chemical reagents used in our experiments were purchased from Merck or Aldrich Chemical Company with high purity. Melting points were measured on an Electrothermal 9100 apparatus. ¹H NMR and ¹³C NMR spectra were recorded on a Bruker Avance (DPX 500 MHz and DPX 125 MHz) in pure deuterated CDCl₃ solvent using tetramethylsilane (TMS) as an internal reference. FT-IR spectra were recorded using KBr pellets on a Nicolet IR-100 infrared spectrometer. The powder X-ray diffraction spectrum was recorded at room temperature using a Philips X-Pert 1710 diffractometer. The latter appeared with Co K α (α =1.79285 Å) voltage: 40 kV, current: 40 mA and was in the range of 20°–80° (2 θ) with a scan speed of 0.02°/s. The particle morphology was examined by scanning electron microscopy using SEM (HITACHI S-4160) on gold coated samples. Magnetic properties were obtained by a vibrating magnetometer/Alternating Gradient Force Magnetometer (VSM/AGFM, MDK Co., Iran).

Preparation of magnetic CoFe₂O₄ nanoparticles (MNPs)

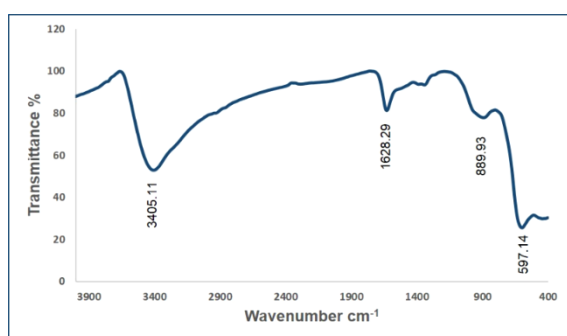
Magnetic CoFe₂O₄ nanoparticles were prepared by chemical co-precipitation chlorine salt of Fe³⁺ and Co²⁺ ions with a molar ratio of 2:1. Typically, FeCl₃·6H₂O (5.8g, 0.02mol) and CoCl₂ (1.3g, 0.01mol) were dissolved in 100 mL deionized water at 80 °C under N₂ atmosphere and vigorous stirring. Then, 10 mL of 25% NH₄OH was quickly injected into the reaction mixture in one portion. The Addition of the base to the Co²⁺/Fe³⁺ salt solution resulted in immediate formation of a black precipitate of MNPs. The reaction was continued for another 60 min and the mixture was cooled to room temperature. The black precipitate was washed with doubly warm distilled water.

General procedure for direct amidation of methylarenes with amine hydrochloride salts

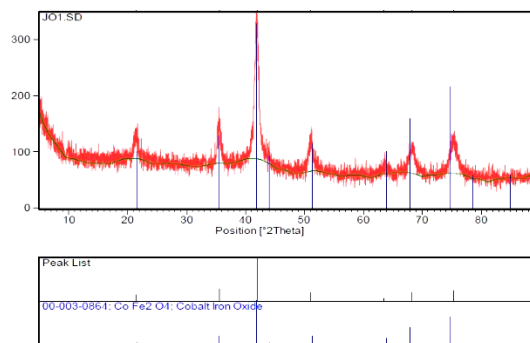
A mixture was made that consisted of catalyst (20 mg), an amine hydrochloride salt (1.5 mmol), CaCO_3 (3 equiv.), methylarenes (1 mmol), and $t\text{-BuOOH}$ (70 wt% in H_2O , 6 equiv.), in CH_3CN (2 mL), under an argon atmosphere for appropriate time at 80 °C. After completion of the reaction (monitored by TLC), the reaction mixture was cooled to room temperature and diluted with EtOAc. The catalyst was separated using an external magnet, washed several times with EtOAc and dried under vacuum at room temperature to be ready for a later run. The mixture was extracted with EtOAc, then the combined organic phases were dried over anhydrous MgSO_4 and the solvent was evaporated under reduced pressure. The crude product was purified by silica gel column chromatography to provide the desired amides.

Results and discussion

We reported the use of a heterogeneous cobalt ferrite nanocatalyst with high efficiency for the oxidative amidation of methylarenes with amine hydrochlorides. Cobalt ferrite was prepared and characterized via fourier transform infrared (FT-IR), vibrating sample magnetometry (VSM), energy-dispersive spectrum (EDS), scanning electron microscopy (SEM), thermal gravimetric analysis (TGA), and X-ray diffraction (XRD) analyses.



FT-IR Spectrum of CoFe_2O_4 NPs.



XRD Pattern of the catalyst CoFe_2O_4 NPs.

Conclusions

This protocol provides high yield, short reaction time, and operational simplicity, green and low cost procedure for the synthesis of all types of amides (primary, secondary and tertiary). The highlights of this work are the reusability and rather high efficiency of the synthesized nanocatalyst.

References

- [1] E. Valeur; M. Bradley. *Chem. Soc. Rev.*, **2009**, 38, 606–631.
- [2] J. B. Feng; X. F. Wu. *Appl. Organomet. Chem.*, **2015**, 29, 63-86.

Nano-crystalline TiO₂, *via* green combustion synthesis, as an efficient and reusable catalyst for preparation of 1,8-dioxooctahydroxanthenes and 1,8-dioxodecahydroacridines

Akram Farrokhi, Esmail Eidi, Zahra Nasresfahani, Mohammad Zaman Kassaei*

Department of Chemistry, Tarbiat Modares University, P. O. Box 14155-4838, Tehran, Iran

(kassaeem@modares.ac.ir)

Introduction

Development of new catalysts at nano-scale has emerged as a fertile field for research and innovation [1]. In particular, metal oxides appear efficient heterogeneous catalysts that are used in various organic transformations [2]. The ability of nanotechnology to enhance catalytic activity opens the potential to replace expensive catalysts with lower amounts of inexpensive nanocatalysts. Nitrogen-containing heterocyclic compounds are widespread in nature and their applications in biologically active pharmaceuticals, agrochemicals and functional materials are becoming more and more important [3].

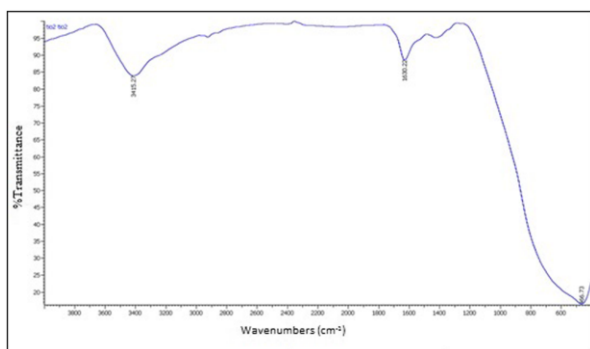
Experimental

Preparation of nano-crystalline TiO₂

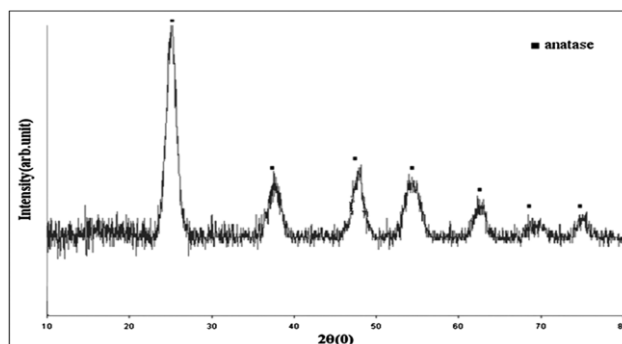
Nano-sized TiO₂ is prepared by the solution combustion method using titanyl nitrate [TiO(NO₃)₂] precursor and citric acid fuel (C₆H₈O₇). The titanyl nitrate is synthesized by the reaction of titanyl hydroxide [TiO(OH)₂] obtained by hydrolysis of tetra-n-butylorthotitanat with nitric acid. Assuming that the titanyl nitrate and fuel undergo complete reaction.

Results and discussion

Here we discuss the combustion synthesis of nano-crystalline TiO₂ NPs as a catalyst in one pot, multicomponent synthesis of 1,8-dioxooctahydroxanthenes and 1,8-dioxodecahydroacridines. The heterogeneous catalyst is fully characterized by FT-IR, XRD, SEM, and TEM.



FT-IR spectrum of nano-TiO₂ prepared by combustion synthesis.



XRD pattern of the as-synthesized nano-TiO₂ powder.

Conclusion

Pure anatase TiO₂ is synthesized by green microwave assisted combustion method, whose advantages include: use of relatively simple equipments, high purity, durable metastable phase, and lower cost compared to the conventional ceramic processes. The resulting TiO₂ NPs acts as a heterogeneous, highly efficient and recyclable novel catalyst for preparation of 1,8-dioxo-octahydroxanthenes and 1,8-dioxo-decahydroacridines.

References

- [1] A. A. Erumpukuthickal; K. Paromita; A. D. Parag; M. Giridhar; R. Narayanan. *ACS Nano*. **2011**, *1*, 8049-8061.
- [2] B. Prabal; S. Manisha; G. K. Prasad; S. Pratibha; M. P. Kaushik. *J. Mol. Catal. A. Chem.* **2011**, *341*, 7306-7309.
- [3] V. P. Litvinov. *Russ. Chem. Rev.* **2003**, *72*, 69-85.

Chitosan synergistically enhanced by successive Fe₃O₄ and silver nanoparticles as a novel green catalyst in one-pot, three-component synthesis of tetrahydrobenzo[*a*]xanthene-11-ones

Seyed Ali Moosavi Mashhadi, Reza Mohammadi, Esmail Eidi, Mohammad Zaman Kassaei*

Department of Chemistry, Tarbiat Modares University, P.O.Box 14155-175, Tehran, Iran
(kassaeem@modares.ac.ir)

Introduction

Fabrication of nanoparticles with desired properties through their surface modification has attracted growing attention in recent years. There is an ever increasing interest in the synthesis, characterization and surface modification of magnetic nanoparticles because of their potential applications in biotechnology, biomedicine, environmental, material science and catalysis [1-2]. Intriguing feature of these nanoparticles is the possibility to tune their properties through a molecular-level design by varying the size of the core and by surface modification with suitable functionalities. Polysaccharides are among the various stabilizing agents used to prevent nanoparticles from aggregating, and represent an attractive choice for preparation of functional materials. In particular, an increasing attention has recently been focused on the synthesis of CS coated Fe₃O₄ NPs [3-4].

Experimental

Synthesis of silver nanoparticles coated magnetic chitosan: Fe₃O₄@CS-Ag NPs

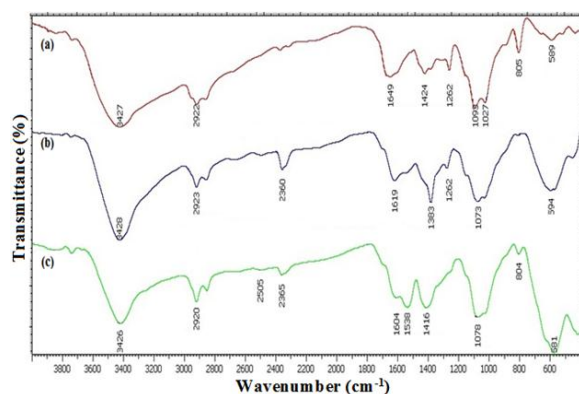
500 mg of Fe₃O₄@CS NPs is dispersed in water (30 mL) in an ultrasonic bath for 30 min, then an aqueous solution of AgNO₃ (300 mg in 5 mL) is added drop-wise over a period of 10 min, at room temperature. The mixture is mechanically stirred vigorously for 4 h. Subsequently, 2 mL of 0.1 M ascorbic acid is gradually added to the mixed solution of chitosan magnetic nanoparticles and AgNO₃ while stirring for 3 h. The solution changes from colorless to gray green, indicating the completion of the reaction. Finally, Fe₃O₄@CS-Ag NPs is separated by an external magnet, washed several times with water and dried under vacuum at room temperature.

General procedure for synthesis of 12-aryl-8,9,10,12-tetrahydrobenzo[*a*]xanthene-11-one

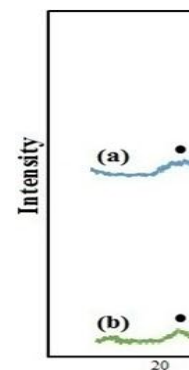
Fe₃O₄@CS-Ag NPs (15 mg) is added to a mixture of benzaldehydes (1 mmol), 2-naphthol (1 mmol), and 1,3-cyclohexadiones (1 mmol) in water (5 mL), and the reaction mixture is stirred at 80 °C. The progress of the reaction is monitored by TLC. After the reaction is completed, the catalyst is separated by an external magnet and reused as such for the next experiment. The crude product is extracted from the aqueous phase by EtOAc, and then the organic layer is washed with saturated brine and dried over anhydrous MgSO₄. Finally the combined organic layers are evaporated under reduced pressure and the resulting crude product is recrystallized from hot ethanol.

Results and discussion

The heterogeneous catalyst, Fe₃O₄@CS-Ag NPs, is fully characterized by FT-IR, XRD, TGA, VSM, SEM, TEM, and ICP-OES.



FT-IR Spectra of CS (a); Fe₃O₄@CS NPs (b); and Fe₃O₄@CS-Ag NPs (c).



XRD Patterns of Fe₃O₄@CS NPs (a); Fe₃O₄@CS-Ag NPs (b).

Conclusion

Preparation and characterization of antibacterial silver NPs implanted on nontoxic, biocompatible chitosan (CS) magnetic nanoparticles (Fe₃O₄@CS-Ag NPs) is described. The results Fe₃O₄@CS-Ag NPs acts as a “green” heterogeneous, highly efficient and recyclable novel catalyst for preparation of 12-aryl-8,9,10,12-tetrahydrobenzo[*a*]xanthene-11-one through one-pot, three-component reactions of benzaldehyde, 2-naphthol, and 1,3-dicarbonyl compounds in water. Green solvent, high yields, short reaction time, operational simplicity, practicability, applicability to various substrates and product purity are among the advantages of this protocol.

References

- [1] K.M. Ho; P. Li. *Langmuir* **2008**, *24*, 1801-1807.
- [2] T. Gelbrich; M. Feyen; A. M. Schmidt. *Macromolecules* **2006**, *39*, 3469-3472.
- [3] G.D. Carlo; A. Curulli; R.G. Toro; C. Bianchini; T.D. Caro; G. Padeletti; D. Zane; G.M. Ingo. *Langmuir* **2012**, *28*, 5471-5479.
- [4] K.H. Bae; M. Park; M.J. Do; N. Lee; J.H. Ryu; G.W. Kim; C. Kim; T.G. Park; T. Hyeon. *ACS Nano* **2012**, *6*, 5266-5273.

A one-pot synthesis of functionalized 2-oxo-4-(phenylamino)-5-(phenylimino)-2,5-dihydro-1H-pyrrole-3-carbonitrile

Nooshin Zahedi, Issa Yavari*

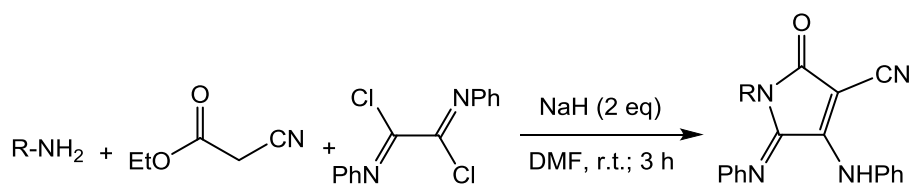
Department of Chemistry, Tarbiat Modares University, PO Box 14175-115, Tehran, Iran

(E-mail address: yavarisa@modares.ac.ir)

Introduction: Heterocycles are widely used in the development of modern pharmaceuticals, this being one of the reasons why continuous efforts are placed towards the design of amenable synthetic approaches for the synthesis of new heterocyclic systems [1]. Our research group reported the synthesis of a novel series of heterocycles using the reaction of dianionic compounds with various electrophiles [2-4].

Experimental: Primary amine, ethyl cyanoacetate and solvents were obtained from *Merck* and used without further purification. *N,N'*-diphenyloxalimidoyl dichloride was synthesized according to the reported procedure [5]. M.p.: Electrothermal-9100 apparatus. IR spectra: Shimadzu IR-460 spectrometer; band positions in cm^{-1} . ^1H and ^{13}C NMR spectra: Bruker DRX-500 Avance instrument at 500 and 125 MHz, respectively; δ in ppm, J in Hz. MS: Finnigan-MAT-8430EI-MS mass spectrometer; at 70 eV; in m/z (rel. %). Elemental analyses: Vario EL III CHNOS elemental analyzer.

Results and Discussion: A simple one-pot synthesis of 2-oxo-4-(phenylamino)-5-(phenylimino)-2,5-dihydro-1H-pyrrole-3-carbonitrile derivatives through the reaction of primary amines and ethyl cyanoacetate derivatives in the presence of bis(imidoyl)chloride compounds at room temperature is described (scheme 1). The structures of compounds 4 were assigned by IR, ^1H NMR, ^{13}C NMR and mass spectral data.



scheme 1

Conclusion: In conclusion, we report a one-pot synthesis of 2-oxo-4-(phenylamino)-5-(phenylimino)-2,5-dihydro-1H-pyrrole-3-carbonitrile. The present procedure has the advantage that the reactants can be mixed without any prior activation or modification and

this procedure has advantages of good yields. The products were crystallized out from the reaction mixture in pure form.

References:

- [1] C. H. Oh; H. W. Cho; D. Baek; J. H. Cho; *Eur. J. Med. Chem.* 2002, 37, 743–754.
- [2] I. Yavari; N. Zahedi; L. Baoosi. *J. Iran. Chem. Soc*, **2016**, 13, 1847-1851.
- [3] I. Yavari; M. Nematpour; E. Sodagar. *Monatsh Chem.* **2015**, 146, 2135-2138.
- [4] I. Yavari; Sh. Mosaferi. *Monatsh Chem.* **2016**, DOI: 10.1007/s00706-016-1834-3.
- [5] F. Helmholtz; R. Schroeder, PZ. Langer. *Naturforsch* **2005**, 60b, 1192-1196.

Aza Crown Macrocyclic-functionalized Fe₃O₄/SiO₂ magnetic nanoparticles as a new heterogeneous reusable catalyst for the synthesis of acridinone derivatives under solvent free conditions

SattarEbrahimi^{a*}

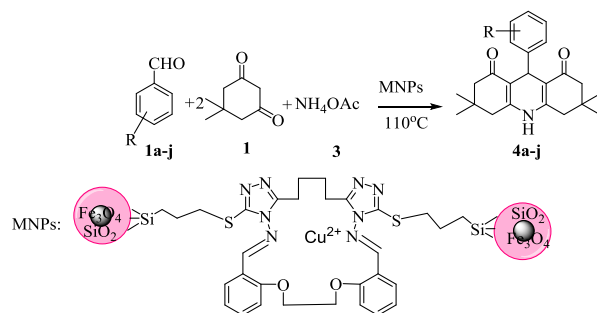
^a *Department of Chemistry Malayer Branch, Islamic Azad University, Malayer, Iran*

Email Address: seyonesi@gmail.com, seyonesi@iau-malayer.ac.ir

Introduction: Acridinedione compounds are generally synthesized by one-pot three-component cyclocondensation of dimedone or 1,3-cyclohexanedione, aromatic or aliphatic aldehydes and ammonium acetate or aromatic amines. Recently several methods have been reported in the literature for the synthesis of these compounds using of different types of catalysts.[1-3] In recent years, magnetic nanoparticles (MNPs) (e.g. Fe₃O₄) have been extensively investigated as catalyst supports in the synthesis of organic-inorganic catalysts, because of their good easy synthesis, stability, and high surface area, as well as low toxicity and price.[4,5] An important feature of these nano-catalysts is their separation from the reaction mixture using an external magnet, thereby obviating the need for filtration.[6]

Experimental: 0.5 g of Fe₃O₄@SiO₂- Propyl-Cl nanoparticles [7] were dispersed in 50 mL methanol by sonication over 1 h. To this suspension, 0.3 g of aza crown ether in 30 mL methanol was added, then, the reaction mixture was refluxed for 24 h under nitrogen. The solid material was obtained by magnetic separation and washed with methanol, and dried at 80 °C for 5 h under vacuum. Then, A mixture of an aromatic aldehyde (1 mmol), dimedone (2mmol), ammonium acetate (1 mmol) and 0.02 g of nano catalyst were stirred magnetically at 110 °C under solvent-free conditions for the 60 min. After completion of the reaction, the resulting solidified mixture was diluted with hot ethanol (15 mL) and the catalyst easily separated by a magnet. The residual solution was concentrated under vacuum and cooled to room temperature, and then, the obtained solid product was filtered and purified by recrystallization from ethanol.

Result and discussion:The magnetic nanoparticle supported Aza Crown Macrocyclic catalyst (MNPs- ACM-Cu²⁺) was prepared following the procedure shown in Scheme 1. Magnetite (Fe₃O₄) nanoparticles were easily prepared via the chemical co-precipitation of Fe²⁺ and Fe³⁺ ion basic solution. These were subsequently coated with silica (Fe₃O₄@SiO₂) through the well-known Stober method. The Fe₃O₄@SiO₂core-shell structures were then sequentially treated with 3-chloropropyltriethoxysilane (CPTS), which can bind covalently to the free-OH groups at the surface of the particles. Then, the reaction of the 3-chloropropyl-functionalized magnetic silica nanoparticles (Fe₃O₄@SiO₂-Cl) with 2,3:14,15-Dibenzo-6,7:10,11-bis[3-mercapto-4H-1,2,4-triazolo]-[1,16,5,6,11,12]dioxatetraaza cyclooctadeca-4,12-diene [8] gives the Aza Crown Macrocyclic-functionalized silica-coated magnetite nanoparticles (MNPs-ACM). Finally, reaction of the (MNPs-ACM) with Cu²⁺ gives the ACM-functionalized silica-coated magnetite nanoparticles (MNPs-ACM-Cu²⁺) (Scheme 1). After the characterization of the nano catalyst, its role as a catalyst was evaluated for the synthesis of acridinone derivatives (Scheme 1) using benzaldehyde, dimedone and ammonium acetates.



Scheme 1

Conclusion: In summary, ACM-functionalized magnetic silica nanoparticles were successfully prepared and their performance as heterogeneous catalyst for the synthesis of acridinone derivatives under solvent-free conditions was investigated. Moreover, the catalyst can be conveniently separated and recovered from the reaction system by a magnet, and can be reused for at least five times without noticeable loss of its activity

References

- [1] Jung D. H.; Lee Y. R.; Kim S. H.; Lyoo W. S. *Bull. Korean Chem. Soc.* **2009**, *30*, 1989-1995.
- [2] Javid A.; Khojastehnezhad A.; Heravi M.; Bamoharram F. *Synthesis and Reactivity in Inorganic, Metal-Organic, and Nano-Metal Chemistry*, **2012**, *42*, 14-17.
- [3] Nakhaei A.; Davoodnia A.; Morsali A. *Res Chem Intermed*, **2014**, *14*, 1861-1869.
- [4] Polshettiwar V.; Luque R.; Fihri A.; Zhu H.; Bouhrara M.; Basset J. M. *Chem. Rev.*, **2011**, *111*, 3036-3075.
- [5] Shylesh S.; Schunemann V.; Thiel W. R. *Angew. Chem. Int. Ed.*, **2010**, *49*, 3428-3459.
- [6] Yi D. K.; Lee S. S.; Ying J. Y. *Chem. Mater.*, **2006**, *18*, 2459-2461.
- [7] Moghanian H.; Mobinikhaledi A.; Blackman A. G.; Sarough-Farahani E. *RSC Adv.*, **2014**, *4*, 28176-28185.
- [8] Foroughifar N.; Mobinikhaledi A.; Ebrahimi A. *Synthesis*, **2009**, *15*, 2557-2560.

Highly Selective Electrochemical Sensor based on Modified Carbon Paste Electrode/ Multi-Walled Carbon Nanotubes/ Schiff base for the Determination of Trace Amount Of Hg(II), Cd(II), Ni(II), Co(II) and Pb(II)

Maryam Abbasi Tarighat^{a*}, Arash REzaei^a, Mehdi Fathinezhad^a
^aDepartment of science, Persian Gulf University, Bushehr, 7516913817, Iran

**matarighat@gmail.com, matarighat@pgu.ac.ir, arashrezaei634@gmail.com*

Introduction: Heavy metal pollution has become a serious threat to human health, living resources, animal and ecological systems. To a small extent, they enter the body system through food, air, vegetable, drinking water and bio-accumulate over a period of time [1]. Exposing people to moderate levels of lead resulted to a greater risk of experiencing changes in hearing ability, decreased mental ability in infants, learning difficulties, reducing growth in young children, kidney damage, increasing blood pressure; anemia; reducing sperm count, digestive issues, fertility and immune systems[2].

Experimental: Chemicals were purchased from Sigma–Aldrich and Merck (Darmstadt, Germany) and used as received with no further purification. Stock solutions chloride of Hg²⁺, Cd²⁺, Ni²⁺, Co²⁺ and Pb²⁺ (100 mg L⁻¹) were prepared by dissolving them in water. A 10⁻³ mol L⁻¹ solution was prepared by dissolving it in 50,50 (v/v) dimethylformamide (DMF), H₂O. A buffer solution of pH 4.5 (0.2 mol L⁻¹) was prepared from KH₂PO₄ and Na₂HPO₄. Schiff base according to literature.

Result and discussion: In the present study, the analytical potential of synthetic Schiff base was examined for the simultaneous determination of Hg²⁺, Cd²⁺, Ni²⁺, Co²⁺ and Pb²⁺ in aqueous samples without any separation steps. Typical spectra depicting complexes at the optimum conditions of pH 4.5 in the wavelength range 200–400 nm performed. The analytical conditions for the simultaneous determination of analyte elements were investigated. The composition of complexes was determined by the mole ratio method. The mole ratio plot for Hg²⁺, Cd²⁺, Ni²⁺, Co²⁺ and Pb²⁺ complexes confirmed a 2:1 (M:L) composition complexes, respectively.

Conclusion: Simultaneous determination of Hg²⁺, Cd²⁺, Ni²⁺, Co²⁺ and Pb²⁺ directly performed by DPV and CV measurements using a new Schiff base, as an analytical reagent, and chemometric modeling was performed. The proposed method provides a good reproducibility and gives a precise, highly sensitive and selective procedure with low LODs values. Also, there is a good agreement between results obtained by the proposed method and results obtained by FAAS .

Keywords: Hg(II); Cd(II); Ni(II); Co(II); Sn(II); MWCNTs; Schiff base

References

- [1] M. Abbasi Tarighat, Food Chemistry 192(2016)548-56
- [2] M. Abbasi Tarighat, M.R. Mohammadizadeh, Gh.Abdi, *J. Agric. Food Chem.* 61(2013)6832-40.
- [3] B.S. Sherigara, Y. Shivaraj, J. Ronald, J. Mascarenhas, A.K. Satpati, *Electrochim. Acta* 52 (2007) 3137–3142.

Preparation and characterization of polyvinyl alcohol hydrogel /grafted modified Fe₃O₄ nanoparticles through hexamethylene diisocyanate

Vahid Hooshangi^{a,*}, Ziba Jahanbakhsh Naghadeh^b,

^{a,*},^b Department of Chemistry, Faculty of Science, Payam Noor University, Tabriz- Iran

E-mail: vahidhooshangi@yahoo.com

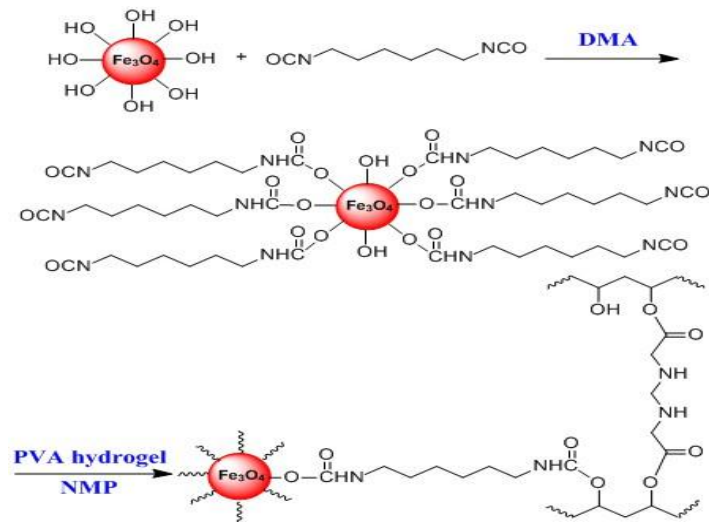
Telefax: +98 41 35419220

Introduction: Magnetic nanoparticles (MNPs) Due to the unique properties, have become one of the most useful materials in numerous applications in biomedical and other fields since their discovery [1, 4]. In this study, we report a novel type of magnetite nanocomposite of the PVA hydrogel/ grafted on modified Fe₃O₄ nanoparticles. Finally, the swelling behavior of prepared magnetite nanocomposite was investigated and Fe₃O₄/PVA crosslinked with hexamethylen diamine showed a fast initial swelling followed by a mild increase until to attaining equilibrium.

Keywords: Hydrogel, Polyvinyl alcohol, Magnetite.

Methods / Experimentals: For this propose firstly the PVA was bromoacetylated. Then the bromoacetylated PVA (BAPVA) for synthesis of hydrogel network was crosslinked by hexamethylenediamine (HMDA), (c-PVA/HMDA). Secondly, the surface of Fe₃O₄ was chemically modified with hexamethylene diisocyanate (HMDI) to improve its compatibility and interphase interaction with the polymeric matrix. Then the c-PVA/HMDA was added to the mixture under Ar atmosphere in room temperature. The grafting process was further carried out at 85 °C for a period of 21 h, then cooled down to room temperature.

Results and Discussion: The characterization of PVA hydrogels-grafted on modified Fe_3O_4 nanocomposite is presented as follow, and its schematic synthetic route is illustrated in



Scheme 1.

Scheme1. Synthetic path for the Preparation of c-PVA-g- Fe_3O_4

The swelling studies of c-PVA-g- Fe_3O_4 were evaluated by the gravimetric method. To determination of the Degree of Swelling (DS) Values of the prepared c-PVA-g- Fe_3O_4 .

Table I. DS Values for the Prepared c-PVA-g- Fe_3O_4 with different pH.

DS	Time (min)	15	30	60	120	240	480	24h
pH								
(c-PVA/HMDA-g- Fe_3O_4)	4	2	4	5	6	4.7	3	1
	5	3.1	5	7	7.5	5.9	4.5	1.2
	7.5	4	6	9	11	7	5	2

Figure 1(i) shows the FT-IR spectrum of the PVA indicates the presence of OH groups due to the bands that appeared in the region between $3300\text{-}3416\text{ cm}^{-1}$.By comparing the spectrum corresponds to the c-PVA/HMDA Fig.1(ii) with PVA the O-H stretching band at 3416 cm^{-1} was shifted to 3475 cm^{-1} as a result of the partly esterification of the O-H and hydrogen bond decreasing. a broad peak at around 3388 cm^{-1} corresponds to the N-H stretching vibration of

the secondary amine group in the polymer chain. The appearance of a sharp peak at 1726 cm^{-1} showed the formation of esteric carbonyl band.

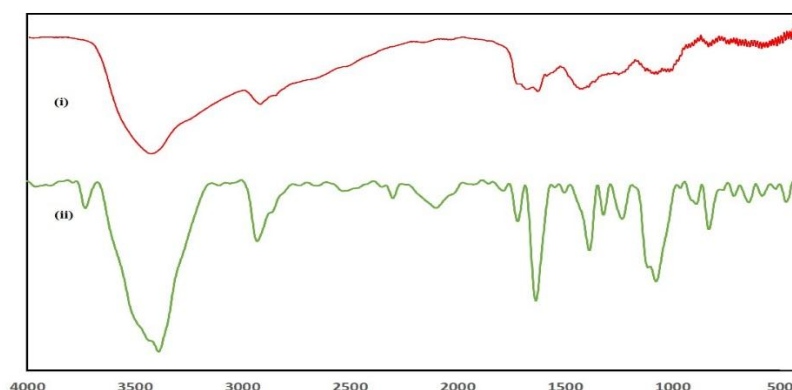


Figure 1: IR spectra of (i) PVA, (ii) c-PVA/HMDA

The morphologies of the products were investigated by SEM images in Figure 2.

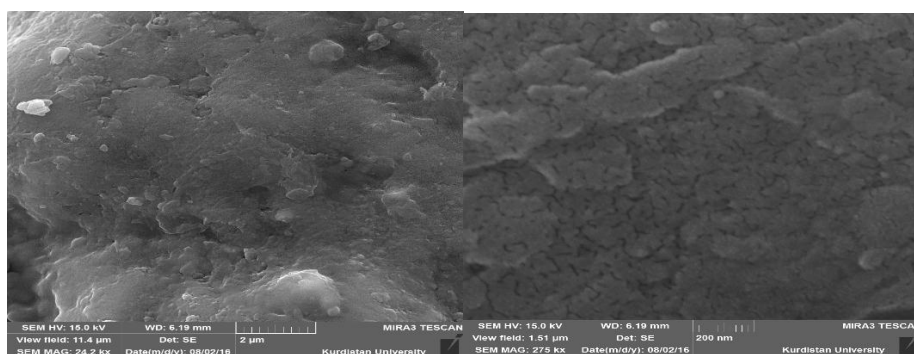


Figure 2. SEM images of the Fe₃O₄-g-c- PVA/EDA

Conclusion: In the present work we report the development of novel PVA hydrogels/grafted Fe₃O₄ suitable different applications. The main difference between the present project and the past similar works lies in not using a solvent to modify PVA prior to crosslinking stage. This matter (the separation of solvent from the product) in turn will be beneficial economically.

References

1. Mou X; Ali Z; Li S; He N. Applications of magnetic nanoparticles in targeted drug delivery system, 2015, 15, 54-62.
2. Kolhatkar AG; Jamison AC; Litvinov D; Willson RC; Lee TR. Tuning the magnetic properties of nanoparticles, 2013, 14, 15977-6009
3. Mody VV; Cox A; Shah S; Singh A; Bevins W; Parihar H. Magnetic nanoparticle drug delivery systems for targeting tumor, 2014, 4, 385-392
4. Faraji M; Yamini Y; Rezaee M. Magnetic nanoparticles: synthesis, stabilization, functionalization, characterization, and applications, 2010, 7, 1-37

Synthesis of Spirooxindole pyrimidines by Acidic Catalyst in Aqueous Media

Khodabakhsh Niknam^{a*}, Mohammad Bashkar^a

^aChemistry Department, Faculty of Sciences, Persian Gulf University, Bushehr, 75169, Iran.

Corresponding author E-mail address: khniknam@gmail.com; Participants author E-mail address: mohammad.bashkar@yahoo.com

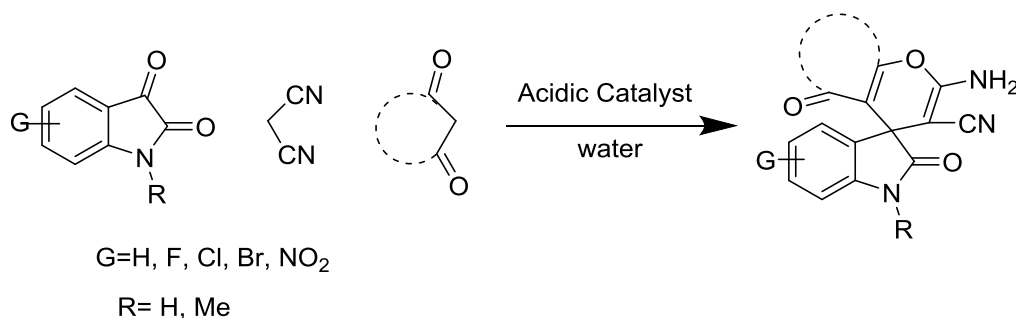
Introduction: Spirooxindoles are commonly occurring heterocyclic ring systems and are important structural motifs found in many natural products and pharmaceuticals [1]. They are recently isolated from plants. Also, they are useful as antibacterial [2], anticancer [3], antiproliferative agents [4], HIV antiviral [5] and antitubercular activities [6].

In recent years, numerous efficient transformations have been developed for the construction of spirooxindole structures, such as Lewis acids, heteropoly acids, solid acids, and ionic liquids [7,8].

Herein, we investigated an efficient and useful one-pot synthesis of spirooxindole derivatives using alumina acidic catalyst in aqueous media.

Experimentals: A mixture of isatin (1 mmol), reactive methylene compound (1 mmol), and 1,3-dicarbonyl compound (1 mmol) in the presence of catalyst in (3 ml) water was refluxed with stirring in an oil bath for 15 min. After completion of the reaction, the mixture was filtered and washed with water to separate catalyst. The crude product was purified by recrystallization from ethanol (95 %).

Results and Discussion: First, to study the reaction of isatin, malononitrile and 1,3-dicarbonyl compound as a simple model substrate, different conditions such as solvent and catalyst was tested. The best result was obtained when alumina acidic catalyst in aqueous media was used according to the yield and the reaction time.



Different substituted isatins electron donating groups such as 5-Me or electron-withdrawing groups 5-NO₂ and halogen substituted could be tolerated in this condensation. Corresponding spirooxindole derivatives were synthesized by the one-pot, three-component reaction in excellent yields under optimized conditions.

Conclusion: In conclusion, we have prepared spirooxindole derivatives by three-component condensation reaction of isatin, reactive methylene reagents with 1,3-dicarbonyl compounds in the presence acidic catalyst in refluxing water. This method has many advantages such as high yields, mild reaction conditions, short reaction time, convenient procedure and environmental friendliness.

Reference:

- [1] Cheng D, Ishihara Y, Tan B, Barbas CF. *A.C.S. Catal.* **2014**, 4, 743
- [2] Ghozlan, S. A. S.; Mohamed, M. F.; Ahmed, A. G.; Shouman, S. A.; Attia, Y. M.; Abdelhamid, I. A. *Arch. Pharm.* **2015**, 348, 113
- [3] Kamal, A.; Reddy, V. S.; Karnewar, S.; Chourasiya, S. S.; Shaik, A. B.; Kumar, G. B.; Kishor, C.; Reddy, M. K.; Narasimha Rao, M. P.; Nagabhushana, A.; Ramakrishna, K. V. S.; Addlagatta, A.; Kotamraju, S. *Chem. Med. Chem.* **2013**, 8, 2015.
- [4] Karthikeyan, K.; Kumar, P. M. S.; Doble, M.; Perumal, P. T. *Eur. J. Med. Chem.* **2010**, 45, 3446.
- [5] Jiang, T.; Kuhen, K. L.; Wolff, K.; Yin, H.; Bieza, K.; Caldwell, J.; Bursulaya, B.; Tuntland, T.; Zhang, K.; Karanewsky, D.; He, Y. *Bioorg. Med. Chem. Lett.* **2006**, 16, 2109.
- [6] Deraeve, C Dorobantu, I. M.; Rebbah, F.; Le Quéméner, F.; Constant, P.; Quémard, A.; *Bioorg. Med. Chem.* **2011**, 19, 6225
- [7] Edmondson S, Danishefsky SJ, Sepp-Lorenzino L, Rosen N. *J. Am. Chem. Soc.* **1999**, 121, 2147
- [8] Rad-Moghadam K, Youseftabar-Miri L. *Tetrahedron.* **2011**, 67:5693

***Biebersteinia multifida* L. Extract as a New Eco-friendly Corrosion Inhibitor for Carbon Steel in HCl Solution**

N. Soltani^{a,*}, N. Tavakkoli^a, A. Nejatian^a

^a Department of Chemistry, Payame Noor University, P.O. Box 19395-3697 Tehran, Iran

^aE-mail addresses: nasrin.soltani@pnu.ac.ir, nasrin_soltani2056@yahoo.com

Abstract: Metals used in industrial applications such as carbon steel are protected from corrosion in different ways that the use of corrosion inhibitors is one of the most popular, efficient, and practical methods especially in aggressive acidic media [1]. In recent years, due to increased environmental warnings and needs to develop environmentally friendly corrosion inhibitors, the researchers have been great attention to natural products derived from plants [2, 3. Among the large number of plants, some of them, such as leaf extracts of *Dacryodis edulis* [4], and the aqueous extract of olive (*Olea europaea* L.) leaves [5] have been reported as corrosion inhibitor of carbon steel in corrosive environments. In this research, the inhibition action of non-toxic *Biebersteinia multifida* L. extract on the corrosion of carbon steel in 2 M HCl has been reported. The corrosion behavior of carbon steel in acidic environment without and with various concentration of *Biebersteinia multifida* L. extract was studied by using the classical method of weight loss and electrochemical methods including potentiodynamic polarization method and electrochemical impedance spectroscopy (EIS) method. The results obtained from all three methods designated that the inhibition effeciancy is highest for 2.0 g/L of *Biebersteinia multifida* L. extract and inhibition effect increased with increasing concentration of extract in order 2.5 g/L \approx 2.0 g/L >1.5 g/L>1.0 g/L>0.5g/L>0.1 g/L. Potentiodynamic polarization measurements in the temperature range of 25-65 °C was performed for different concentration of extract to define the effect of temperature on the behavior of extract on the surface of carbon steel. The results indicated that the adsorption of *Biebersteinia multifida* L. extract is well described by Langmuir isotherm model under all of the studied temperatures. Thermodynamic adsorption parameters show that *Biebersteinia multifida* L. extract was adsorbed by a spontaneous exothermic process and a physisorption process can be suggested for that.

Keywords: *Biebersteinia multifida* L. extract; Non-toxic Corrosion Inhibitor; electrochemical impedance spectroscopy (EIS); Potentiodynamic polarization.

References

- [1] A.K. Singh, M. Quraishi, Investigation of the effect of disulfiram on corrosion of mild steel in hydrochloric acid solution, *Corrosion Science*, 53 (2011) 1288-1297.
- [2] O.K. Abiola, A. James, The effects of Aloe vera extract on corrosion and kinetics of corrosion process of zinc in HCl solution, *Corrosion Science*, 52 (2010) 661-664.
- [3] M. Behpour, S. Ghoreishi, M.K. Kashani, N. Soltani, Inhibition of 304 stainless steel corrosion in acidic solution by *Ferula gumosa* (galbanum) extract, *Materials and corrosion*, 60 (2009) 895-898.
- [4] E. Oguzie, C. Enenebeaku, C. Akalezi, S. Okoro, A. Ayuk, E. Ejike, Adsorption and corrosion-inhibiting effect of *Dacryodis edulis* extract on low-carbon-steel corrosion in acidic media, *Journal of Colloid and interface Science*, 349 (2010) 283-292.
- [5] A. El-Etre, Inhibition of acid corrosion of carbon steel using aqueous extract of olive leaves, *Journal of Colloid and Interface Science*, 314 (2007) 578-583.

Synthesis and application of in-situ molecularly imprinted silica monolithic in pipette-tip solid-phase microextraction for the separation and determination of gallic acid in orange juice samples

Maryam Arabi^a, Mehrorang Ghaedi^a, Abbas Ostovan^{b*}

^a*Chemistry Department, Yasouj University Yasouj, 75914-35, Iran

^b Department of Chemistry, Kerman Branch, Islamic Azad University, Kerman, Iran

E-mail address: saman.ostovan@yahoo.com

Introduction: we focused on the synthesis of hydrophilic, porous, flexible, crack-free and mechanically stable molecularly imprinted polymer as monolithic sorbent with non-covalent interaction at the tip of micropipette. Furthermore, it was applied for separation and preconcentration of gallic acid from orange juice samples. The reagents and organic solvents as well as evaporation step time were reduced while achieving high throughput, MIP monolithic via in-situ and direct polymerization inside micropipette.

Methods / Experimentals: 0.5 mmol gallic acid and 0.2 mmol thiourea were dissolved in 0.62 mL water and 2 mL methanol. 1.31 mL of TEOS and 0.29 mL of HCl were added to the prepared solution under stirring. Then, 0.23 mL of APTMS was added to it followed by continuous stirring until the hydrolysis was completed. A micropipette tip sealed at two ends with rubber was filled by 90 μ L of the solution. It was covered and kept at 40-45 °C for 24h.

Results and Discussion: The preparation of molecularly imprinted silica monolithic within the confinement of a micropipette-tip includes two steps: the hydrolyzation of the silanes of

TEOS and APTMS and the condensation of the hydrolyzed precursors [1]. To form a homogenous, permeable and mechanical stable monolithic matrix within the pretreated micropipette-tip, two vital parameters including the amount of thiourea and the condensation temperature were examined in the preparation of this MIP-monolithic. Experimental observation showed that the use of thiourea in the silica monolithic promotes the uniform mesoporous structure without any crack in the prepared monolithic skeleton. Interestingly, it was observed that the absence of thiourea in the reaction mixture monolith makes the monolithic fragile. The use of thiourea as an additive in the reaction mixture, resulted in non-cracked homogenous monolithic. Additionally, different condensation temperatures were adopted to examine the monolith formation. At higher condensation temperature (45 °C), the monolithic skeleton was seriously cracked that is attributed to the evaporation of methanol from silica matrix. With the decrease of the condensation temperature (down to 30 °C), the obtained monolithic matrix became homogeneous and denser in cost of the prolonged condensation time. Thus, the condensation temperature was set at 30 °C to obtain mechanical stable and permeable monolithic.

Conclusion: A novel in-situ hydrophilic molecular imprinting was developed for preparing silica-based monolithic at the tip of micro-pipette. Moreover, the addition of thiourea resulted in a crack-free monolithic. No interference with other constituents of orange juice was observed on surface of MIP-monolithic. The significant advantages of the current method include its cost-effectiveness, extremely low consumption of precursor and solvent and enhanced ease of operation.

References

[1] Raquel Gomes da Costa Silva, Fabio Augusto, Sol-gel molecular imprinted ormosil for solid phase extraction of methylxanthines

Development of a lower toxic approach based on one-pot green synthesis of water compatible molecularly imprinted nanoparticles for extraction of antihypertensive drug from human urine

Maryam Arabi^a, Mehrorang Ghaedi^a, Abbas Ostovan^{b}, Javad Tashkhourian^c*

^{a}Chemistry Department, Yasouj University Yasouj, 75914-35, Iran*

^bDepartment of Chemistry, Kerman Branch, Islamic Azad University, Kerman, Iran

^cDepartment of Chemistry, College of Science, Shiraz University, Shiraz 71454, Iran

E-mail address: maryamarabi63@yahoo.com

Introduction:

Hydrochlorothiazide (HCT) has been one of the most widely used diuretic and antihypertensive agents [1]. Because of the incidence of various side effects such as hyperglycemia, hyperuricemia, and hypokalemia [2], it may prove useful to monitor serum and urine levels of HCT in individual cases in order to obtain optimal therapeutic response and minimal side effects and also to assure compliance with therapy. Advances in solid phase extraction (SPE) usually refer to improvements in the specific and selective recognition of a particular component, which has a great potential for biological process. Molecularly imprinted polymers (MIPs) have attracted much attention for their outstanding mechanical and chemical robustness, low cost of preparation and high selectivity to target molecule. The aims of this study are as follows: (a) One-pot and green synthesis of Fe₃O₄@Molecularly imprinted polymers (Fe₃O₄@MIPs) (b) investigation of the basic characteristics of Fe₃O₄@MIPs by various instrumental analyses and (c) application of the Fe₃O₄@MIPs as SPE sorbents for purification and extraction of HCT.

Methods / Experimentals:

The sol-gel reaction was employed for hydrolysis of the silanes of tetraethyle orthosilicate (TEOS) and 3-aminopropyltrimethoxysilane (APTMS) to achieve molecularly imprinted particles anchored by hydrogen bonding to poly ethylene glycol [3]. All data were collected

and processed according to Freundlich isotherm (FI) to estimate binding parameters of the magnetic molecularly imprinted polymers (MMIPs) and magnetic non imprinted polymers (MNIPs).

Results and Discussion:

Typically, 50.0 mg of MMIPs or MNIPs were suspended in 10.0 mL of various concentrations of HCT solutions. After the samples were shaken, the MMIPs or MNIPs were separated by an external magnetic field and the solution was analyzed by high performance liquid chromatography. Under the optimized conditions the calibration curve was obtained by using the linear regression method and peak areas were plotted versus concentrations. The linearity of the established method was estimated over the range of 2.5–1000 $\mu\text{g L}^{-1}$ resulting in a regression equation $y = 121.33x - 5.87$ and a correlation coefficient of 0.9994. The average recoveries were in the range of 90.75% to 110.0% for urine whiles their intra-day and inter-day precision expressed as a relative standard deviation (RSD) was found to be 0.81% to 6.63%. These results demonstrated the good repeatability and accuracy of the method. In order to evaluate the selectivity of MMIPs, three compounds of similar structure, were investigated. For sampling, 50.0 mg MMIPs was added into a glass tube containing 10.0 mL methanol solution of studied species at two concentrations (0.5 and 1 mg mL^{-1}). Then, the above solutions kept stirring for 24 h at room temperature and subsequently the particles were collected by exposure of an external magnet filed and the supernatant monitored periodically. The result show that MMIPs had the highest affinity for HCT compared to other compounds.

References

- [1] Razak. O. A. *Journal of Pharmaceutical and Biomedical Analysis*, **2004**, 34, 433-440.
- [2] Cooper, M.; Sinaiko, A.; Anders, M.; Mirkin, B. *Analytical chemistry*, **1976**, 48, 1110-1111.
- [3] Smatt, J. H.; Schunk, S.; Lindén, M. *Chemistry of Materials*, **2003**, 15, 2354-2361.

Curcumin nanoparticles embedded into bacterial nano cellulose as a colorimetric gas sensor for ammonia

Pourreza N^{a,*}, Lotfizadeh N^a, Golmohammadi H^b

^aDepartment of Chemistry, Faculty of Sciences, Shahid Chamran University of Ahvaz, Ahvaz, Iran

^bACECR-Production Technology Research Institute, Ahvaz, Iran

*npourreza@scu.ac.ir

Introduction

Ammonia is a toxic, hazardous, corrosive and environmental pollutant causing lung disease, burning of skin and permanent blindness [1]. It is a marker for spoilage of meat and chicken. Because of these, detection of ammonia has gained worldwide attention. Curcumin (1,7-bis (4-hydroxy-3-methoxyphenyl)-1,6-heptadiene-3,5-dione), a natural product of the rhizomes of *curcuma longa* has been used as coloring agent and spice in food, drugs, and cosmetics [2]. Bacterial nanocellulose has been used for a wide range of applications such as wound-healing, tissue engineering, and sensing [3,4]. The present work describes an efficient gas sensor for detecting ammonia using curcumin nanoparticle (CURNs) embedded in bacterial nanocellulose as a safe and green nano material.

Method:

CURNs were embedded into bacterial nanocellulose via zinc ions as a linker and stirring at 60°C for 6 h. The absorption intensity of CURNs embedded in bacterial cellulose is decreased in the presence ammonia vapor. Curcumin molecules suffer rapid hydrolytic degradation at basic conditions and change color from yellow to red. New red shifted absorption bands appear at $\lambda = 460$ nm. This decrease in the absorption intensity of CURNs embedded in bacterial nanocellulose is proportional to ammonia concentration and was utilized for the colorimetric detection of ammonia..

Results

The effect of experimental parameters such as concentration of CUNPs, concentration of zinc, heat and time on the sensing probe was examined. Under optimum experimental conditions, the absorption intensity was linear with the concentration of ammonia in the range of 2.25 to 22.5 mg. The detection limit was 1.59 μg . The developed method was successfully employed for the detection of ammonia in swage water, meat and cosmetic samples with satisfactory results.

.

Conclusion

In this work the CURNs as a natural, inexpensive, non-toxic and environmental friendly nano material have been embedded into bacterial nanocellulose and utilized as a gas sensor for ammonia detection rotten meat and chicken and cosmetic products.

Keywords: Ammonia; Colorimetric; Curcumin nanoparticles; Nano cellulose;

References

- [1] S. B. Khan, M. M. Rahman, E.S. Jang, K. Akhtar, H. Han, Talanta 84 (2011) 1005–1010.
- [2] R.A. Sharma, A.J. Gescher, W.P. Steward, Eur. J. Cancer 41 (2005) 1955-1968.

[3]Abdul Khalil, H.P.S., Davoudpour, Y., Nazrul Islama, Md., Mustapha, A., Sudesh, K., Dungani, R., Jawaid, M. Carbohydr. Polym, 2014, 99, 649–665.

[4]N. Pourreza, H. Golmohammadi, T. Naghdi and H. Yousefi, Biosens. Bioelectron, 2015, 74, 353–359.

ZnTiO₃ nano particles as a sorbent for removal of an azo dye from aqueous solutions

Saeedeh Hashemian*

Department of chemistry, Islamic Azad University, Yazd Branch, Yazd, Iran

Abstract

ZnTiO₃ nano particles were synthesized by sol-gel method. The nano particles were characterized by FTIR, XRD and SEM methods. Adsorption of an azo dye, methyl red (MR) by ZnTiO₃ nano particles was studied. Effect of different factors, including agitation time, pH and adsorbate concentration on adsorption capacity of adsorbent for DR dye was investigated. Experimental results demonstrated MR could be effectively removed from aqueous solution by ZnTiO₃ nano particles within 10 min of contact time and pH 11. The adsorption kinetics of DR well matched with pseudo-second order rate expression.

Keywords: Adsorption, Dispersed red 1, Nano particles, ZnTiO₃

Introduction

Zinc titanate is an interesting ternary oxide system showing different polymorphs like cubic defect spinel Zn₂Ti₂O₇, cubic inverse spinel ZnTiO₃, and hexagonal ilmenite type ZnTiO₃. ZnTiO₃ has the ilmenite structure [1].

There are several methods to prepare ZnTiO₃ powder including solid state reaction, sol-gel, etc [2, 3]. These mixed oxides are important inorganic metalloid materials and are widely used in different fields [4-6]. These compounds with ilmenite structure are important and wide for chemical and electrical applications due to their weak magnetism, catalyst, adsorptive and semiconductivity properties [7].

Methods / Experimentals

All chemical were analytical grade purity and were used as received and were purchased from Merck. The ZnTiO₃ nanoparticles were synthesized by sol gel method. The ZnTiO₃ was prepared by sol-gel method. 1 mmol Zinc acetate and 1 mmol titanium ethoxide were dissolved in de-ionized water and ethanol separately then mixed. Then, citric acid and ethylene glycol (equal molar ratio) were added. The mixed solution was stirred at 80 °C, and was refluxed for 12 h at 80 °C and then was calcined at 500 °C for 2 h [8].

Results and Discussion

The morphology of as prepared ZnTiO₃ was determined by SEM image and showed in Fig. 1. The SEM image shows spherical uniform size of in nano scale. The average size of nano particles were determined 30 nm.

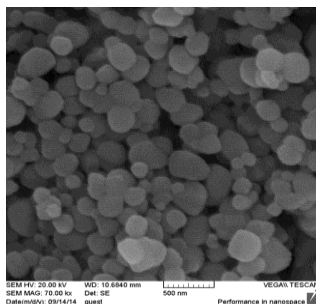


Fig. 1. SEM image of ZnTiO₃ nano particles

Effect of contact time

The effect of contact time on the adsorption of DR by ZnTiO₃ nano particles is shown in Fig. 2. The results show the rate of uptake of DR on ZnTiO₃ nano particles is quite rapid and adsorption occurs within the first 10 min of contact time.

* Corresponding author; Sa_hashemian@iauyazd.ac.ir

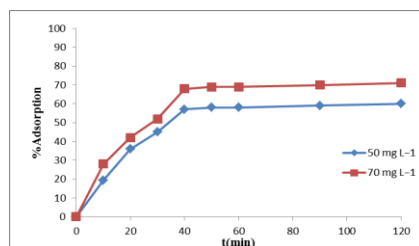


Fig. 2. Effect of contact time for adsorption of MR by ZnTiO₃ nano particles

Effect of initial solution pH

The pH of wastewater containing dyes is one of the most important factors that control the adsorption of dye onto adsorbent. The effect of pH for adsorption of DR was investigated for concentration of 50 and 70 mg L⁻¹ and results are presented in Fig. 3. The results showed that sorption was strongly dependent on pH. As pH increases from 2-12, the percentage of DR removal by ZnTiO₃ nano particles was increased.

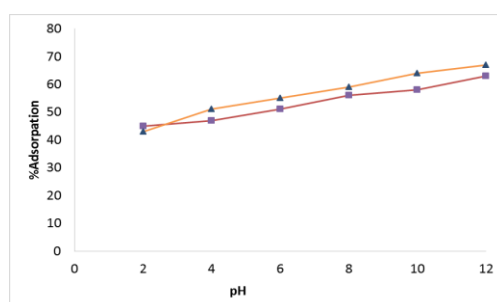


Fig. 3. Effect of pH on the adsorption of MR by ZnTiO₃ nano particles

Conclusion

ZnTiO₃ nano particles were successfully synthesized. The results show the illmenite type compound. The zinc titanate nano particles had sufficient capacity adsorptive property.

References

- [1] A. D. Bachvarova-Nedelcheva, R. D. Gegova, A. M. Stoyanova, R. S. Iordanova, V. E. Copicia, N. K. Ivanova, I. Sandu, *Bulgarian Chemical Communications*, 2015, 47(7) 540-543.
- [2] Y. L. Chai, Y. S. Chang, G.J. Chen, Y. J. Hsiao, *Materials Research Bulletin*, 2008, 43, 1066-1073.
- [3] B. Lokesh, S. Kaleemulla, N. Madhusudhana Rao, *International Journal of ChemTech Research*, 2015, 6(3) 1929-1932.
- [4] C. Y. Jimmy, Z. Lizhi, Y. Jiaguo, *Chemistry Materials*, 2002, 14, 4647-4653.
- [5] J. B. Yin, X. P. Zhou, *Chemistry Materials* 2002, 14, 4633-4640.
- [6] C. SH, H. ML, W. SC, L. HC, C. Ts, H. TH, *Journal of American Ceramic Society*, 2011, 94, 201-200.
- [7] S. Hashemian, A. Foroghimoqhadam, *Chemical Engineering Journal*, 2015, 230, 299-306.

Spherical Carbon Resin as Supporting Ni -nanocatalyst for the Heck Reaction

Atefe Valikhani^a, Jamaladin Shakeri^{a,b,*}

^a *Department of Chemistry, Isfahan University of Technology, Isfahan, Iran*

^b *Faculty of Chemistry, Razi University, Kermanshah, Iran*

Email Address: ja.shakeriharandi@ch.iut.ac.ir

Introduction:

Uniform nanoparticles have attracted a lot of attention in scientific studies due to the variety of their applications. Spherical particles with featured properties have a lot of important applications in target drug delivery [1], and biomedicine [2]. They are particularly utilized as catalyst support [3]. The Stober method is a facial way to synthesize the silica and carbon spherical particles. The process was discovered in 1968 by W. Stober *et al.* This method has some advantages such as particle-size controlling, narrow-size distribution, and a smooth spherical morphology of the resulting silica. Recently, this method has been utilized for carbon spherical particles by resorcinol-formaldehyde (RF) precursors. This resin is synthesized by the polymerization of resorcinol (a derivative of phenol) and formaldehyde, and calcination to achieve a carbon sphere [4,5]. Carbon particles develop more oxygen-containing groups through oxidizing, a process helping the modifying process of the carbon sphere in supporting metal nanoparticles [6,7,8] In the current work, we report the synthesis of carbon- Ni core shell structures by utilizing carbon spheres obtained via the Stober method and NiCl₂, using microwave. The main advantage of using this catalyst of Carbon Sphere-Ni (CS@ Ni) is for the Heck reaction.

Experimental:

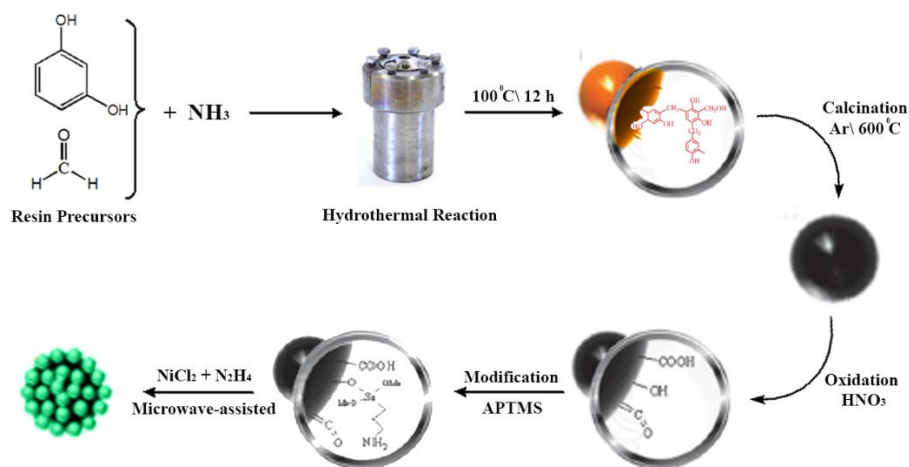
Ammonia aqueous solution (0.15 mL) was mixed with a solution containing absolute ethanol (15 mL) and deionized water (30 mL), and then stirred for more than 1 h. Subsequently, resorcinol (0.3 g) was added and continually stirred for 30 min. The formaldehyde solution (0.45 mL) was added and stirred for 24 h at room temperature, and then heated for 12 h at 100 °C

under a static condition in Teflon-lined autoclave. The solid product was recovered by centrifugation and was air-dried at 100°C . For carbonization, the RF spheres were heated at 600°C for ε h under Ar atmosphere. Next, these carbon spheres were oxidized with nitric acid (0 M). The mixture was filtered and the product was rinsed with distilled water and dried at 80°C . The process was carried out by placing the oxidized carbon spheres (0.3 g) with 300 mL toluene. Subsequently, 3 mL of APTMS was added and the solution was refluxed for 18 h . Finally, Ni nanoparticles were decorated onto the carbon-sphere surface in a microwave-assisted reduction process performed in a mixture of NiCl_2 salt, N_2H_4 , NaOH , and ethylene glycol (named: CS@ Ni).

Procedures for the Heck reaction: In a typical experimental procedure, K_2CO_3 (0.06 g) and CS@ Ni (0.05 g) were added to DMF ($\varepsilon\text{ mL}$) in a 10 mL beaker, subsequently was degassed. Then bromobenzene derivative (0.65 g) and n-butyl acrylate (0.05 g) were added and was refluxed at 130°C . Then the reaction mixture was cooled to room temperature and an aliquot was removed for gas chromatography (GC) analysis.

Result and Discussion:

Schematic illustration of consecutive steps of the synthesis of CS and CS@ Ni structures are depicted in Scheme 1.



Scheme 1. Schematic illustration of consecutive steps of the synthesis of CS and CS@ Ni structures.

Figure 1 shows SEM image of the carbon spheres (CS). As can be seen from this figure the resulting carbon spheres possessed diameters between 400–500 nm. They are quite uniform and smooth with a few structural defects.

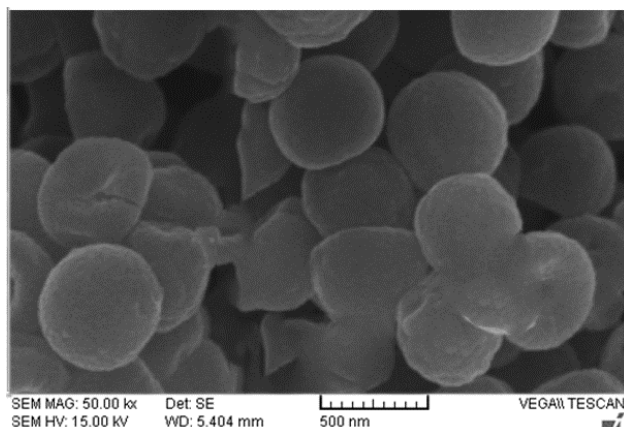


Fig 1. SEM image of carbon spheres (CS) prepared by the Stober method.

The SEM image of carbon- Ni core shell structures (CS@ Ni) is depicted in Figure 2. The results reveal that Ni nanoparticles are successfully loaded onto the carbon spheres surface with an average particle size around 10 nm.

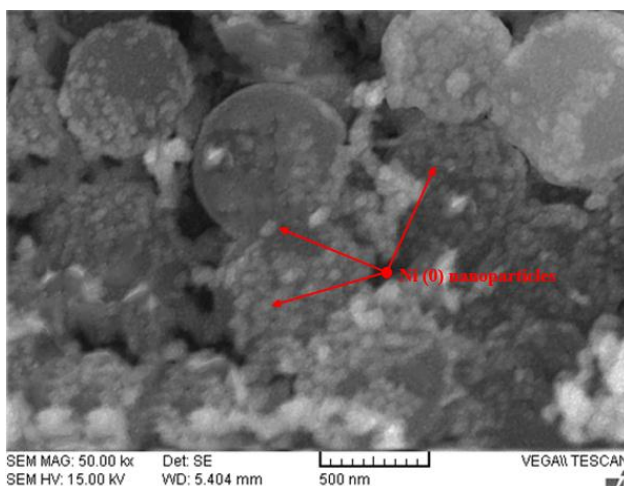


Fig 2. SEM image of Ni-nanoparticle carbon spheres (CS@ Ni) prepared by the microwave-assisted reduction.

These Ni-nanoparticle carbon spheres (CS@ Ni) were further investigated for the Heck coupling reaction. The effect of aryl derivative, base and reaction time were investigated and the results are summarized in Table 1.

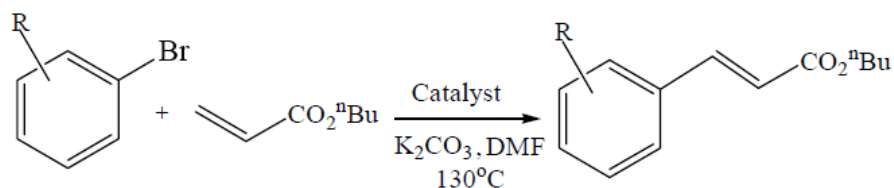


Table 1: Details of the Heck coupling of bromobenzene derivatives and n-butyl acrylate.

Entry	Ar-Br	Time (h)	Yield (%)	Base
1		6	30	K ₂ CO ₃
2		3	40	NaO ^t Bu
3		6	40	K ₂ CO ₃
4		6	32	K ₂ CO ₃

Conclusions:

We have reported herein deposition of Ni nanoparticles on the carbon spheres prepared by the Stober method. The Heck reactions of aryl bromides with n-butyl acrylate were carried out efficiently at short reaction times and moderate yields.

References:

- [1] U. Jeong; Y. L. Wang, M. Ibisate; Y. N; Xia. *Adv. Funct.Mater*, 2009, 19, 1907.
- [2] Y. Fang; D. Gu; Y. Zou; Z. X. Wu; F. Y. Li; R. C. Che; Y. H. Deng; B. Tu; D. Y. Zhao. *Angew. Chem*, 2010, 122, 8109
- [3] X. M. Sun; Y. D. Li. *Angew. Chem*, 2004, 116, 707
- [4] J. Liu; S. Z. Qiao; H. Liu; J. Chen; A. Orpe; D. Zhao; G. Q. Lu. *Angew. Chem*, 2011, 123, 0947, 0950.
- [5] Y. R. Dong; N. Nishiyama; Y. Egashira; K. Ueyama. *Ind. Eng. Chem. Res*, 2008, 47, 4712.

[6] J. Choma; D. Jamio; K. Augustynek; M. Marszewskib; M. Jaroniec. *Chem. Commun*, 2012, 48, 3972–3974.

[7] A. B. Chen;Y. F. Yu;Y. T. Li; Y. Y. Wang; Y. Q. Li; S. H. Li; K. C. Xia; *J. Mater. Sci*, 2016, 51, 4601.

[8] H. J. Lu;y. Li; L. Q. Zhang; H. N. Li;Z. X. Zhou; A. R. Liu; Y. J. Zhang; S. Q. Liu. *RSC Adv*, 2016, 6, 52126.

[9] H. Wru; G. Wu; Q. Wu; L. Wang. *Material Characterization*, 2014, 122.

Theory of Surface-Enhanced Raman Spectroscopy: Charge-Transfer Mechanism

Zahra Jamshidi

Chemistry and Chemical Engineering Research Center of Iran, P.O. Box: ۱۴۳۳۰-۱۸۷, Tehran, Iran

*Corresponding author: jamshidi@ccerci.ac.ir, na.jamshidi@gmail.com

Introduction

Surface-enhanced Raman scattering (SERS) is one of the most sensitive spectroscopic techniques for a wide range of applications such single molecule spectroscopy.^۱ The spectral sensitivity is due to the great enhancement effect, which mainly arises from two mechanisms; electromagnetic and chemical mechanisms. The chemical enhancement can be classified as the non-resonant chemical mechanism and a resonant charge-transfer (CT) chemical mechanism,^۲ that in the CT mechanism a new charge transfer state appears when molecule adsorb on the surface. Theoretical simulation of resonance Raman spectra has considerable challenge. The goal of this study is to shed light on the CT mechanism of SERS by considering the properties of CT excited states, and the crucial factor which affect this mechanism.

Method of calculation

The intensity of resonance Raman spectra is related to the calculation of the transition polarizability tensor. This tensor is calculated with several approaches which divided into two main groups, time-dependent and time-independent methods. In this work, we obtain polarizability tensor by using the excited state gradient method which is developed and implemented by Petrenko and Neese.^۳

$$\alpha_{i \rightarrow f} = \sum_n (M_{\cdot n})^* \int_0^\infty dt \left[\prod_k \frac{\Delta_k^n}{\sqrt{\gamma}} (1 - e^{-i\omega_k t}) \right] e^{-\sum_j s_j^n (1 - e^{-i\omega_j t}) + i(E_L - E_{\cdot n})t - \Gamma_n t} \quad (۱)$$

where n labels electronic states (index \cdot correspond to the ground state); $M_{\cdot n}$ is the transition dipole moment; ω_k is the vibrational frequency of k th mode; Δ_k^n is the dimensionless origin shift of the n th excited-state PES along the k th normal mode; $s_k^n = (\Delta_k^n)^2 / \gamma$; $E_{\cdot n}$ is the adiabatic minima separation energy between the ground and n th excited state; E_L is the incident photon energy; Γ_n is the homogeneous linewidth parameter. As can be found in Eq. ۱, for simulating resonance Raman spectra, several steps should be performed to determine: ω_k , $M_{\cdot n}$, $E_{\cdot n}$ and Δ_k^n . These steps are the optimization of structure, frequency calculation, excited state gradient calculation along normal modes upon optimized ground state geometry, and finally, dimensionless displacements should obtain to produce resonance Raman spectra.^۴

Result and discussion

The type of excitation and the effect of excited state vector gradient on the pattern of resonance Raman spectra have been obtained for pyridine molecule interacted with silver cluster and compared with experiment to verify the charge transfer mechanism (see Figure 1(I)). However, as in chemical mechanism of SERS, it was known that the chemical nature of surface and also electronic potential of interface play an important role. The effect of electric potential has been modelled by applying external electric field for selected CT transitions and the enhancement of ν_{1a} and ν_{9a} modes and decline in the intensity of ν_{6a} mode at negative electric field (which is directed toward cluster) have been observed (see Figure 1(II)). On the other hand, it is believed that alloying may serve as an illustrative evidence for studying the influence of the chemical nature. In order to study this effect, six and twenty atomic pure as well as bimetallic silver and gold clusters have been used as models. Figure 1(III) shows the effect of binding site and composition on the pattern of SERS-CT spectra.

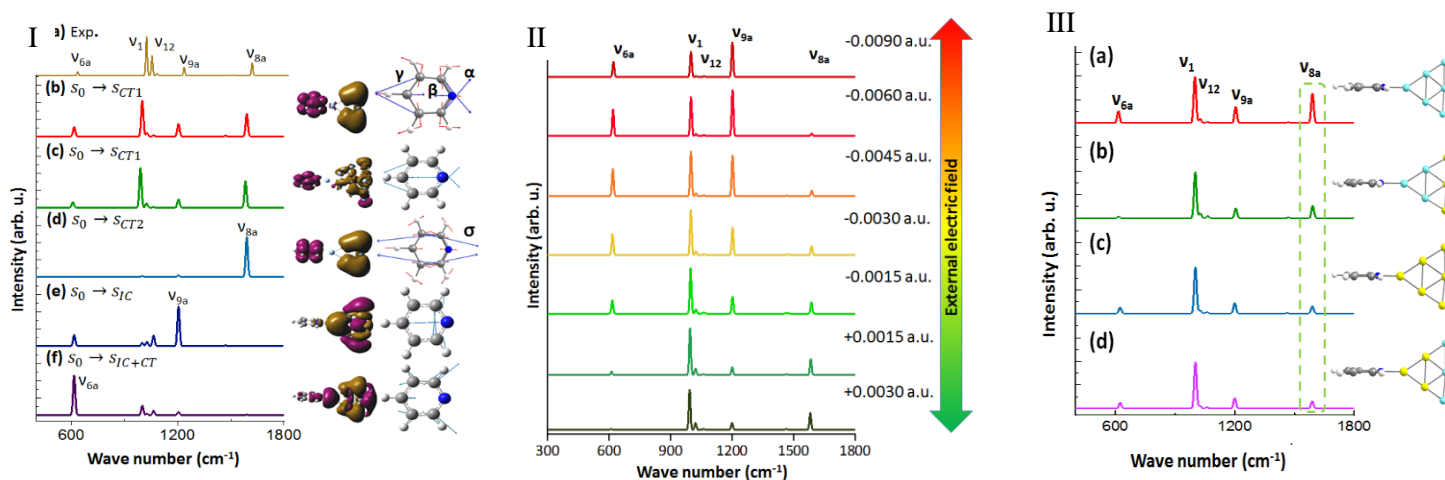


Figure 1. SERS spectra for I) different type of transitions. II) CT transitions by applying external electric field for Py-Ag₇. III) CT transitions of different surface a) Py-Ag₇, b) Py-Ag₇Au₇, c) Py-Au₇ and d) Py-Au₇Ag₇.

Conclusion

This study demonstrated that the excited state vector gradient can be used as a distinguishing factor to explain the SERS-CT selection rules. These results match well with the experimental studies, and also explained the effect of electrode potentials and nature of surface on the pattern of spectra as an experimental evidence of CT mechanism. This knowledge help us to develop Raman applications and design highly enhancing devise.

[1] P. L. Stiles, J. A. Dieringer, N. C. Shah and R. P. Van Duyne, *Annu. Rev. Anal. Chem.*, 2008, 1, 101.

[2] M. G. Albrecht and J. A. Creighton, *J. Am. Chem. Soc.*, 1997, 99, 5215.

- [^۳] (a) T. Petrenko and F. Neese, *J. Chem. Phys.*, ۲۰۱۲, ۱۳۷, ۲۳۴۱۰۷. (b) T. Petrenko and F. Neese, *J. Chem. Phys.*, ۲۰۰۷, ۱۲۷, ۱۶۴۳۱۹.
- [^۴] M. Mohammadpour and Z. Jamshidi, *J. Chem. Phys.*, ۲۰۱۶, ۱۴۴, ۱۹۴۳۰۲.

Variation of the electronic property of zigzag boron nitride nanotubes by Al doping, A DFT study

Zahra Tavangar^{1,*}, Hadi Basharnavaz²

¹Department of Physical Chemistry, Faculty of Chemistry, University of Kashan, Iran.

²Institute of Nano Science and Nano Technology, University of Kashan, Kashan, Iran.

(z.tavangari@kashanu.ac.ir)

Introduction:

Boron nitride nanotubes (BNNTs) are a binary compounds with equal numbers of boron and nitrogen atoms, which are isoelectronic with carbon nanotubes [1,2]. BNNTs have been paid much attention by the scientific communities because of their important and unique properties, ideal for electronic and structural applications. Several attempts have been done to reduce the band gap energy by proposing the doping of BNNTs particularly single doping. For example, energy gap of the system with carbon doping is reduced to about 1 eV [3-5]. All mentioned calculations about BNNTs were performed using the density functional theory (DFT) in the gas phase.

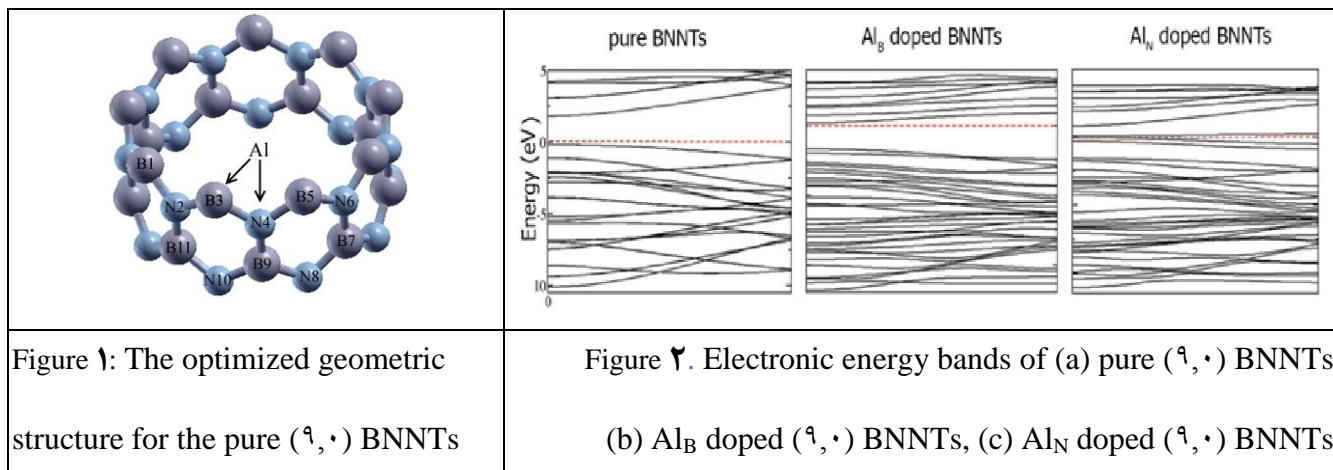
Computational method:

Our calculations have been done with PWSCF from Quantum Espresso distribution [6]. The Brillouin-zone integration was performed with a Monkhorst–Pack k-points mesh set of $1 \times 1 \times 1$ which represents the convergence of our systems, along the U–Z direction. An 10 \AA vacuum layer was considered to avoid interaction between the nanotubes. A Kinetic energy cut offs for the wave function was determined using an appropriate convergence test and set to 10 Ry for all structures.

Results and Discussion:

The structural and electronic properties of pure and Al-doped BNNTs have been examined using DFT calculations. The results of calculations of band structure and density of states show that Al-doped BNNT exhibited better semiconductor properties in comparison with pure BNNTs. Doping BNNTs with Al reduced energy gap and consequently improved the conductivity of BNNTs. Our results show that by doping of the B atom by Al atom the energy gap of zigzag BNNTs has small changed while the energy gap significantly influenced by Al-doping instead of N atom. The results do not show specific trend between diameter of nanotube and band gap energy in both pure and AIB BNNTs. Thus, these forms of nanotubes can be suitably used in sensors, biosensors, motors, drivers, cell batteries and energy storage of lithium and hydrogen. Also, band gap and fermi energy level rise with the increasing

of the diameter of the BNNTs from (2, 2) to (10, 10). This behavior revealed that semiconducting properties of BNNTs are reduced by increasing their diameter.



Conclusion:

The results of calculations of density of states (DOS) and band structure (band) showed that the band gap between the valence and conduction level increases as a result of the enhancement of tube diameter of BNNTs. Finally, the results showed that the electronic properties of the pristine BNNTs can be improved by doping Al atom in the zigzag configuration of tubes.

References:

- [1] E. Zahedi, A. Seif, Effect of tube radius on the electronic and magnetic properties of finite boron nitride zigzag nanotubes using DFT, *Physica E: Low-dimensional Systems and Nanostructures*, 2011, 44, 179-180.
- [2] Y. Song, Y. Sun, D. Hoon Shin, K. Nam Yun, Y.-H. Song, W.I. Milne, C. Jin Lee, Excellent oxidation endurance of boron nitride nanotube field electron emitters, *Applied Physics Letters*, 2014, 104, 163102.
- [3] Y. Chen, J. Zou, S.J. Campbell, G. Le Caer, Boron nitride nanotubes: Pronounced resistance to oxidation, *Applied Physics Letters*, 2004, 84, 2430-2432.
- [4] D. Golberg, Y. Bando, C.C. Tang, C.Y. Zhi, Boron Nitride Nanotubes, *Advanced Materials*, 2007, 19, 2413-2432.
- [5] J. Li, G. Zhou, Y. Chen, B.-L. Gu, W. Duan, Magnetism of C Adatoms on BN Nanostructures: Implications for Functional Nanodevices, *Journal of the American Chemical Society*, 2009, 131, 1796-1801.

Application of response surface methodology for modeling and optimizing of photocatalytic properties of S/Fe/TiO₂ nanoparticle prepared

Masood Hamadani^{1,*}, Maryam Ostadi²

¹Institute of Nanosciences and Nanotechnology, University of Kashan, Kashan, IRAN

²Department of Physical Chemistry, Faculty of Chemistry, University of Kashan, Kashan, IRAN

(hamadani@kashanu.ac.ir)

Introduction:

One of the probable methods for eliminating organic Pollutants from sewage is utilizing photocatalytic oxidation by semiconductors. Among utilized semiconductors, Titanium dioxide is a perfect photocatalytic because of high sensitivity, Non-toxicity, availability, High oxidation power and long-term stability [1-3]. The high band gap of TiO₂ limits Absorption wavelength to less than 388 nm and needs a UV source for practical application. It comprises a small part of the Sunlight (3%-5%). We tried to build a new photocatalytic system with increased photocatalytic activity under the UV and visible irradiation in comparison with TiO₂ so as to improve efficiency in the utilization of solar energy.

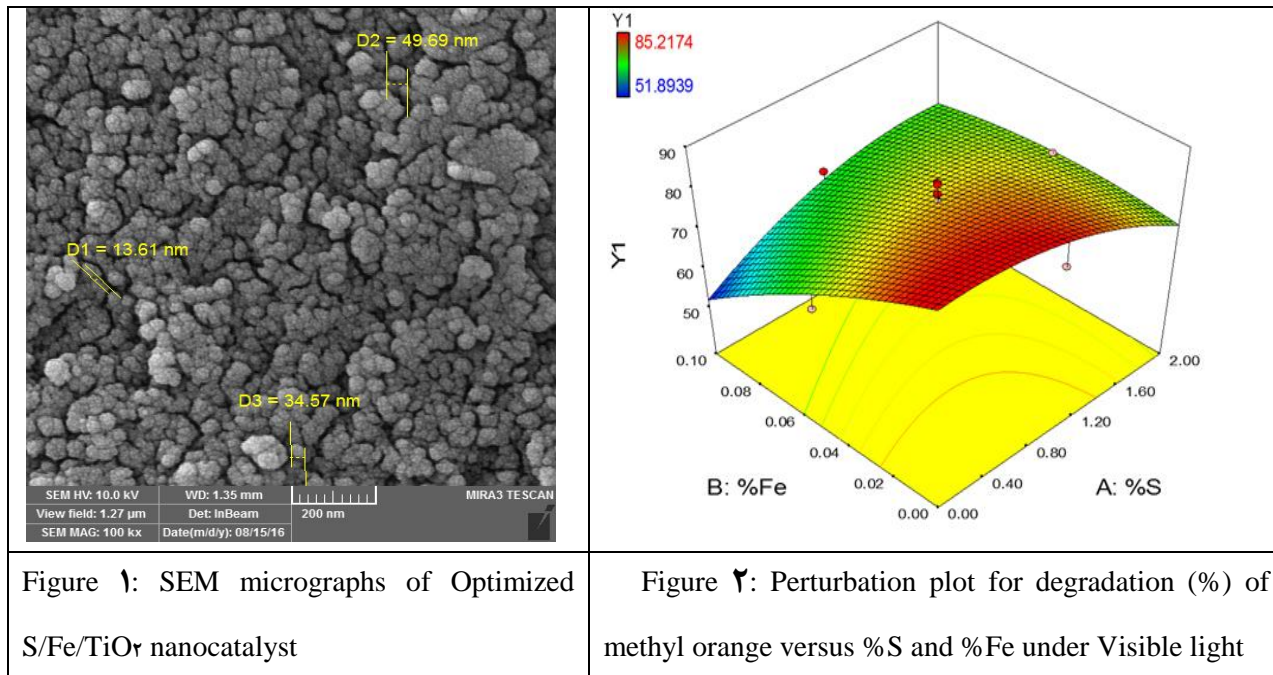
Experimentals:

TTIP was used as the TiO₂ source and Fe(NO₃)₃·9H₂O and S-Benzylthiuronium chloride salt were used as Fe and S dopants, respectively. The utilized synthetic method for all steps is the Sol-gel method. For investigation of photocatalyst performance, methyl orange was used as a combination of wastewater pollutant under UV and visible light irradiation. For analysis, we used XRD, DRS, SEM-EDX and FT-IR methods. Modeling and optimization of the photocatalytic performance of S/Fe/TiO₂ nanoparticles is done by using the RSM method [4].

Results and Discussion:

Firstly, we doped TiO₂ by S-Benzylthiuronium chloride and prepared the x%S/TiO₂ nanoparticles. The results showed that 1%S/TiO₂ catalyst with 92.36% degradation after 180 minutes in visible irradiation and 2%S/TiO₂ catalyst with 97.60% degradation after 60 minutes in UV irradiation were the best results. In next section, codoped TiO₂ with varying amounts of iron plus the optimal amount of sulfur (in visible irradiation) were synthesized. 1%S-0.1%Fe/TiO₂ catalyst with 98.38% degradation after 180 minutes in visible irradiation and with 98.44% degradation after 60 minutes in UV irradiation had the best results. The central composite design, which is a widely used form of RSM was employed for the optimization of photocatalytic properties S/Fe/TiO₂ nanoparticle under visible and UV light irradiation. In order to evaluate the influence of operating parameters on the photocatalytic properties, three influential factors were

chosen: weight percent of sulfur (x_1), weight percent of Iron (x_2) and time aging (x_3). Figure 1 shows SEM micrographs of Optimized S/Fe/TiO₂ nanocatalyst and Figure 2 shows the Perturbation plot for degradation (%) of methyl orange versus %S and %Fe under Visible light



Conclusion:

Modeling and optimization of the photocatalytic performance of S/Fe/TiO₂ nanoparticles is done using the RSM method. Suggested optimized doping through software calculations for making the catalyst is 0.41% S-0.02% Fe/TiO₂-45h time aging in visible irradiation and 0.41% S-0.02% Fe/TiO₂-29h time aging in UV irradiation. Studying their photocatalytic activity showed 99.06% degradation after 180 minutes for catalyst optimal visible and 99.00% degradation after 60 minutes for catalyst optimal UV.

References:

- [1] K. Rajeshwar, M. Osugi, W. Chanmanee, C. Chenthamarakshan, M. V. B. Zanoni, P. Kajitvichyanukul, R. Krishnan-Ayer, Journal of photochemistry and photobiology C: photochemistry reviews 2008, 9, 171-192.
- [2] D. Spasiano, R. Marotta, S. Malato, P. Fernandez-Ibanez, I. Di Somma, Applied Catalysis B: Environmental 2010, 100, 90-123.
- [3] J. Carneiro, S. Azevedo, F. Fernandes, E. Freitas, M. Pereira, C. Tavares, S. Lanceros-Méndez, V. Teixeira, Journal of materials science 2014, 49, 7476-7488.
- [4] A. I. Khuri, Response surface methodology and related topics, World scientific, 2006.

Mild Synthesis of Novel Zinc Metal Organic Polymer and its Hybrid with Activated Carbon: Application for Bromocresol Purple Removal and Antibacterial Agent

Tahere Taghipour^a, Gholamreza Karimipour^{b*}, Mehrorang Ghaedi^{b*}

^{a, b, c} Department of Chemistry, Yasouj University, Yasouj, ۷۵۹۱۸ - ۷۴۸۳۱, Iran

E-mail: m_ghaedi@yahoo.com

Introduction:

Metal-organic polymers (MOPs) are a subclass of coordination polymers by linkage of inorganic transition metal clusters and organic ligands. MOPs have shown great potential for the removal of dyes and other toxic chemicals [۱]. Moreover, we can improve MOPs by intermixing porous activated carbon (AC) with MOPs that form novel composites with advanced novel physical and chemical properties compared to their pristine counterparts.

On the other hand, many researchers have focused their studies on the synthesis and characterization of new metal based antibacterial agents in order to design complexes with better biological activity and lower toxicity [۲,۳].

Experimentals:

۲,۴-phenylenedioxy diacetic acid and Zinc nitrate tetrahydrate were dissolved in deionized water, individually. The zinc salt solution was then added to the ۲,۴-phenylenedioxy diacetic acid solution with stirring at room temperature. The solution was filtered and the precipitate was washed with cold water. The MOP was loaded onto activated carbon (AC). AC and MOP were dispersed in deionized water under sonication. The mixture was then stirred and the MOP-AC was separated by centrifugation and dried at ۵۰ °C.

Results and Discussion:

The morphology of the resulting crystals of MOP and MOP-AC are shown in the SEM micrograph. The sizes of MOP particles were about ۱۰۰ nm (Fig. ۱a, b).

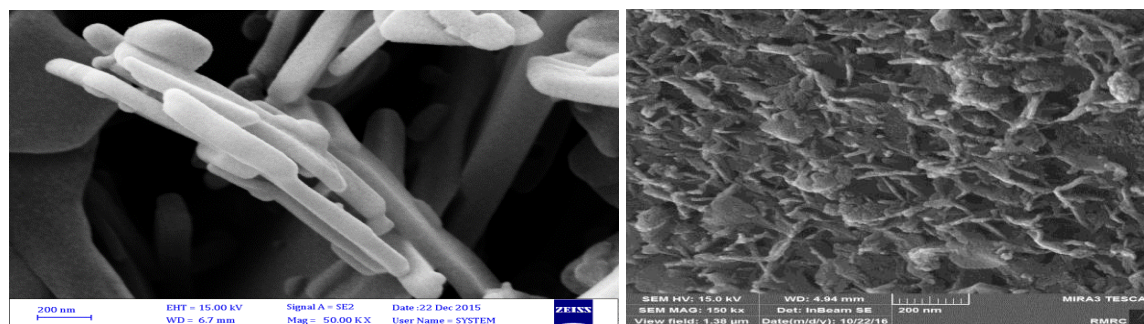


Fig. 1 SEM image of MOP (a) and MOP-AC (b).

Optimum values obtained for all factors, corresponded desirability and R% value for BCP are shown in Table 1.

Table 1. Optimum conditions.

Factors	Unit	Optimum value
X_1 : BCP concentration	mg L ⁻¹	10.22
X_2 : sonication time	min	2.41
X_3 : adsorbent dosage	g	0.09
Desirability value		1.0
R% BCP		98.7942

Conclusion:

In conclusion, we have successfully synthesized a nanosized zinc (II) coordination polymer. The results showed that MOP-AC had good activity during dye removal and central composite design method. Also, on the results obtained, it can be concluded that MOP acts as an effective antibacterial agent against *Proteus vulgaris* bacteria.

References

- [1] A. Abbasi; M. Gharib; M. Najafi; J. Janczak. *Journal of Solid State Chemistry*, 2016, 230, 12-17.
- [2] M. Barsukova-Stuckart; L.F. Piedra-Garza; B. Gautam; G. Alfaro-Espinoza; N.V. Izarova; A. Banerjee; B.S. Bassil; M.S. Ullrich; H.J. Breunig; C. Silvestru; U. Kortz. *Inorg Chem*, 2012, 51, 12010-12022.
- [3] K. Giannousi; G. Sarafidis; S. Mourdikoudis; A. Pantazaki; C. Dendrinou-Samara. *Inorg Chem*, 2014, 53, 9607-9616.

Efficient Oxygen Evolution Reaction on Ni Loaded Hydroxyapatite- Carbon Nanotubes Composite

Mohsen Sorouri^a, AfsanehSafavi^{a,*}, AbdolkarimAbbaspour^a

^aDepartment of Chemistry, College of Sciences, Shiraz University, Shiraz 71454, Iran

safavi@chem.susc.ac.ir

Introduction: The oxygen evolution reaction (OER) always proceeds on oxidized surfaces [1]. Ni and its oxides were discovered to exhibit electrocatalytic activity towards OER in alkaline solution in the early last century [1]. Hydroxyapatite (HA) is the most stable calcium phosphate salt and it could act as a super-lattice to immobilize catalytic particles and provides an alternative chemical environment as a catalyst support [2]. To enhance the electrical conductivity of HA to be applied in an electrocatalyst structure, the composites of HA with conductive phases especially with carbon nanotubes (CNTs) could be suggested [3]. Here, the Ni substituted HA-MWCNT composite (Ni/HA-MWCNTs) will be examined for OER in alkaline media.

Experimental: The HA-MWCNT composite mainly was prepared via the solventless solid state metathesis procedure using the activated MWCNTs [3]. In a particular synthesis of 100 mg of 40% HA-MWCNTs composite, 60 mg of the activated MWCNTs was mixed with 23 mg of $\text{CaCl}_2 \cdot 9\text{H}_2\text{O}$ and 46.3 mg of $\text{Na}_3\text{PO}_4 \cdot 12\text{H}_2\text{O}$. The materials were finely mixed with a pestle and mortar, and then delivered to a quartz tube situated in a microwave oven. After the microwave irradiation (power of 900W and time of 3 min), the product was washed three times with double distilled water and then dried at 100 °C overnight. The loading of Ni was attained by soaking 10 mg of HA-MWCNTs substrate into the 5 ml of 50 mM solution of $\text{NiCl}_2 \cdot 6\text{H}_2\text{O}$, for 48 h.

For testing the catalysts, the clear GCE surface was modified via the casting of 2 μl of 4 mg ml^{-1} of the suspension of Ni/HA-MWCNTs in water. After drying in air, 2 μl of 0.5% of Nafion solution was casted on the electrode and left to dry.

Results and Discussion: The TEM image of Ni/HA-MWCNTs is represented in Figure 1A. The mixed layer of Ni substituted HA and MWCNTs could be seen. In addition, the XRD patterns of HA-MWCNTs and Ni/HA-MWCNTs are depicted in Figure 1B. According to the similar XRD patterns of Ni/HA-MWCNTs and non-substituted composite, the apatitic structure has been preserved during the Ni loading step. However, the sample could be regarded as the calcium nickel phosphate mineral with the general formula of $\text{Ca}_{19}\text{Ni}_2(\text{PO}_4)_{14}$ and JCPDS # 00-049-1224. The featured peaks of the rhombohedral lattice were detectable in the spectrum a, at 2 θ degrees of 13.75, 22.00, 28.05, 31.30, 34.68, 53.48°. However, some main diffraction peaks of $\text{Ni}(\text{OH})_2$ structure are also detectable. These peaks are positioned at 11.35°, 22.74°, 33.46°, 34.41°, 38.77° and 59.99° and are in good accordance with the pattern of the JCPDS# 038-0715.

Figure 2 represents the OER voltammograms of HA-MWCNTs and Ni/HA-MWCNTs in alkaline electrolyte. The non-substituted HA-MWCNTs composite is not active toward the OER (voltammogram a). However, the OER behavior of electrodeposited Ni/MWCNTs as a rival catalyst, is depicted in Figure 2 (voltammogram b). The higher OER current density as well as about 40 mV of onset potential shift were observed for Ni/HA-MWCNTs in comparison to Ni/MWCNTs(ED) catalyst. The higher performance of Ni/HA-MWCNTs catalyst toward OER could be also attributed to incorporation of Ni into the HA matrix. However, due to the flexibility

of HA substrate, the conversion of nickel phosphate species into oxides and hydroxides is feasible during the potential alterations.

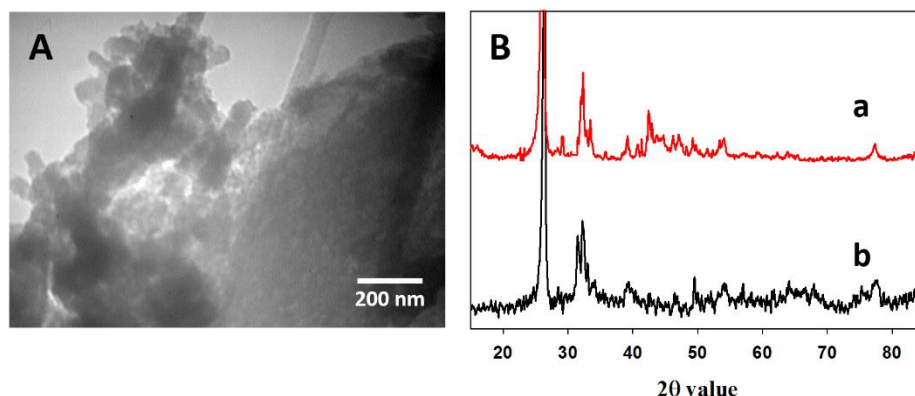


Figure 1A: TEM micrograph of Ni/HA-MWCNTs composite. B: XRD patterns of a) HA-MWCNTs composite and b) Ni/HA-MWCNTs.

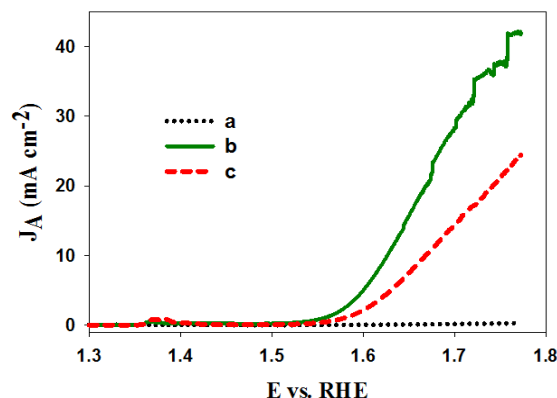


Figure 2 Comparison of OER activity of a) HA-MWCNTs, b) Ni/HA-MWCNTs, c) Ni/MWCNTs(ED). Conditions: 1 M of O₂ saturated KOH, rotation rate of 2500 rpm and scan rate of 1 mV s⁻¹.

Conclusion: HA/MWCNT could be applied as a proper substrate for immobilization of Ni species as an OER active catalyst. The high activity of Ni/HA-MWCNTs toward OER, is explained by the flexibility of HA moiety for immobilizing the reactive phases of mixed oxides and/or oxide hydroxides of constituted Ni metal. The 40 mV shift of onset potential toward the more negative values has also been achieved over Ni/HA-MWCNTs compared to HA free Ni/MWCNTs(ED).

References

- [1] M. Gong, H. Dai, *Nano Research*, **2015**, 8, 23-39.
- [2] J. H. Kim; S. H. Kim; H. K. Kim; T. Akaike; S. C. Kim, *Journal of Biomedical Materials Research*, **2002**, 62, 600–612.
- [3] A. Safavi; M. Sorouri, *Materials Letters*, **2013**, 91, 287–290.

Hypochlorite Triggered De-alloying of AuAg@Carbon Nanodots: Towards Fabrication of a Colorimetric Assay using the Tunable Plasmonic Property of Bimetallic Alloy Nanoparticles

Zahra Mohammadpour, Seyyed Hossein Abdollahi, Afsaneh Safavi*

Department of Chemistry, Faculty of Sciences, Shiraz University, Shiraz, ۷۱۹۴۶۸۴۷۹۵, Iran.

*E-mail: safavi@susc.ac.ir;

Introduction: Nanoscale bimetallic Au-Ag with distinctive optical, electrical and chemical properties offers superior advantages in catalysis, antimicrobial properties, and surface-enhanced Raman spectroscopy (SERS) sensing compared to their monometallic counterparts.^{۱-۴} In this report, Au-Ag alloy and carbon nanodots (C-dots) were integrated into a single platform resulted in a new sensing assay for hypochlorite. Hypochlorite is an extensively used disinfectant for water treatment. Accumulation of this ion in environmental samples is associated with neuron degeneration, cancer, arthritis and inflammatory diseases.^{۴-۷} This assay is fast, selective, sensitive, simple and robust for environmental monitoring of hypochlorite in bleach and tap water samples.

Methods/Experimentals: Sodium hypochlorite (۶-۱۴%) was purchased from Merck. The UV-Vis absorption spectra were measured using a Shimadzu spectrophotometer. For measurement of ClO^- , the as-synthesized bimetallic nanoparticles solution was added drop-wise to the electrolyte (۷۰ mM sodium nitrate, ۲ mM sodium carbonate). ۱ mL of colloidal nanoparticles solution was added to the glass vials followed by the addition of ClO^- standard solution with different concentrations (۰-۶۰ μM). After ۱۰ min incubation at room temperature, the absorption spectra were collected.

Results and Discussion: A chemical co-reduction process proceeded for production of AuAg@C-dots. TEM image and the particle size histogram of AuAg@C-dots (**Fig. ۱A**) showed that the average particle size was ۵.۶ nm (۱۵۰ particles), which was in close agreement with the average size measured by dynamic light scattering (DLS) (۶-۷ nm). Large aggregated particles after treatment with hypochlorite were observed in the sample (**Fig. ۱B**) in support of the particle agglomeration confirmed by DLS. Under the optimized experimental conditions, the spectral change of AuAg@C-dots upon exposure to different concentrations of hypochlorite (**Fig. ۲**) followed a linear trend over the hypochlorite concentration range of ۱.۷ to ۱۹ μM . Analysis of spiked real samples revealed recovery percentage values over the range of ۹۵.۶-۱۰۹.۴% suggesting the potential applicability of the present assay in environmental monitoring. Particularly, we successfully measured the ClO^- concentration in the bleach. The concentration determined using the present system (۶.۲۵ μM) was in close agreement with the value measured spectrophotometrically (۶.۶۱ μM).

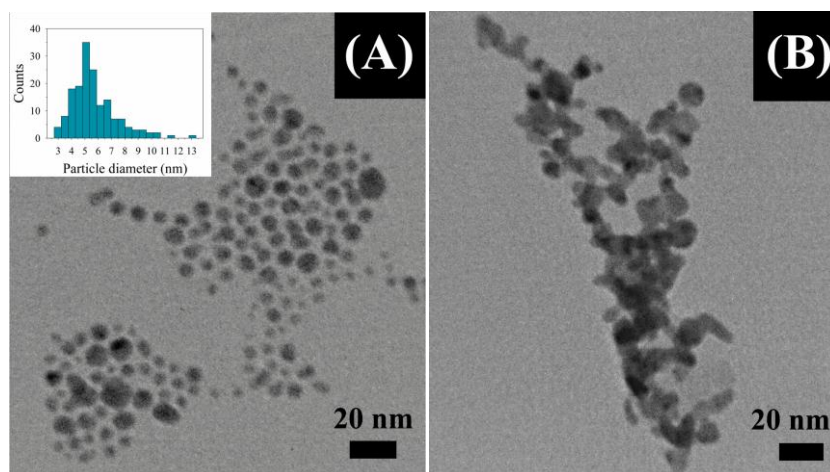


Fig. 1 TEM image of AuAg@C-dots (A) before and (B) after hypochlorite addition.

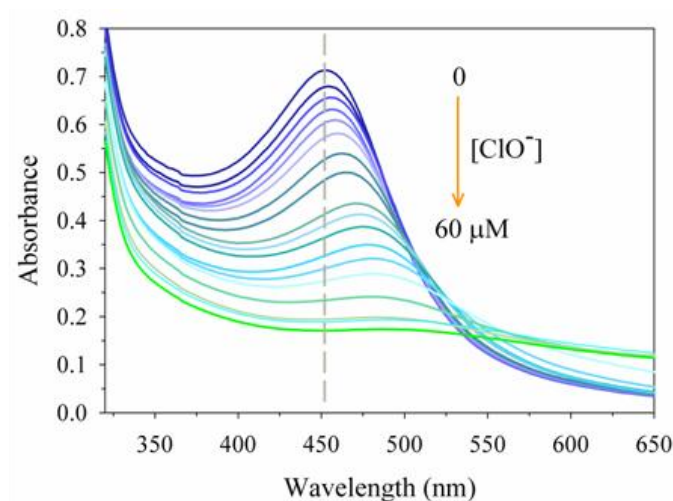


Fig. 2 UV-Vis absorption decay and SPR shift of AuAg@C-dots following the increasing amount of hypochlorite over the concentration range of 0 to 60 μM .

References

- (1) Cortie, M. B.; McDonagh, A. M. *Chem. Rev.* 2011, 111, 3713-3730.
- (2) Liu, X.; Wang, D.; Li, Y. *Nano Today* 2012, 7, 448-466.
- (3) Banerjee, M.; Sharma, S.; Chattopadhyay, A.; Ghosh, S. S. *Nanoscale* 2011, 3, 5120-5125.
- (4) Wu, S. M.; Pizzo, S. V. *Arch. Biochem. Biophys.* 2001, 391, 119-126.
- (5) Chen, J.; Mo, Y.; Schlueter, C. F.; Hoyle, G. W. *Toxicol. Appl. Pharmacol.* 2013, 272, 408-413.
- (6) Benhar, M.; Engelberg, D.; Levitzki, A. *EMBO reports* 2002, 3, 420-425.
- (7) Pattison, D. I.; Davies, M. J. *Chem. Res. Toxicol.* 2001, 14, 1403-1464.

High-Yield Synthesis and Characterization of Extremely Thin Gold Nanosheets in Natural Deep Eutectic Solvents

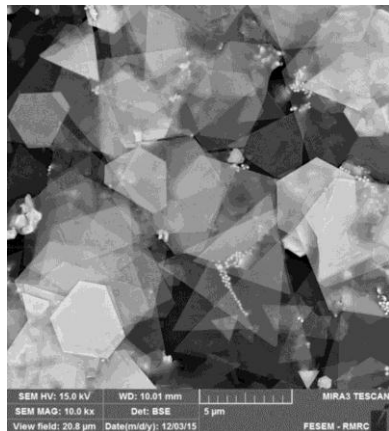
Afsaneh Safavi ^{a*}, Amin Reza Zolghadr ^a, Mahsa Shekarnoush ^a, Maral Ajamian ^a

Email address: safavi@susc.ac.ir

Introduction: Introduction: Gold nanosheets are nanostructures of gold which have the size over microscopic area and thickness in the range of a few to 100 nanometers [1]. Gold nanosheets have made significant advances in hyperthermia of cancer tumors [2], gas sensors [3] and catalysis [4]. Numerous papers were published on synthesis of gold nanosheets but the main disadvantage of most of the suggested procedures is applying organic toxic or unsafe materials as solvent, reducing agent, surfactant and also stabilizers.

Methods: The NADES that was used was made up of the 1:1:1 molar ratios of glucose, fructose, sucrose, and water and synthesized as described previously [5]. ~ 1 g of the synthesized NADES was diluted to 10 mL with distilled water (10% w/v) and stirred for 10 min. After obtaining a clear, colorless and homogenous solution, 100 mg GA was added to the above solution with continuous stirring under ambient conditions for 10 min and this solution was used to synthesize gold nanosheets. (Solution A). After that 400 µL of HAuCl₄ solution (0.005 M) was injected to the solution A with continuous stirring. The appearance of golden suspension after about 2 h indicated the presence of gold nanosheets.

Results and discussion: The field emission scanning electron microscopy (FESEM) images show that the as prepared products are mainly composed of gold nanosheets with regular shapes (hexagonal and triangular) together with a few semi-spherical particles.



The height profile results from atomic force microscopy (AFM) image clearly show that the average thickness of gold nanosheets was 1.0 nm. The XRD pattern analysis confirmed the presence for gold nanosheets as the main product. The 2θ values of peaks in the XRD pattern are analogues to the corresponding standard values of gold. A strong diffraction in XRD pattern stems from gold {111} planes and weak diffractions in XRD patterns result from the other planes. The zeta potential distribution showed a sharp peak in -27.0 mV which indicates that the surface charges of gold nanosheets are mostly negative. Both NADES and GA in the solution play important role in formation and morphology of Au nanosheets. In addition, the concentrations of HAuCl₄, the reaction time and temperature are also crucial for the morphology and size of the final product.

Conclusion: A simple, green and cost effective method was suggested for synthesis of ultrathin and large gold nanosheets with a vast variety of triangular and hexagonal shapes. The FESEM image analysis of gold nanosheets suggests that the size and morphology of gold nanosheets are strongly dependent on experimental parameters such as the amounts of NADES, GA, HAuCl₄, temperature and time.

References:

- [1] X. Fan, Z. R. Guo, J. M. Hong, Y. Zhang, J. N. Zhang and N. Gu. *Size-controlled growth of colloidal gold nanoplates and their high-purity acquisition*, Nanotechnology, 2010, 21, 105602-105609.
- [2] M. Tohidi, F. A. Mahyari and A. Safavi. *A seed-less method for synthesis of ultra-thin gold nanosheets by using a deep eutectic solvent and gum arabic and their electrocatalytic application*, RSC Adv., 2015, 5, 32744-32754.
- [3] S. S. Shankar, A. Rai, B. Ankamwar, A. Singh, A. Ahmad and M. Sastry. *Biological synthesis of triangular gold nano prisms*, Nat. Mater., 2004, 3, 482-488.
- [4] H. I. Karunadasa, E. Montalvo, Y. Sun, M. Majda, J. R. Long and C. J. Chang. *A molecular mos edge site mimic for catalytic hydrogen generation*, Science, 2012, 335, 798-802.
- [5] Y. Dai, J. van Spronsen, G.-J. Witkamp, R. Verpoorte and Y. H. Choi. *Natural deep eutectic solvents as new potential media for green technology*, Anal. Chim. Acta, 2013, 777, 71-78.

Simultaneous Determination of Dopamine and Serotonin at Carbon Molecular Wire Electrode

Maryam Mohammadzadeh, Afsaneh Safavi*

Department of Chemistry, College of Sciences, Shiraz University, Shiraz, ۷۱۹۴۶۸۴۷۹۰, Iran.

Corresponding author: safavi@susc.ac.ir

Introduction: Dopamine (DA) is an important neuron transmitter existed in brain [۱]. Serotonin (۵-HT) is an ubiquitous compound in the animal and plants [۲]. It has a basic role in aggression, body temperature, sleep and etc [۳]. Many reports have shown the coexistence of dopamine and serotonin in biological systems and that they affect each other in their respective activities [۴, ۵].

In this work, a recently constructed carbon molecular wire electrode (CMWE)[۶] has been used for the simultaneous determination of ۵-HT and DA without any additional modification such as addition of electron transfer mediator or specific reagent.

Methods/ Experimental: CMWE was prepared by hand mixing diphenyl acetylene as molecular wire, graphite powder and CNT with a mass ratio of ۳۰/۳۰/۴۰, respectively. The resulting paste was heated on a heater at ۷۰ °C. The paste was packed into the cavity of a Teflon tube and warmed up to ۷۰ °C again.

Voltammetric measurements were performed using an electrochemical system equipped with GPES software and a three electrode electrochemical cell: an Ag/AgCl/KCl as reference and a platinum wire as a counter electrode.

Results and Discussion: Cyclic voltammograms of DA and ۵-HT in ۰.۱ M PBS (pH ۷.۰) at CMWE are shown in Fig. ۱. The peak separation is about ۰.۱۷ V and it is enough for simultaneous determination of DA and ۵-HT at CMWE (Fig. ۱d).

Differential pulse voltammetry was used for the simultaneous determination of DA and ۵-HT. In here, the concentration of either DA or ۵-HT was kept constant and that of the other was changed. As shown in Fig. A, the oxidation peak current of DA increased with increasing its concentration and without an appreciable change of the oxidation peak current due to ۵-HT. These measurements are repeated for ۵-HT and the results are shown in Fig. B.

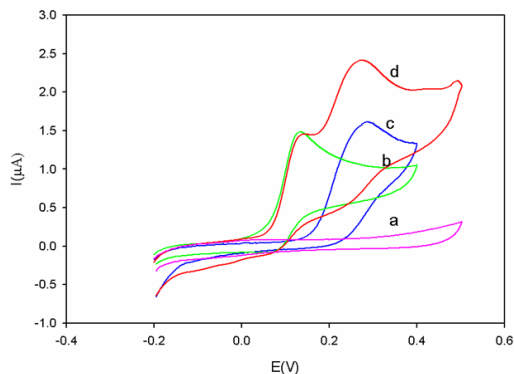


Fig. 1 Cyclic voltammograms of a) PBS (pH 7.0) as electrolyte solution, b) 100 μM DA c) 100 μM 5-HT and d) a mixture containing 100 μM DA and 100 μM 5-HT. Scan rate 50 mVs⁻¹

A good linear relationship was obtained between the oxidation peak currents and the concentrations of DA and 5-HT. For oxidation peaks of DA, the linear range was 5.0 - 500 μM with a correlation coefficient of 0.9976. For 5-HT, two linear ranges were obtained; 5.0-100 μM and 100-500 μM with correlation coefficients of 0.9988 and 0.9990, respectively. The theoretical detection limits were obtained as 1.02 and 1.78 μM for DA and 5-HT, respectively at S/N ratio of 3. The electrode was applied for the determination of DA and 5-HT in human serum.

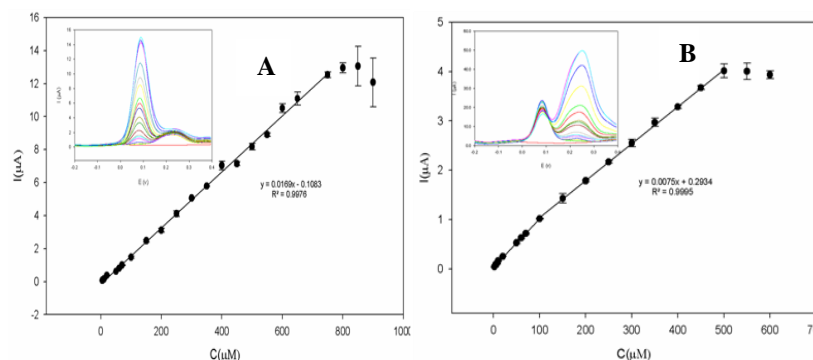


Fig. 2 Calibration curves for (A) oxidation peaks of DA in the presence of 100 μM 5-HT and (B) 5-HT in the presence of 100 μM DA. The error bars indicate mean \pm SD (n=5). Insets are Differential pulse voltammograms of (A) DA in the presence of 100 μM 5-HT in PBS (pH 7.0) (DA concentration: 0.1-100 μM), and (B) 5-HT in the presence of 100

Conclusion: The applicability of a newly constructed carbon molecular wire electrode (CMWE) was investigated for the determination of biological compounds. As reported above, suitable results were obtained for simultaneous determination of dopamine and serotonin. Moreover, this sensor exhibited attractive features such as good peak separation, high sensitivity, low detection limit, resistance towards electrode fouling, excellent repeatability and reproducibility. The electrode was successfully used in analysis of the human serum.

References

- [1] A.A. Ensafi; M. Taei; T. Khayamian, *Journal of Electroanalytical Chemistry*, 2009, 733, 212-220.
- [2] A. Pletscher, *Essays in Neurochemistry and Neuropharmacology*, 1978, 3, 49.
- [3] L. Descarries; M.A. Audet; G. Doucet; S. Garcia; S. Oleskevich; P. Séguéla. J.J., *Annals of the New York Academy of Sciences*, 1990, 700, 81-92.
- [4] S. Shahrokhian; A. Mahdavi-Shakib; M. Ghalkhani; R.s. Saberi, *Electroanalysis*, 2012, 24, 420-432.
- [5] W. Zhang; Y. Chai; R. Yuan; S. Chen; J. Han; D. Yuan, *Analytica Chimica Acta*, 2012, 707, 7-12.

[۶] A. Safavi; M. Mohammadzadeh; M. Sorouri, *Microchemical Journal*, ۲۰۱۶.

Synthesis of highly stable and biocompatible gold nanoparticles: Application as a new X-ray contrast agent

Maral Ajamian^a, Pooya Iranpour^{b,*}, Abdolkarim Abbaspour^a, Afsaneh Safavi^{a,*}

^aDepartment of Chemistry, College of Sciences, Shiraz University, Shiraz, 71345, Iran.

^bMedical Imaging Research Center, Shiraz University of Medical Sciences, Shiraz, Iran.

E-mail: pooya_iranpour@yahoo.com; safavi@chem.susc.ac.ir

1. Introduction

X-ray-computed tomography (CT) is an imaging technique which is applied for variety of research and clinical diagnostics. Consequently, X-ray attenuation elements such as barium, iodine and gold are mostly used for clinical tissue imaging [1-3]. Iodine molecules as contrast agents are mostly used for CT imaging due to high X-ray absorption coefficient of iodine, but they have rapid pharmacokinetics and high viscosity for injection to body. Because of these shortcomings, a new class of contrast agent such as gold nanoparticles has been introduced. For in vivo biomedical applications, the use of stable and biocompatible gold nanoparticles is inevitable. For this purpose, nontoxic and green materials such as Gum Arabic (GA), a plant extract, and glucosammonium formate ionic liquid have been introduced for stabilizing and reducing of gold nanoparticles, respectively.

2. Experimental

2.1 Synthesis of gold nanoparticles

GA solution was prepared by mixing 10 mg of GA in 10 ml of deionized water. Different amounts of HAuCl₄ · 3H₂O (0.1 mM) were added to this solution, then the prepared solution was placed under mild heating at 60 °C. 10 mg of the ionic liquid was added to the stirring solution and the stirring was continued for 10 to 20 min depending on the concentration of HAuCl₄ · 3H₂O (100-1000 μM). During the synthesis process, the color of solution changes from light yellow to red color which indicates the formation of gold nanoparticles. Furthermore, to evaluate the stability of the synthesized gold nanoparticles in physiological media, 1.0 ml of the prepared gold nanoparticles solution was treated with 1.0 mL of 1 mg mL⁻¹ human serum albumin (HAS) and bovine serum albumin (BSA) in phosphate buffer (PBS, 0.1 M pH 7.4) solutions.

3. Results and discussion

The stability of prepared gold nanoparticles in biological media was examined by monitoring the change in their SPR band in HAS and BSA within a seven days period. As it is obvious in Fig. 1A and B, the SPR of gold nanoparticles has low variation after seven days and no precipitation has been revealed in solutions. The obtained results indicate that the synthesized gold nanoparticles clearly are intact in biological media at physiological pH value. Moreover, the HSA and BSA were not adsorbed on the surface of gum arabic capped gold nanoparticles, while these proteins have extreme tendency to the surface of bare gold nanoparticles. It could be concluded that the GA molecule framework around the synthesized gold nanoparticles has

effective coating for producing intact gold nanoparticles. Another point that should be noted is biocompatibility of gum arabic and the prepared ionic liquid as capping and effective reducing agents, respectively.

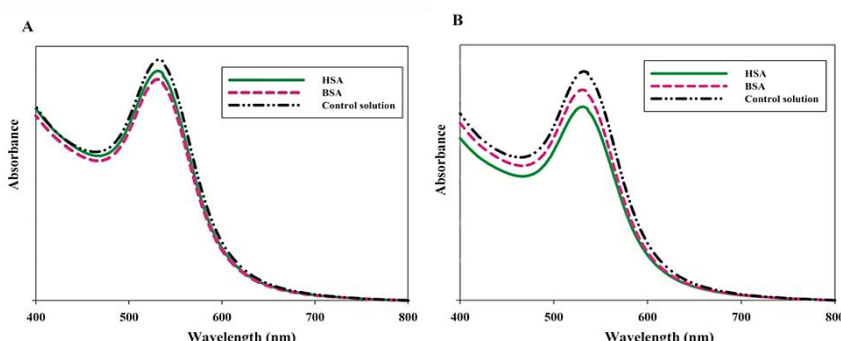


Fig. 1 (A and B) UV-Vis spectra of GA capped-gold nanoparticles in the absence as (control solution) (a) and presence of (b) HAS and (c) BSA solutions after incubation times of 1 h (B) and one week, respectively. [BSA] = [HAS] = 1 mg mL⁻¹ in phosphate buffer (pH = 7.4, 0.1 M).

The X-ray attenuation coefficient of the synthesized gold nanoparticles is approximately 3.3 times higher than Visipaque which is a conventional iodine-based contrast agent (Fig. 2).

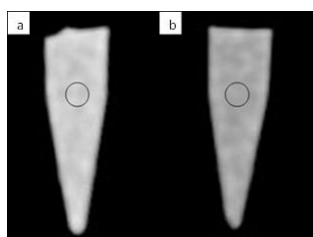


Fig. 2 X-ray CT in vitro images. The vials are containing of 0.5 mg mL⁻¹ (a) GA-AuNPs and (b) Visipaque.

4. Conclusion

In conclusion, a new procedure has been reported for synthesis of biologically stable gold nanoparticles using GA as coating agent. The GA-protected gold nanoparticles can be easily and rapidly prepared by in situ chemical reduction using glucosammonium formate ionic liquid. For synthesis of gold nanoparticles, the nontoxic and biocompatible materials were used. Furthermore, the stable GA-capped gold nanoparticles were applied as effective contrast agents for CT imaging.

References

- [1]. Lusic, H.; Grinstaff, M. W. *Chemical reviews*, 2012, 112, 1641-1666.
- [2]. Kojima, C.; Umeda, Y.; Ogawa, M.; Harada, A.; Magata, Y.; Kono, K. *Nanotechnology*, 2010, 21, 2450104.
- [3]. Kim, D.; Park, S.; Lee, J. H.; Jeong, Y. Y.; Jon, S. *Journal of the American Chemical Society*, 2007, 129, 7661-7665.

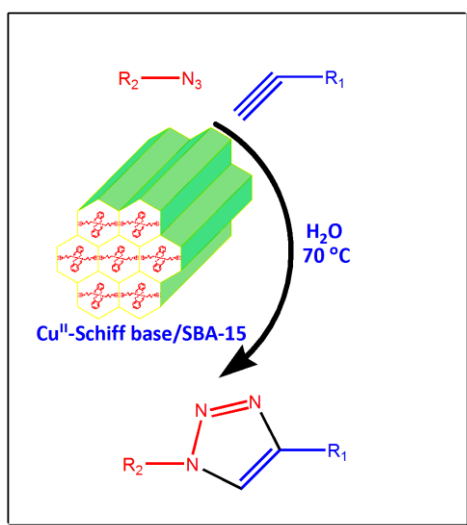
SBA-15-Supported Copper (II) Complex: An Efficient Heterogeneous Catalyst for Azide–alkyne Cycloaddition in Water

Mojtaba Bagherzadeh,* Hamed Mahmoudi

Chemistry Department, Sharif University of Technology, Tehran, P.O. Box 11365-3716, Iran;

bagherzadeh@sharif.edu

Introduction: The copper-catalyzed azide–alkyne cycloaddition (CuAAC) for synthesis of 1,4,5-triazole derivatives is one of the most attractive and a fundamental reaction in nature and synthetic organic chemistry [1]. Both copper(0) and copper(I)-containing compounds have recently emerged as effective catalysts in the 1,3-dipolar azide–alkyne cycloaddition [2]. However, these compounds are prone to redox processes so it is desirable to protect and stabilize the active copper catalysts during CuAAC-cycloaddition reaction. This limitation can be overcome by utilizing of a Cu (II)-containing catalyst [3].



Experimentals: The reaction of the functionalized mesoporous SBA-15 in absolute ethanol with copper(II) acetate afforded a novel Cu^{II}-Schiff base/SBA-15 catalyst. The compound Cu^{II}-Schiff base/SBA-15 was characterized by IR, SAX, EDXS, XANES, SEM, TEM and BET studies.

Results and Discussion: Cu^{II}-Schiff base/SBA-15 catalyst was applied as catalyst for three-component copper-catalyzed azide–alkyne cycloaddition (CuAAC) reactions to obtain 1,4-disubstituted-1,2,3-triazoles. The catalyst can catalyze the azide–alkyne cycloaddition of terminal alkynes with organic azides generated in situ from sodium azide and different organic

halides in the presence water. The process is environmentally friendly and uses an easily available solvent to produce excellent yields. Furthermore, the recyclability and reusability of catalyst for up to five consecutive cycles in the reaction of phenylacetylene and benzyl chloride substrates without a significant loss of efficiency indicate the potential of the Cu^{II}-Schiff base/SBA-100 as an efficient catalyst.

Conclusion: In summary, the present study illustrates the feasibility and applicability of utilizing the Cu^{II}-Schiff base/SBA-100 material to catalyze the azide–alkyne cycloaddition for the synthesis of the corresponding 1,2,3-triazoles through 1,3-dipolar cycloaddition of terminal alkynes with organic azides generated in situ from sodium azide and different organic halides in the presence of water.

References

- [1] P. Thirumurugan, D. Matosiuk, K. Jozwiak, Chem. Rev., 113 (2013) 4900–4979.
- [2] A. Akbari, N. Arsalani, M. Amini, E. Jabbari, J. Mol. Catal. A: Chem., 414 (2016) 47–54.
- [3] I. Jalia, F. Gallier, N. Brodie-Linder, J. Uziel, J. Augé, N. Lubin-Germain, J. Mol. Catal. A: Chem., 393 (2014) 56–61.

Epoxidation of Alkenes Catalyzed by the Nanocluster Polyoxometalates Supported on the Clinoptilolite Zeolite

Mojtaba Bagherzadeh,* Hadigheh sadat Hosseini

Chemistry Department, Sharif University of Technology, Tehran, P.O. Box 11159-3613, Iran;

bagherzadeh@sharif.edu

Introduction: Polyoxometalates (POMs) form a particular class of inorganic metal oxygen nanosized cluster, which exhibits a great structural diversity of shapes, sizes and nuclearities. [1] POMs have deserved general attention as efficient homogenous catalysts for the oxidation of olefins, aromatics and alcohols because of their tuneable catalytic reactivity and stability toward oxidation. Thus, the immobilization of soluble POMs onto surfaces is preferred due to advantages in product separation, accessibility of the active sites deposited on the support whiles are maintained the activity and selectivity of homogeneous catalysts properties. [2]

Experimentals: Polyoxomolybdate was prepared and supported on the Clinoptilolite Zeolite. The prepared catalyst was characterized by means of FT-IR, atomic absorption spectroscopies, powder X-ray diffraction (XRD), N₂ absorption-desorption, scanning electron microscopy (SEM) and transmission electron microscopy (TEM).

Results and Discussion: BET surface area analysis, atomic absorption and FT-IR spectroscopies confirmed the immobilization of polyoxomolybdate. XRD and TEM analyses reveal that the structure of support remains intact after immobilization of polyoxomolybdate. Furthermore, the recyclability and reusability of catalyst for up to six consecutive cycles in epoxidation of alkenes without a significant loss of efficiency indicate the potential of polyoxomolybdate as an efficient catalyst.

Conclusion: In summary, the catalytic investigations disclosed that Nanocluster Polyoxomolybdate immobilized on the Clinoptilolite Zeolite as a green support was found to be efficiently active and selective catalyst in liquid phase olefin epoxidation in dichloroethane at 40 °C.

References

- [^١] M. Mirzaei, H. Eshtiagh-Hosseini, M. Alipour, A. Frontera, *Coord.Chem.Rev.*, ٢٧٥ (٢٠١٤) ١-١٨.
- [^٢] Y. Zhou, G. Chen, Z. Long, J. Wang, *RSC Adv.*, ٤(٢٠١٤) ٤٢٠٩٢-٤٢١١٣.

Ag/CoFe₂O₄/Graphene oxide nanocomposite photo-catalytic antibacterial activity under visible light

Naghdi Sedeh A^{a*}, Kooti M^a, Motamedi H^b

^a Department of Chemistry, Shahid Chamran University of Ahvaz, ۶۱۳۵۷- ۴۳۱۶۹, Iran

^b Department of Biology, Shahid Chamran University of Ahvaz, ۶۱۳۵۷- ۴۳۱۶۹, Iran

E.mail: azarnaghdisedeh۲۲@yahoo.com

Introduction:

The treatment of organic pollutants and bacteria in wastewater is a major aspect of environmental issues[۱]. Graphene oxide (GO) with many of oxygen containing functional groups is a highly oxidative form of graphene have also shown the ability to inhibit the growth of bacteria. Silver nanoparticles have shown antibacterial activity to kill bacteria. However, these Ag/GO-based photocatalysts face difficulty of separation after photocatalytic reactions, which limit their application. To solve it, introducing magnetic nanoparticles in the photocatalyst has been proposed to achieve efficient separation and recycling of Ag-based materials for water treatment [۲-۳]. We have, therefore, synthesized Ag/CoFe₂O₄/Graphene oxide nanocomposite and examined its photocatalytic activity for killing bacteria.

Methods / Experimentals

Preparation of Ag/CoFe₂O₄/GO composite

This three-component composite was synthesized through an easy procedure. Graphene oxide (GO) was first prepared by oxidation of graphite powder according to the Hummers' method, with a minor modification of removing [۳۸,۳۹]. In the second step, ۰.۲ g of the pre-synthesized GO was coated with cobalt ferrite nanoparticles using co-precipitation method to give CoFe₂O₄/GO. Silver nanoparticles were then deposited onto the surface of CoFe₂O₄/GO via chemical reduction to obtain Ag/CoFe₂O₄/GO composite.

Result and Discussion:

In case of treatment of *E. coli* in the presence of visible light bacterial growth was inhibited and no bacterial colony formation was happened following culture on Mueller-Hinton agar while in dark condition bacterial growth was observed as the number of colonies was innumerable. Nearly, a similar result was found for *S. aureus*. In first hours of treatment of this bacterium with the synthesized compound in under visible light, limited bacterial growth was found but with time lapse the number of appeared colonies was significantly reduced. These data suggest that the synthesized compound has photocatalytic activity and following visible light irradiation this property with free radical production potential cause bacterial damage especially in bacterial cytoplasmic membrane and in case of gram negative bacteria. i.e., *E. coli*, in outer membrane envelope. The delay in bacterial killing in case of *S. aureus* can be related to this fact that the cell wall of this species has pentaglycine bridge between its tetrapeptide side chains that causes more than 90% of side chains be involved in transpeptidation reactions and hence has more rigid cell wall in comparison with other bacterial species. The growth of both tested bacteria in dark condition confirms that the antibacterial activity of this compound is related to the presence of visible light, i.e., its photocatalytic activity.

Conclusion

This experiment proved the synergistic effect between Ag/GO and CoFe₂O₄ and it could promote photoactivity efficiency of antibacterial. The trapping experiments showed that $\bullet\text{O}^{\cdot-}$ and h^+ are the major reactive species for the Ag/CoFe₂O₄/GO photocatalytic system. Thus, this research shows that Ag/CoFe₂O₄/GO nanocomposite possess excellent photocatalytic antibacterial properties and magnetic recovery performance. This work provides a facile way to prepare the new magnetic photocatalyst by using for the treatment antibacterial properties.

References

- [1] Ma Sh, Zhan S, Jia Y, and Zhou Q, Highly Efficient Antibacterial and Pb(II) Removal Effects of Ag-CoFe₂O₄-GO Nanocomposite, *ACS Appl. Mater. Interfaces*, 2018, 10, 10576-10586.
- [2] Zhu X, Wu D, Wang W, Tan F, Wong P-F, Wang X, Qiu X, Qiao X, Highly effective antibacterial activity and synergistic effect of Ag-MgO nanocomposite against Escherichia coli, *J Alloy Compd*, 2016, 684, 282-290.
- [3] Jing L, Xu Y, Huang Sh, Xie M, He M, Xu H, Li H, Zhang Q, Novel magnetic CoFe₂O₄/Ag/AgVO₄ composites: Highly efficient visible light photocatalytic and antibacterial Activity, 2016, 199, 11-12.

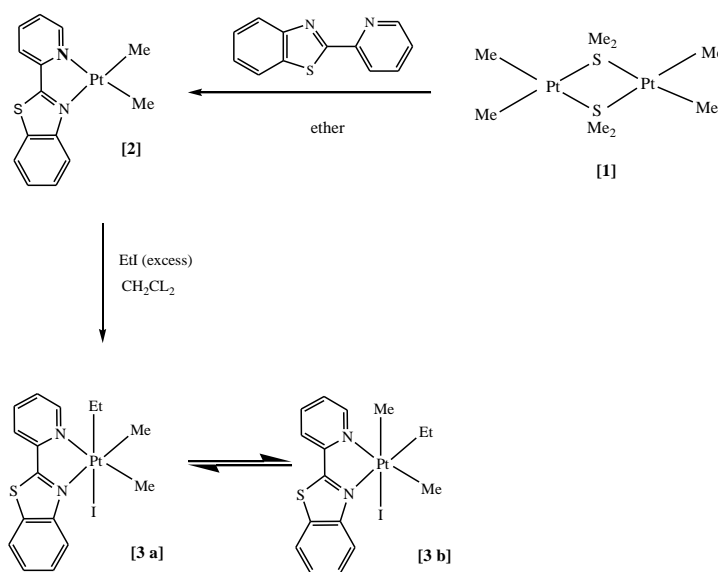
Oxidative Addition of EtI to a Dimethylplatinum (II) Complex Containing 2-(2-Pyridyl)-4,5-Benzothiazole Ligand

Lale Shafiee Sarvestani^a, Mehdi Rashidi^{*a}

^a Department of Chemistry, College of Sciences, Shiraz University, Shiraz, Iran
rashidi@chem.susc.ac.ir

Introduction: Benzothiazole and its derivatives are important pharmacophores of heterocyclic compounds. 2-(2-pyridyl) benzothiazole (pbt), is one of the benzothiazole-based compounds. This ligand acts as a bidentate ligand, coordinating through both nitrogen atoms. It coordinates with metal ions mainly by the nitrogen atoms of pyridyl and thiazole, to give complexes which exhibit various photochemical and photophysical properties besides biological activities.¹ This ligand is expected to bind to soft acceptor centres in S,N-chelating mode, but the only observed binding mode of pbt is N,N-chelation.² Platinum complexes of pbt, as biologically active compounds, are candidates for replacing cisplatin with more effective drugs that can be administered orally and with reduced side effects.³

Experimentals: The reaction of organoplatinum (II) complex [1] with 2 equivalents of 2-(2-Pyridyl)-4,5-Benzothiazole in ether at room temperature gave complex [2]. Reaction of complex (2) with was added a large excess of EtI, in dichloromethane gave complex [3] (Scheme 1).



Scheme 1. The synthetic pathway to [PtEtMe₂(pbt)]

Result & Discussion: In the ¹H NMR spectrum (Figure 1) the major isomer **3a** gave a triplet at $\delta = 0.12$ due to the CH₃ group of Et ligand with ¹J(HH) = 7.6 Hz, and with satellites due to coupling to ¹⁹⁵Pt with ¹J(PtH) = 16.4 Hz. The CH₂ group of the Et ligand appeared as overlapping multiplet around $\delta = 1.39-2.06$. These parameters are comparable with previously reported data for [PtEtI(pbt)] complex, in which the Et ligand being *trans* to the I atom. Thus, the two different Me groups must be *trans* to N ligating atoms.

The second isomer **2b** gave a triplet at $\delta = 0.29$ for the CH_2 group of Et with $^1J(\text{PtH}) = 11.6\text{ Hz}$, and $^1J(\text{HH}) = 7.6\text{ Hz}$. The CH_2 group of Et ligand were located as overlapping multiplet around $\delta = 1.39\text{--}2.06$.

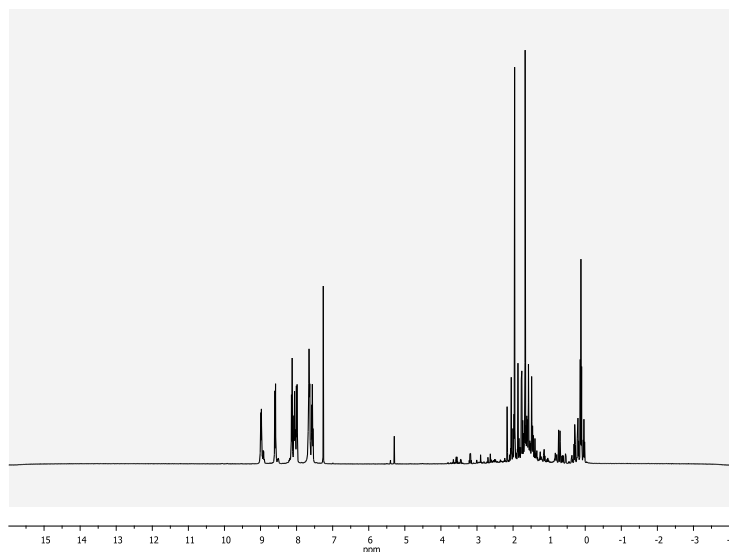


Figure.1 ^1H NMR spectrum (400.22 MHz) of $[\text{PtEtMe}_7(\text{pbt})]$, in CDCl_3

The cyclometalated Pt(II) complex $[\text{PtMe}_7(\text{pbt})]$ contains an MLCT band in the visible region that could be used to monitor its oxidative addition reaction with EtI and study the kinetics of the reaction by using UV-Visible spectroscopy. Thus, an excess of EtI was used at different temperatures and the disappearance of the MLCT band at $\lambda_{\text{max}} = 563\text{ nm}$ in toluene solvent or $\lambda_{\text{max}} = 520\text{ nm}$ in acetone solution were used to monitor the reaction.

Conclusion: This complex, was reacted with excess EtI. The structure of the final product with Pt(IV) center, as determined by NMR studies. This complex, with an octahedral platinum(IV) center, contains two different nitrogen atoms with different Pt–N distances. According to the kinetic results, the oxidative addition reaction of EtI with $[\text{Pt}(\text{pbt})\text{Me}_7]$ follows a good second order kinetics, first order with respect to both reactants. The entropy of activation, ΔS^\ddagger , has a large negative value which is consistent with an $\text{S}_{\text{N}}2$ -type mechanism.

References:

- [1] X. B. Fu, G. T. Weng, D. D. Liu, X. Y. Le. *J. Photochem. Photobio. A.: Chem*, 2014, 277, 83.
- [2] S. Chowdhury, S. Majumder, A. Bhattacharya, P. Mitra, J. P. Naskar. *J. Coord. Chem*, 2013, 77, 3360.
- [3] K. Marjani, M. Mousavi, D. L. Hughes. *Transition. Met. Chem*, 2009, 34, 80.

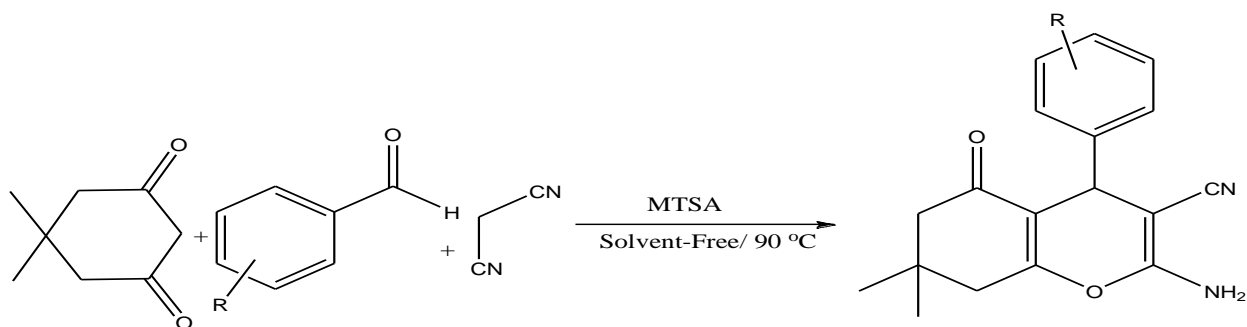
Melamine Trisulfonic Acid as a Highly Efficient and Reusable Catalyst for the One-Pot Synthesis of 4H-Chromene Derivatives under Solvent-Free Conditions

Farhad Hatamjafari*

Department of Chemistry, Faculty of Science, Tonekabon Branch, Islamic Azad University, Tonekabon, Iran

Email address of the corresponding author: hatamjafari@yahoo.com

Introduction: The multi-component reactions (MCRs) were an important tool in the organic synthesis as they possess ability of building up the pharmaceuticals [1]. 4H-chromenes are an important class of oxygen-containing heterocyclic compounds which have attracted significant synthetic interest due to their reactivity and biological activity. These compounds had shown interesting biological properties including antimicrobial, antiviral, antitumor cancer therapy and central nervous system activity. These derivations were used in the treatment of hypertension, Alzheimer's disease and Seizures [2]. Therefore, we report herein the MTSA as a new catalyst for the one-pot solvent-free synthesis of 4H-chromene derivatives high yields by condensation of aromatic aldehydes, dimedone and malononitrile (Scheme 1).



Scheme 1: Synthesis of 4H-chromene derivatives the presence of MTSA as a catalyst

Methods / Experimentals: A mixture of aromatic aldehyde (1 mmol), dimedone (1.1 mmol), malononitrile (1.2 mmol), and MTSA (1.5 mol%) was heated in at 90 °C for 1 h. After completion of the reaction, as indicated by TLC, the reaction mixture was cooled to room temperature, CH₂Cl₂ (3 mL) was added, stirred for 5 min, and filtered to separate the catalyst. The solvent was evaporated to give the crude product which was purified by recrystallization from ethanol (90%) to give pure products.

Results and Discussion: Nowadays, MTSA is often used as a Bronsted–Lowry acid catalyst in the synthesis of organic compounds. Features of this catalyst that are of interest include: easy separation, environmentally friendly, reusable, clean, and economical [3]. We started our study of one-pot, three-component condensation using MTSA as a catalyst and undertaking reactions using benzaldehyde, dimedone and malononitrile to create corresponding 4H-chromenes products as the model reaction. The synthesis of compound 1 was selected as a model to determine suitable reaction conditions in the presence of MTSA with various amounts of catalyst

and under solvent-free conditions. Best results were obtained under solvent-free conditions in the presence of 10 mol% catalyst at 90 °C for 1 h. All compounds were characterized using melting point, IR, ¹H NMR techniques. The results for the preparation of substituted *ε*H-chromene derivatives are summarized in Table 1.

Table 1. MTSA catalyzed synthesis of *ε*H-chromene derivatives^a

Entry	Ar	Yield (%)	M.P. °C (Found)	M.P. °C (Reported in Lit.) [29]
1	Ph	92	228-229	229-231
2	γ-FC ₇ H ₅	88	233-235	235-237
3	ε-MeC ₇ H ₅	94	218-220	219-221
4	γ-ClC ₇ H ₅	90	201-203	201-205
5	ε-ClC ₇ H ₅	91	213-214	212-214
6	ε-MeOC ₇ H ₅	93	192-195	192-194

Reaction condition: ^a aldehyde (1 mmol), dimedone (1 mmol), malononitrile (1.2 mmol), MTSA (10 mol%), Isolated yield.

The catalyst was easily recovered by simple filtration after dilution of the reaction mixture with ethyl acetate and was reused after being vacuum dried. MTSA was reused for four runs without significant loss of activity (Run 1: 89%; Run 2: 88%; Run 3: 87%; Run 4: 84%).

Conclusion: In conclusion, we have demonstrated a novel method for the synthesis of substituted *ε*H-chromene derivatives by MTSA under solvent-free conditions. Moderate to high yields of the corresponding *ε*H-chromenes were obtained. The advantages of this method include high yields, available time, one-pot, experimental simplicity, under solvent-free conditions, environmentally friendly and easy separation with reuse of the catalyst.

References

- [1]. Kappe C.O., *Accounts Chem Res.* 2005, 38(12), 879-888.
- [2]. Kumar D., Reddy V.B., Sharad S., Dube U., Kapur S., *Europ J Med Chem.* 2009, 44, 3805-3809.
- [3]. Zare A. E., *J. Chem.*, 2012, 9(4), 2322-2331.

Experimental and DFT Calculation Studies of Some Macrocyclic Schiff Base Complexes

Sheida Esmailzadeh*

Department of Chemistry, Darab branch, Islamic Azad University, Darab, I. R. Iran

Email address: esmailzadehsheida@yahoo.com

Introduction: Stability constant can be key parameters for the investigation of equilibria in solution. They are very important in many fields such as environmental studies, medicinal, analytical and industrial chemistry. Therefore complexation reactions of metal ions with different ligands have been widely studied [1,2]. As an important class of compounds, Schiff bases have received much attention in the wide variety of fields due to structural varieties and unique characteristics [3]. In this paper in order to make sense between the experimental and theoretical results, formation constants of some Schiff base complexes were calculated by using DFT method.

Methods/Experimentals: The formation constant measurements were carried out by a titration method at constant ionic strength 0.1M (NaClO₄) at 10, 20, 30 and 35±1°C. UV-Vis spectra were recorded in the range 200-700 nm. The SQUAD program [4] was used to calculate the formation constant. To investigate the stability of [H₂L] Schiff base ligand and their complexes, in gas phase some properties such as HOMO-LUMO energies, chemical hardness and binding energy were obtained by using the DFT method.

Results and Discussion: The formation constant, K_f , of complexes were calculated at several temperatures using SQUAD computer program. Then the standard Gibbs free energy (ΔG), enthalpy (ΔH) and entropy (ΔS) changes of the formed complex were calculated. On the basis of the results, the formation constant of the complexes with respect to bivalent transition metal ions were found in the order $\text{Co}^{2+} > \text{Cu}^{2+} > \text{Ni}^{2+} > \text{Zn}^{2+}$. In the studies systems, Schiff base ligand act as donor species and metal ion act as acceptor. This order ($\text{Co}^{2+} > \text{Cu}^{2+} > \text{Ni}^{2+} > \text{Zn}^{2+}$) largely reflect the changes in the heat of complex formation across the series from a combination of the influence of both the polarizing ability of the metal ion and the crystal field stabilization energies (CFSE) [5,6].

To investigate the stability of [H₂L] Schiff base ligand and their complexes, in gas phase some properties such as HOMO-LUMO energies, chemical hardness and binding energy were obtained by using the gradient corrected density functional theory (DFT) method with the B³LYP functional and 6-311G** basis sets.

Table 1. Thermodynamic parameters of the complexes in DMF

Complex	logK _f				-ΔH° (kcal mol ⁻¹)	-ΔS° (cal K ⁻¹ mol ⁻¹)	-ΔG° (kcal mol ⁻¹) ^b
	288	293	298	303			
CoL	8.23(0.21) ^a	7.96(0.13)	7.43(0.26)	7.02(0.11)	168.39(2.0)	491.93(3.7)	39.74(0.32)
CuL	7.90(0.33)	7.08(0.03)	5.83(0.09)	5.26(0.07)	160.43(1.2)	463.78(4.2)	36.34(1.1)
NiL	4.83(0.14)	4.20(0.20)	3.88(0.08)	3.21(0.28)	127.00(1.7)	367.34(2.6)	27.69(0.9)
ZnL	4.06(0.24)	3.69(0.16)	3.12(0.01)	2.94(0.16)	120.02(1.8)	269.76(1.4)	23.73(1.2)

^a Standard deviations are given in parentheses, ^b at T= 303 K

Table 2. HOMO, LUMO, band gap and interaction energies of the complexes

Complex	HOMO (eV)	LUMO (eV)	Δ Band gap (eV)	Hardness (η)	ΔE (kcal mol ⁻¹)
CoL	-0.19014	-0.00116	0.18898	0.07199	-980.88.49
CuL	-0.19170	-0.04891	0.14279	0.07142	-909.07718
NiL	-0.18783	-0.04603	0.14180	0.07040	-934.83823
ZnL	-0.18190	-0.04788	0.13402	0.07103	-800.34.36

Conclusion: The present study allowed us to obtain the formation constant of Co(II), Ni(II), Cu(II) and Zn(II) Schiff base complexes. The trend of the complex formation of the Schiff base ligand (H₂cdacacMeen) with four metal cations decreases as follow: [CoL] > [CuL] > [NiL] > [ZnL]. The molecular properties of the structures have been investigated by means of computational studies. This finding is further supported by the fact that the experimental formation constants of these complexes.

[1] Golbedaghi, R.; Khajavi, F. *Bull. Chem. Soc. Ethiop.* 2014, 28, 1-8.

[2] Kanchi, S.; Singh, P.; Bisetty, K. *Arab. J. Chem.* 2014, 7, 11-20.

[3] Jia, Y.; Li, J. *Chem. Rev.* 2010, 110, 1097-1621.

[4] Leggett. D. L. *Computational Methods for the Determination of Formation Constant*, Plenum Press, New York; 1980.

Theoretical Study of the Reaction Mechanism and Solvent Effect on the rate of Diels- Alder Reaction between Cyclopentadiene and C₇₀.

Abbas Amini Manesh^{*}, Mohammad Haqgu, Nahid Rahimi

Department of Chemistry, Payame Noor University, ۱۹۳۹۵-۴۶۹۷ Tehran, I. R. of IRAN.

Email: a_aminima@yahoo.com

Introduction: Fullerene has received much attention with respect to its physicochemical properties as well as its synthetic applications in biological and materials science [۱].

Diels-Alder reaction has proved to be a powerful way to functionalize these conjugated π systems and have offered wide opportunities for the creation of new nanocarbon structures with potential application in biological, biotechnology, material science and medicinal chemistry. Also the reaction and functionalizations are carried out in organic solvents and thus the solution behavior of C₇₀ will provide useful information on selecting solvents for practical processing.

Method: In this work, mechanism and solvent effect on the rate of Diels–Alder reaction of C₇₀-cyclopentadiene was studied using Two-layered ONIOM method.

The ONIOM method is performed using a combination of density functional theory and AM۱ semiempirical method for reactants and transition state [۲]. Reacting system-solvent interactions are taken into account by employing the conductor polarized continuum model (CPCM) and the conductor like screening model, (COSMO).

Results and Discussion: Figure ۱ shows the energies of Stationary Points:

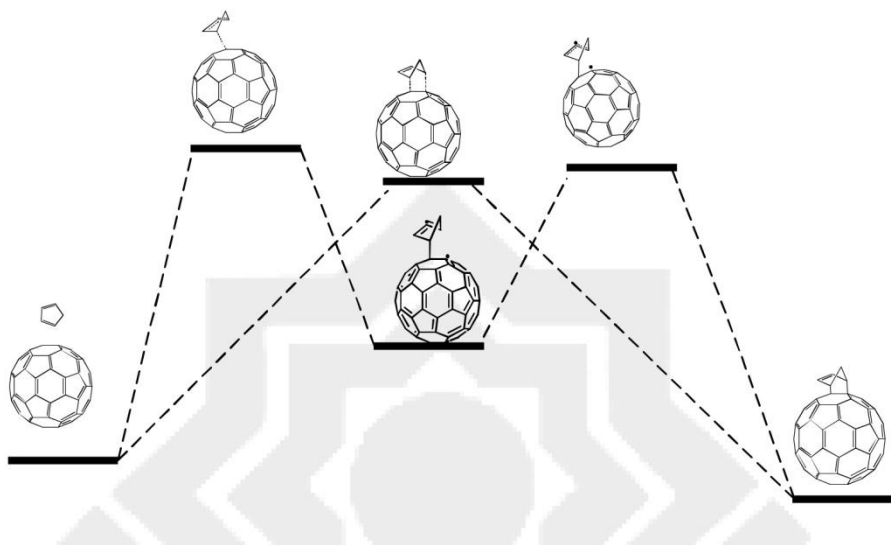


Figure ۱: ONIOM (B³LYP/۶-۳۱G(d): AM۱): Energies of Stationary Points.

Conclusion: The results show that the Diels–Alder reaction between cyclopentadiene and C₇₀ proceeds by the concerted mechanism and the rate increased as the polarity of the solvent increased.

References

۱. Kroto, H. W., Fischer, J. E., Cox, E. D., *The Fullerenes*, ۱۹۹۳, New york, U.S.A: Oxford: Pergamon Press.
۲. Silvia O., Morera, J., Cases, M., Morokuma, K., and Sola, M., *J. Phys. Chem. A* ۲۰۰۹, ۱۱۳, ۹۷۲۱–۹۷۲۶.

Electrochemical Properties of Clindamycin Antibiotic as Potassium Exchange Membrane

Mohsen Oftadeh^{a,*}, Faramarz Dehdar^b, Zahra Askari^a, Ziba Ghasemi Shervedani^c, Sahar Babadi Bakhtiari^a, Daniel Omidghaemi^d

- a. Chemistry Department, Payame Noor University, ۱۹۳۹۵-۴۶۹۷ Tehran, I. R. Iran
- b. Department of Chemical Engineering, Amirkabir University of Technology, Tehran, Iran
- c. Department of Chemistry, Isfahan University of Technology, Isfahan, Iran
- d. Department of Chemical Engineering, University of Arak, Arak, Iran

m_oftadeh@pnu.ac.ir

Introduction: Ionophores are moderate molecular weight compounds that are mobile ion carriers. Because ionophores are highly lipophilic, they rapidly dissolve into bacterial cell membranes. Ionophores bind ions, shield the ionic charges and translocate ions across the bacterial membrane, disrupting crucial ion gradients [۱-۳]. The first neutral ionophores used in ion-selective electrode (ISE) membranes were antibiotics. They were followed by a large number of natural and synthetic, mainly uncharged carriers for cations and a series of charged and uncharged ones for anions [۴]. The structure of clindamycin raises additional possibilities for its mode of transport. This antibiotic is composed of an amino acid (hygrinic acid) linked to an amino sugar. [۵, ۶]

Experiments: Potassium exchange membranes were first prepared and then clindamycin pure powder was dispersed in above solution. The solutions were poured on a flat clean glass and let to be relaxed and then put into an oven to be dried. The test cell used in measuring the membrane electrochemical properties is shown in Fig. ۱-a. The water content was measured as the weight difference between the dried and swollen membranes. Ion exchange capacity (IEC) was determined through titration. Membrane potential, transport number and permselectivity were measured using a two-cell glassy apparatus.

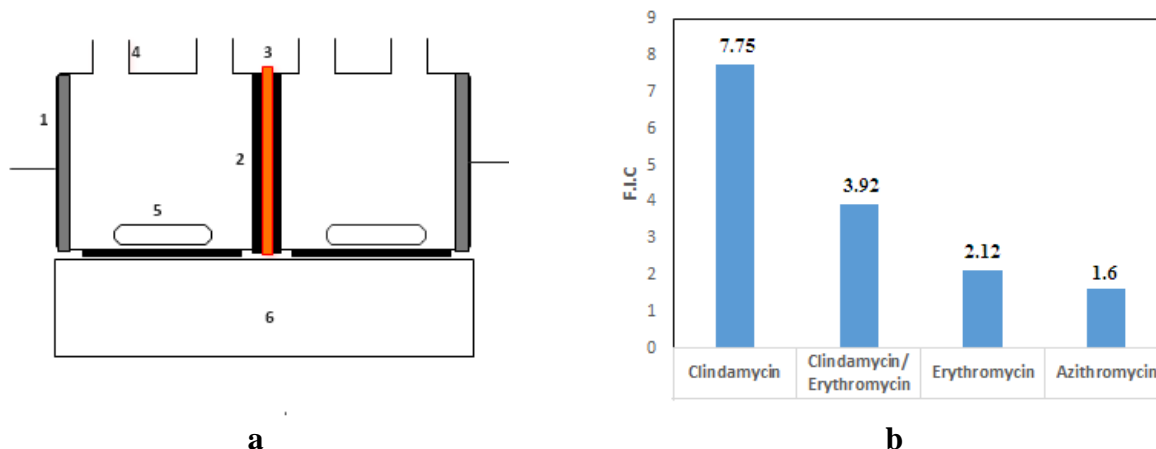


Figure ۱. a) Schematic diagram of test cell: (۱) Pt electrode, (۲) rubber ring, (۳) membrane, (۴) Orifice, (۵) magnetic bar, (۶) stirrer; b) Fixed ion concentration for prepared membranes with various antibiotic content (mequiv/g absorbed water).

Results and Discussion: Using a relationship between the IEC and water content, the effect of these parameters can be optimized on each other during the process. Fixed ion concentration (FIC) or the equivalent of functional group per absorbed water content can be used for this purpose (Fig. 1-b). The presence of clindamycin ionophores in the membranes leads to an improvement in ion exchange capacity in comparison with erythromycin, azithromycin and even mixture of clindamycin/erythromycin ionophores due to their functional groups. In the absence of clindamycin ionophores, the membranes are not much accessible to ion exchange. Membrane potential increases with adding of clindamycin ionophore in comparison with the other used ionophores in KCl solution. The membranes were put in the cell and their selectivity for potassium cations was studied. The average conductivity of clindamycin, erythromycin, azithromycin and the mixture of clindamycin and erythromycin tested by the cell test is 600, 389.75, 319.91 and 502 μ S, respectively (Fig. 2-a). As shown in Figure 2-b, perm-selectivity and transport number of prepared membranes increase with an increment of clindamycin ionophore for K⁺ ions. The prepared membrane samples were immersed in oxidant aqueous solution for oxidative stability measurements. Figure 2-b shows that oxidative stability of the prepared membranes decreases with decreasing of clindamycin as ionosphere. This may be due to an increase of aqueous solution and water diffusion in a membrane matrix and also due to lower oxidative stability of particles than the polymer binder.

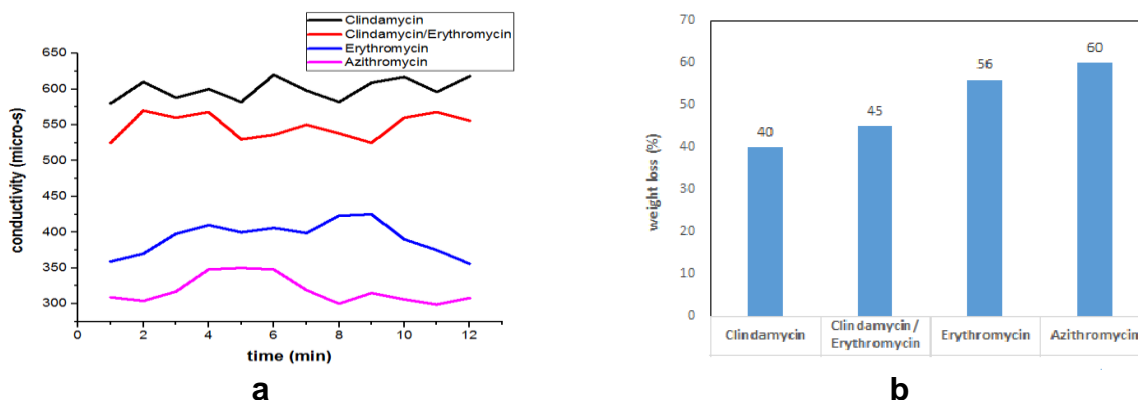


Figure 2. a) Comparison of membranes' conductivity; b) Oxidative stability of prepared membranes with various antibiotics

Conclusion: According to the investigations, it can be realized that pure powder of clindamycin plays as an ionophore into polymeric membrane, so that its structure causes this property and makes the membrane able to translocate the huge cations such as potassium and then other smaller cations including sodium, lithium, proton and etc.

References

- [1] Mulder, J., Basic Principles of Membrane Technology, 2nd.ed, Springer, 1996.
- [2] Li, X.; Wang, Z.; Lu, H.; Zhao, C.; Na, H.; Zhao, C. *J. Membrane Sci.* 2005, 254, 147-190.
- [3] Callaway, T. R., et al. *Curr. Issues Intes. Microbiol.* 2003, 4, 43-51.
- [4] Hosseini, S. M., et al. *Desalination* 2011, 279, 306-314.

[۵] Gohil, G. S.; Binsu, V. V.; Shahi, V. K. *J. Membrane Sci.* ۲۰۰۶, ۲۸۰, ۲۱۰-۲۱۸.

[۶] Khodabakhshi, A. R., Madaeni, S. S. and Hosseini S. M.. *Ind. Eng. Chem. Res.* ۲۰۱۰, ۴۹, ۸۴۷۷-۸۴۸۷.

Synthesis and antimalarial activity of new nanocopolymer β -lactams and molecular docking study of their monomers

Edris Ebrahimi,¹ Aliasghar Jarrahpour*,² Nahid Heidari,³ Amin R. Zolghadr

Department of Chemistry, College of Sciences, Shiraz University, Shiraz ۷۱۴۰۴, Iran.

E-mail: edris.ebrahimi@yahoo.com;

Introduction:

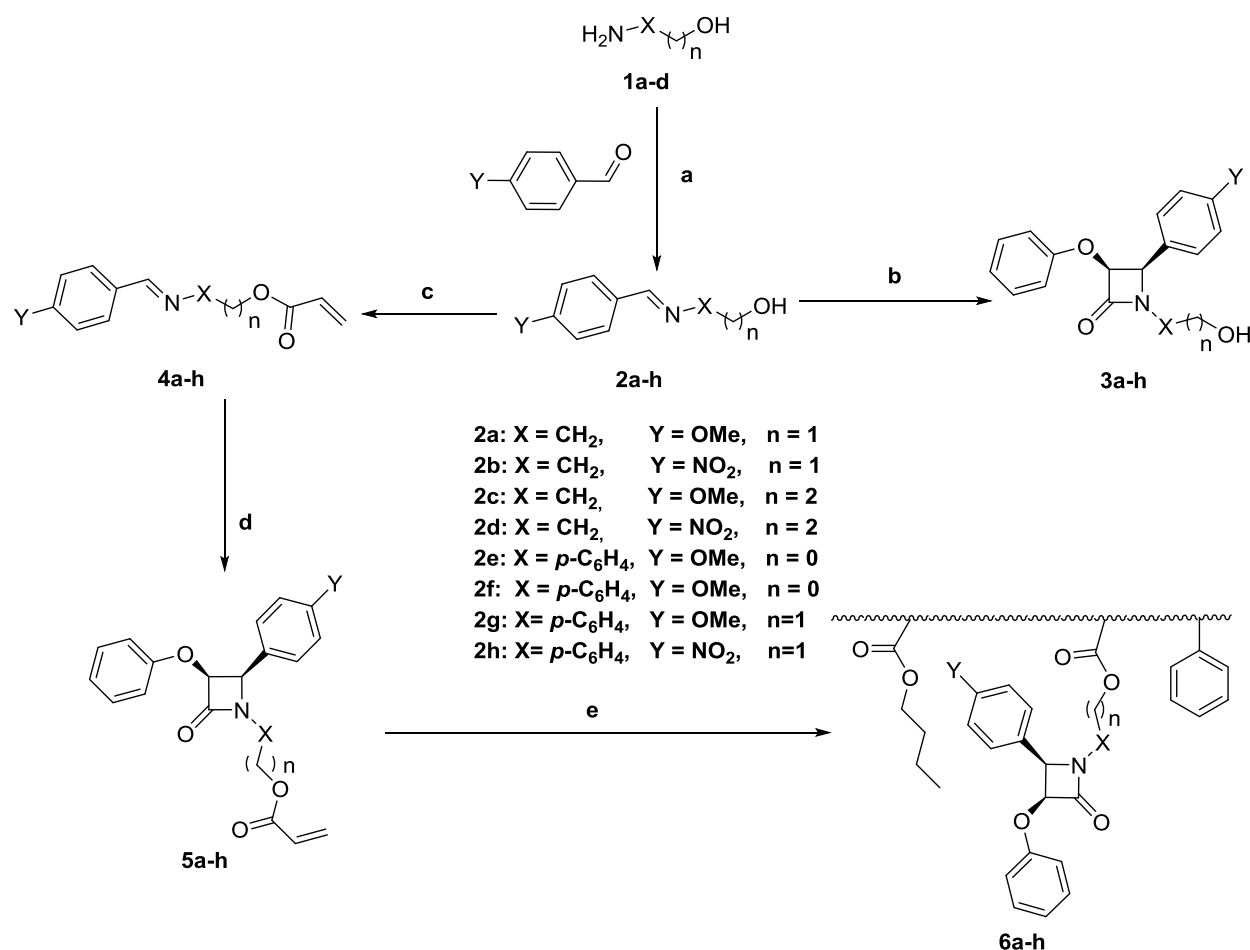
β -Lactams form a class of antibiotics characterized by the presence of a β -lactam (γ -azetidinone) ring.[¹] This four-membered ring is responsible for biological activity in penicillins, cephalosporins, carbapenems, nocardicins and monobactams, which have been widely used as chemotherapeutic agents for treating microbial diseases.[²] Nanomedicine is designed and synthesized drug delivery vehicles that can carry drug and efficiently cross physiological membranes to reach target sites.[³] The unique properties of polymeric micelles as carriers of hydrophobic drugs have been reported in recent years.[⁴] The preparation of different ampicillin, amoxicillin,[⁵] or penicillin[⁶] entrapped polycyanoacrylates, carbohydrate[⁷] and antibiotic conjugated polyacrylate nanoparticles formed by emulsion polymerization in water has been reported.[⁸]

Methods / Experimentals:

A mixture of Schiff base, triethylamine in dry CH_2Cl_2 was stirred at 0°C . Chlorotrimethylsilane was added dropwise to the mixture and stirred for 1 hour. Then, phenoxyacetic acid and tosyl chloride were added and the mixture was stirred at room temperature for 12 h. Then it was washed with HCl 1 M, saturated NaHCO_3 , and brine. The organic layer was dried (Na_2SO_4), filtered and the solvent was evaporated to give the crude β -lactams. Then desired products were purified by silica gel column chromatography or recrystallization from EtOAc.

Result and discussion:

Some free hydroxyl imines **1a-h** were synthesized from aliphatic and aromatic amines containing the hydroxyl group and aromatic aldehydes in refluxing ethanol. To prepare β -lactams **2a-h**, hydroxy imines **1a-h** were protected by trimethylsilyl chloride (TMSCl) in the presence of Et_3N in dry CH_2Cl_2 . Then, phenoxyacetic acid and *p*-toluenesulfonyl chloride were added to the above crude mixture. The new mixture was stirred for 12 h to afford N-substituted hydroxy β -lactams **2a-h** in good to excellent yields. The silyl group was deprotected during aqueous workup. In the next step, the acrylated- β -lactam monomers **3a-h** were used for the preparation of β -lactam nanocopolymers **4a-h**. These nanocopolymeric emulsions were prepared easily in water by radical initiator emulsion polymerization using warmed mixture of butyl acrylate, styrene and an acrylated β -lactam monomer.[⁹] For this, the acrylated- β -lactam monomers **3a-h** were dissolved in a mixture of butyl acrylate and styrene 3:1 (w:w) at 70°C under Ar atmosphere. Then the mixture was pre-emulsified in deionized water and sodium dodecyl sulfate (SDS) (1 %w) was added as the surfactant. After about 30 min, the homogenous solution was treated with potassium persulfate (0.5 % w/w) to start free radical polymerization for 2 h (Scheme 1).



Conclusions

Several nanopolyacrylate β -lactams have been synthesized from the corresponding monomeric β -lactams by emulsion polymerization. The polyacrylated β -lactam nanoparticles showed average diameter of 26–58 nm. Finally, moderate antimalarial activities were obtained against chloroquine resistant *Plasmodium falciparum* K1 strain with IC₅₀ varying from 14 to up to 50 μM . Molecular docking results showed that these compounds could create crucial hydrogen bonding and hydrophobic interactions to the *Pf*-SSB tetramer within protein binding pocket.

References

- [1] D. Giomi, F. Cordero, F. Pisaneschi, A. Brandi in *Comprehensive Heterocyclic Chemistry III*, Vol. 4, Vol. (Ed. ^Eds.: Editor), Oxford: Elsevier, City, 2008.
- [2] A. K. Halve, D. Bhaduria *Bioorganic & medicinal chemistry letters*. 2007, 17, 341-345.
- [3] A. El-Ansary, S. Al-Daihan *Journal of Toxicology*. 2009, 2009.
- [4] A. L. Lee, S. Venkataraman, S. B. Sirat, S. Gao, J. L. Hedrick, Y. Y. Yang *Biomaterials*. 2012, 33, 1921-1928.
- [5] G. Fontana, M. Licciardi, S. Mansueto, D. Schillaci, G. Giammona *Biomaterials*. 2001, 22, 2857-2865.
- [6] S. Henry-Michelland, M. Alonso, A. Andremon, P. Maincen, J. Sauzieres, P. Couvreur *International journal of pharmaceutics*. 1987, 35, 121-127.
- [7] S. C. Abeylath, E. Turos, S. Dickey, D. V. Lim *Bioorganic & medicinal chemistry*. 2008, 16, 2412-2418.
- [8] J. C. Garay-Jimenez, E. Turos *Bioorganic & medicinal chemistry letters*. 2011, 21, 4589-4591.
- [9] A. Jarrahpour, R. Heiran *Journal of the Iranian Chemical Society*. 2014, 11, 75-83.

An Experimental Study on the Surface Properties of *N*-Methylmorpholinium-Based Ionic Liquids

Mohammad Hadi Ghatee*, Tahereh Ghaed-sharaf

Department of Chemistry, College of Science, Shiraz University, Shiraz, Iran

Email: ghatee@susc.ac.ir

Introduction: Ionic liquids are a new type of solvents composed of large organic cations and organic or inorganic anions unable of forming an ordered crystal and thus remaining liquid at or near room temperature. Among different ILs Morpholinium-based protic ILs exhibit a large electrochemical window as compared to other protic ILs (up 2.91 V) and possess relatively high ionic conductivities of 10-16.8 mS.cm⁻¹ at 298.15 K and 21-29 mS.cm⁻¹ at 373 K [1].

Experimentals: The surface tension of ILs was determined at vapor/liquid equilibrium using the capillary apparatus [2, 3]. The surface tension is calculated from:

$$2\gamma \cos \theta = r\rho g(h + \frac{r}{2}), \quad (1)$$

where γ is the surface tension, ρ is the density, g is the acceleration of gravity, r is the capillary radius, h is the height of liquid in capillary and θ is the contact angle.

Result and Discussion: We used the Eq. (1) and calculated the surface tension in the range 298.15-348.15 K. The surface tensions obtained for all ILs demonstrate high correlation in the whole temperature range. For *N*-methylmorpholinium ILs, surface tension is decreased by increasing anion chain length and temperature as shown in Figure 1.

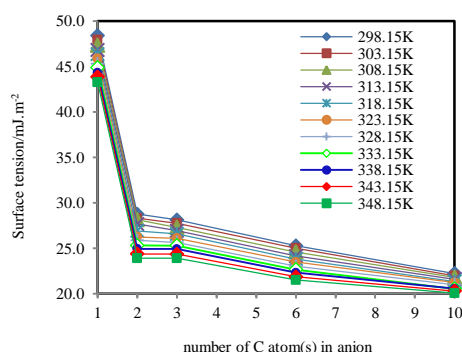


Figure 1. Surface tension of *N*-methylmorpholinium ILs versus number of C atom(s) in anion.

The surface thermodynamics functions, namely the surface entropy and surface energy, can be calculated with high accuracy. Essentially, surface tension decreases as the temperature is increased and fits to the linear equation:

$$\gamma = E^s - TS^s, \quad (2)$$

where E^s is surface energy and S^s is surface entropy. The plot of surface entropy and surface energy versus the number of carbon atoms of the anion alkyl chain are shown in Figures 2 and 3.

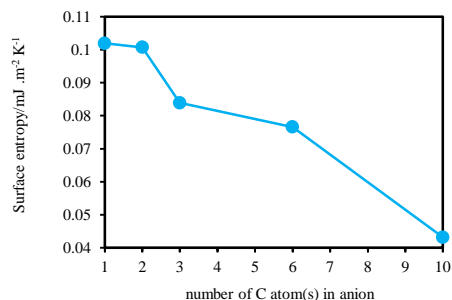


Figure 2. Surface entropy of *N*-methylmorpholinium-based ILs obtained by surface tension measurement.

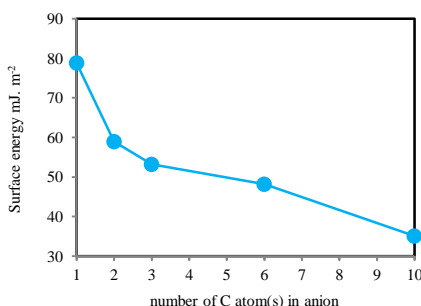


Figure 3. Surface energy of *N*-methylmorpholinium-based ILs obtained by surface tension measurement.

Conclusion: The results show that, as the anion alkyl chain length of the ILs increases, surface tension, surface energy, surface entropy decreases. The variation of surface properties versus anion chain length is sharp for short alkyl chain length of anion and is smooth for those of long alkyl chain length. Basically, the properties of morpholinium-based ILs are very sensitive to the alkyl chain length of the anion particularly at low chain length.

References:

- [1] Brigouleix, C.; Anouti, M.; Jacquemin, J.; Caillon-Caravanier, M.; Galiano, H.; Lemordant, D. Physicochemical characterization of morpholinium cation based protic ionic liquids used as electrolytes. *The Journal of Physical Chemistry B* 2010, 114, 1707-1716.
- [2] Ghatee, M. H.; Zolghadr, A. R. Surface tension measurements of imidazolium-based ionic liquids at liquid-vapor equilibrium. *Fluid Phase Equilibria* 2008, 263, 168-170.
- [3] Ghatee, M. H.; Bahrami, M.; Khanjari, N.; Firouzabadi, H.; Ahmadi, Y. A Functionalized High-Surface-Energy Ammonium-Based Ionic Liquid: Experimental Measurement of Viscosity, Density, and Surface Tension of (2-Hydroxyethyl)ammonium Formate. *Journal of Chemical & Engineering Data* 2012, 57, 2090-2101.

Synthesis and characterization of Mg-Co-Al Nano Hydrotalcites

Khadijeh Shekoohi^{*,a}, Amir Hossein Haghighi^b, Fatemeh Sadat Hosseini^c

^a Department of Chemistry, Darab branch, Islamic Azad University, Darab ۷۴۸۱۷۸۳۱۴۳-۱۹۶, I. R. Iran

^b Department of Polymer Engineering, Shiraz Branch, Islamic Azad University, Shiraz ۷۱۹۸۷ ۷۴۷۳۱, Iran

^c Young Researchers and Elite Club, Shiraz Branch, Islamic Azad University, Shiraz ۷۱۹۸۷ ۷۴۷۳۱, Iran

E-mail address: sh.shekoohi@gmail.com, sh.shekoohi@iaudarab.ac.ir .

Introduction: Nano Hydrotalcites are as anionic clays or layered double hydroxides (LDH). Hydrotalcite compounds are a class of two-dimensional nanostructured anionic clays that consist of two types of metallic cations[۱,۲]. Synthesis methods play important role to produce nano-sized crystals of hydrotalcite, so the preparation methods are always an important research subject in this field. Coprecipitation method is the most basic and commonly used synthetic method of hydrotalcite in which a mixed alkaline solution is added to a mixed salt solution and the resultant slurry is aged at a desired temperature. In this paper, binary and ternary Nano Hydrotalcites that contains magnesium, aluminum and cobalt have been synthesized by coprecipitation method[۳,۴].

Experimentals: Mg-Al Nano hydrotalcite with Mg/Al molar ratio of ۱:۱, ۳:۱, ۵:۱ and ۸:۱ and Co-Mg-Al Nano hydrotalcite with Co/Mg/Al molar ratio of ۱:۸:۱ and ۳:۸:۱ was synthesized. we study of the molar ratio influences structure and performance of Nano hydrotalcite . The synthesized Nano hydrotalcites were then characterized by X-ray diffraction (XRD) and scanning electron microscope (SEM).

Results and Discussion: The XRD pattern of Mg-Al Nano hydrotalcites is represented in Figure ۱. The difference in the intensities of the reflections indicates different degrees of crystallinity .When the cationic composition varies, these peaks became broad and their intensity decreased with increasing the molar ratio of $M^{۲+}$ to $M^{۳+}$. The XRD pattern of Co-Mg-Al Nano Hydrotalcite shown in Figure ۲. Table ۱ lists the maximum diffraction intensity and the corresponding d values of the ۴ samples for the (۰۰۳), (۰۰۶), and (۰۰۹) crystal planes.

The sharp peak (۰۰۳) indicates the formation of highly crystalline materials. The X-ray data indicate a decrease in the crystallinity and increase in the interlayer spacing of the materials with increase in the cobalt composition [۵]. In order to determine the morphology and particle size distribution of the synthesized hydrotalcites we have different respective samples which were studied by SEM.

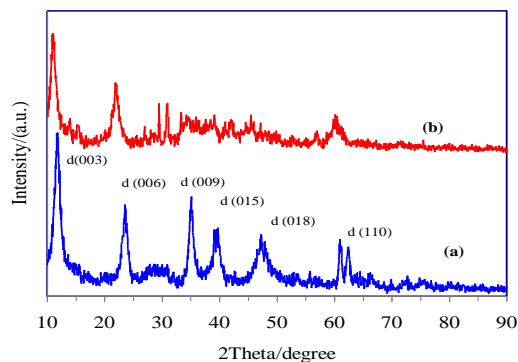


Figure 1. XRD pattern of Mg-Al Nano Hydrotalcite molar ratio (a) 1:1, (b) 1:2.

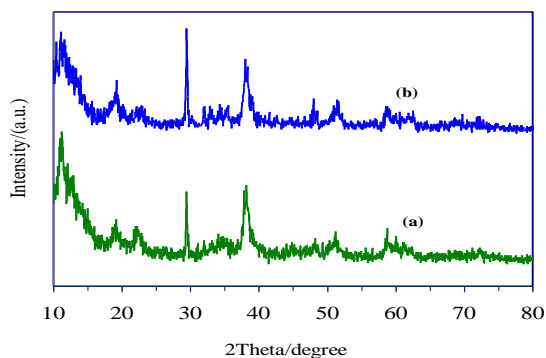


Figure 2. XRD pattern of Co-Mg-Al Nano Hydrotalcite molar ratio (a) 1:1:1, (b) 1:2:1.

Table 1. XRD patterns of synthesized Nano hydrotalcites.

Nano hydrotalcite	(1:1)		(1:2)		(1:1:1)	
	$2\theta (^{\circ})$	d (nm)	$2\theta (^{\circ})$	d (nm)	$2\theta (^{\circ})$	d (nm)
Mg/Al (1:1)	11.82	0.700	23.08	0.377	30.13	0.290
Mg/Al (1:2)	11.10	0.802	21.99	0.404	34.08	0.269
Co/Mg/Al (1:1:1)	10.97	0.807	22.16	0.401	34.47	0.260
Co/Mg/Al (1:2:1)	11.00	0.801	22.06	0.394	34.13	0.263

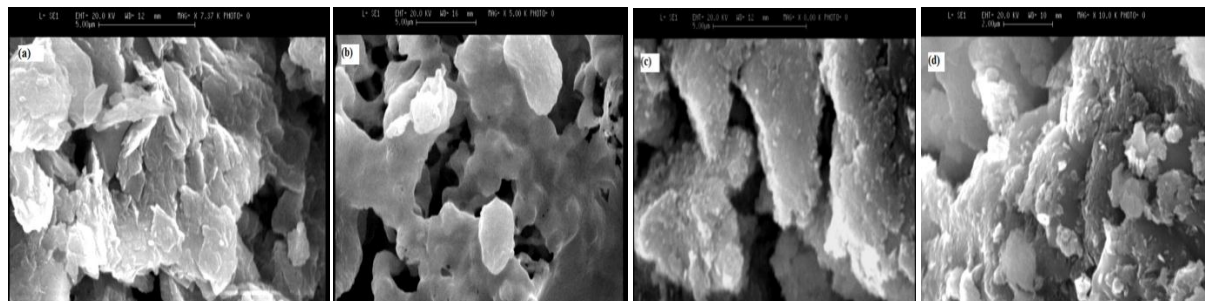


Figure 3. The SEM images of Nano hydrotalcites synthesized samples (Mg-Al) a- 1:1, b- 1:2, (Co-Mg-Al) c- 1:1:1, d- 1:2:1

Conclusion: The crystallinity and crystallite size of the hydrotalcite were observed to Varying with molar of M^{2+}/M^{3+} ratio. When the M^{2+}/M^{3+} ratio increases case the changes in the layer spacing. The crystallinity of Mg-Al hydrotalcite with ratio 1:1 was highest and that Co-Mg-Al hydrotalcites was lowest. Morphological analysis, by SEM method, revealed the formation of layered double hydroxides crystals, but also their cohesion, resulting in different particle sizes.

References

- [1] A. Brito; M. E. Borges; M. Garin M; A. Hernandez. *Energy & Fuels*, 2009, 23, 2902-2908
- [2] K. Setshedi; J. Ren; M. S. Onyango. *Int. J. Phy. Sciences*. 2012, 7, 63-69
- [3]. Vaccari A, *Catal. Today*. 1998, 41, 53-71
- [4]. G Defontaine; L J Michot; I Bihannic . *Langmuir*, 2004, 20, 1213-1222
- [5]. K. Motokura; N. Fujita; K. Mori; T. Mizugaki ; K. Ebitani; K. Kaneda. *J. Am. Chem. Soc.*, 2000, 122, 9674-9676

Efficient photocatalytic Suzuki cross-coupling reactions on Pd/ZnO nanoparticles under visible light irradiation.

Mona Hosseini-Sarvari^{*a}, Zahra Bazyar^a

^aDepartment of Chemistry, Faculty of Science, Shiraz University, Shiraz ۷۱۴۵۴, Iran

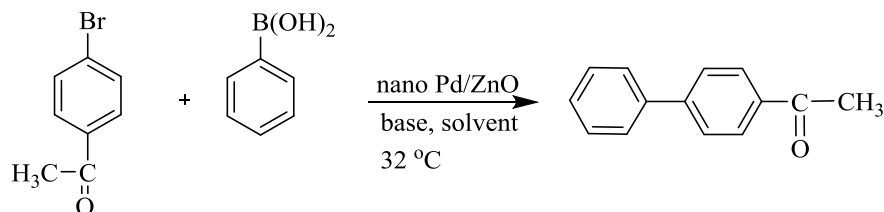
E-mail: Bazyarzahra@yahoo.com, Monahosseini@yahoo.com

Introduction: In the recent years, attention has been paid to design and fabrication of Nanoscale hybrid composite materials containing metal and semiconductor components show great performance in optics , electronics , catalysis, and other applications [۱]. There are three basic types of hybrid nanomaterials such as alloy, core/shell and blending nanostructures which they show many interesting and unique properties [۲]. Among these nanostructures, semiconductor/metal composites are studied due to their unique structure [۳]. Heterogeneous photocatalytic processes based on noble metals are used for various applications such as novel organic synthesis, environmental remediation [۳,۴]. construction and architecture [۴], energy sources [۵], biological detection [۴].The convert solar energy into chemical energy (photosynthesis) to drive catalytic reaction, has received wide attention. photocatalyst processes have prominent advantages such as the facility of being driven at ambient conditions, the ability of using solar light for chemical reaction, green and renewable energy source[۶].

Experimentals: To a solution of p-bromoacetophenone(۱ mmol) , phenylboronic acid(۱ mmol) and Cs₂CO₃ (۰.۲۴ mmol) in deionized water(۱ mmol), was add Pd/ZnO (۰.۰۰۱ g) . The reactant mixture was carried out under air atmospheres and stirred under visible light irradiation a ۱۱ W LED lamp . After reaction completion catalyst was separated by centrifuging and the solvent removed under reduced pressure, the crude product was purified by column chromatography.

Results and Discussion: For the coupling reaction of p-bromoacetophenone and phenylboronic acid (Scheme ۱), the reaction did not occur using only pure ZnO as catalyst or without any catalyst under irradiation. However, the Pd/ ZnO catalyst exhibited excellent photocatalytic activity under the given conditions.

After optimized conditions in the air and room temperature condition, the photocatalytic performance Of Pd/ZnO catalyst for coupling reactions were investigated with a series of differently substituted aryl halides (Br ,Cl) and phenylboronic acid.



Scheme 1. Representative reagent for the reaction.

Conclusion: In conclusion, We have successfully demonstrated that a heterogeneous Pd/ZnO catalyst used for cross-coupling reactions under visible light irradiation at ambient temperatures, even natural sunlight. The catalytic activity of Pd nanoparticles under visible light irradiation can be evidently increased by using the photoactive semiconductor ZnO as the support.

References:

1. X. Liu, Z. Li, W. Zhao, C. Zhao, J. Yang, Y. Wang. J. Colloid and Interface Science. 2014, 432, 170-175.
2. J. Kim, K. Yong. J. Nanoparticle Research. 2012, 14, 1033.
3. P. Georgieva, N. K., A. Bojinovab, K. Papazovab, K. Mirchevaa, K. Balasheva. Colloids and Surfaces A: Physicochemical and Engineering Aspects. 2014, 460, 240-247.
4. C. G. Silva, M. J. Sampaio, S. A.C. Carabineiro, J. W.L. Oliveira, D. L. Baptista, R. Bacsa, B. F. Machado, P. Serp, J. L. Figueiredo, A. M.T. Silva, J. L. Faria. J. Catalysis. 2014, 316, 182-190.
5. Q. Chen, Y. Xin, X. Zhu. Electrochimica Acta. 2010, 55, 34-42.
6. Q. G. J. Long, L. Fan, L. Chen, L. Zhao, H. Lin, X. Wang. J. Catalysis. 2013, 303, 141-150.
7. J. Manna, T.P. Vinod, K. Flomin, R. linek. J. Colloid and Interface Science. 2010, 460, 113-118.

Simple, fast and regioselective synthesis of novel 2-aminospiro[benzopyrano[2,2-a]phenazine-quinoxaline]-2-carbonitrile derivatives via a one-pot, two-steps and five-component reaction by a magnetically recyclable heterogeneous Chitosan-supported Fe_3O_4 nanoparticle catalyst

Maryam Mirzazadeh^a, Ali Reza Sardarian^{a*}

^a Department of Chemistry, College of Sciences, Shiraz University, Shiraz 71946-84790, Iran

Email address: Mirzazadeh_maryam@yahoo.com

Introduction:

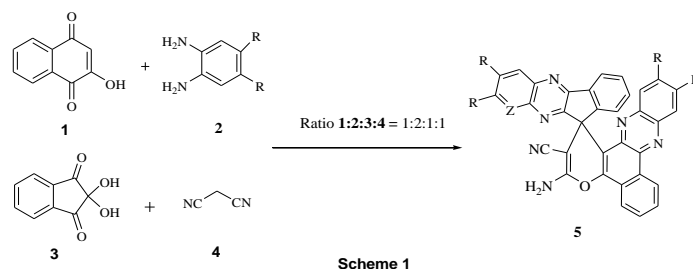
Synthesizing multifunctional and regioselective compounds which have a skeleton resembling those found in natural compounds and drug-like molecules alongside presenting efficient and ecofriendly methods for their synthesis is one of the main challenges in modern organic synthesis^[1]. Phenazine is a natural compound and synthetic products exhibit a wide range of biological activities. Such as antimalarial, trypanocidal, fungicidal and antiplatelet. Also, some of benzophenazines show anti-tumor activity in leukemia and solid tumors by their DNA intercalating ability^[2-4]. quinoxaline is another unique and privileged lead intermediate for designing synthesis of multifunctionalized compounds, especially those containing quaternary carbon centers and spiro-rings and chromene nucleus.

Experimental:

Fe_3O_4 @chitosan(20 mg) was added to a mixture of 2-hydroxynaphthalene-1,4-dione (1.0 mmol), benzene-1,2-diamine (1.0 mmol), in Ethanol and water (1:3, 10.0 mL). The resulting mixture was sonicated for 10 minutes. Then, benzene-1,2-diamine (1.0 mmol), 2,2-dihydroxy-2H-indene-1,3-dione (1.0 mmol) and malononitrile (1.0 mmol) were added and sonicated for an appropriate time. After completion of the reaction, the catalyst was easily separated from the reaction mixture with an external magnet and the precipitated product was filtered and washed with ethanol (2 mL) and water (10 mL) to afford the pure product.

Results and discussion:

We investigated different situations to find the best and most efficient method for synthesis of these multifunctionalized spiro compounds.



In the ^1H NMR spectra of these compounds, two isomers were seen which can be the result of electronic inductive and conjugative effects of aromatic rings played a principal role in controlling regioselectivity of amino groups at the time of formation of benzo[a]phenazin-9-ol or 1*H*-indeno[1,2-*b*]quinoxaline.

Conclusion:

Here, we have described a facile, efficient and regioselective one-pot, five-component synthesis of 3-aminospiro[benzo[*c*]pyrano[3,4-*a*]phenazine-1,1'-indeno[1,2-*b*]quinoxaline]-3-carbonitrile derivatives with formation of up to seven σ bonds including four C-N, two C-C and one C-O bonds and two spiro rings by using symmetrical and asymmetrical benzene-1,3-diamines, 3-hydroxynaphthalene-1,4-dione, 3,4-dihydroxy-1*H*-indene-1,3-dione and malononitrile.

Prominent among the advantages of this method are novelty, operational simplicity, broad substrate scope, good regioselectivity, excellent chemical yields, short reaction time and easy workup procedures employed. This approach is therefore potentially useful for the synthesis of structurally diversified spiro heterocyclic compounds with the crumene nucleus for the sake of medicinal or biological research.

References:

- 1) Polshettiwar, V.; Varma, R. S. *Chem. Soc. Rev.* 2008, 37, 1056–1097; (b) Ganem, B. *Acc. Chem. Res.* 2009, 42, 473–474; (c) Padwa, A. *Chem. Soc. Rev.* 2009, 38, 3072–3081; (d) Domling, A. *Chem. Rev.* 2006, 106, 17–89.
- 2) Hafez, H. N.; Hegab, M. I.; Ahmed-Farag, I. S.; El-Gazzar, A. B. A. *Bioorg. Med. Chem. Lett.* 2008, 18, 4038–4043.
- 3) Laursen, J. B.; Nielsen, J. *Chem. Rev.* 2004, 104, 1663–1686.
- 4) Neves-Pinto, C.; Malta, V.; Pinto, M.; Santos, R.; Castro, S.; Pinto, A. *J. Med. Chem.* 2002, 45, 740–743.

Nano-Sized Cu/Zn-Modified MCM-41 (Cu/Zn-MCM-41): Preparation, Characterization and Catalytic Application in A New More Atom Efficient Synthesis of Tetrasubstituted Imidazoles

Mohsen Shekouhy^a, Ali Moaddeli^a, Ali Khalafi-Nezhad^{a,*}

^a *Department of Chemistry, College of Sciences, Shiraz University, Shiraz 71345, Iran*

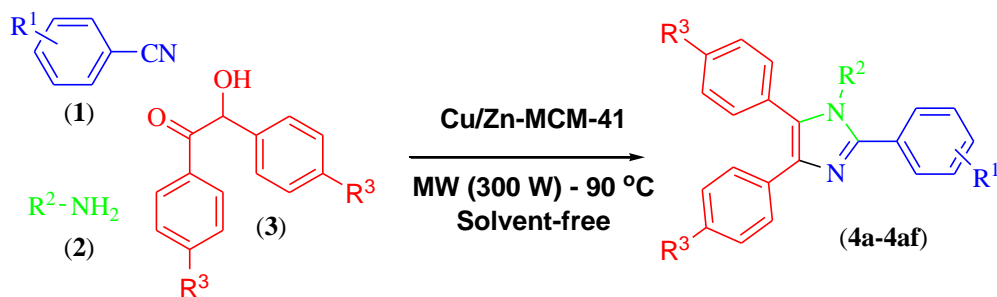
Email address: khalafi@chem.susc.ac.ir, m.shekouhy@gmail.com

Introduction:

More recently we introduce a novel and more atom efficient method for the synthesis of tetrasubstituted imidazoles *via* a one-pot three-component condensation of benzoin, nitriles and amines in the presence of trifluoroacetic acid under microwave irradiation [1]. This is noteworthy that the application of this method is in combination with some highlighted advantages, but, it is in combination with a crucial drawback, the application of trifluoroacetic acid that is a highly toxic and no recoverable material. So, we herein report the preparation of nano-sized Cu/Zn-modified MCM-41 as a new highly efficient and reusable mesoporous nano-catalyst for one-pot condensation of nitriles (1), amines (2) and benzoin (3) (Scheme 1).

Methods or Experimental: The method of direct insertion of Cu and Zn ions in the sol gel preparation step was applied for the synthesis of nano-sized Cu/Zn-MCM-41. For the preparation of tetrasubstituted imidazoles, In a pressure-resistance microwave glass tube, nitriles (1 mmol), amines (1 mmol), benzoin (1 mmol) and Cu/Zn-MCM-41 (20 mg) were added and then exposed to microwave irradiation. After the completion of reaction, ethyl acetate was added and resulting mixture was stirred magnetically at 80 °C for 10 minutes. Insoluble catalyst was separated with centrifugation, washed with ethyl acetate, dried at 120 °C for 2 and reused. The separated solution was kept at room temperature for 24 h and precipitated crystals were filtered and dried under reduced pressure to afford pure products.

Results and Discussion: In the first step, nano-sized copper/zinc-modified MCM-41 was prepared and the structure of synthesized catalyst was fully characterized with XRD, IR, Fe-SEM, HR-TEM, ICP, EDX and BET methods. After this, the reaction parameters were optimized under various conditions and the best results were obtained at 90 °C with 10 min microwave irradiation with the maximum power of 300 W in the presence of 20 mg of catalyst under solvent-free conditions. In the next step, the scope and efficiency of the process were explored under optimized conditions with the one-pot condensation of a broad range of structurally diverse aromatic nitriles (1), amines (2) and benzoin (3) (Scheme 1),



Scheme 1.

Obtained results are approximately similar to results of the application of trifluoroacetic acid [1]. All reactions were completed in short times (5-10 min) and corresponding products were obtained in good to excellent yields (82-95%). Besides, aryl nitriles bearing an electron withdrawing substitution on aromatic ring were reacted faster than the others bearing an electron donating group. In addition, the reaction was not proceeded in the case of aromatic primary amines with a strong electron withdrawing groups even after a long time of microwave irradiation (30 min). Application of substituted benzoin was lead to the similar results and halide or alkyl substituted benzoin were successfully converted to desired tetrasubstituted imidazoles whereas only a mixture of unknown products was obtained with the application of methoxy (as an electron donating group) substituted benzoin even after a long time of microwave irradiation (30 min). These results obviously establishes the similar catalytic efficiency of nano-sized Cu/Zn-modified MCM-41 and trifluoroacetic acid, while the application of Cu/Zn-MCM-41 is in combination with some other advantages such as recoverability and reusability of catalyst that will prevent the generation of toxic wastes.

Conclusion: In summary, the nano-sized copper/zinc-modified MCM-41 was prepared and fully characterized as a new heterogeneous mesoporous nano-catalyst and was then successfully applied in our recently reported more atom efficient one-pot synthesis of tetrasubstituted imidazoles with the aim of the enhancement in the ecofriendly aspects and avoid of the production of toxic waste.

References

[1] Khalafi-Nezhad, A.; Shekouhy, M.; Sharghi, H.; Aboonajmi, J.; Zare, A.; *RSC Advances*, 2016, 6, 67281-67289.

Tetrabutylammonium *L*-Prolinate (TBALP): A New Biodegradable Amino Acid-Based Ionic Liquid for the synthesis of ϵ -*H*-Benzo[*b*]pyrans

Reza Kordnezhadian^a, Mohsen Shekouhy^a, Ali Khalafi-Nezhad^{a,*}

^a Department of Chemistry, College of Sciences, Shiraz University, Shiraz 71345, Iran

Email address: khalafi@chem.susc.ac.ir, rezakd8830@gmail.com

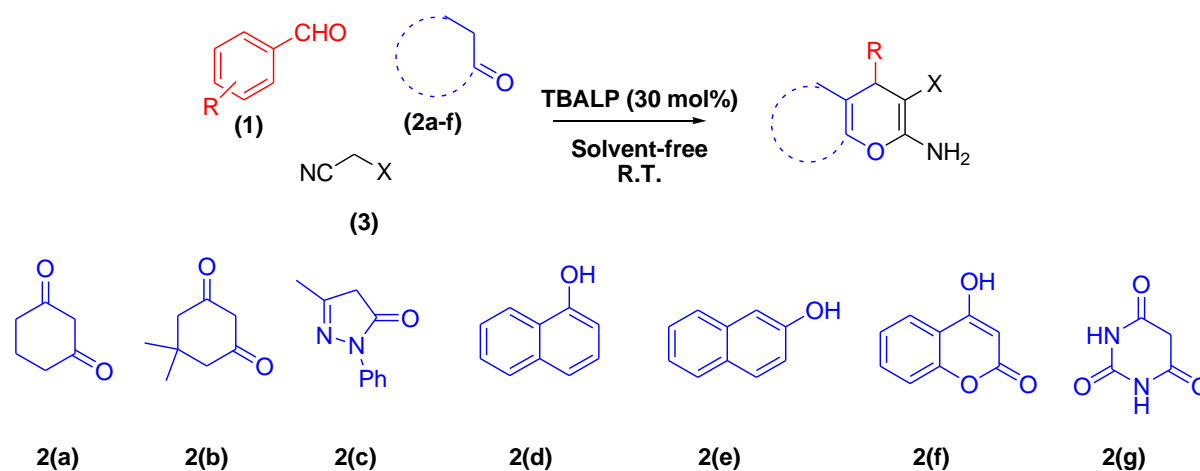
Introduction:

Ionic liquids (ILs) have captured the attention of the chemical community across the globe as green alternatives to classical environmentally destructive media [1]. However, most of them are neither sustainable nor biodegradable, and in many cases exhibit relatively high toxicities [2]. Biomolecules are generally biodegradable and many are non-toxic, as well as more sustainable than fossil resources. Many biomolecules can be incorporated into ILs, amino acids, however, have a special position amongst biomolecules as they can be easily converted into both anions and cations. Considering these facts, we herein report the TBALP as a new amino acid-based biodegradable ionic liquid for the synthesis of ϵ -*H*-benzo[*b*]pyrans. (Scheme 1)

Methods or Experimental: Tetrabutylammonium *L*-Prolinate (TBALP) was prepared with the direct reaction of equimolars of tetrabutylammonium hydroxide and *L*-proline. The chemical structure of obtained IL was then characterized with IR, Mass and NMR techniques. For the preparation of ϵ -*H*-benzo[*b*]pyrans, Ketone (1 mmol), malononitrile or ethyl cyanoacetate (1 mmol), aldehyde (1 mmol) and TBALP (0.5 mmol) were added in a 50 mL round-bottomed flask and the resulting mixture was stirred at room temperature. After completion of the reaction (as monitored by TLC), water (10 mL) was added to the mixture, stirred for 5 min and filtered to separate the catalyst. Separated catalyst was obtained in 99.7% after the evaporation of water under reduced pressure. Separated solids were then recrystallized from hot ethanol to afford the pure products.

Results and Discussion: In the first step, tetrabutylammonium *L*-Prolinate (TBALP) as a new biodegradable IL was prepared with the direct reaction of equimolars of tetrabutylammonium hydroxide and *L*-proline and the chemical structure of obtained IL was then characterized with IR, Mass and NMR techniques. After this, the reaction parameters for the one-pot three component synthesis of ϵ -*H*-benzo[*b*]pyrans were optimized under various conditions and the best results were obtained in the presence of TBALP (5 mol%) under solvent-free conditions at room temperature. In the next step, the scope and efficiency of the process were explored under optimized conditions with the one-pot condensation of a broad

range of structurally diverse aldehydes (1), carbonyl compounds possessing a reactive α -methylene group (2) and alkyl malonates (3) (Scheme 1),



X: CN, Et

Scheme 1.

Using this method, all reactions proceeded efficiently and the desired products were produced in good to excellent yields (80-93%) in very short reaction times (3-5 min) without formation of any side products. Aromatic aldehydes having electron withdrawing groups reacted at faster rate compared with those that substituted with electron releasing groups. Besides, our methodology has been used successfully for acid and base sensitive materials such as heteroaromatic aldehydes (furfural and thiophene-2-carbaldehyde), and corresponding 4H-pyrans were obtained in excellent yields and without any by-product.

Obtained results are approximately similar to results of the application of trifluoroacetic acid

Conclusion: In summary, we have reported a highly efficient, solvent-free-free and green method for very fast one-pot three-component synthesis of 4H-pyran derivatives using TBALP as a new and biodegradable amino acid-based IL. This method not only offers substantial improvements in the reaction rates and yields, but also avoids the use of hazardous catalysts or solvents.

References

[1] Amarasekara, A.S.; *Chemical Reviews*, 2016, 116, 613-6183.

[2] Jordan, A.; Gathergood, N.; *Chemical Society Reviews*, 2015, 44, 8200-8237.

Cyclizations and Unexpected C–C-Bond Cleavage Reaction

Somayeh Firoozi^a, Mona Hosseini-Sarvari^{a*}

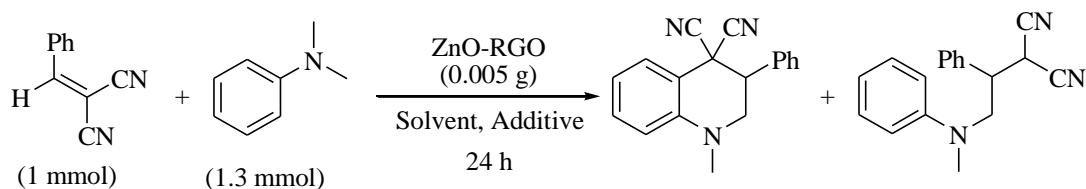
^a Department of Chemistry, Faculty of Sciences, Shiraz University

Email address : hossaini@shirazu.ac.ir , firoozi.org.chem@gmail.com

Introduction: C-H activation is C-H bonds conversion into C-C or carbon-heteroatom bonds. This concept allows the chemists to exploit organic compounds in unimaginable ways resulting a revolution in synthetic approaches [1-3]. It faces two challenges: the activation of inactive C–H bond in molecule and selective activation of specific C–H bond between all of which [4-6]. Herein, we present novel, green, and practical method for cyclization and C–C bond cleavage through this method.

Experimental: Zinc oxid-reduce graphene oxide was added to stirring mixture of γ -arylidene malononitrile, *N,N*-dimethyl aniline, and hydrogenperoxid in CH₃CN. The progress of reaction was followed by TLC and after reaction quench, the obtained reaction mixture was centrifuged. Obtained residue was filtered and washed by CH₃CN. The main product was finally separated by silica gel plate.

Results and Discussion: We used the reaction between phenylidene malononitrile and *N,N*-dimethyl aniline with zinc oxid-reduce graphene oxide as catalyst in the presence of various gases such as Ar, O₂ and air atmosphere in acetonitrile at room temperature (Scheme 1). There is no differences between reaction atmospheres (table 1). Various solvents including CH₃CN, CHCl₃, THF, DMF, EtOH, H₂O, CH₃CN / H₂O, and EtOH / H₂O were also applied in this reaction. Although the products were not synthesized using CH₃CN, CHCl₃, THF and DMF, two products were found in EtOH, H₂O, CH₃CN / H₂O, and EtOH / H₂O. In this while, using CH₃CN / H₂O presents more yields and we decided to apply it for further investigations.



Scheme 1.

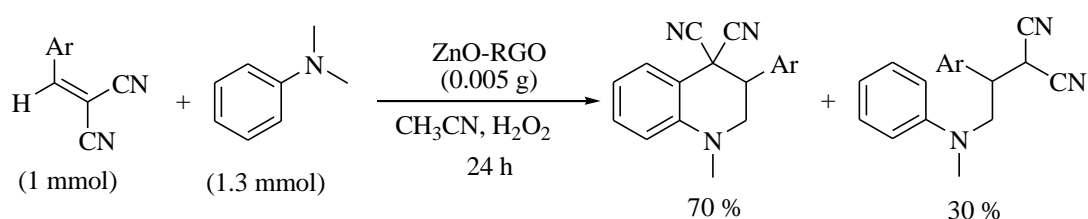
Table 1. The optimization data of reaction.

Entry	Solvent	Atmosphere	Additive	Conversion (%)
1	CH ₃ CN	Air	-	-
2	CH ₃ CN	O ₂	-	-
3	CH ₃ CN	Ar	-	-

4	CHCl ₃	Air	-	-
5	THF	Air	-	-
6	DMF	Air	-	-
7	EtOH	Air	-	10, 0
8	H ₂ O	Air	-	10, 0
9	CH ₃ CN / H ₂ O	Air	-	20, 0
10	EtOH / H ₂ O	Air	-	10, 0
11	CH ₃ CN	Air	H ₂ O ₂ (1 mmol)	70, 30
12	CH ₃ CN	Air	t-BuOOH (0.5 mmol)	Trace
13	CH ₃ CN	Air	t-BuOOH (1 mmol)	>Trace
14	CH ₃ CN	Air	t-BuOOH (1.5 mmol)	>Trace
15	CH ₃ CN	Air	I ₂	Trace
16	CH ₃ CN	Air	DDQ	Trace

The effect of oxidative reagents such as H₂O₂, t-BuOOH, I₂ and DDQ was investigated in table 1 and the best result was observed in the presence of H₂O₂ (table 1, entry 11) in 70:30 ratio of products. To find the effect of photo on the reaction, we study the reaction under dark condition and it was surprisingly observed that the reaction progress is notable. Herein, it was confirmed the reaction has no dependence to photo. Based on these results, all derivatives have been synthesized in these optimized conditions (Scheme 2).

Scheme 2



Ar : C₆H₅, 4-Cl-C₆H₄, 4-OH-C₆H₄, 3-Me C₆H₄, 2-Br C₆H₄, 4-NO₂-C₆H₄

Conclusion: In conclusion, we have successfully developed a new strategy of α sp² C-H activation of t-amines at the present zinc oxid-reduce graphene oxide and hydrogenperoxid for C-C bond formation reaction.

References

- [1] Davies, H. M. L.; Daniel, M. J. *Org. Chem.*, 2016, 41, 243-250.
- [2] Chen, D. Y. K.; Youn, S. W. *Chem. Eur. J.*, 2012, 18, 9402-9414.
- [3] White, M. C. *Synlett*, 2012, 2746-2748.
- [4] Huang, L.; Zhao, J. *Chem. Commun.*, 2013, 49, 3701-3703.
- [5] Chen, D. Y. K.; Youn, S. W. *Chem. Eur. J.*, 2012, 18, 9402-9414.

Synthesis of Two Novel Diastereoselective Amonafide β -Lactam Conjugates

Javad Ameri Rad^a, Aliasghar Jarrahpour^{a*}

^a Department of Chemistry, College of Sciences, Shiraz University, Shiraz ۷۱۴۰۴, Iran

Email address: jarrah@susc.ac.ir; aliasghar7683@yahoo.com

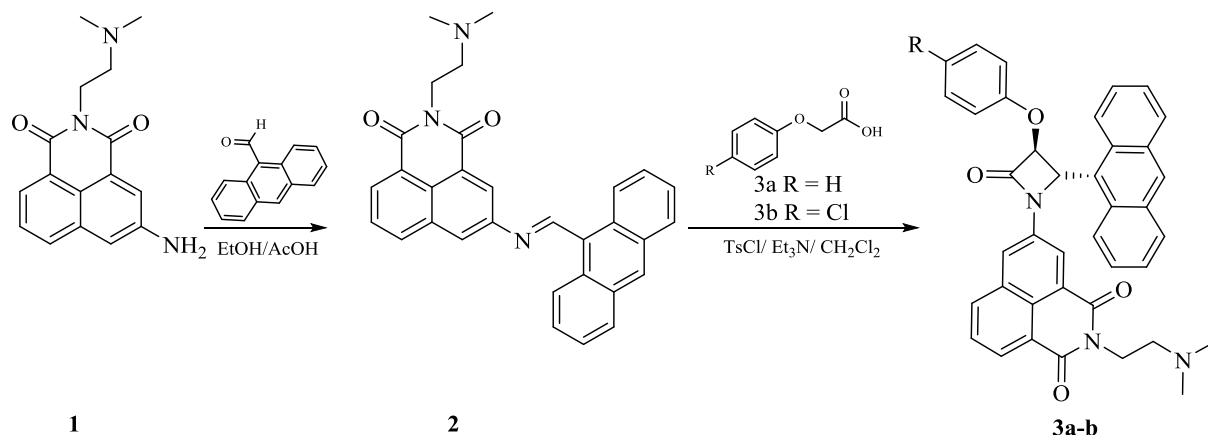
Introduction: The β -lactam ring is the important functional group responsible for the incomparable effectiveness antibacterial property of the most widely employed antibacterial agents. The β -lactam has been widely recognized as an important synthetic intermediate in organic synthesis due to its presence in most widely used antibiotics such as penicillins and cephalosporins. Recent decades have witnessed the modification of β -lactam ring to prove their broad range of pharmacological activities such as cholesterol absorption inhibitors, thrombin inhibitors,[۱] antimalarial activities, anti-fungal[۲-۳]. On the other hand, cyclic imides have received special attraction due to their widely potential pharmaceutical applications [۴]. The design of highly efficient antitumor agents is important in organic and medicinal chemistry fields. Isoquinolindione (naphthalimide) based anticancer drugs constitute an indispensable part in the development of anticancer drugs. Since the first lead compound, Amonafide which was discovered by Braña et al, the development of naphthalimide anticancer agents has resulted in a series of drug candidates such as amonafide, mitonafide, elinafide and bisnafide.[۵]

Experimental: General procedure for the synthesis of amonafide β -lactam conjugates ۲a-b:

The amonafid have been synthesized according to a report [۶], A mixture of amonafide (۱.۰۰ mmol) and anthracene-۹-carbaldehyde (۱.۱۰ mmol) was refluxed in ethanol (۲۰ mL) for ۵ h. Then the solvent was evaporated under vacuum to afford the crude Schiff base ۲. This compound was filtered and washed with ethanol to afford pure solid Schiff base. Finally a mixture of Schiff base ۲ (۱.۰۰ mmol), triethylamine (۵.۰۰ mmol), phenoxy acetic acid derivatives (۱.۵۰ mmol) and tosyl chloride (۱.۵۰ mmol) in dry CH_2Cl_2 (۱۵ mL) was stirred at room temperature for several hours. Then the mixture was washed with HCl ۱N (۲۰ mL), saturated NaHCO_3 (۲۰ mL) and brine (۲۰ mL). The organic layer was dried (Na_2SO_4), filtered and the solvent was evaporated to give the crude products. Crude conjugates were purified by recrystallization from ethylacetate (Scheme ۱).

Results and Discussion: The synthesis of β -lactam conjugates ۲a-b were achieved according to the outlined procedure in Scheme ۱. The structure of β -lactam ۲a-b was characterized by FT-IR, ^1H -NMR, ^{13}C -NMR, Mass and elemental analysis. Under these experimental conditions, this reaction afforded the *trans*- β -lactams. The stereochemistry of compounds were assigned from the coupling constants of the two β -lactam ring protons H-۳ and H-۴ ($J_{3,4}$ Hz $> J_{3,4}$ for the *trans* stereoisomer). The ^1H -NMR spectrum of *trans*- β -lactam ۲b showed a doublet at ۵.۶۹ and ۵.۹۴ ppm ($J = ۲.۵۰$ Hz) for H-۴ and H-۳ respectively. Two singlets at ۰.۸۱ ppm and ۰.۸۳ ppm for the two methyl groups and a multiplet at ۱.۴۷-۱.۷۱ ppm for two CH_2 protons. The aromatic protons exhibited in appropriate chemical shifts. The ^{13}C -NMR spectrum exhibited the following signals: Aliphatic groups at ۳۷.۲, ۴۴.۹, ۵۶.۲ and ۶۰.۹ ppm, the β -lactam ring carbons C-۳ and C-۴ at ۸۱.۶ and ۸۶.۷ ppm, aromatic carbons at

117.0-133.3 ppm, the β -lactam carbonyl appeared at 161.0 ppm and amonafide carbonyl groups at 180.1 and 172.6 ppm. The IR spectrum of **2b** showed the characteristic absorption of the β -lactam carbonyl at 1709 cm^{-1} .



Scheme 1: Synthesis of Amonafide β -Lactam Conjugates **3a-b**

Conclusion: In this study, we have described the synthesis of two amonafide β -lactam hybrid by a stereoselective ketene-imine cycloaddition (Staudinger reaction). To the best of our knowledge, this is the first time that amonafide has been used for the synthesis of γ -azetidinones. This novel imine afforded good to excellent yield of the desired β -lactams and with exclusive diastereoselectivity. Further studies are now under investigation to study anti-cancer and DNA intercalation bioactivity and drug-like properties of the β -lactam and it will be reported in due course.

References:

- [1] Claudio, P.; Jesu's, A. M.; In'aki, G.; Mikel, O. Synlett 2001, 1113. P.D. Mehta, N.P.S. Sengar, A.K. Pathak. Eur. J. Med. Chem. 45 (2010) 5541-5560.
- [2] A. Jarrahpour, E. Ebrahimi, R. Khalifeh, H. Sharghi, M. Sahraei, E. De Clercq, V. Sinou, C. Latour, L. Djouhri Bouktab, J.M. Brunel. Tetrahedron 68 (2012) 4740-4744
- [3] A. Jarrahpour, E. Ebrahimi, V. Sinou, J.M. Brunel, Eur. J. Med. Chem. 87 (2014) 364-371.
- [4] Zhang, Y-Y.; Zhou, Ch-H. Bioorganic & Medicinal Chemistry Letters 21 (2011) 4349-4352.
- [5] Braña, M. F.; Ramos, A. Curr. Med. Chem.-Anti-Cancer Agent. 1 (2001) 237-250.
- [6] Ares, J. J., Kador, P. F.; Miller D. D. J. Med. Chem. 29 (1986) 2384-2389.

Nano-rods Zinc Oxide as a heterogeneous recyclable and efficient catalyst for the solvent free synthesis of α -hydroxyl phosphonate derivatives

Mona Hosseini-Sarvari^{*a}, Hossein Sheikh^a

^aDepartment of Chemistry, Faculty of Science, Shiraz University, Shiraz ۷۱۴۱۴, Iran

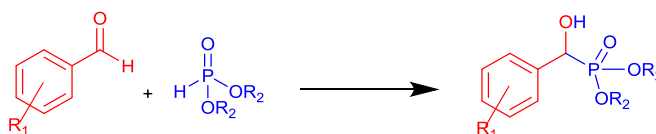
E-mail: orgchemist77@gmail.com, Monahosseini@yahoo.com

Introduction: In green chemistry, researcher tries to prevent environmental problems which are caused due to the negative impacts of chemical substances. One of the major efforts of chemists to fulfill this idea is to avoid toxic organic solvents which are the main reason of pollution in underground water resources. To this purpose, many solvent free protocols have been developed for various kinds of organic reactions.[۱-۴]

Carbon-Phosphor (C-P) bond formations have been noticed in recent decade. Among all reasons of these significant attentions, the biological activity of phosphonated molecules including enzyme inhibitors such as EPSP synthetase, reain, HIV protease, PTPases and herbicides, is particularly the main attitude.[۵]

So, it is important to find a simple and eco-friendly method for the synthesis of this important category of compounds. Consequently in continuation of our previous report on the application of nano-rod ZnO,[۶] herein we use this catalysts as a reusable and efficient catalyst for the synthesis of α -hydroxyl phosphonate in a green protocol.

Experimentals: To begin attempts to optimize the reaction parameters for the Synthesis of hydroxylphosphonate derivatives, a reaction of benzaldehyde and dialkylphosphonate as model substrates was performed in the presence of nano-rod ZnO. In the model reaction, a mixture of dimethyl phosphonate (۱ mmol) and benzaldehyde (۱ mmol) in the presence of nano-rod ZnO as a catalyst was stirred continually.(Scheme ۱)



Scheme ۱. Representative reagent for the reaction.

The reaction was pursued with TLC till the starting material was finished. According the reaction yield we decided to optimize the solvent, catalyst amount and temperature.

Results and Discussion: Starting material (1 mmol) and ZnO nano-rod (5 mol %) as catalyst were admixture in 10 ml flask, heated in an oil bath to 80 °C and stirred for suitable time. completion of the reaction was followed by TLC.

After optimized conditions in the air and 80 °C, the performance Of ZnO catalyst for (C-P) bond formations were investigated with a series of differently substituted benzaldehyde and dialkylphosphonate.

Conclusion: In conclusion, we have successfully demonstrated that a ZnO nano-rod catalyst used for (C-P) bond formations under mild condition at ambient temperatures.

References:

1. X. Liu, Z. Li, W. Zhao, C. Zhao, J. Yang, Y. Wang. J. Colloid and Interface Science. 2014, 432, 170-175.
2. J. Kim, K. Yong. J. Nanoparticle Research. 2012, 14, 1033.
3. P. Georgieva, N. K., A. Bojinovab, K. Papazovab, K. Mirchevaa, K. Balasheva. Colloids and Surfaces A: Physicochemical and Engineering Aspects. 2014, 260, 240-247.
4. C. G. Silva, M. J. Sampaio, S. A.C. Carabineiro, J. W.L. Oliveira, D. L. Baptista, R. Bacsa, B. F. Machado, P. Serp, J. L. Figueiredo, A. M.T. Silva, J. L. Faria. J. Catalysis. 2014, 316, 182-190.
5. M. Hosseini-Sarvari and M. Tavakolian. Canadian Journal of Chemistry 2012, 90, 11, 1117-1122.

بسمه تعالی

عنوان سخنران :

نقش شیمی و فارغ التحصیلان شیمی در توسعه واقعی کشور

خلاصه مباحث سخنرانی:

در این سخنرانی تلاش شده است تا با بررسی اجمالی موارد زیر و همچنین یک سری تجربیات عملی به نقش شیمی و فارغ التحصیلان شیمی در توسعه واقعی کشور پرداخته شود:

(۱) وضعیت کلی علم شیمی در جهان و ایران

(۲) پتانسیل های مختلف کشور برای توسعه

(۳) توانمندی های ویژه شیمیدان های کشور برای توسعه

(۴) نقش و رابطه علم شیمی در مقایسه با دیگر علوم

البته لازم به ذکر است که آنچه تاکنون در کشور توسط شیمیدانان کشور بواسطه علم شیمی صورت گرفته فاصله زیادی را تا حالت ایده آل دارد. بنابراین ضمن برشمردن برخی از این عوامل تلاش شده است تا راهکارهایی نیز پیشنهاد گردد .

آیا تحقیقات در کشورهای در حال توسعه در انطباق با مسائل زیست محیطی است؟

Application of Ketene Dithioacetals, Ketene Aminals, and Enaminones in the
Synthesis of Heterocyclic Compounds *via* Multicomponent Reactions

Abdolali Alizadeh

A short review of electrochemical, solid phase extraction and resonance rayleigh scattering research works

Hooshang Parham
Shahid Chamran University, Ahvaz
Email:hoparham@yahoo.com

We established a method for simultaneous determination and detection of I^- , Br^- and Cl^- using SWV as a sensitive end-point detection system. The method is based on the combination of a coulometric titration technique (constant current chronopotentiometry) that is electronically switched to SWV on the same electrochemical instrument. An electronic device which could electronically change two different working electrodes (working electrodes switching circuit) was designed and applied. The switching circuit changed the working electrodes (Ag or static mercury drop electrode, SMDE) according to different electrochemical methods under run (SMDE for SWV and Ag electrode for constant current chronopotentiometry)[¹]. This method can determine 5×10^{-6} mol of Br^- and I^- and also 5×10^{-6} mol of Cl^- in a sample solution.

A major advantage of using MIONs as solid phase extractor is the possibility of collecting of the particles by application of a magnetic field in a batch system. This makes magnetic nanoparticles excellent candidates for combining adsorption properties with ease of phase separation. We have introduced an efficient method for the removal of Hg (II) ion from polluted water using modified magnetic iron oxide nanoparticles with γ -mercaptobenzothiazole (MBT) which forms strong complex with Hg (II) ion. The proposed method shows high potential for effective removing of traces of Hg (II) ion from water solution in a short time via an easy procedure and lowers the concentration of this ion close to the standard healthy levels announced by the World Health Organization (WHO), that declared there is no safe level of mercury for human beings, in other words, mercury is so poisonous that no amount of mercury absorption is safe [²].

In our current research we used Resonance Rayleigh Scattering (RRS) as a detection technique for different analytes using nanoparticles. Resonance Rayleigh scattering has drawn much more attention in recent years and made important contributions in many scientific areas. When a particle is exposed to an electromagnetic radiation, the electrons in the particle oscillate at the same frequency as the incident wave. Resonance Rayleigh scattering takes place when the wavelength of Rayleigh scattering is located at or close to the molecular absorption band. The properties of scattered light depend on the size, composition, shape, homogeneity of the nanoparticles, and refractive index of the medium.

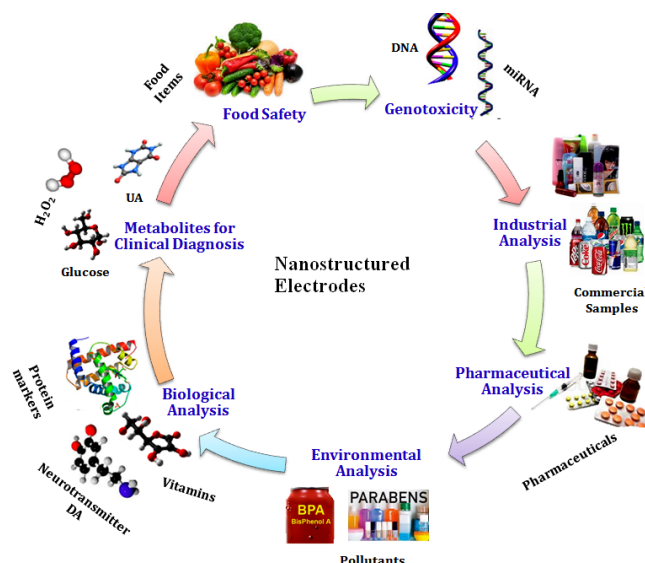
Simple, novel and sensitive methods were developed to determine ethion, thiram and γ -mercaptobenzothiazole in water samples [³⁻⁵]. These methods were based on that ethion or thiram can interact with silver and gold nanoparticles (AgNPs, AuNPs) and change the resonance Rayleigh scattering (RRS) intensity of them. The change in RRS intensity (ΔI_{RRS}) is linearly correlated with the concentration of ethion, thiram and γ -mercaptobenzothiazole added over the wide ranges of analytes in $\mu\text{g L}^{-1}$ ($1.0-900.0$, $1.0-200.0$ and $0.0-300.0$, respectively). Analytes can be measured in a short time (3-5 min) without any complicated or time-consuming sample pretreatment processes.

[¹]- H. Parham; B. Zargar. Anal Chim Acta, 464, 2002, 110-122.

- [۲]-H. Parham; B. Zargar; R. Shiralipour. J Hazard Mat, ۲۰۵-۲۰۶, ۲۰۱۲, ۹۴-۱۰۰.
- [۳]-H. Parham; S.Saeed. Talanta, ۱۳۱, ۲۰۱۵, ۵۷۰-۵۷۶.
- [۴]-H. Parham; N. Pourreza; F. Marahel. Talanta, ۱۴۱, ۲۰۱۵, ۱۴۳-۱۴۹.
- [۵]-H. Parham; N. Pourreza; F. Marahel. Spectrochim Acta Part A: Molecular and Biomolecular Spectroscopy, ۱۵۱, ۲۰۱۵, ۳۰۸-۳۱۴.



Nanostructured Electrochemical Sensors and Biosensors



Saeed Shahrokhian

Department of Chemistry, Sharif University of Technology, Tehran ۱۱۱۵۵-۹۵۱۶, Iran

Today, sensing and biosensing approaches comprising electroanalytical principles have been emerged as a scintillating analytical tool for rapid onsite monitoring of a diverse range of compounds. Electroanalytical methods based on chemically modified nanostructured electrodes offer a versatile platform for analytical sensing and biosensing of redox moieties with various advantages of high sensitivity and defined response characteristics with accuracy, good reproducibility and precision. Significant modifications have been made for designing robust and stable sensors from the time of tiny mercury drop electrodes to the today's advanced nanosensors based on a variety of functional nanomaterials, peptides, conducting polymers, enzymes, whole cells, antibodies and aptamers.

In our research group, promising electrochemical sensors based on composites of carbon nanostructures, e.g. functionalized carbon nanotubes, carbon nanoparticles, nanodiamond and graphene with various metals nanoparticles and also conducting polymers are developed. Under the optimized experimental conditions, the prepared nanostructured modified electrodes were successfully applied for the accurate determination of some pharmaceutically important compounds in drug formulations and clinical preparations (blood serum and plasma).

Improved dye-sensitized solar cells properties by using modulated electrical field in the electrophoretic deposition and advanced electrocatalyst for highly efficient hydrogen and oxygen evolution reaction

Behzad Rezaei

Department of Chemistry, Isfahan University of Technology, Isfahan ۸۴۱۵۶-۸۳۱۱۱, IR Iran

Concerns about energy encourage many researchers to find trustful, clean and equitable replacements for the finite resources of energy. So solar cells, fuel cell and hydrogen and oxygen evolution systems, have being attracted many attentions. Although silicon p–n junctions basis are most commercialized photovoltaic solar cells, dye-sensitized solar cells (DSSCs) can be a promising future generation of solar energy devices. This can be ascribed to their low cost, clean, simple processing operations and renewability for transferring inexhaustible sunlight into electrical energy. DSSCs have lower efficiencies compared to silicon solar cells, so for improving their performance, new modification methods with a facile transport pathway have been extensively investigated. Accordingly, surface modification of TiO_2 by quantum dots, metal doping and nano-sized noble metals, coupling to semiconductor and designing new morphologic photo-anodes have been developed to enhance efficient electron transport in DSSCs.

One of the main problem for the preparation of DSSCs is uniformity of prepared photoelectrodes [۱,۲]. Electrophoretic deposition method (EPD) under electrical field conditions as a very simple and powerful method has gained extensive attentions in photoelectrodes preparation for DSSCs systems (Fig.۱). This method is especially attractive due to the preparation of uniform coated layer, its low-cost, simple equipment, controllable situation and binder-free process during less time, compared to the other coating techniques. Accordingly, the potential of EPD in large-scale production and usage in future commercialization can not be ignorable.

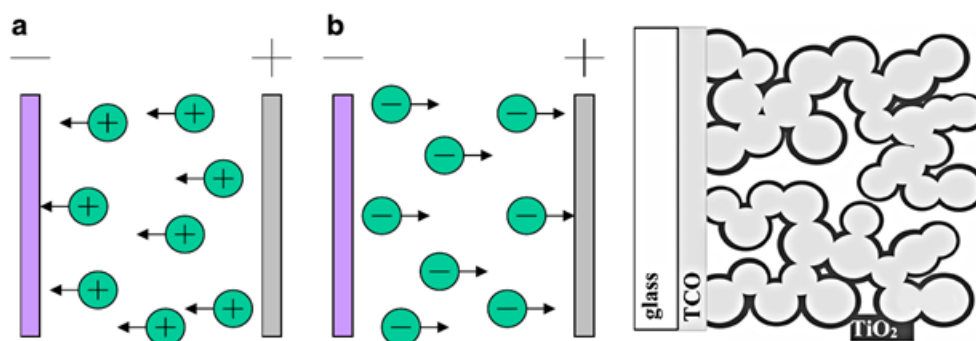


Fig. ۱: Electrostatic is driving force in deposition of nano-particles by EPD method.

So in our research, investigated some different pulsed EPD methods to prepare suitable DSSCs photoelectrodes and obtained results represented advantages compared to the conventional DC-EPD methods (Fig. ۲). A Film-coated on FTO using pulsed EPD method has better morphology, inter-particle connectivity, and also fewer particles aggregation.

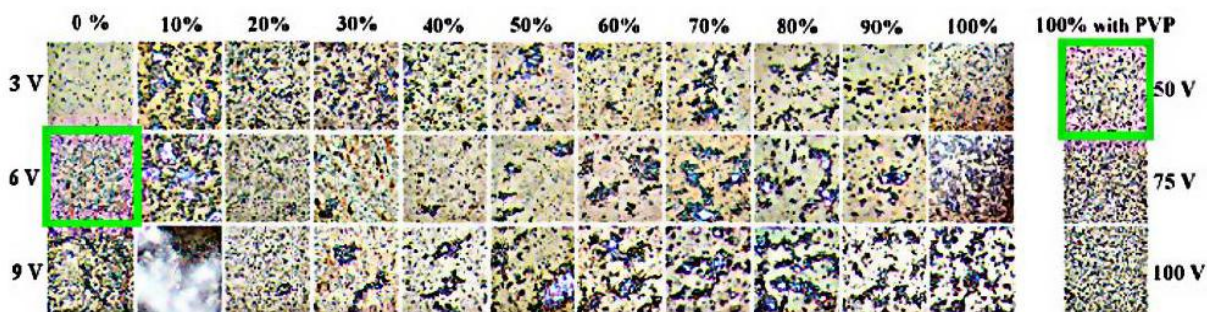


Fig. ۲: Optical microscope images of deposited TiO_2 nanoparticles at the surface of FTO

The structure of film leads to the highest specific surface area, which can allow for more absorption of dye molecules and provide appropriate blocking properties preventing recombination reactions and also increase the injected electrons lifetime.

Hydrogen as a fuel is also one of the most capable candidates to replace petroleum fuels in future. Consequently, efficient technologies of hydrogen production are required. In some of the other works, developed different modification methods to produce suitable electrodes for high performance electrochemical hydrogen and oxygen evolution reaction by fabricating bi or three metallic or carbon nanoparticles on suitable substrates such as nanoporous stainless steel (NPSS). NPSSs were prepared by electrochemical anodization process that was used as a cheap, stable and powerful support for loading of catalysts.

References:

۱. H. C. Weerasinghe, F. Huang, and Y.-B. Cheng, Nano Energy ۲, ۱۷۴ (۲۰۱۳).
۲. H.-W. Chen, C.-P. Liang, H.-S. Huang, J.-G. Chen, R. Vittal, C.-Y. Lin, K. C.-W. Wu, and K.-C. Ho, Chem. Commun. (Camb). ۴۷, ۸۳۴۶ (۲۰۱۱).

From classical to advanced analytical instrumentations and material science

H. Bagheri

Environmental and Bio-Analytical Laboratories, Department of Chemistry, Sharif University of Technology, P.O. Box 11365-9516, Tehran, Iran

bagheri@sharif.edu

The construction of combined capillary gas chromatography-fluorescence spectrometry was our research focal point in 1986-1991. Some applications of this sensitive and selective instrumentation was extended to the determination of two- and three-ring aromatic hydrocarbons in commercial light hydrocarbon fractions and determination of carbaryl and 1-naphthol in English apples and strawberries. The progress in the hyphenation of liquid chromatography and mass spectrometry using thermospray and particle beam was a hot topic in early 90's and led to the ultra-trace analysis of aquatic samples in conjunction with *off-line* and *on-line* solid phase extraction. Since then, sample preparation step prior to the instrumental analysis for biological and environmental analyses has become our major research field. Some research aspects of sample preparation are oriented toward the development of efficient, economical, miniaturized and environmentally friendly methods to overcome the limitations of traditional approaches. Electrospinning provides an approach to generate a wide variety of nonwoven fiber mats of polymers, composites, and ceramic precursor solutions. Various nanofibers have been implemented to the extraction of different analytes [1,2]. Polymeric nanocomposites are a class of materials in which nanoscale particulates such as spherical inorganic minerals are dispersed within the polymeric networks. Polymeric nanocomposites, depending on type and content of the incorporated nanoparticles, exhibit improved properties in compared with pure polymers [3,4]. On the other hand, superhydrophobic surfaces exhibit extreme water repellency, with water droplets resting on them with high contact angles. Artificial superhydrophobic surfaces are fabricated by combining rough surface morphology and low surface energy coatings. Here, very recent approaches toward preparation of some extracting media comprising electrospun nanofibers, nanocomposites, dendrimeric nanomagnetic, superhydrophobic materials and microfluidic system [5] toward microextraction techniques will be addressed.

References

- [1] H. Bagheri, O. Rezvani, S. Banihashemi, J. Chromatogr. A, 2016, 1434, 19-28.
- [2] H. Bagheri, P. Khanipour, A. Roostaie, J. Chromatogr. A, 2016, 1433, 34-40.

[۳] H. Bagheri, H. Javanmardi, A. Abbasi, S. Banihashemi, J. Chromatogr. A, ۲۰۱۶, ۱۴۳۱, ۲۷-۳۵.

[۴] H. Bagheri, S. Banihashemi, Anal. Chim. Acta, ۲۰۱۵, ۸۸۶, ۵۶-۶۵.

[۵] H. Bagheri, M. Allahdadlalani, C. Zamani, J. Sep. Sci., ۲۰۱۶, ۳۹, ۴۲۲۷-۴۲۳۳.

On the theory of electrochemical metal deposition

Wolfgang Schmickler

Department of Theoretical Chemistry, Ulm University, Ulm, Germany

During the last decade, in search of better fuel cells and batteries, the theory of electrochemical reactions has focused on electrocatalysis. In contrast, the field of metal deposition and dissolution, which includes corrosion, has been neglected, even though its economic importance is at least as great. This fundamental class of reactions poses a principal problem, which has been aptly called the enigma of metal deposition [1]: Ions in aqueous electrolytes are strongly solvated; univalent ions have hydration energies of the order of 2 eV, di- and trivalent ions of the order of 4 eV and 6 eV. When these ions are deposited on a metal electrode, they have to shed their solvation sheath, and one would expect activation energies of the order of half the solvation energies, which would make these reactions extremely slow. However, in practice these reactions are quite fast, and silver deposition is one of the fastest electrochemical reactions.

In order to investigate this problem, we have developed a quantum theory which contains ideas from Marcus-Hush theory, the Anderson-Newns model, and our own work. The corresponding model Hamiltonian contains a few interaction parameters, which we have obtained from density functional theory and molecular dynamics simulations. We have performed explicit calculations for the deposition of silver, copper, and zinc. Monovalent ions like Ag^+ fit well into the structure of water, and can approach the electrode surface without loss of solvation. In addition, their valence s electrons interact strongly with the sp bands of the corresponding metal, which catalyses the reaction. For silver deposition we obtained an activation energy of about 0.4 eV, in good agreement with experimental values [2]. In this case the rate-determining step is the diffusion of the deposited silver atom to a kink site, where it is incorporated.

The deposition of the two divalent ions Cu^{++} and Zn^{++} occurs in two steps [3]; the transfer of the first electron occurs in the outer sphere mode. Our calculated energies of activation for copper deposition are in line with experiments, but for zinc we obtain an energy of activation that is much too high. The problem is the energy of the univalent ion, which is much higher than

that of the divalent. We suggest that zinc depositions is aided by the formation of complexes, and present experimental evidence for this suggestion.

[¹] E. Gileadi, J. Electroanal. Chem. 660 (2011), 247.

[²] L. M.C. Pinto, E. Spohr, P. Quaino, E. Santos and W. Schmickler, *Ange-
wandte Chemie Int. Ed.*, 52 (2013) 7883.

[³] L. M.C. Pinto, P. Quaino, E. Santos and W. Schmickler, *ChemPhysChem*
15 (2014) 132.

**Design, synthesis and characterization of some transition metal compounds
(coordination polymers, nanocatalysts) for oxidation reactions and
biodiesel production**

Faezeh Farzaneh

*Department of Chemistry, Faculty of Physics & Chemistry, Alzahra University, P.O.Box ۱۹۹۳۸۹۱۱۷۶, Vanak,
Tehran , Iran*

Email address: faezeh_farzaneh@yahoo.com, farzaneh@alzahra.ac.ir

The design of new heterogeneous catalysts for selective and environmentally friendly transformation of some organic reactions is nowadays a remarkable research goal. Different solid materials, such as microporous, nanoporous or silica and silicate layers have been used as supports. The utilization of magnetic nanoparticles as solid supports is a new approach in recent years. Preparation of new transition metal complexes followed by immobilization on magnetic nanoparticles surface is a suitable method for using them as heterogeneous catalyst. Herein, the synthesis, characterization and investigation on catalytic behavior of some new prepared complexes with Schiff base ligands of amino acids with α -hydroxynaphthaldehyde or polypyridyl ligands followed by immobilization on modified magnetic nanoparticles or other solid supports will be described. Nanomagnetic particles are also one of the most popular materials with increasingly use in immobilizing proteins, enzymes, and other bioactive agents in analytical, biochemistry, medicine, and biotechnology [1-4].

More recently, another class of materials attracted the attention of scientists from university and industry are coordination polymers, or metal-organic frameworks (MOFs), also called porous coordination polymers (PCPs). They are constituted by multi-functionalized organic molecules that are bound together by inorganic units to form porous solids with a regular and sometimes predictable geometry. These compounds containing redox active ions of transition metals such as Fe, Co, Ni, Cu, Mn, Mo and V may also have catalytic activity for some transformation of organic reactions. The expansion of this research area is not only interesting in terms of structural diversity and fascinating properties but also regarding the wide range of applications in catalysis, drug delivery, adsorption, gas storage and separation. Recently, many attempts have been made on using mixed-ligands for preparation of MCPs especially mixed N-

containing and polycarboxylate ligands. In fact, combination of different ligands, resulting in greater tunability of structural frameworks seems to be a good choice for preparation of new polymeric structures. In this study, synthesis of new coordination polymers and investigation on catalytic behavior of some of them as catalyst for oxidation reactions and biodiesel production will be presented [6-7].

References:

- [1] **Faezeh Farzaneh**; Yasaman Sadeghi. J. Mol. Catal. A: Chem. 2015, 398, 270–281.
- [2] Elham Zamanifar; Faezeh Farzaneh; Jim Simpson; Mahboobeh Maghami. Inorg. Chim. Acta, 2014, 414, 63–70.
- [3] Masoomesh Sharbatdaran ; **Faezeh Farzaneh**; Majid Mojtahedzadeh Larijani; Alireza Salimi; Mina Ghiasi; Mehdi Ghandi. Polyhedron, 2016, 110, 264–270.
- [4] Zeinab Asgharpour; **Faezeh Farzaneh**; Alireza Abbasib. RSC Adv. 2016, 6, 90729–90739.
- [5] Ming-Hui Sun; Shao-Zhuan Huang; Li-Hua Chen; Yu Li; Xiao-Yu Yang; Zhong-Yong Yuan; Bao-Lian Su. Chem. Soc. Rev. 2016, 45, 3479–3563.
- [6] Lida Hamidipour; Maciej Kubicki; **Faezeh Farzaneh**; Mehdi Ghandi; Mahbobeh Maghami. Inorg. Chem. Commun. 2013, 36, 227–231.
- [7] Elnaz Rashtizadeh; **Faezeh Farzaneh**; Zahra Talebpour. Bioresource Technol. 2014, 154, 32–37.

Schiff base complexes: Synthesis and applications

M. Montazerozohori

Department of Chemistry, Yasouj University, Yasouj, Iran

E-mail: mmzohori@yu.ac.ir

Schiff bases (also named as imine or azomethine compound), named after Hugo Schiff, are prepared via a condensation reaction between a primary amine and an aldehyde or a ketone under specific conditions. Schiff base complexes have been amongst the most widely studied coordination compounds in the past few years due to their facile synthesis with very high yield, large diversity and wide range of application including: antifungal, antibacterial, anticancer, antimicrobial and anthelmintic activities; catalytic activity in many organic reactions; as models of reaction centers of metalloenzymes, as non-linear optical and luminescent materials; as precursor in nanotechnology and etc. These are used as pigments and dyes and intermediates in organic synthesis, and as polymer stabilizers. In coordination chemistry point of view, Schiff base complexes have been caused a considerable development in structural studies. Accordingly synthesis and characterization of new Schiff base compounds and investigation of their properties especially their biological and catalytic activities are in demand yet. In this direction, among many other researchers, our research group has focused on preparation and structure of new Schiff base complexes (IIB group) especially four and five coordinated complexes containing N^{\vee} and N^{∇} -Schiff base. Antibacterial/antifungal of these compounds was evaluated against some gram positive and negative bacteria and some fungal strains that led to acceptable results for their antimicrobial activities. DNA cleavage potential of the complexes was also investigated. On some complexes theoretical studies such as DFT and Hirshfeld surface analyses were performed to investigate various interactions between molecules in solid state network. Some of the synthesized complexes were prepared in nanostructure size and used as precursor for the synthesis of metal oxide nano-particles [1-7].

References

- [1] S. Amer, N. El-Wakiel, H. El-Ghamry, J. Mol. Struct. 1049 (2013) 326-330.
- [2] K. Hariprasath, B. Deepthi, I.S. Babu, P. Venkatesh, S. Sharfudeen, V. Soumya, J. Chem. Pharm. Res. 2 (2012) 496-499.
- [3] P. Ghosh, A.R. Chowdhury, S.K. Saha, M. Ghosh, M. Pal, N.C. Murmu, P. Banerjee, Inorgan. Chim. Acta 429 (2015) 99-108.
- [4] A. Afkhami, H. Keypour, F. Khajavi, M. Rezaeivala, J. Lumin. 131 (2011) 1472.
- [5] M. Montazerozohori, A. Nazaripour, A. Masoudiasl, R. Naghiha, M. Dusek, M. Kucerakova Mater. Sci. Eng. C, 50(2015) 462-470.
- [6] A. Masoudiasl, M. Montazerozohori, R. Naghiha, A. Assoud, P. McArdle, M. Safi Shalamzari, Mater. Sci. Eng. C, 61(2016) 809-823.
- [7] S. Ghanbari Niyaky, M. Montazerozohori, A. Masoudiasl, J.M. White, J. Mol. Struct. 1131(2017)201-211.

Inorganic Photochemistry and Photophysics: Recent Advances and Applications

Mehdi Amirnaser

Department of Chemistry, Isfahan University of Technology, Isfahan ۸۴۱۵۶۸۳۱۱۱, Iran, E-mail: amirnaser@cc.iut.ac.ir

The interaction of light with matter is one of the most significant and fascinating areas in the physical sciences. Applications of photochemistry and photophysics are now expanding at a huge rate. The subject spans a full range of disciplines from the immediately practical to those that are still emerging. Dye-sensitized solar cells, photocatalytic production of H_2 and reduction of CO_2 using metal complexes or MOFs and CQDs, light-driven molecular electronic devices or molecular machines, information processing, quantum dots, photodynamic therapy for medical applications, theranostics, and biological optical imaging and sensing, highlight strong examples of new multidisciplinary research frontiers.

Detection of many biologically important species and construction of molecular logic gates have also received special attention. Nitric oxide, the odd-electron diatomic gaseous molecule, produced endogenously by nitric oxide synthase (NOS), plays several important roles in various biological processes including blood pressure control, immuneresponse, neurotransmission, and cell apoptosis [۱]. The biological activity of NO is heavily dependent on the dose, duration of exposure, and cellular sensitivity to NO. It is therefore desirable to develop procedures for rapid and direct detection of NO concentration.

Small molecular fluorogenic probes are of great value in selective detection of various metal ions in biological systems. From a biological point of view, Zn(II) is the second most abundant metal ion in the human body and an essential cofactor in many biological processes such as brain function and pathology, DNA synthesis, immune function, enzyme activity and neurotransmission [۲]. It is supposed that disorder of zinc homeostasis is linked to a number of pathological processes, such as Alzheimer's disease and epilepsy [۳]. Therefore, the monitoring of zinc ion with a selective chemical probe is highly desired.

An overview of the aforementioned topics will be presented and in an effort towards the development of new applications for carboxamide ligands, selective "On-Off" switching behavior of small fluorogenic molecules, Hbpq and Hqcq, for detection of NO and Zn(II) ion as selective chemical probes will be discussed [۴,۵]. In the presence of Zn^{2+} , the Hqpzc fluorescence exhibits reversibility with SCN^- , and as an illustrative example the construction of an INHIBIT type logic gate at the molecular level, resulting from the fluorescent signals of Hqpzc, is described.

References

- [۱] S.R. Weckler, A. Mikhailovsky, D. Korystov, P.C. Ford, *J. Am. Chem. Soc.* ۱۲۸ (۲۰۰۶) ۳۸۳۱.
- [۲] C.J. Frederickson, J.Y. Koh, A.I. Bush, *Nat. Rev. Neurosci.* ۶ (۲۰۰۵) ۴۴۹.
- [۳] S.M. Hancock, D.I. Finkelstein, P.A. Adlard, *Frontiers in Aging Neuroscience*, ۶ (۲۰۱۴) Article ۱۳۷, ۱.
- [۴] S. Meghdadi, M. Amirnaser, A. Amiri, Z.M. Mobarakeh, Z. Azarkamanzad, *C. R. Chim.* ۱۷ (۲۰۱۴) ۴۷۷.
- [۵] M. Amirnaser, R. Sadeghi Erami, S. Meghdadi, *Sens. Actuators, B* ۲۳۳ (۲۰۱۶) ۳۵۵.

Carbon capture and chemical fixation by metal-organic frameworks (MOFs)

Global warming resulting from the emission of greenhouse gases, especially CO₂, has become a widespread concern in the recent years. Carbon capture and storage (CCS) is widely regarded as an effective approach to reduce the total CO₂ emission in the atmosphere. The removal of CO₂ from low pressure gas mixture can be achieved with solid porous adsorbents. The CO₂ involved chemical synthesis has been widely investigated in the past decades because carbon dioxide is a naturally abundant, inexpensive and recyclable as well as non-toxic and non-flammable compound. One of the most prominent and environmentally friendly methods for chemical fixation of CO₂ is its conversion to cyclic carbonates via reaction of epoxides with carbon dioxide. Cyclic carbonates are valuable intermediates in organic synthesis, aprotic polar solvents and raw materials for plastics.

In continues of our recent works in the field of heterogeneous catalyst, we succeed to design new catalyst based on MOF for producing cyclic carbonates. In this manner, new metal nanoparticles doped MOFs and different functionalized MOFs as efficient heterogeneous catalysts with high surface area and Lewis acid sites for cycloaddition reactions of epoxides with CO₂ has been introduced. High activity, which result in a higher local concentration of CO₂, selectivity, easy work up, reusability and extremely mild reaction conditions are unique features of these novel and efficient immobilized catalysts.

1) F. Zadehahmadi, F. Ahmadi, S. Tangestaninejad, M. Moghadam, V. Mirkhani, I. Mohammadpoor-Baltork, R. Kardanpour, Catalytic CO₂ fixation using tin porphyrin

supported on organic and inorganic materials under mild conditions, *J. Mol. Catal. A: Chem.*, **398** (2015) 1-10.

2) F. Ahmadi, S. Tangestaninejad, M. Moghadam, V. Mirkhani, I. Mohammadpoor-Baltork, R. Kardanpour, Electron-deficient tin (IV) tetraphenylporphyrin perchlorate: A highly efficient catalyst for chemical fixation of carbon dioxide, *polyhedron*, **32** (2012) 68-72.

3) M. Montazerolghaem, S. F. Aghamiri, S. Tangestaninejad, M. R. Talaie, Metal-organic framework MIL-101 doped with metal nanoparticles (Ni & Cu) and its effect on CO₂ adsorption properties, *RSC Adv.*, **6** (2016) 632-640.

Organometallic Fluoro Complexes; Swimming against the Stream?

Mohsen Golbon Haghighi^{a*}

^a *Department of Chemistry, Shahid Beheshti University, Evin, Tehran, 19839-69411 Iran*
mohsen_golbon@yahoo.com; m_golbon@sbu.ac.ir

Considering the scarcity of the naturally occurring organofluorine compounds on one hand, and their omnipresence in drugs,[1] agrochemicals,[2] and advanced materials[3] on the other, there is a great interest in the development of new synthetic methodologies allowing the introduction of fluorine into organic molecules. A myriad of potent fluorinating reagents have been prepared and used in fluorination of many classes of organic compounds. Yet, by the beginning of the new century, it became evident that some important fluorination reactions could not be performed by simply picking the right fluorinating reagent. In particular, the selective introduction of fluorine into nonactivated aromatic rings remained a significant challenge. Isolated efforts to expand the scope of fluorinating reagents to include late transition metal complexes, particularly palladium complexes, did not provide viable alternative fluorination methods despite their efficiency in the formation of C–C, C–N, and C–O bonds. By the early 2000s, there were no experimental data on the formation of the C–F bond assisted by transition metal complexes, and all attempts to observe aryl–fluoride reductive elimination reaction have been unsuccessful. Furthermore, very few late organotransition metal fluoro complexes were convincingly characterized, as the synthetic methods toward such complexes were insufficiently developed, in particular with regard to metals in a high oxidation state.

Although likely the most important, aryl–F elimination can be considered a particular case of a more general elimination of aryl–halogen bonds and can be influenced by the same factors. Surprisingly, only few literature reports described aryl–halide elimination from isolated transition metal complexes. While the feasibility of such reaction was established, more synthetic and mechanistic information was necessary to make predictions regarding the most suitable systems for the formation of carbon–halogen bonds. It was important to perform detailed studies of aryl–halide reductive elimination reactions with regard to the nature of the metal and ligands, halogenation mechanism, complex geometry, solvent effect, and so forth. Deciphering the influence of these parameters could guide the development of strategies toward making new C–X bonds including in fluoroarenes. This presentation discuss our studies on the mechanism of electrophilic halogenation–reductive elimination transformations. Particular emphasis is placed on understanding the requirements for formation of carbon–fluorine bonds usually in competition with other reductive elimination reactions.

References:

[1] Wang, J.; Sánchez-Roselló, M.; Aceña, J. L.; del Pozo, C.; Sorochinsky, A. E.; Fustero, S.; Soloshonok, V. A.; Liu, H.; *Chem. Rev.*, **2014**, *114*, 2432–2506.

- [2] Theodoridis, G. *Fluorine-Containing Agrochemicals: An Overview of Recent Developments*. In *Advances in Fluorine Science*; Tressaud, A., Ed.; Elsevier: Amsterdam, **2006**; 2, 121– 175.
- [3] Babudri, F.; Farinola, G. M.; Naso, F.; Ragnia, R.; *Chem. Commun.*, **2007**, 1003– 1022.

Designing a Garden, Fuel Cell Power Plant and Pharmaceutical Factory in the Nano World by Using of Organometallic Complexes at Oil/Water Interface

S. Jafar Hoseini*

Department of Chemistry, Faculty of Sciences, Yasouj University, Yasouj, ۷۵۹۱۸۷۴۸۳۱, Iran

Introduction

Richard Feynman gave an idealistic and now oft-quoted talk entitled “There’s Plenty of Room at the Bottom” in December ۱۹۵۹. The event was an American Physical Society meeting at the California Institute of Technology. Although he didn’t intend it, but he was defining moment in nanotechnology, long before anything “nano” appeared. The “oil–water interfacial assembly” strategy provides a powerful bottom-up approach for the nanofilm fabrication due to low cost and low environmental impact. Most important advantages of this assembly strategy are the significant simplicity and universality found in almost all of the related low dimensional nanostructures. The product formed by the reaction at the interface contains ultra-thin nanocrystalline particles [۱, ۲]. Here I would like to talk on the manipulating of platinum nanoparticles self-assembly at oil/water interface to produce a beautiful garden by application of organometallic complexes. Then, I design a nano-fuel cell power plant to generate electricity for a nanogarden and a pharmaceutical nano-factory that produces different medicines by using of carbon-carbon coupling reactions.

Experimental

The method used to prepare thin film at the oil–water interface involves dissolving relevant precursor in organic layer and injecting appropriate reducing reagent in the aqueous layer. The onset of reduction was marked by a coloration of the liquid–liquid interface. With the passage of time, the color became more vivid, finally resulting in a film at the liquid–liquid interface. The aqueous and organic layers below and above the film were, however, transparent. Transferring of thin film from the toluene–water interface to the solid substrate (glass or electrode) was generally carried out using a lifting-up approach of the substrate from the liquid phase. Thus, the toluene phase was removed slowly by a syringe and then a solid substrate was inserted into the liquid phase and pulled out.

Results and Discussion

Designing of beautiful trees is the fundamental step in the producing a nanogarden. We used liquid/liquid interface to produce dendritic tree-like nanostructures of platinum–aminoclay at the toluene–water interface [۱]. Nanosheets of platinum nanoparticles were used to cover the floor of the garden. They were synthesized by reduction of platinum complex in the presence of polyvinylpyrrolidone (PVP) as stabilizer at toluene / water interface [۱]. Different and beautiful floor are very breathtaking. Monodisperse and small platinum nanoparticles assembled near to other were synthesized from reduction of $[PtCl_4(cod)]$ ($cod = 1,5$ -cyclooctadiene) complex at oil/water interface and can be used as second type of floor [۲]. To build a fence around the garden to a large nanotube is needed. We have synthesized different inorganic nanotubes such as TiO_2 , ZnO , Al_2O_3 and BN [۳]. Decorating the garden with

snowman was another of our demands. Pt/Pd nanohybrid thin film was produced at toluene/water interface as snowman like structure [٤]. Instead of the sunlight, nanogarden needs lighting which promotes the growth of plants. We synthesized different platinum based electrocatalyst to build a nano-fuel cell power factory with methanol fuel. We produced Pt-Sn/reduced-graphene oxide [٥], Pt/Fe/Fe₃O₄, PtPdZn, PtPdCu and other nanohybrids to catalyze methanol oxidation reaction in fuel cells [٦]. Suzuki–Miyaura cross-coupling reactions provide a general and powerful method for the synthesis of pharmaceuticals due to functional group compatibility, mild reaction conditions and accessibility of organoboron reagents. We have used different nanocomposite to design a pharmaceutical nano-factory [٧, ٨]. Oxidative addition reaction is a rate-determining step in carbon-carbon coupling reactions. Organoplatinum complexes were used to find effective factors on the rate and mechanism of the oxidative addition reactions [٩, ١٠].

Conclusion

As the final result, I can only say that there is a very great world at the bottom that many people- like live there and behave similar to us.

References

- [١] S. J. Hoseini, M. Rashidi and M. Bahrami, *J. Mater. Chem.*, ٢٠١١, ٢١, ١٦١٧٠-١٦١٧٦.
- [٢] S. J. Hoseini, N. Mousavi, M. Roushani, L. Mosadeghi, M. Bahrami and M. Rashidi, *Dalton Trans.*, ٢٠١٣, ٤٢, ١٢٣٦٤-١٢٣٦٩.
- [٣] A. Gomathi, S. J. Hoseini, C. N. R. Rao, *J. Mater. Chem.*, ٢٠٠٩, ١٩, ٩٨٨-٩٩٥.
- [٤] S. J. Hoseini, M. Bahrami and M. Dehghani, *RSC Adv.*, ٢٠١٤, ٤, ١٣٧٩٦-١٣٨٠٤.
- [٥] S. J. Hoseini, Z. Barzegar, M. Bahrami, M. Roushani and M. Rashidi, *J. Organomet. Chem.*, ٢٠١٤, ٧٦٩, ١-٦.
- [٦] S. J. Hoseini, M. Bahrami and M. Roushani, *RSC Adv.*, ٢٠١٤, ٤, ٤٦٩٩٢-٤٦٩٩٩.
- [٧] S. J. Hoseini, M. Dehghani and H. Nasrabadi, *Catal. Sci. Technol.*, ٢٠١٤, ٤, ١٠٧٨-١٠٨٣.
- [٨] R. H. Fath, S. J. Hoseini, *J. Organomet. Chem.*, ٢٠١٧, ٨٢٨, ١٦-٢٣.
- [٩] S. J. Hoseini, H. Nasrabadi, M. Rashidi, *Organometallics*, ٢٠١٥, ٣٤, ٦١٦-٦٢١.
- [١٠] S. J. Hoseini, H. Nasrabadi, R. H. Fath, Z. Moradi, *Organometallics*, ٢٠١٤, ٣٣, ١٦٨٩-١٦٩٩.

Influence of ancillary ligands in Dye-sensitized solar cells (DSSCs) and Organic light emitting diodes(OLEDs)

Hashem Shahroosvand

Chemistry Department, University of Zanjan, Zanjan, Iran

Email: shahroos@znu.ac.ir

Dye-sensitized solar cells (DSSCs) and organic light emitting diodes (OLEDs) have motivated many researchers to develop various complexes with tailored properties involving anchoring and ancillary ligands [1]. Ancillary ligands carry favorable light-harvesting abilities and are therefore crucial in determining the overall power conversion efficiencies and luminescence efficiencies. The use of ancillary ligands having aliphatic chains and/or π -extended aromatic units decreases charge recombination and permits the collection of a large fraction of sunlight in DSSCs [2]. This presentation aims to provide insight into the relationship among the ancillary ligand in ruthenium polypyridyl complexes, DSSC and OLED properties, which can further guide the function-oriented design and synthesis of different sensitizers and emitter for DSSCs and OLEDs, respectively [3]. Finally, Ru polypyridyl complexes have gained increasing interest for feasible large-scale commercialization of DSSCs and OLEDs due to their more favorable light-harvesting abilities and long-term thermal and chemical stabilities compared with other conventional sensitizers. Therefore, the main idea is to inspire scientists to explore new avenues in the design of new sensitizers and emitters based on ruthenium polypyridyl complexes for DSSCs and OLEDs application.

References:

- [1] O'Regan B, Grätzel M, A low-cost, high-efficiency solar cell based on dye-sensitized colloidal TiO_2 films. *Nature* 1991; 353: 737-740.
- [2] Pashaei B, Shahroosvand H, Graetzel M, Nazeeruddin Md. K. Influence of ancillary ligand in dye-sensitized solar cells, *Chem. Rev.* 2016; 16, 9480-9564.
- [3] Shahroosvand H, Najafi L, Sousaraei A, Mohajerani E, Janghour M, Bonaccorso F. Ruthenium tetrazole-based electroluminescent device: the key role of counter-ions for the light emission properties. *J Phys Chem C* 2016; 120 (43):24960-24972.

Different Cycloplatinated(II) Complexes with Allyldiphenylphosphine as Ancillary Ligand: Photophysical Study

Reza Babadi Aghakhanpour,^{a,c} Hamid R. Shahsavari,^{a*} Mojgan Babaghasabha,^a Mohsen Golbon Haghighi,^b S. Masoud Nabavizadeh^c and Behrouz Notash^b

^aDepartment of Chemistry, Institute for Advanced Studies in Basic Sciences (IASBS), Yousef Sobouti Blvd., Zanjan 45137-6931, Iran.

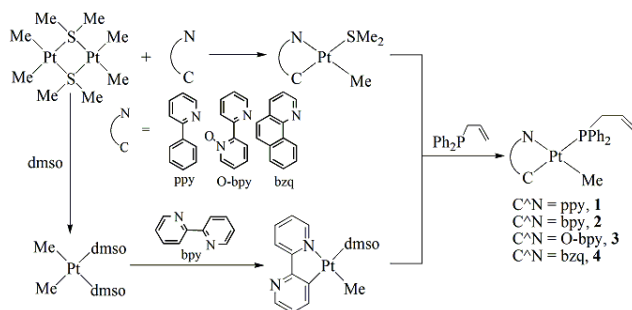
^bDepartment of Chemistry, ShahidBeheshti University, Evin, Tehran 19839-69411, Iran.

^cDepartment of Chemistry, College of Sciences, Shiraz University, Shiraz 71454, Iran.

Email: shahsavari@iasbs.ac.ir

Introduction: In the past years, hybrid ligands with the hemilabile character has been one the most attractive areas in organometallic chemistry because of their high potential in homogeneous catalytic systems [1-5]. The phosphine containing weakly coordinating carbon moieties, in particular olefins, can sterically and electronically affect the properties of the complexes. As part of our ongoing research into the cyclometalation chemistry of platinum, Herein, we expand our investigation by the synthesis and characterization of a closely related series of cycloplatinated(II) complexes featuring allyldiphenylphosphine ligand [6-9]. We decided to investigate how an allylic substituent on the phosphine ligand affects the photophysical properties of the cycloplatinated(II) complexes.

Experimental: The synthetic methods of the complexes are presented in Scheme 1. The product complexes [Pt(C^N)(Me)(PPh₂allyl)], 1-4, (C^N = ppy, 1; bpy, 2; O-bpy, 3; and bzq, 4, respectively, and PPh₂allyl is allyldiphenylphosphine) were synthesized using the reaction of above-mentioned precursor complexes with 1 equivalent of PPh₂allyl ligand under inert atmosphere at room temperature. All the new complexes were isolated as pure and stable solids that are also quite stable in solution.



Scheme 1. Synthetic route for preparation of the complexes 1-4.

Results and Discussions: The structures of the complexes **1-4** in solution were accurately deduced from their ^1H , ^{13}C , ^{31}P , and ^{195}Pt NMR spectra together with the help of two dimensional (HH COSY, HSQC) and DEPT ^{13}C techniques. Crystals of X-ray diffraction quality were obtained for the complexes **1** and **4** from CH_2Cl_2 solution with slow layer diffusion of *n*-hexane. The complexes **1**, **2** and **4** exhibit a strong green emission in solid state at room (298 K) and low temperatures (77 K) and in glassy solution (CH_2Cl_2). None of these complexes is emissive in solution at ambient temperature (Figure 1).

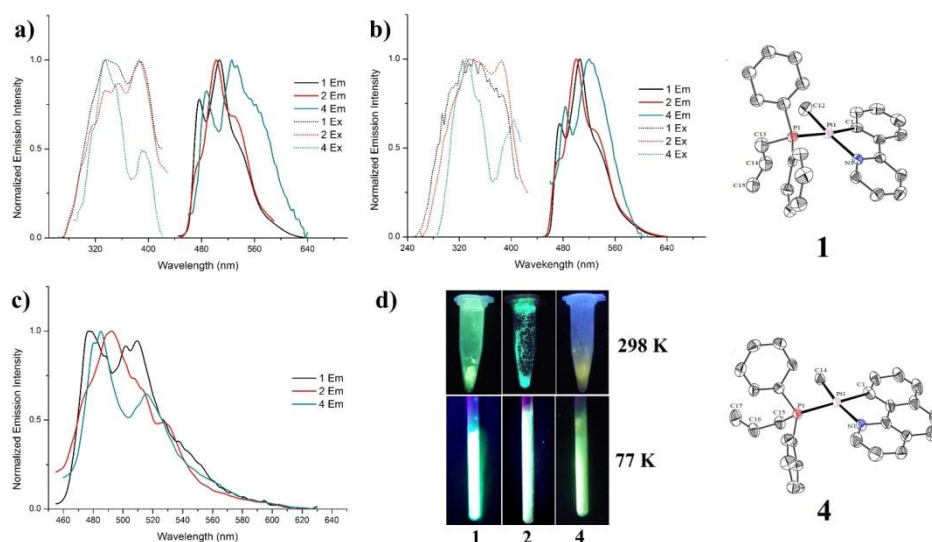


Figure 1. Emission spectra with the excitation spectra for the complexes **1**, **2** and **4** in a) solid state at 298 K , b) solid state at 77 K , c) CH_2Cl_2 glassy state. d) Photographic images of the complexes **1**, **2** and **4** under UV light.

Conclusion: In summary, a series of closely related cycloplatinated(II) complexes $[\text{Pt}(\text{C}^{\wedge}\text{N})(\text{Me})(\text{PPh}_2\text{allyl})]$, **1-4**, were synthesized from the appropriate precursor complexes and allyldiphenylphosphine ligand. This study also investigates the effect of allyl substituent of phosphine ligand on the photophysical properties of the complexes.

References

- [1] Gavrilova, A. L.; Bosnich, B., *Chem. Rev.* **2004**, *104*, 349-384.
- [2] Braunstein, P., *J. Organomet. Chem.* **2004**, *689*, 3903-3967.
- [3] Diéguez, M.; Pàmies, O.; Ruiz, A.; Díaz, Y.; Castellón, S.; Claver, C., *Coord. Chem. Rev.* **2004**, *248*, 2160-2192.
- [4] Bassetti, M., *Eur. J. Inorg. Chem.* **2006**, *2006*, 4473-4482.
- [5] Lee, H. M.; Lee, C.-C.; Cheng, P.-Y., *Curr. Org. Chem.* **2007**, *11*, 1491-1524.
- [6] Niazi, M.; Shahsavari, H. R., *J. Organomet. Chem.* **2016**, *803*, 82-91.
- [7] Niazi, M.; Shahsavari, H. R., *ChemistrySelect* **2016**, *1*, 1780-1783.
- [8] Niazi, M.; Shahsavari, H. R.; Golbon Haghighi, M.; Halvagar, M. R.; Hatami, S.; Notash, B., *RSC Adv.* **2016**, *6*, 76473-76474.
- [9] Niazi, M.; Shahsavari, H. R.; Golbon Haghighi, M.; Halvagar, M. R.; Hatami, S.; Notash, B., *RSC Adv.* **2016**, *6*, 90073-90084.

Surface Chemistry: From Theory to Experiment

Saeid Azizian

Department of Physical Chemistry, Faculty of Chemistry, Bu-Ali Sina University, Hamedan, Iran

E-mail: saizian@basu.ac.ir

Interfacial science is the study of processes between two phases. Interfaces and processes involving interfaces have gained growing interest from theoretical, experimental and industrial viewpoints.

Five classes of interfaces including, solid/liquid, solid/gas, solid/solid/ liquid/liquid and gas/liquid led to the application of this subject in chemistry, physics, chemical engineering, biotechnology and environmental science. Adsorption as one of the subjects of surface chemistry is of great technological importance. So the study of theoretical and experimental aspects of adsorption is important too.

We will summarize some research progresses in our group about theoretical aspects of adsorption kinetics, adsorption isotherm equations and some of studied experimental systems.

Review of Quantum Scattering Formulation via Non-Local Potentials

Ali Maghari

Department of Physical Chemistry, College of Science, University of Tehran, Tehran, Iran

maghari@ut.ac.ir

Introduction: The non-local separable potentials (NLSP) have been widely used in many branches of physics, such as nuclear physics, condense matter and reactive collisions. The two-body NLSP has been used to theoretically describe the few-body scattering problems, since the Lippmann-Schwinger (LS) equation can analytically solved. We proposed a novel approach to solve the two- and three-body quantum scattering equations and obtained the analytical expressions for coupled and uncoupled scattering properties in terms of partial-wave resolvent matrix with an arbitrary angular momentum quantum numbers. Moreover, our work is concerned with the theoretical study of an electron-hole pair (exciton) confined in a harmonic quantum dot (QD) and calculated an analytic expression for exciton wave function in terms of hypergeometric functions and the scattering parameters within the effective mass approximation. The actual Coulomb potential is replaced by a projective operator such as a 3D nonlocal separable potential (NSP) and the form factor of the interaction potential is chosen as the Yukawa (screened coulomb) form. The obtained analytical expressions for cross-sections as well as phase shifts and time delays have been used for calculating the quantum statistical mechanical properties of fluids. The natural extension of two-body scattering formulations for the case of full few-body scattering may be within the Faddeev equation approach. The method leads to a unique formulation for both equilibrium and non-equilibrium statistical mechanical properties as well as the collision reaction dynamics. However, our approach are recently used for electron-hole pair interactions in quantum dots, but the method can be extended to any quantum system such as quantum wells and wires.

Mathematical Model: Consider a two-channel separable potential for two-particle system as

$$\hat{V}_{NL} = -\frac{\hbar^2}{\mu} \sum_{k=1}^n v_k |\chi_k\rangle \langle \chi_k| \quad (1)$$

where n is the rank of the potential, v_k is the coupling strength and $|\chi_k\rangle$ is an arbitrary state of the system. The Hamiltonian of the system confined in a harmonic trap as:

$$\hat{\mathcal{H}} = \frac{\hat{p}^2}{2\mu} + \frac{1}{2}\mu\omega^2 r^2 + \hat{V}_C \quad (2)$$

where μ the reduced mass, ω the confining frequency and $\hat{V}_C(r) = -\frac{e^2}{\epsilon|r_e-r_h|}$ is the Coulomb potential between two-charged particles. The actual Coulomb potential can be replaced by a projective operator defined in Eq. (1). The LS equation for the wave function and transition matrix operator via Hamiltonian $\hat{\mathcal{H}}$ is given by

$$|\psi(z)\rangle = |\varphi\rangle + \frac{1}{z - \hat{\mathcal{H}}_0} \hat{V}_{NL} |\psi(z)\rangle \quad (3)$$

$$\hat{T}(z) = \hat{V} [1 - \hat{V} \hat{G}_0(z)]^{-1} \quad (4)$$

where $\hat{H}_\epsilon = \frac{\hat{p}^2}{2\mu} + \frac{1}{2}\mu\omega^2 r^2$, $|\varphi\rangle$ refers to the eigenvector of \hat{H}_ϵ , $z \equiv E - i\epsilon$ is the complex energy parameter and $G_\epsilon(z) = (z - \hat{H}_\epsilon)^{-1}$ is the Green's operator. The transition matrix explicitly shows the contributions from the bound states, resonances and distinct singularities in the complex plane and plays an important role in calculation the statistical mechanical properties of system. In our works, we have chosen the Yamaguchi type model potential.

Results and Discussion: Using the two-particle NLSP model and analytical solving the LS equation, a new formulation of the equilibrium and non-equilibrium statistical mechanical properties of a gas are presented in terms of partial-wave scattering amplitude. For this model potential, the bound states and resonances are also calculated. Moreover, the three-body transition matrix and its poles (bound states and resonances) and consequently other related quantities like scattering amplitudes, scattering length, phase shifts and cross sections are calculated from the analytical solution of Faddeev equations. Also, we obtained a new analytical expression for the third virial coefficient in terms of three-body transition matrix. Furthermore, a theoretical study of an electron-hole pair confined in a harmonic QD has been recently done and an analytic expression for exciton wave function is obtained. The actual Coulomb potential is replaced by a projective operator such as a 3D- NLSP and the form factor of the interaction potential is chosen as the Yukawa form. This trapped system perturbed with a non-Hermitian complex absorbing Scarf potential is also studied using a LS formalism. This allows to describe the scattering of a gas in a tight smooth trapping surface and to analyze the scattering bound and resonance states. The analytical expressions for wave functions and transition matrix as well as the absorption probabilities of atom-surface collision were calculated. The analytical expressions for wave functions and transition matrix as well as the absorption probabilities of atom-surface collision were calculated.

References

- [1] A. Maghari and N. Tahmasbi, *J. Phys. A: Math. Gen.* **38** (2005) 4469.
- [2] A. Maghari and M. Dargahi, *J. Phys. A: Math. Theor.* **41** (2008) 2753.
- [3] N. Tahmasbi and A. Maghari, *Physica A* **382** (2007) 537.
- [4] A. Maghari and M. Dargahi, *J. Stat. Mech.* (2008) P10007.
- [5] A. Maghari, and V. Moheb Maleki, *Comm. Theoret. Phys.* **64** (2010) 22.
- [6] Z. Ahmed, *Phys. Lett. A*, **377** (2013) 957.
- [7] S. López and F. D. Adame, *Semicond. Sci. Technol.* **19** (2002) 227.
- [8] C. G. Santander and F. Adame, *Phys. Lett. A* **370** (2011) 314.

A Brief Review on Confined Fluids; Curvature Dependency of Structure, and their Application in Super Capacitors

Ezat Keshavarzi

Department of Chemistry, Isfahan University of Technology, Isfahan, Iran, ۸۴۱۵۶۸۳۱۱۱

E-mail: keshavrz@cc.iut.ac.ir

The structure and phase transition of fluids in nanopores may show a dramatic discrepancy with macroscopic bulk fluids, these include new kind of properties and phase transitions do not observed in the macroscopic fluids systems; examples include layering and wetting transitions as well as shifts in regular bulk transitions. The main reasons for these differences are the systems wall effects. The fundamental measure density functional results, represented in this work indicate the happening of layering phase transition in hard sphere fluid confined in a nanoslit with hard and structure less walls. The excess adsorption, interfacial tension, wall pressure for both confined and bulk fluids at contact of different curvature walls have been investigated. Our results show that the confining of a fluid in a nanopore causes an oscillatory behavior for all of the above mentioned properties around those values for bulk. The study of an anisotropic and electrolyte confined fluids are more complicated because of their orientation degree of freedoms, and the long range interactions respectively. These kind of fluids have several and important applications in industrial tools and super capacitors.

Quantum Dynamics of Electron Transfer and Free Electron Capture

Hassan Sabzyan*, Mohammad Jafar Jenabi, Nasrin Sadeghi, Fatemeh Alavi

Department of Chemistry, University of Isfahan, Isfahan 81746-73441, I. R. Iran.

sabyan@sci.ui.ac.ir

Introduction: So far, a number of theoretical methods have been developed for the study of electron transfer (ET) between two atomic, molecular and/or ionic species, and free electron capture (FEC) by a charged particle. All of these studies (including potential model, kinetics, scattering, and state-to-state quantum mechanical) were based on models and approximations not matching exactly the conditions of the real problem, and their major failure is the neglect of the time-dependent nature of the core phenomenon which is the evolution of the electronic wavepacket at the 10^{-15} sec time scale [1]. In this lecture, results of the works on the quantum dynamics of the ET and FEC during $\text{He}^{+} - \text{H}$ and $\text{He}^{+}/\text{p}^{+} - \text{e}^{-}$ collisions, will be presented.

Computational Method: The two-dimensional time-dependent Schrödinger equation is solved numerically by time propagator operator method using a third-order split operator technique in the coordinate space and an FFT/IFFT technique to switch between coordinate and momentum spaces to treat respectively the potential and kinetic energy operators. The simulation box setups used in this series of studies are shown in Fig. 1. The ET phenomenon is studied for two cases of fixed and moving nuclei. For the former case, effects of the charge of the acceptor nucleus and its distance to the donor H atom are investigated, and for the latter effect of the wavefunction of the incoming H atom on the ET dynamics is studied.

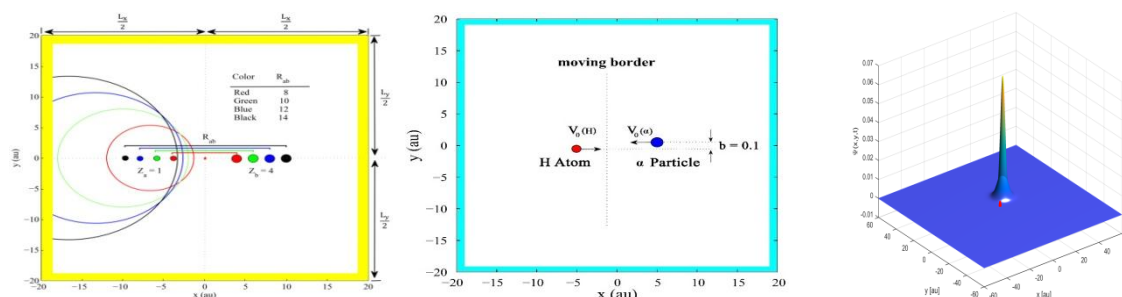


Fig. 1: Simulation box used for the study of ET (left: fixed, middle: moving nuclei) and FEC (right).

For the FEC, the free electron wavepacket is set at a certain distance and allowed to move in a defined direction towards the nucleus. Evolution (and trajectory) of the wavepacket, and its decomposition into hydrogen-like atomic orbitals are followed with time.

Results and Discussion: Typical results are presented in Fig. 2. For the case of fixed nuclei, the ET dynamics is investigated by calculating and following the electron densities belonging to the two nuclei based on a partitioning by zero-force borders (Fig. 1). These densities

oscillate with time after a significant decay from their initial ρ_s and ρ_p values. Quantum dynamics of the ET, for the case of moving nuclei, strongly depends on the charges of the nuclei and their distance and velocities, and especially on the initial orbital (ρ_s , ρ_p , ρ_{p_x} and ρ_{p_y}) of the incoming donor H atom. This ET transfer dynamics is also detailed by calculating expansion coefficients of the projection of the evolving wavepacket onto the stationary eigenfunctions of the H and He^+ species to investigate evolution of the electron density around each nucleus during the ET. The instantaneous and overall electron densities captured by the He^+ nucleus from the H atom are also calculated and analyzed. The FEC dynamics depend on the static (shape and width) and dynamic (momentum and direction of motion) characteristics of the incoming wavepacket.

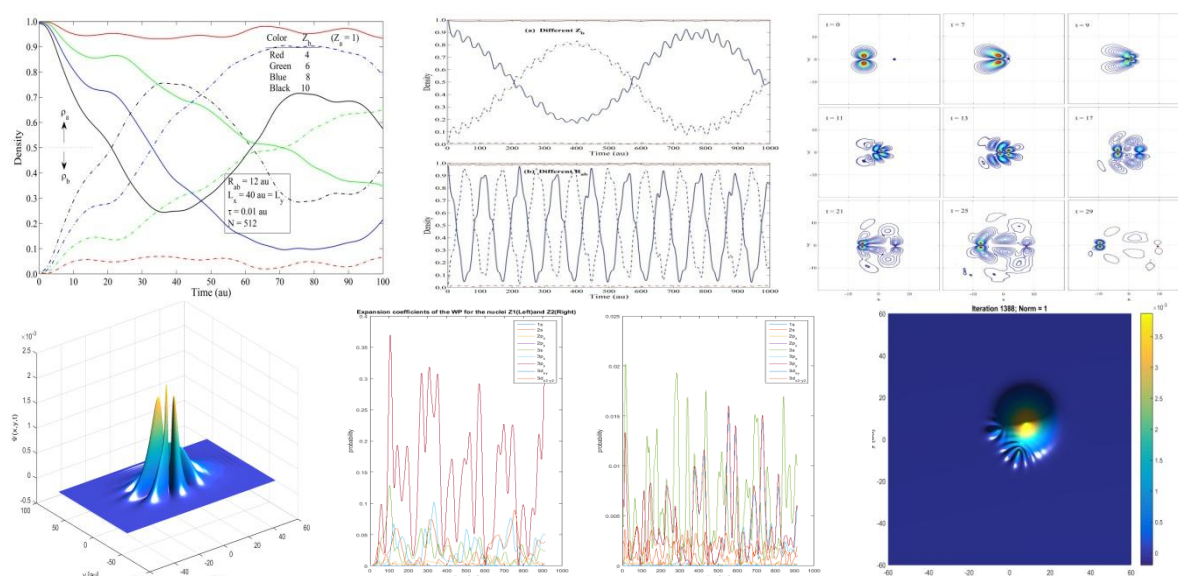


Fig. 9: Typical results obtained in the study of ET (top row) and FEC (bottom row) phenomena.

Conclusion: In an ET process, electron density oscillates between the two fixed nuclei, while evolves transiently in a complex scheme among different orbitals of the donor and acceptor nuclei prior to a damped oscillation between and decay to a couple of them. The instantaneous and overall captured electron density by the He^+ particle from the H atom during H- He^+ collision depend on the impact parameter, relative velocity (collision energy) and the initial state of the H atom. For a specific setup, ET occurs by 70%, 76%, 78% and 79% when starting with ρ_s , ρ_p , ρ_{p_x} and ρ_{p_y} orbitals, respectively. Results of this series of studies show evidently that due to its quantum nature, electron *crawls* from one nucleus to the other in the ET, and from a point in the free space towards an attractor nucleus in the FEC phenomena.

References:

[1] Hassan Sabzyan and Mohammad Jafar Jenabi, The Journal of Chemical Physics, 2016, 144, 134306; and references therein.

Structural properties and phase transition of confined hard and dipolar hard ellipsoids - density functional theory approach

M Moradi. Physics Department, Shiraz University

The density profiles and corresponding order parameters of the hard ellipsoids confined between two hard walls and also in contact with a single hard wall are studied using the density functional theory. The Hyper-Netted Chain (HNC) approximation is used to write excess grand potential of the system with respect to the bulk value. To simplify the calculations we use restricted orientation model (ROM) for the orientation of ellipsoids to find the density profiles and order parameters. Density functional theory shows that there is a uniaxial-biaxial phase transition near a single hard wall and also between two hard walls for a fluid consisting of uniaxial hard ellipsoidal particles with finite elongation. Also the density and polarization profiles of the dipolar hard ellipsoids confined between hard walls are studied using the density functional theory. The number density is expanded up to zero and first order in polarization to find the results. For the zero order in polarization, the coupled integral equations for the directional densities are obtained. Then for the first order in polarization the coupled integral equations for the directional densities and polarization profiles are obtained. Finally we calculate the density and polarization profiles for different cases and compare the obtained results.

Green protocol for the synthesis of quinoxaline derivatives using $\text{SiO}_2\text{-H}_3\text{PW}_{12}\text{O}_{40}$ as an efficient and reusable catalyst

Heshmatollah Alinezhad^a, Elham Soleimani^a

^aDepartment of Organic Chemistry, Faculty of Chemistry, University of Mazandaran, Babolsar, Iran

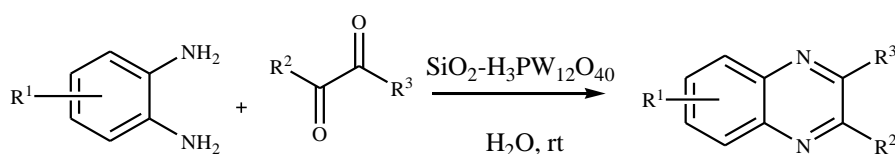
Corresponding Author E-mail: Heshmat@umz.ac.ir

Email: heshmat@umz.ac.ir

Introduction: Quinoxalines are important class of heterocyclic compound in pharmaceutical chemistry [1]. These compounds have broad biological activities such as antitumor [2], antiviral [3], antibacterial [4], and anticarcinogen [5]. Furthermore, some antibiotics such as levomycin, actinoleutin and echinomycin also have a quinoxaline ring in their structures and these are known to inhibit the growth of Gram positive bacteria [6] and are active against various transplantable tumors [7]. Various kinds of synthetic methods toward quinoxalines have been developed, including the condensation of aryl 1,2-diamines with ketones, α -hydroxyketones, α -halo- β -ketoesters and 1,2-diketones. Among them the condensation of 1,2-diamine with 1,2-diketone is one of the simplest and the most direct method for the synthesis of quinoxaline derivatives. Various acid catalysts such as SSA [8], $\text{H}_3\text{PW}_{12}\text{O}_{40} \cdot x\text{H}_2\text{O}$ [9], InCl_3 [10], MnCl_2 [11], [MOEI]-BSA [12], Nanoparticle-supported [13], cobalt Nitritoltris (methylenephosphonic acid) [14] have been employed to achieve this transformation. Even though, some of these methods suffer from several drawbacks such as low product yields, long reaction times, use of volatile organic solvents, harsh reaction conditions, use of homogeneous catalysts and tedious work-up procedures. Therefore, development of simple, efficient, eco-friendly and high yielding methods for synthesizing quinoxalines are still required.

Heterogeneous solid acid catalysts are preferred over conventional homogeneous, because these catalysts can be easily separated from the reaction mixture by simple filtration. Heteropoly acids supported on silica gel have received considerable importance in organic synthesis because of their ease of handling, simple workup, enhanced reaction rates, and recoverability of catalysts [15].

We report herein a facile, efficient and practical method for preparation of quinoxaline derivatives in excellent yields using $\text{SiO}_2\text{-H}_3\text{PW}_{12}\text{O}_{40}$ in water at room temperature (scheme 1).



Scheme 1

Methods / Experimentals: A solution of 1,2-diamine (1 mmol), 1,2-diketone (1 mmol), and PW/SiO₂ (20 mg) in water (2 mL) was stirred at room temperature. After completion of the reaction, as indicated by TLC (ethyl acetate–*n*-hexane, 3:7), water was removed by simple filtration. Then the mixture of crude solid product and catalyst was dissolved in acetone (2 mL), and filtered for separation of the catalyst. The filtrate was evaporated under reduced pressure. The solid products were purified further by crystallization from ethanol to afford the pure quinoxalin and characterized by ¹H NMR, ¹³C NMR, IR, melting point and compared with literature data.

Results and Discussion: To establish the generality and scope of our method, various 1,2-diketones were reacted with different substituted *o*-phenylenediamines. In all cases, the reactions were very clean and the quinoxaline derivatives were obtained in excellent yields under the optimized reaction conditions. The effect of electron-releasing and electron-withdrawing substituents on the aromatic ring of aryl-1,2-diamines on the reaction was investigated. When *o*-phenylenediamines are substituted with electron withdrawing groups, lower rates and yields of reaction are observed than the ones bearing electron-donating groups.

Conclusion: We have demonstrated a very simple, high efficient and green protocol for the preparation of quinoxalin using 12-tungstophosphoric acid supported on silica gel (PW/SiO₂) as a recyclable solid acid catalyst. Our method offers several advantages including short reaction time, high yield with high purity, easy work up, easy recovery and reusable catalyst, cost-effective use of cheap and commercially available starting materials.

References

- 1) a) A. Jaso; B. Zarranz; I. Aldana; A. Monge. *J. Med.Chem.*, 2005, 48, 2019. b) A. Carta; G. Paglietti; M. E. R. Nikookar; P. Sanna; L. Sechi; S. Zanetti. *Eur. J. Med.Chem.*, 2002, 37, 300. c) A. Dell; D. H. William; H.R. Morris; G. A. Smith; J. Feeney; G. C. K. Roberts. *J. Am. Chem. Soc.* 1975, 97, 2497. d) C. Bailly; S. Echepare; F. Gago; M. J. Waring; *Anti- Cancer Drug Des.*, 1999, 10, 291.
- 2) P. Corona; A. Carta; M. Loriga; G. Vitale; G. Paglietti. *Eur. J. Med. Chem.* 2009, 44, 1079.
- 3) M. Loriga; S. Piras; P. Sanna; G. Paglietti. *Farmaco* 1997, 52, 107.
- 4) Y. B. Kim; Y. H. Kim; J. Y. Park; S. K. Kim. *Bioorg. Med. Chem. Lett.*, 2004, 14, 541.
- 5) P. Haldar; B. Dutta; J. Guin; J. K. Ray. *Tetrahedron Lett.* 2007, 48, 5850.
- 6) C. Bailly; S. Echepare; F. Gago; M. J. Waring. *Anti-Cancer Drug Des.* 1999, 10, 291.
- 7) S. Sato; O. Shiratori; K. Katagiri. *J. Antibiot.*, 1977, 20, 270.
- 8) X. Hui; J. Desrivot; C. Bories; P. M. Loiseau; X. Franck; R. Hocquemiller; B. Figadère. *Bioorg. Med. Chem. Lett.* 2006, 16, 810.
- 9) C. Srinivas; C. N. S. S. P. Kumar; V. Jayathirtha Rao; S. Palaniappan. *J. Mol. Catal. A Chem.* 2007, 260, 22.
- 10) M. M. Heravi; Kh. Bakhtiari; F. F. Bamoharram; M. H. Tehrani. *Monatsh. Chem.* 2007, 138, 460.
- 11) P. Hazarika; P. Gogoi; D. Konwar. *Synth. Commun.* 2007, 37, 3447.
- 12) M. M. Heravi; Kh. Bakhtiari; H. A. Oskooie; Sh. Taheri. *Heteroat. Chem.* 2008, 19, 218.
- 13) S. Sajjadifar; M. Norollahi; S. Miri. *Iran j catal.*, 2014, 4, 50.
- 14) F. Rajabi; D. Alves; R. Luque. *Synthesis. Molecules*, 2015, 20, 2079.
- 15) S. Fathi; A. R. Sardarian. *PHOSPHORUS SULFUR*, 2015, 190, 1471.
- 16) M. M. Heravi; Sh. Taheri; Kh. Bakhtiari; H. A. Oskooie. *Catal. Commun.* 2007, 8, 211.